Synthesis of Boron and Silicon Complexes Coordinated with Quinolate-Type Ligands

Yuichiro TOKORO

2013

Department of Polymer Chemistry

Graduate School of Engineering

Kyoto University

Preface

The studies presented in this thesis have been carried out under the direction of Professor Yoshiki Chujo at Department of Polymer Chemistry, Graduate School of Engineering, Kyoto University. The studies are concerned with "Synthesis of Boron and Silicon Complexes Coordinated with Quinolate-Type Ligands".

The author wishes to express his sincerest gratitude to Professor Yoshiki Chujo for his kind guidance, valuable suggestions, and warm encouragement throughout this work. The author is deeply and heartily grateful to Dr. Kazuo Tanaka and Dr. Atsushi Nagai for their constant advices and helpful discussions during the course of this work. The author is indebted to Mr. Hyeonuk Yeo and Mr. Syohei Shiotsu for their great contribution to this work. The author would like to thank Dr. Yasuhiro Morisaki, Dr.Yuuya Nagata and Dr. Kenta Kokado for their valuable suggestions and discussions. The author wishes to acknowledge all the members of Professor Chujo's group. The author is obliged to Ms. Masako Kakutani for her assistance during the author's laboratory life.

Furthermore, the author would like to thank Professor Kenneth B. Wagener, Dr. Paula Delgado and Dr. Frank Arroyave at Department of Chemistry, University of Florida, U.S.A. for their supports and valuable suggestions during the author's stay in U.S.A. The author is grateful to Japan Society for the Promotion of Science (JSPS) for financial support from April 2011 to March 2013.

Finally, the author expresses his deep appreciation to his friends and family, especially his parents, Jun-ichi Tokoro and Noriko Tokoro, and his wife Yuko Tokoro for their constant assistance and encouragement.

Yuichiro Tokoro

March 2013

Table of Contents

Part II. Pentacoordinate Silicon Induced by a Benzo[h]quinolyl Ligand

General Introduction

General Introduction

1. Conjugated Organoboron Compounds

Organoboron complexes with the tricoordinate state possess three covalent bonds and one vacant p-orbital. The vacancy gives Lewis acidity to organoboron compounds, resulting in the enhancement of sensitivity toward moisture and Lewis base. In order to stabilize them, there are two conventional methods, introducing bulky substituents[1] and structural constraint.[2] The former prevents nucleophilic attacks to the boron center, and the latter forces the boron compounds to adopt the planar structure ideal for tricoordinate state (Figure 1). These methods have been applied to synthesize π-conjugated low-molecular-mass organoboron compounds such as boroles[3] and borepins,[4] and π-conjugated polymers (Figure 2).[5] In these compounds, the vacant p-orbital of boron interacts with the adjacent occupied p-orbitals of carbon and extends π-conjugation. The vacant orbital works as an n-type dopant in the organic semi-conducting materials, so that the organoboron compounds possess high electron affinity and belong to n-type π-conjugated polymers which involve smaller number of establish material compared with p-type π-conjugated polymers. The π-conjugated organoboron compounds were also reported as selective optical sensors for fluoride anion with high selectivity (Scheme 1).[6] Coordination of fluoride anion to the organoboron compounds changes the hybridization at the boron atom from sp^2 to sp^3, and this change would interrupt the extension of π-conjugation and alter emission properties. Thereby, the addition of fluoride ions to a chloroform solution of the π-conjugated organoboron compounds induced hypsochromical shifts of the absorption maximum and the annihilation of intense blue emission.

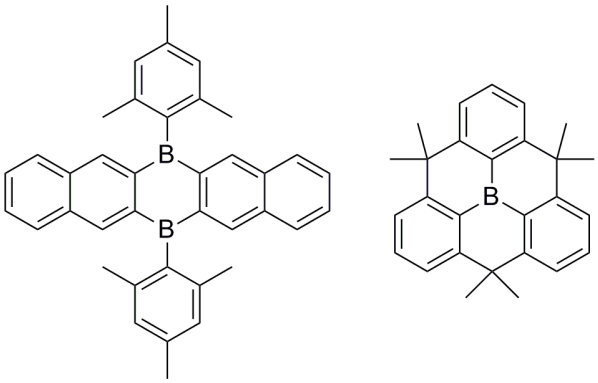

Figure 1. Examples of tricoordinate organoboron compounds stabilized by bulky substituents (left) and by structural constraint.

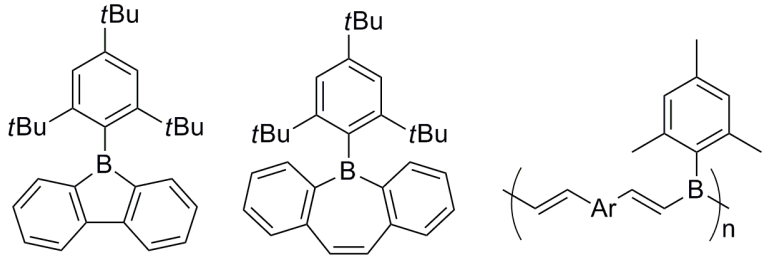

Figure 2. Examples of boroles (left), borepins (centre) and organoboron polymers (right).

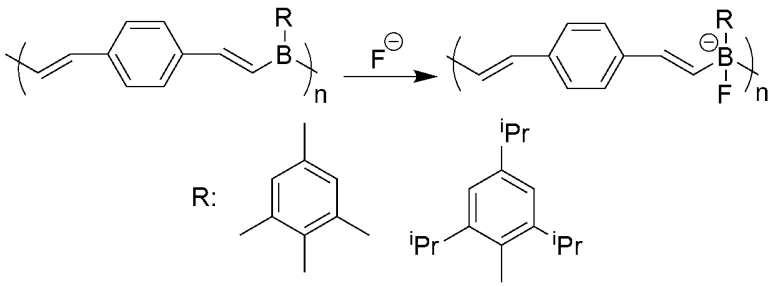

Scheme 1. Reaction of organoboron polymer with fluoride.

Boron can form not only the tricoordinate state but also the tetracoordinate state by accepting a lone pair, and there are a lot of compounds containing a tetracoordinated boron such as boron dipyrromethenes (BODIPYs),[7] boron diketonates[8] and boron quinoloates (Figure 3).[9]

Their rigid structures with the boron center often provide strong emission. BODIPYs are widely used to label proteins and DNAs due to their sharp fluorescence peaks and insensitivity to the polarity and pH of local environments.[10] Furthermore, boron diketonates easily bring about intersystem crossing without heavy atoms, leading to unusual phosphorescent materials.[11]

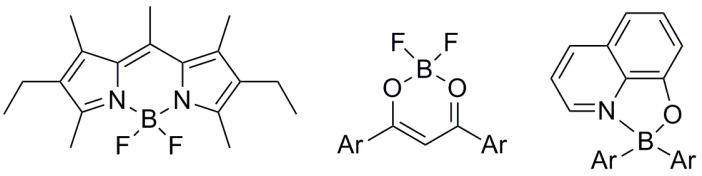

Figure 3. Examples of BODIPYs (left), boron diketonate (centre) and boron quinolate (right).

Organoboron quinolates are valuable light-emitting materials potentially useful in organic light-emitting devices (OLEDs). Organoboron quinolates with high luminescent efficiency and high thermal stability were first reported by Wang *et al.* as an alternative to tris(8-hydroxyquinolinato)aluminium (Alq_3),[12] which is widely used in electron-transport and luminescence layers of OLEDs. The first synthesis of boron quinolate polymers and boron aminoquinolate polymers having π-conjugated backbones was recently accomplished by Nagata and Chujo (Figure 4).[13] The boron quinolate monomer attached diiodophenyl groups on the boron was polymerized by Sonogashira–Hagihara coupling with aromatic diyne comonomers to produce the conjugated alternative polymers incorporating organoboron quinolate into the main chain. The absorption maxima of the polymers from *p*-phenylene-ethynylene unit were slightly changed even in the presence of the boron atoms. In contrast, the polymers showed intense blue-green emission with good quantum yields from the quinolate moiety under a wide range of excitation wavelengths via efficient energy transfer from the π-conjugated backbone to the quinolate moiety. The organoboron quinolate polymers linked on quuinolate ligand were also prepared via the polymer reaction between the polymer precursors and triarylboranes (Figure 4).[14] The photoluminescence quantum yields of the polymers were not significantly high in

comparison with that of the polymer precursor. On the other hand, drastically bathochromic shifts of the absorption and fluorescence emission maxima were observed. The electron mobilities of the polymers were detected with similar levels to Alq_3, These results give us prospects for the possibility of using the boron quinolate polymers as a new class of electron-transfer materials.

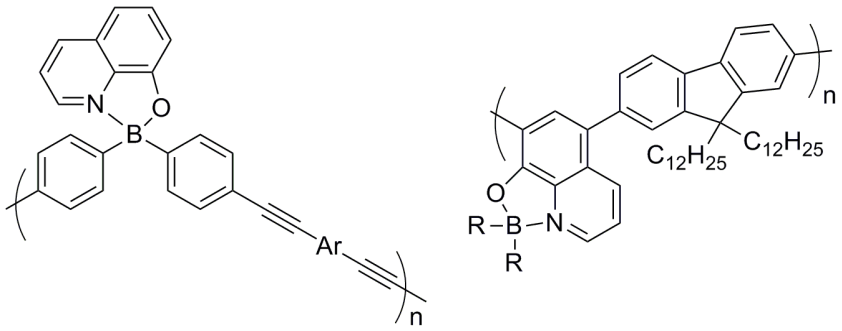

Figure 4. π-Conjugated polymers containing organoboron quinolate moieties.

2. Conjugated Tetracoordinate Silicon Compounds

Silicons in organics usually adopt the tetracoordinate state with stable single bonds between silicon and carbon. A low-lying σ* level of silicon induces significant characteristics particularly in UV-vis absorption spectra. Oligo- and polysilanes showed absorption bands between 300 and 400 nm assignable to σ-σ* transition in Si–Si bonds.[15] Many kinds of organic substituents were introduced to polysilanes, and influenced optical properties. Aryl derivatives displayed bathochromic shift as compared with alkyl ones.[16] The shift was explained by interaction betweeen σ orbitals of polysilanes and π orbitals of aryls. Tetracoordinate silicons were also observed in π-conjugated heterocyclic compounds. Siloles were 5-membered cyclic dienes containing silicon in which σ* orbitals interact with π*orbitals of dienes (Figure 5).[17] The σ*-π* conjugation decreases the LUMO energy levels, leading to good electron-transporting

ability such as Alq_3.[18] The σ*-π* conjugation is valid not only in the plane of the silacycles but also out of the plane. Fluorescence spectra of poly(1,1-silole-vinylene)s show a little bathochromic shift from their respective component units.[19] In addition, the polymers are applicable for detecting explosives due to the unique responsiveness to nitro compounds in solid-states.

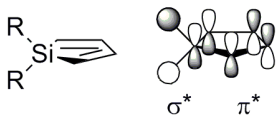

Figure 5. Schematic drawing of the orbital interaction in the LUMOs of a silole ring.

3. Pentacoordinate Silicon Compounds

Pentacoordinate silicon adopts the trigonal-bipyramidal structure and offers two kinds of substitution sites, apical and equatorial.[20] The silcon centre and two apical atoms form a three-centre four-electron bond. A bonding orbital should be delocalized through three atoms and nonbonding orbital localized on the apical atoms. The localization gave partially negative charge to the apical atoms, so that electronegative substituents and electron donors directed to the apical positions.

Pentacoordinate silicon compounds are important reactive intermidiates in S_N2 and Hiyama coupling reactions.[21] They are stabilized by structural constraint or electronegative substituents. Polydentate ligands such as trialkanolamines[22] or N_2O_2-type dipyrrins, which contain 2-hydroxyphenyl group at the pyrrole α-position,[23] compulsively enclose Lewis basic moieties to the silicon centre to make a dative bond (Figure 6). Fluoride and alkoxide ions tend to enhance the formation of tetracoordinate silicon and to generate anionic pentacoordinate silicon species due to their electronegativity and strong affinity to silicon.[24] Although a lot of

pentacoordinate silicon complexes are known, there are a few examples to offer the neutral silicon complexes with bidentate ligands which allow various designs around the silicon centre for functional materials. Diethynylsilanes with 8-aminonaphthyl ligand have been incorporated into main-chains of π-conjugated polymers. High values of third-order nonlinear susceptibility were obtained in these polymers.[25] In 2-silylazobenzene, reversible photoswitching of the coordination numbers have been achieved by *E*/*Z* isomerization of azobenzene, resulting in color changes.[26]

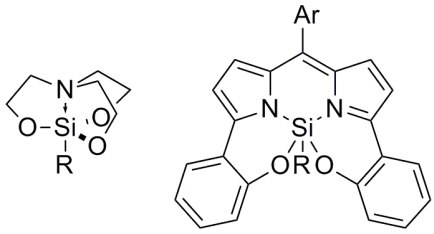

Figure 6. Examples of pentacoordinate silicon compounds generated by trialkanolamines (left) and N_2O_2-type dipyrrins (right).

4. Survey of this thesis

In Part I, the author describes synthesis and a luminescent property of boron quinolates containing π-conjugated polymers. In Chapter 1, low-molecular-mass organoboron quinoline-8-thiolate and -selenolate complexes as model compounds and organoboron polymers containing these complexes with the poly(*p*-phenylene-ethynylene) main chain were prepared (Chart 1). Increasing atomic number of the 16 Group atom adjacent to the boron atom caused emission shift to longer wavelength and decreasing of absolute quantum yields of both the model compounds and the polymers.

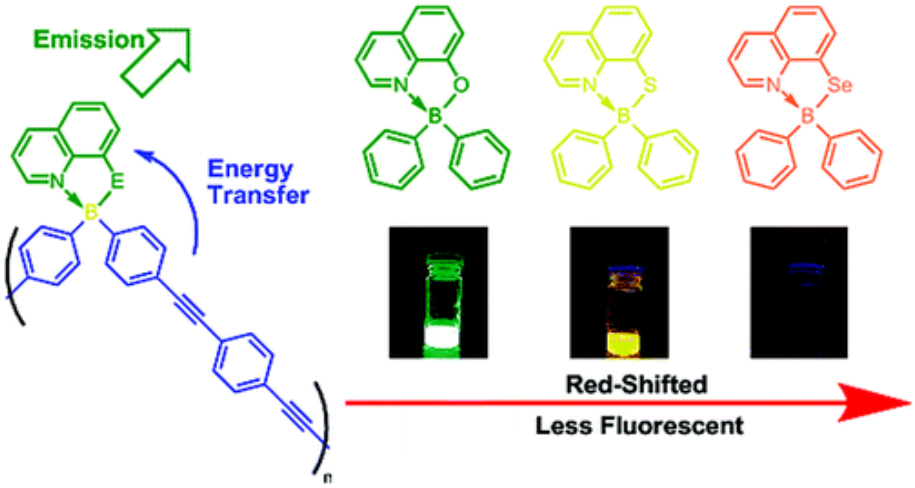

Chart 1

In Chapter 2, the author illustrates the synthesis of poly(*p*-phenylene-ethynylene) derivatives containing organoboron benzo[*h*]quinolate moieties in the main chain via Sonogashira-Hagihara coupling polycondensation (Chart 2). The polymer showed an emission shift to longer wavelength as compared with that from organoboron quinolate.

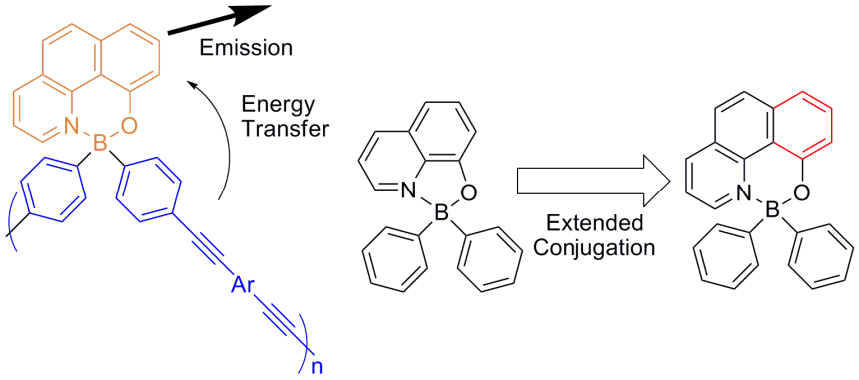

Chart 2

In Chapter 3, the author demonstrates luminescent coordination polymers with both the aminoquinolato ligands and boron centers embedded in the main chain (organoboron aminoquinolate-based coordination polymers) obtained via Sonogashira-Hagihara coupling polycondensation (Chart 3). Their UV–vis absorption and photoluminescence spectra revealed

that the optical behavior of the obtained polymers strongly depended on the electron-donating or -accepting characters of the π-conjugated backbone between boron atoms.

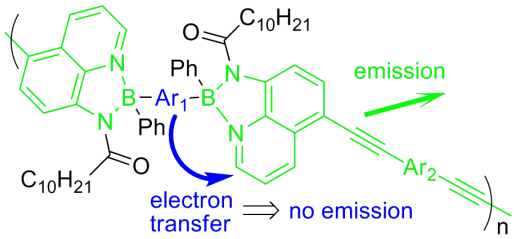

Chart 3

In Chapter 4, the author explains the preparation of optically active organoboron aminoquinolate-based coordination polymers bearing the chiral side chain derived from L-alanine. The circular dichroism (CD) study in the mixed solvents with $CHCl_3$ and DMF demonstrated that the secondary structures of the obtained polymers were stabilized by hydrogen-bonding interaction in the side chains (Chart 4).

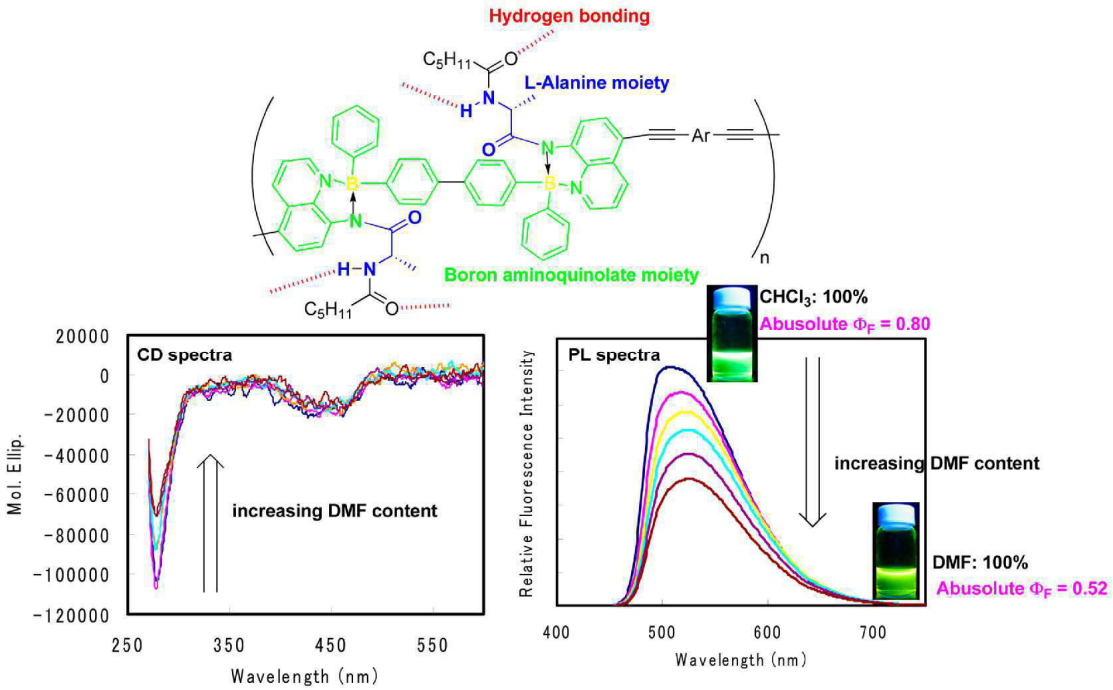

Chart 4

In Chapter 5, the author shows aminoquinolate moieties arranged perpendicularly on borafluorenes constructing main-chain of π-conjugated polymers. The distinct optical properties depending on the energy levels of the main chains were observed (Chart 5).

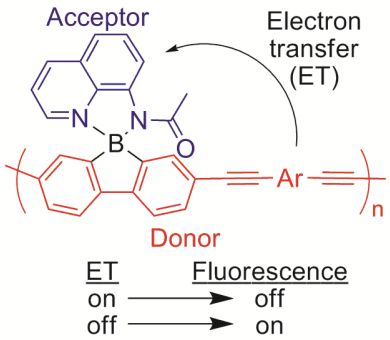

Chart 5

In Part II, the author describes synthesis and properties of pentacoordinate silicon compounds induced by benzo[*h*]quinoline. In Chapter 6, pentacoordinate silicon complexes with a benzo[*h*]quinolyl ligand and various substituents are shown (Chart 6). They formed strong dative bonds between the silicon atom and the ligand. As the bond length was shortened by electrowithdrawing substituents on the silicon centre, the magnitude of fluorescence was enhanced.

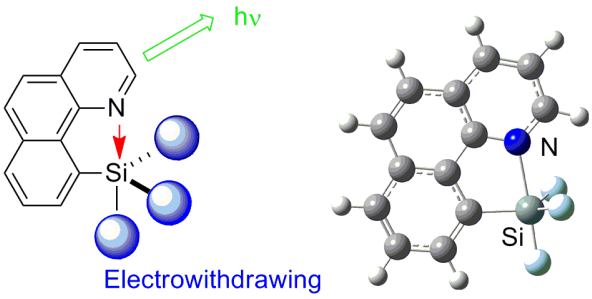

Chart 6

In Chapter 7, the author presents the synthesis of benzo[*h*]quinolyldibenzo[*b*,*f*]silepins. The benzo[*h*]quinolyl ligand provided the pentacoordinate character for silicon in dibenzo[*b*,*f*]silepins. The molecular structures were dominated by the substituents on the silicon centre. The planar-pentacoordinate structure rigidly fixed by fluoride contributed to inducing charge transfer from the dibenzosilepin moiety to the benzoquinolyl ligand after photoexcitation.

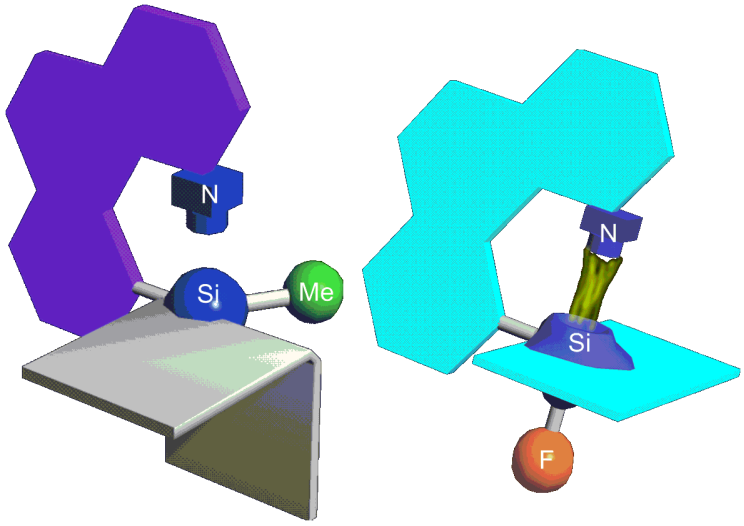

Chart 7

In Chapter 8, the author describes the effect on the electronic properties by the introduction of 4-methoxyphenyl or 4-trifluoromethylphenyl groups to benzo[*h*]quinolated dibenzo[*b*,*f*]silepins at *para*- or *meta*-positions toward the silicon centre (Chart 8). In the *para*-substituted compounds, methoxy group stabilized charge transfer state, leading to the bathochromic shift of fluorescence in the emission spectra. The *meta*-substituted compounds displayed absorption bands derived from π-conjugation through the vinylene group. Bathochromic shifts independent from solvent polarity were observed in both compounds with methoxy and fluorine.

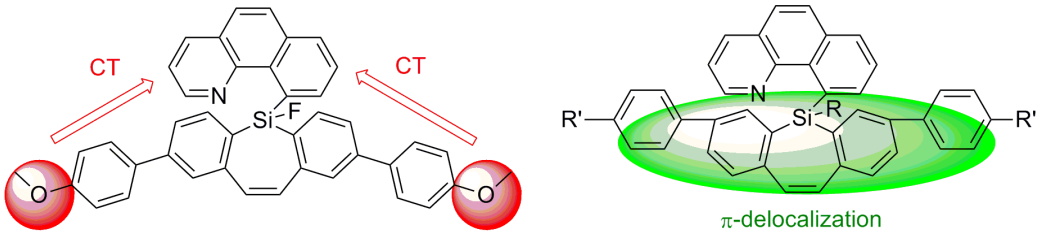

Chart 8

In chapter 9, the author presents the construction of conjugated polymers containing the benzo[*h*]quinolyldibenzo[*b*,*f*]silepin moiety. Conformation determined by substituents on the silicon centre influenced on the extent of the delocalization of π-electron through vinylene group of the dibenzosilepin moiety.

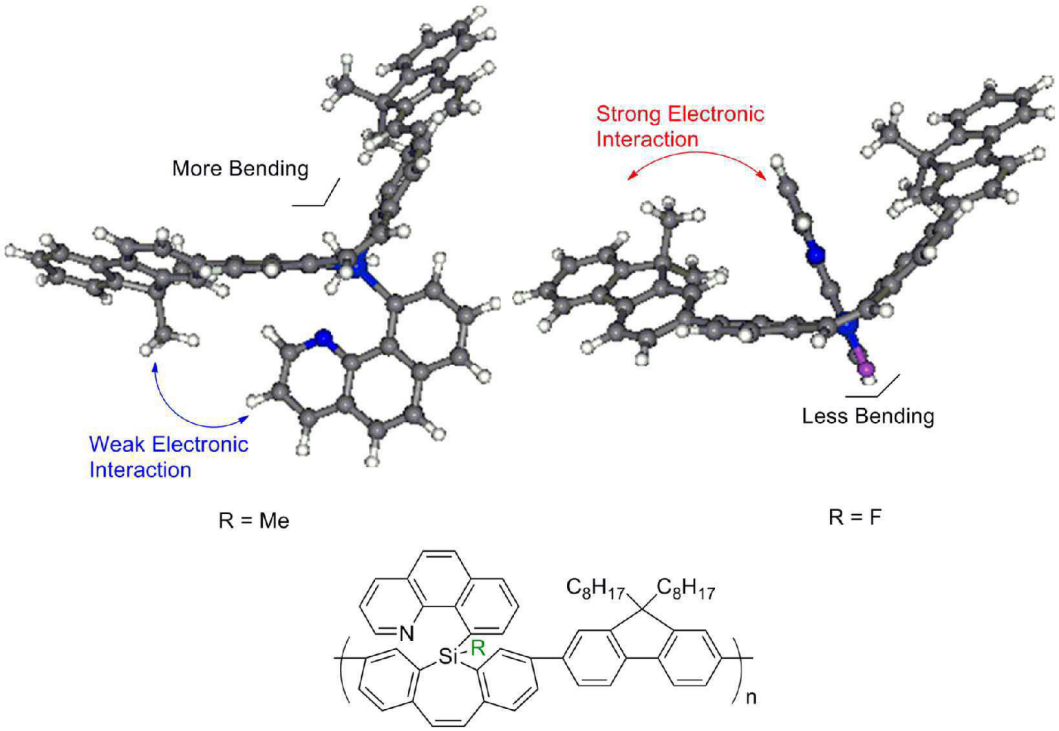

Chart 9

References

(1) Chen, J.; Kamph, J. W.; Ash, A. J., III *Organometallics* **2008,** *27,* 578.

(2) (a) Zhou, Z.; Wakamiya, A.; Kushida, T.; Yamaguchi, S. *J. Am. Chem. Soc.* **2012,** *134,* 4529. (b) Saito, S.; Matsuo, K.; Yamaguchi, S. *J. Am. Chem. Soc.* **2012,** *134,* 9130.

(3) Wakamiya, A.; Mishima, K.; Ekawa, K.; Yamaguchi, S. *Chem.Commun.* **2008,** 579.

(4) Caruso A., Jr.; Siegler, M. A.; Tovar, J. D. *Angew. Chem. Int. Ed.* **2010,** *49*, 4213.

(5) Matsumi, N.; Naka, K.; Chujo, Y. *J. Am. chem. Soc.* **1998,** *120,* 5112.

(6) Miyata, M.; Chujo, Y. *Polym. J.* **2002,** *34,* 967.

(7) Loudet, A.; Burgess, K. *Chem. Rev.* **2007,** *107,* 4891.

(8) (a) Nagai, A.; Kokado, K.; Nagata, Y.; Arita, M.; Chujo, Y. *J. Org. chem.* **2008,** *73,* 8605. (b) Nagai, A.; Kokado, K.; Nagata, Y.; Chujo, Y. *Macromolecules* **2008,** *41,* 8295.

(9) Wu, Q.; Esteghamatian, M.; Hu, N.-X.; Popovic, Z.; Enright, G.; Tao. Y.; D'Iorio, M.; Wang, S. *Chem. Mater.* **2000,** *12*, 79.

(10) (a) Karolin, J.; Johansson, L. B. -A.; Strandberg, L.; Ny, T. *J. Am. chem. Soc.* **1994,** *116,* 7801. (b) Tan, K.; Jaquinod, L.; Paolesse, R.; Nardis, S.; Di Natale, C.; Di Carlo, A.; Prodi, L.; Montalti, M.; Zaccheroni, N.; Smith, K. M. *Tetrahedron* **2004,** *60,* 1099. (c) Yee, M.-c.; Fas, S. C.; Stohlmeyer, M. M.; Wandless, T. J.; Cimprich, K. A. *J. Biol. Chem.* **2005,** *280,* 29053.

(11) Zhang, G.; Evans, R. E.; Campbell, K. A.; Fraser, C. L. *Macromolecules* **2009,** *42,* 8627.

(12) (a) Nagata, Y.; Chujo, Y. *Macromolecules* **2007,** *40*, 6. (b) Nagata, Y.; Chujo, Y. *Macromolecules* **2008,** *41*, 2809. (c) Nagata, Y.; Chujo, Y. *Macromolecules* **2008,** *41*, 3488.

(13) (a) Nagata, Y.; Chujo, Y. *Macromolecules* **2007,** *40*, 6. (b) Nagata, Y.; Chujo, Y. *Macromolecules* **2008,** *41*, 2809. (c) Nagata, Y.; Chujo, Y. *Macromolecules* **2008,** *41*, 3488.

(14) (a) Nagata, Y.; Otaka, H.; Chujo, Y. *Macromolecules* **2008**, *41*, 737. (b) Nagai, A.; Kobayashi, S.; Nagata, Y.; Kokado, K.; Taka, H.; Kita, H.; Suzuri, Y.; Chujo, Y. *J. Mater. Chem.* **2010.** *20,* 5196.

(15) Miller, R. D.; Michl J. *Chem. Rev.* **1989,** *89,* 1359.

(16) Trefonas, P.; West, R.; Miller, R. D.; Hofer, D. *J. Polym. Sci., Polym. Lett. Ed.* **1983**, *21*, 823.

(17) Yamaguchi, S.; Tamao, K. *Chem. Lett.* **2005,** *34,* 2.

(18) (a) Murata, H.; Malliaras, G. G.; Uchida, M.; Shen, Y.; Kafafi, Z. H. *Chem. Phys. Lett.* **2001,** 161. (b) Murata, H.; Kafafi, Z. H.; Uchida, M. *Appl. Phys. Lett.* **2002,** *80,* 189.

(19) Sanchez, J. C.; Trogler, W. C. *Macromol. Chem. Phys.* **2008,** *209,* 1527.

(20) (a) Chuit, C.; Corriu, R. J. P.; Reye, C.; Young, J. C. *Chem. Rev.* **1993,** *93,* 1371. (b) Holmes, R. R. *Chem. Rev.* **1996,** *96,* 927.

(21) Nakao, Y.; Hiyama, T. *Chem. Soc. Rev.* **2011,** *40,* 4893.

(22) Frye, C. L.; Vogel, G. E.; Hall, J. A. *J. Am. Chem. Soc.* **1961,** *83,* 996.

(23) Sakamoto, N.; Ikeda, C.; Yamanaka, M.; Nabeshima, T. *J. Am. Chem. Soc.* **2011,** *133,* 4726.

(24) (a) Klanberg, F.; Muetterties, E. L. *Inorg. Chem.* **1968,** *7,* 155. (b) Schomburg, D.; Krebs, R. *Inorg. Chem.* **1984,** *23,* 1378. (c) Bréfort, J. L.; Corriu, R. J. P.; Guérin, C.; Henner, B. J. L.; Wong Chi Man, W. W. C. *Organometallics* **1990,** *9,* 2080. (d) Kumars Swamy, K. C.; Chandrasekhar, V.; Harland, J. J.; Holmes, J. M.; Day, R. O.; Holmes, R. R. *J. Am. Chem. Soc.* **1990,** *112,* 2341.

(25) (a) Douglas, W. E.; Guy, D. M. H.; Kar, A. K.; Wang, C. *Chem. Commun.* **1998,** 2125. (b) Douglas, W. E.; Kuzhelev, A. S.; Yurasova, I. V.; Antipov, O. L.; Klapshina, L. G.; Semenov, V. V.; Domrachev, G. A.; Lopatina, T. I.; Guy, D. M. H. *Phys. Chem. Chem. Phys.* **2002,** *4,* 109. (c) Bushuk, S. B.; Carré, F. H.; Guy, D. M. H.; Douglas, W. E.; Kalvinkovskya, Y. A.; Klapshina, L. G.; Rubinov, A. N.; Stupak, A. P.; Bushuk, B. A. *Polyhedron* **2004,** *23,* 2615.

(26) Kano, N.; Komatsu, F.; Yamamura, M.; Kawashima, T. *J. Am. Chem. Soc.* **2006,** *128,* 7097.

Part I

Conjugated Polymers Containing Boron Quinolates in the Main-Chain

Chapter 1

Synthesis of Organoboron Quinoline-8-thiolate and -selenolate Complexes and Their Incorporation into π-Conjugated Polymer Main-Chain

Abstract

Low-molecular-mass organoboron quinoline-8-thiolate and –selenolate complexes as model compounds, and organoboron polymers incorporated their complex structures into the poly(*p*-phenylene-ethynylene) main chain were prepared. Tetracoordination states of boron atoms in the obtained compounds were confirmed by ^{11}B NMR spectroscopy, and the detailed structures of the model compounds were determined by single-crystal X-ray diffraction analysis. The polymers were synthesized by Sonogashira-Hagihara coupling reaction of organoboron quinolate-based monomers having diiodo groups with 1,4-diethynylbenzene derivatives bearing electron-donating or -withdrawing groups in moderate yields. Their optical properties were studied by UV-vis absorption and photoluminescence spectroscopies. Increasing atomic number of the 16 Group atom adjacent to the boron atom caused emission shift to longer wavelength and decreasing of absolute quantum yields for both the model compounds and the polymers. There are no differences between the polymers with the donating π-conjugated linker and with the accepting one in the photoluminescence property, resulting from efficient energy transfer from π-conjugated main chain to Q ligand. Further, the obtained polymers showed high refractive indices ($n_d > 1.66$).

Introduction

In recent years, there has been a considerable interest in conjugated polymers due to their potential use in a wide range of applications in electronics and photonics favored by their tunable electronic and optical properties.[1,2] Their prime examples are polymeric light emitting diodes,[2] plastic lasers,[3] nonlinear optical materials,[4] and polymer-based photovoltaic cells.[5] In addition, other advantages of organic conjugated polymers over their inorganic counterparts are the application of device fabrication via solution processing methods including dip coating, spin casting, and, ink-jet printing which receive more and more attention as a potential low cost alternative to vacuum deposition techniques.[6]

More recently, an incorporation of organoboron dyes as electroluminescent chromophores into π-conjugated polymer main chain, i.e., π-conjugated organoboron polymer, is attractive for future applications as electroluminescent devices, organic field-effect transistors, photovoltaics, and so on. Organoboron dyes are well-known in the fields of molecular probes,[7] photosensitizers,[8] and lasers[9] because their dyes possess large molar coefficients, two-photon absorption cross sections, high emission quantum yields and sensitivity to the surrounding medium. Conjugated polymers containing organoboron quinolate, which is one of the organoboron dyes, in their main chains have been synthesized in Chujo laboratory.[10] These polymers showed strong green fluorescence and an efficient energy migration from conjugated linkers to boron quinolate moieties was observed.

Quinolate-type ligands (Q), such as 8-hydroxyquinoline and quinoline-8-thiol, have been widely used to produce luminescent metal complexes, which in many cases emit from a Q-based intraligand charge transfer (ILCT) excited state.[11] This ILCT state is formed when the highest occupied molecular orbital (HOMO) and the lowest unoccupied molecular orbital (LUMO) are localized on the phenolate/thiolate ring and on the pyridyl ring of the Q ligand, respectively. A

few general rules which govern the fluorescence of metal chelates of 8-hydroxyquinoline have been formulated.[12] (i) Fluorescence is reduced with increasing atomic number of the metal ion, caused by an increase in the rate of intersystem crossing known as heavy atom effect. For example, tris(8-hydroxyquinolinato)indium is less fluorescent compared to tris(8-hydroxyquinolinato)gallium which, in turn, is less fluorescent than tris(8-hydroxyquinolinato)aluminum (AlQ_3). (ii) The emission shifts to longer wavelength as the covalent nature of the metal-ligand bonding is increased. For example, the chelates formed with Al, Ga, and In emit at progressively longer wavelengths of 532, 545, 558 nm, respectively. Likewise, metal chelates of 8-hydroxyquinoline and quinoline-8-thiol absorb and emit at increasingly longer wavelengths.[13] In contrast, the application of these rules to organoboron quinolate has not yet been investigated. Herein, the author reports the synthesis and optical properties of the low-molecular-mass organoboron quinoline-8-thiolate and -selenolate complexes and incorporation of the organoboron quinoline-8-thiolate or -selenolate into conjugated polymer main chain.

Results and Discussion

Synthesis of Model Compounds. The reactions between 8-hydroxyquinoline, 8-mercaptoquinoline hydrochloride, or quinoline-8-selenolate, and triphenylborane afforded the corresponding organoboron quinolates **1O**,[22] **1S** and **1Se**, respectively. When these compounds were purified by recrystallization in the mixed solvent (CH_2Cl_2/hexane = 1/2 (v/v)), **1O**, **1S**, and **1Se** were obtained as yellow-green, yellow, and orange color solid, respectively. All three compounds were stable under air and showed high solubility in dichloromethane and chloroform. The tetracoordination states of the boron atoms in **1S** and **1Se** were confirmed by the ^{11}B NMR

spectroscopy in $CDCl_3$ [**1S**: δ_B = 3.57 ppm, **1Se**: δ_B = 3.66 ppm], and the basic structures of **1S** and **1Se** were also characterized by ^1H NMR, ^{13}C NMR and EI mass spectroscopies.

Further, the molecular structures of **1S** and **1Se** as determined by single crystal X-ray analyses are shown in Figure 1. The sp^3 orbital-hybridized boron centers of **1S** and **1Se** appear as a distorted tetrahedron with dihedral angles N(1)-B(1)-S(1) of 99.1° and N(1)-B(1)-Se(1) of 98.9 °, respectively (Table 1). The average of B(1)-N(1) bond length of **1Se** (1.608 Å) was slightly longer than that of **1S** (1.594 Å), probably indicating that the chelating ability of **1Se** is lower than that of **1S** because selenium atom brings about the larger distortion of five-membered chelating ring.

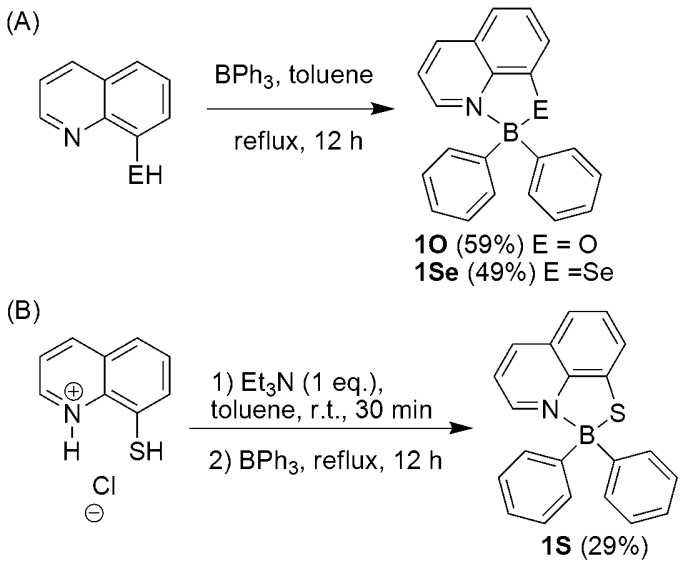

Scheme 1. Synthesis of model compounds (A) **1O** and **1Se**, and (B) **1S**.

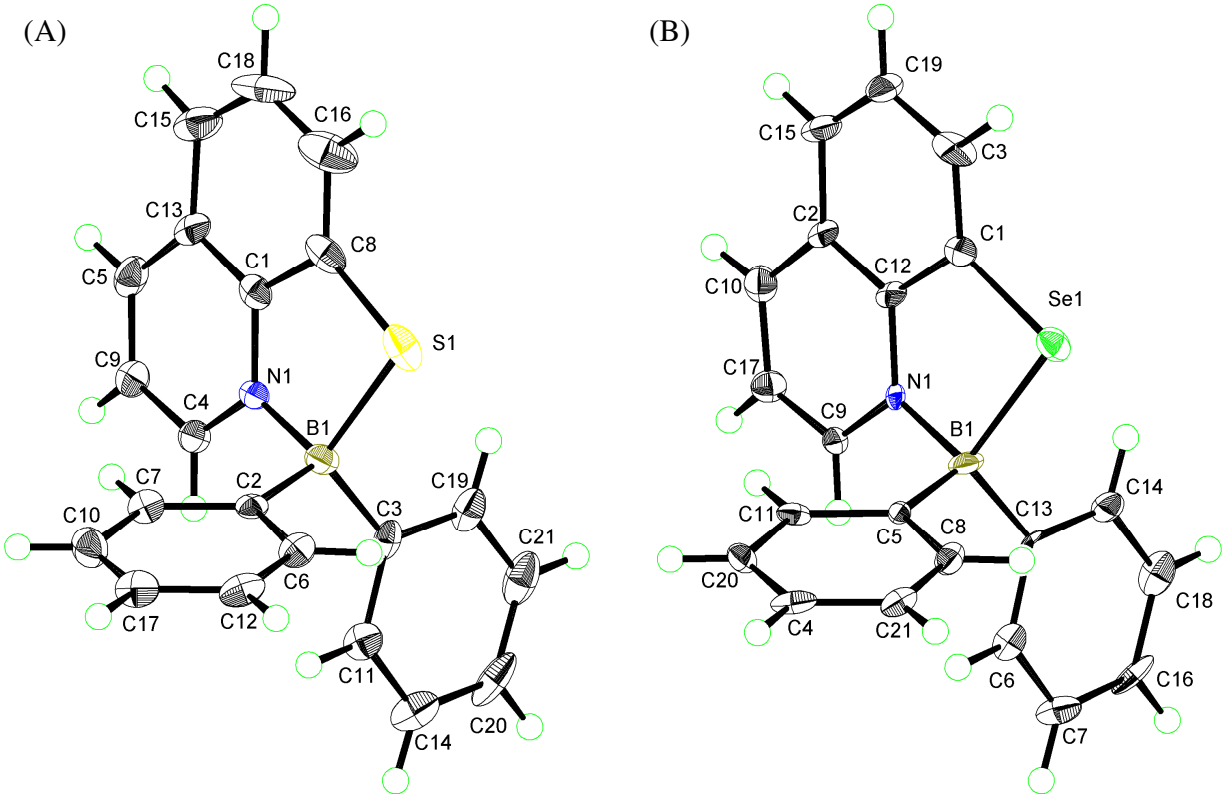

Figure 1. The X-ray crystal structures of (A) **1S** and (B) **1Se** with thermal ellipsoids drawn to the 50% probability level.

Synthesis of Monomers. Organoboron quinolate-based monomers **2O**[10], **2S**, and **2Se** were prepared from the corresponding quinoline derivatives according to Scheme 2. The obtained compounds of **2O**, **2S**, and **2Se** showed yellow-green, yellow, and orange color, respectively, analogous to the model compounds. All three compounds were stable under air and soluble in dichloromethane and chloroform, whereas insoluble in hexane. The tetracoordination state of the boron atoms in **2S** and **2Se** were confirmed by the ^{11}B NMR spectroscopy in $CDCl_3$ [**2S**: δ_B = 7.43 ppm, **2Se**: δ_B = 7.53 ppm]. Because of electronegative property of iodine atom, these signals are downfield-shifted compared to those of the model compounds. Further, the structures of **2S** and **2Se** were also characterized by ^{1}H NMR, ^{13}C NMR and electron-spray-ionization mass spectroscopies, and by elemental analysis.

Table 1. Selected bond lengths (Å) and angles (deg) for **1S** and **1Se**

		1S	
B(1)-N(1)	1.594(5)	N(1)-B(1) -S(1)	99.1(2)
B(1)-S(1)	1.980(4)	B(1)-S(1)-C(8)	93.09(18)
S(1)-C(8)	1.754(4)	S(1)-C(8)-C(1)	113.3(3)
C(8)-C(1)	1.418(5)	C(8)-C(1)-N(1)	115.7(3)
N(1)-C(1)	1.366(4)	C(1)-N(1)-B(1)	117.1(3)
B(1)-C(2)	1.608(6)		
B(1)-C(3)	1.602(6)		
		1Se	
B(1)-N(1)	1.608(8)	N(1)-B(1) -Se(1)	98.9(4)
B(1)-Se(1)	2.119(6)	B(1)-Se(1)-C(1)	88.8(2)
Se(1)-C(1)	1.887(6)	Se(1)-C(1)-C(12)	113.5(5)
C(1)-C(12)	1.429(6)	C(1)-C(12)-N(1)	117.1(6)
N(1)-C(12)	1.358(7)	C(12)-N(1)-B(1)	119.4(4)
B(1)-C(5)	1.599(7)		
B(1)-C(13)	1.604(8)		

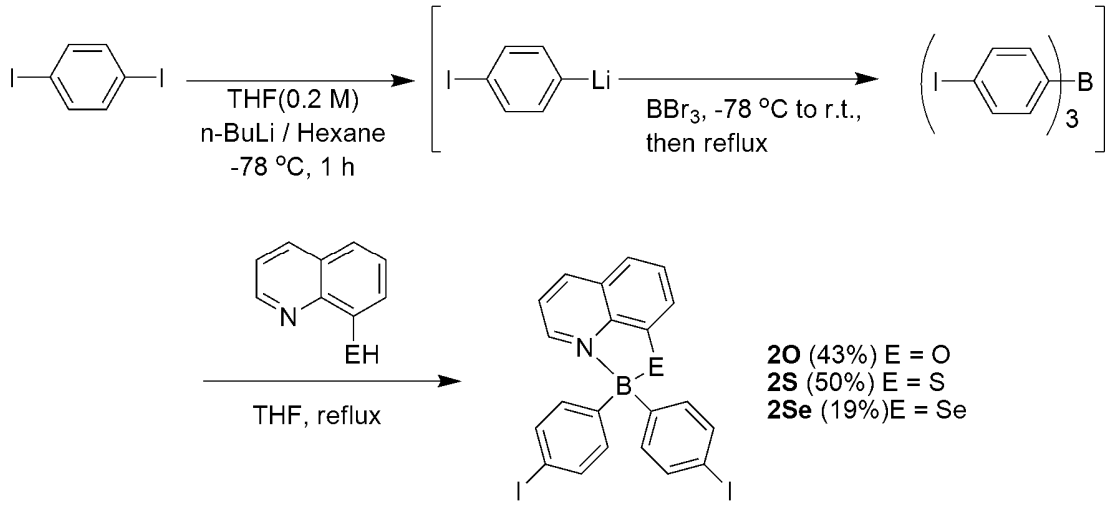

Scheme 2. Synthesis of monomers **2O**, **2S**, and **2Se**.

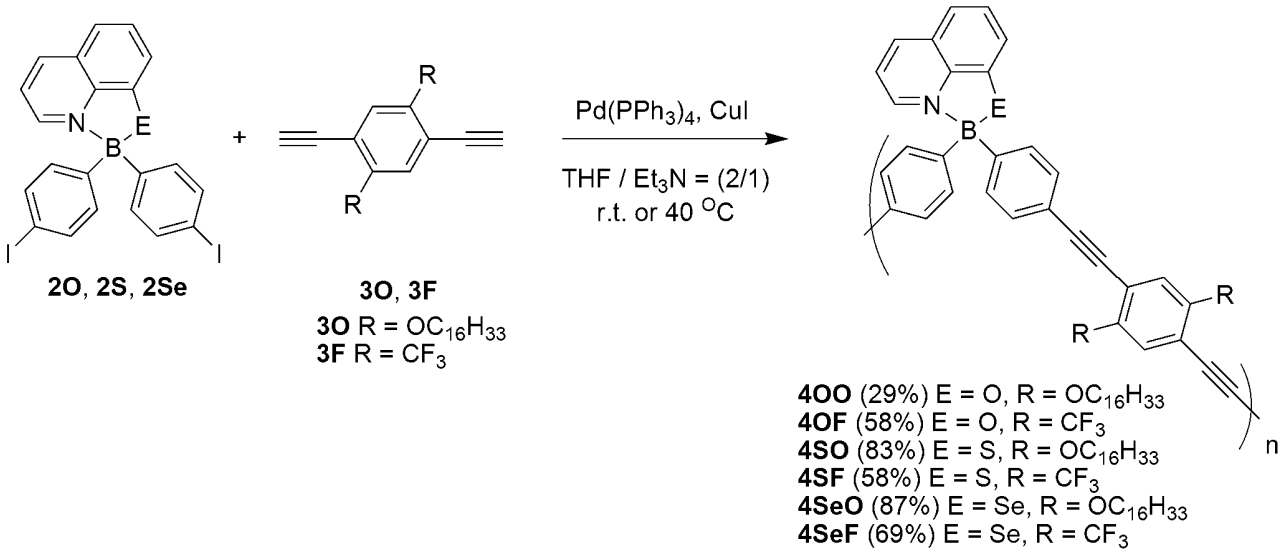

Scheme 3. Synthesis of polymers.

Synthesis of Polymers. Scheme 3 and Table 2 summarize the condition and results of the polymerization of **2O**, **2S**, or **2Se** with 1,4-diethynylbenzene derivatives **3O** or **3F** in the presence of a catalytic amount of $Pd(PPh_3)_4$ and CuI in the mixed solvent of tetrahydrofuran (THF) and triethylamine. The polymers **4OO**, **4OF**, **4SO**, **4SF**, **4SeO**, and **4SeF** were obtained as yellow or orange solids after precipitation into methanol and hexane, respectively, and the polymer yields were 29–87%. The polymers were soluble in THF, CH_2Cl_2, and $CHCl_3$. The ^{11}B NMR spectra of the obtained polymers were observed at δ_B = 8.89–3.91 ppm assignable to the tetracoordination state of the boron atoms in each polymer, indicating that the polymerization proceeded without any damage of the structure in the organoboron quinolate moiety. The IR spectra of the polymers showed the absorption peaks at 2214–2204 cm^{-1}, which are attributable to stretching of the –C≡C– bond in the polymer backbone. Moreover, strong peaks due to the C–F stretching band were observed at around 1157 cm^{-1} in the spectra of **4OF**, **4SF**, and **4SeF**. The number-average molecular weights (M_n) and the molecular weight distribution (M_w/M_n) of the polymers, measured by size-exclusion chromatography (SEC) in THF toward polystyrene standards, were 2200–11200 and 1.4–3.0, respectively (Table 2). Thermal stabilities of the polymers were examined by thermogravimetric analysis. The start of the thermal degradation under air for the polymers lies between 276 and 332 °C, where 5% weight loss was recorded. These data suggest that the obtained polymers present similar thermal stability to general poly(*p*-phenylene-ethynylene)s.[23]

Table 2. Polymerization of organoboron quinolate-based monomers and 1,4-diethynylbenzene derivatives[a]

polymers	Yield[b] (%)	M_n[c]	M_w[c]	M_w/M_n[c]	DPn[d]	T_5/°C[e]	T_{10}/°C[e]
4OO	29	3,200	6,100	1.9	3.5	286	305
4OF	58	3,400	4,900	1.4	6.0	332	363
4SO	83	11,200	24,500	2.2	12.0	293	317
4SF	58	3,100	5,500	1.8	5.3	276	312
4SeO	87	7,800	10,900	1.4	8.0	293	318
4SeF	69	2,200	6,600	3.0	3.5	292	322

[a] Conditions: Sonogashira-Hagihara couplings of organoboron quinolate-based monomer (1 equiv.) and 1,4-diethynylbenzene derivatives (1 equiv.) were carried out in the presence of $Pd(PPh_3)_4$, CuI in the mixed solvent (THF/NEt_3 = 2/1) at room temperature or 40 °C for 96 or 48 h. [b] Isolated yields after precipitation. [c] Estimated by size-exclusion chromatography (SEC) based on polystyrene standard in tetrahydrofuran (THF). [d] Average number of repeating units calculated from M_n and molecular weights of repeating units.[e] Thermogravimetric analysis: heating rate 10 K/min under air; values given for weight loss of 5% and 10%.

Optical Properties. The optical properties of the obtained polymers were investigated by UV–vis absorption and photoluminescence in $CHCl_3$ solution as compared to those of model compounds. The results from the absorption and emission spectra are summarized in Table 3. All emission data given here were obtained after exciting at the longest wavelength of the absorption peaks, i.e., absorption maxima of the polymers and the model compounds are corresponding to phenylene-ethynylene and quinoline, respectively. The model compounds **1O**, **1S** and **1Se** showed the weak absorption peaks at 395 nm, 454 nm, and 480 nm, respectively, arising from the quinolinol ligand and the strong absorption peaks at around 270 nm, derived from the π-π* transition (Figure 2). The absorption peaks of the quinolinol ligand shift to longer wavelength as

the covalent nature of the boron-ligand bonding is increased, that is, the maximum of **1Se** is red-shifted as compared to that of **1S** which, in turn, is red-shifted in comparison with that of **1O**. Despite the absorption peaks of the model compounds, this observation seems to confirm the expected trend from the rule, as mentioned above, which govern the absorption and fluorescence of metal chelates of Q. In contrast to the model compounds, the polymers **4OO**, **4OF**, **4SO**, **4SF**, **4SeO**, and **4SeF** showed the strong absorption peaks in the region from 300 to 400 nm. These peaks should be due to the π-conjugated linkers connecting the Q units each other. It is observed that the polymers which have the same π-conjugated linkers give the same absorption peaks in the region from 300 to 400 nm. This would mean that the electronic structure of the π-conjugated linker is independent from that of the Q ligand.

In the photoluminescence spectra in $CHCl_3$, model compounds **1O**, **1S**, and **1Se** showed emission maxima at 501 nm, 563 nm, and 609 nm, respectively (Figure 3). The emission shifts to longer wavelength as the covalent nature of the boron-ligand bonding is increased. The absolute fluorescence quantum yields of **1O**, **1S**, and **1Se** in $CHCl_3$ at room temperature were determined as Φ_F = 0.47, 0.09, and 0.01, respectively. Fluorescence is reduced with increasing atomic number of the 16 Group atom that is adjacent to the boron atom in each model compound, caused by an increase in the rate of intersystem crossing known as heavy atom effect. From these results, it can be said that the model compounds emit from the Q-based ILCT excited state and follow the rules similar to those govern the fluorescence of metal chelates of Q. The photoluminescence spectra of polymers **4OO**, **4SO**, and **4SeO** are also represented in Figure 3. Noteworthily, the shapes of the emission spectra of the polymers **4OO** and **4SeO** are quite analogous to the corresponding model compounds. Therefore the photoluminescence spectra of these polymers are characteristic of the Q ligands. In other words, the presence of organoboron quinolate in the polymer backbone is crucial in these photoluminescence properties. It can be deduced that the

energy transfer from the π-conjugated linkers in the main-chain to the Q ligands on the boron centers would occur not only in **4OO**, but also in **4SO**. On the other hand, **4SeO** showed the strong peak at 427 nm, emitting the light from π-conjugated linker and the weak peak at 598 nm, emitting from Q ligand in the photoluminescence spectrum. There are no differences between the polymers with the donating π-conjugated linker and with the accepting one in the photoluminescence property, as shown in Table 3. This means that the π-conjugated linker is irresponsible to both the emission spectrum and absolute quantum yield. In comparison with quantum yields, it can be seen that absolute quantum yields of the polymers are nearly equal to the corresponding model compounds, thereby implying the efficient energy transfer from the π-conjugated linkers to the Q ligands. Further, the polymers **4SO** and **4SeO** have high refractive indices, n_d = 1.67 and 1.68, respectively. These values were high enough in comparison with those of S-containing polymers such as polythiourethane known as high refractive materials, indicating the potential applicability to optical devices.[24]

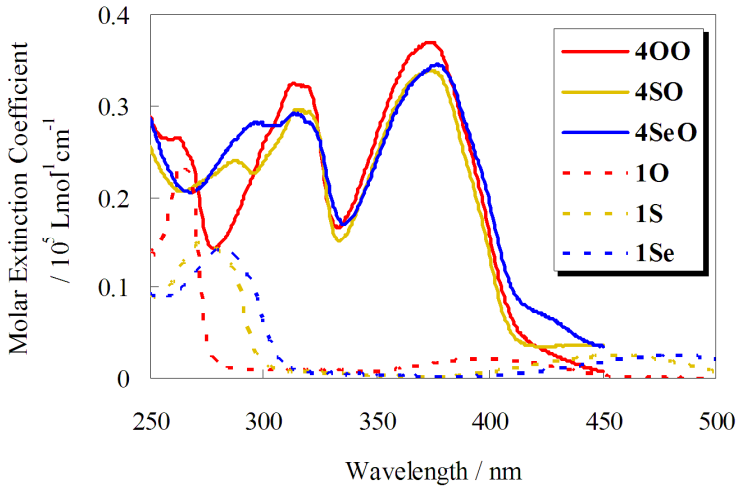

Figure 2. UV-vis spectra of polymers and model compounds in $CHCl_3$ (1.0×10^{-5} M).

Table 3. UV-visible absorption and photoluminescence data

compounds	$\lambda_{abs,max}$ (nm)[a]	$\varepsilon(m^2mol^{-1})$[a]	$\lambda_{em,max}$ (nm)[b]	Φ_F[b, c]
4OO	313, 374	3250, 3700	421, 502	0.54
4OF	264, 356, 372	2910, 5600, 5580	414, 501	0.58
4SO	287, 316, 374	2390, 2950, 3390	433, 564	0.10
4SF	279, 359, 375	1920, 3760, 3810	420, 561	0.14
4SeO	297, 314, 377	2820, 2920, 3450	427, 598	0.01
4SeF	287, 360, 377	1820, 3630, 3680	415, 601	0.00
1O	264, 395	2370, 220	501	0.47
1S	273, 454	1500, 260	563	0.09
1Se	283, 480	1440, 260	609[d]	0.01

[a] UV-vis: $CHCl_3$ (1.0×10^{-5} M). [b] Fluorescence: $CHCl_3$ (1.0×10^{-5} M). [c] Absolute quantum yield. [d] 1.0×10^{-3} M.

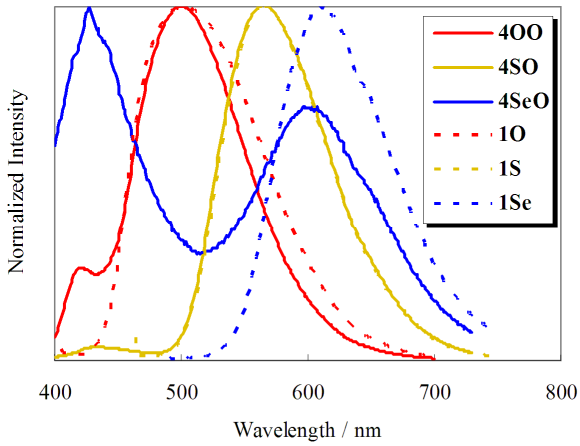

Figure 3. Normalized emission spectra of polymers and model compounds in $CHCl_3$ (1.0×10^{-5} M).

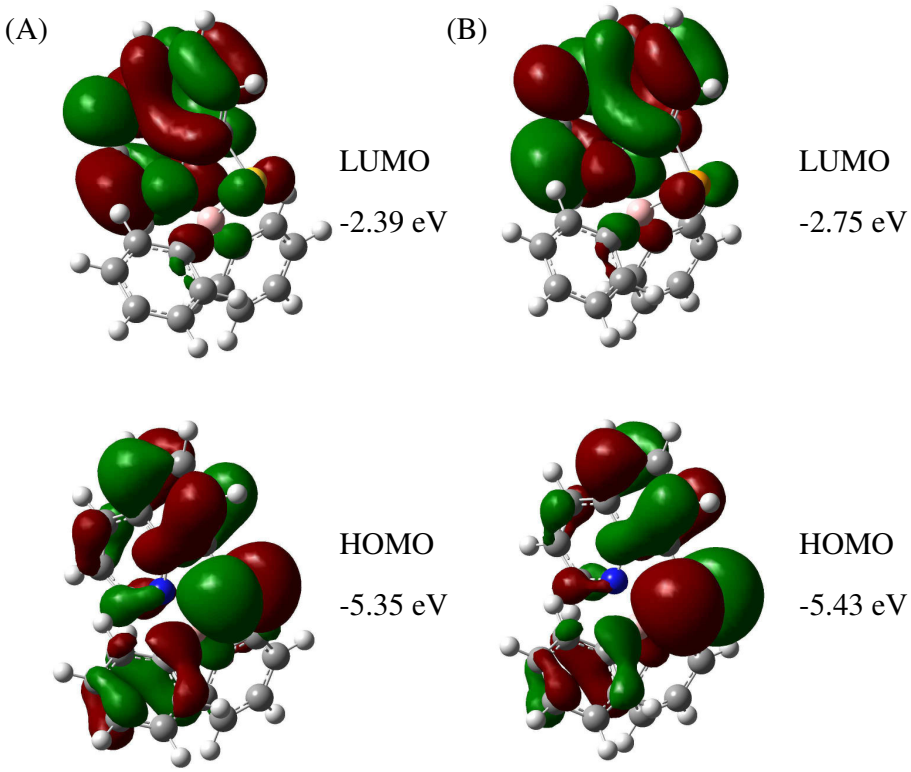

Figure 4. Molecular orbital diagrams for the HOMO and LUMO of (A) **1S** (B3LYP/6-31G(d)// B3LYP/6-31G(d)) and (B) **1Se** (B3LYP/6-311$_+$G(2df, 2p)// B3LYP/6-311$_+$G(2df, 2p)).

Molecular Orbital Calculations. To further understand the nature of optical properties, the author has carried out theoretical calculation for compounds **1S**, **1Se**, **5OO**, **5SO**, and **5SeO** using density-functional theory (DFT) method at the B3LYP/6-31G(d) or B3LYP/6-311$_+$G(2df, 2p).[25] Figure 4A and B exhibit LUMO and HOMO of **1S** and **1Se**, respectively. The LUMOs of these compounds are located predominantly on Q ligands and the HOMOs are on Q ligands and phenyl group. As a result, the HOMO-LUMO transition is not restricted but the molar extinction coefficient is low. In addition, the HOMO and LUMO of these compounds are partly located on S or Se atoms, which leads to a smaller HOMO-LUMO gap for **1Se** (2.68 eV) relative to **1S** (2.96 eV). In contrast, the HOMOs of compounds **5OO**, **5SO**, and **5SeO**, which have π-conjugated

linkers, are not on the Q ligands, but localized on the whole of π-conjugated linkers and the LUMOs are localized on the Q ligands, as shown in Figure 5. These spatial separations of HOMOs and LUMOs probably decrease the electronic transition dipoles and the oscillator strengths of polymers' HOMO-LUMO transitions. In fact, TD-DFT calculations of **1S** and **5SO** support this explanation. The calculated oscillator strengths of HOMO-LUMO transitions were 0.0593 for **1S** and 0.0067 for **5SO**, respectively. From these results, it can be said that the HOMO-LUMO transitions are not allowed but the π-π* transitions of π-conjugated linkers contribute to the absorption peak of lowest energy in the UV-vis absorption spectrum. Moreover, the HOMOs of **5OO**, **5SO**, and **5SeO** are not located on the 16 Group atoms that are adjacent to the boron atom in each polymer, indicating that the π-π* transitions of π-conjugated linkers irresponsible to these atoms.

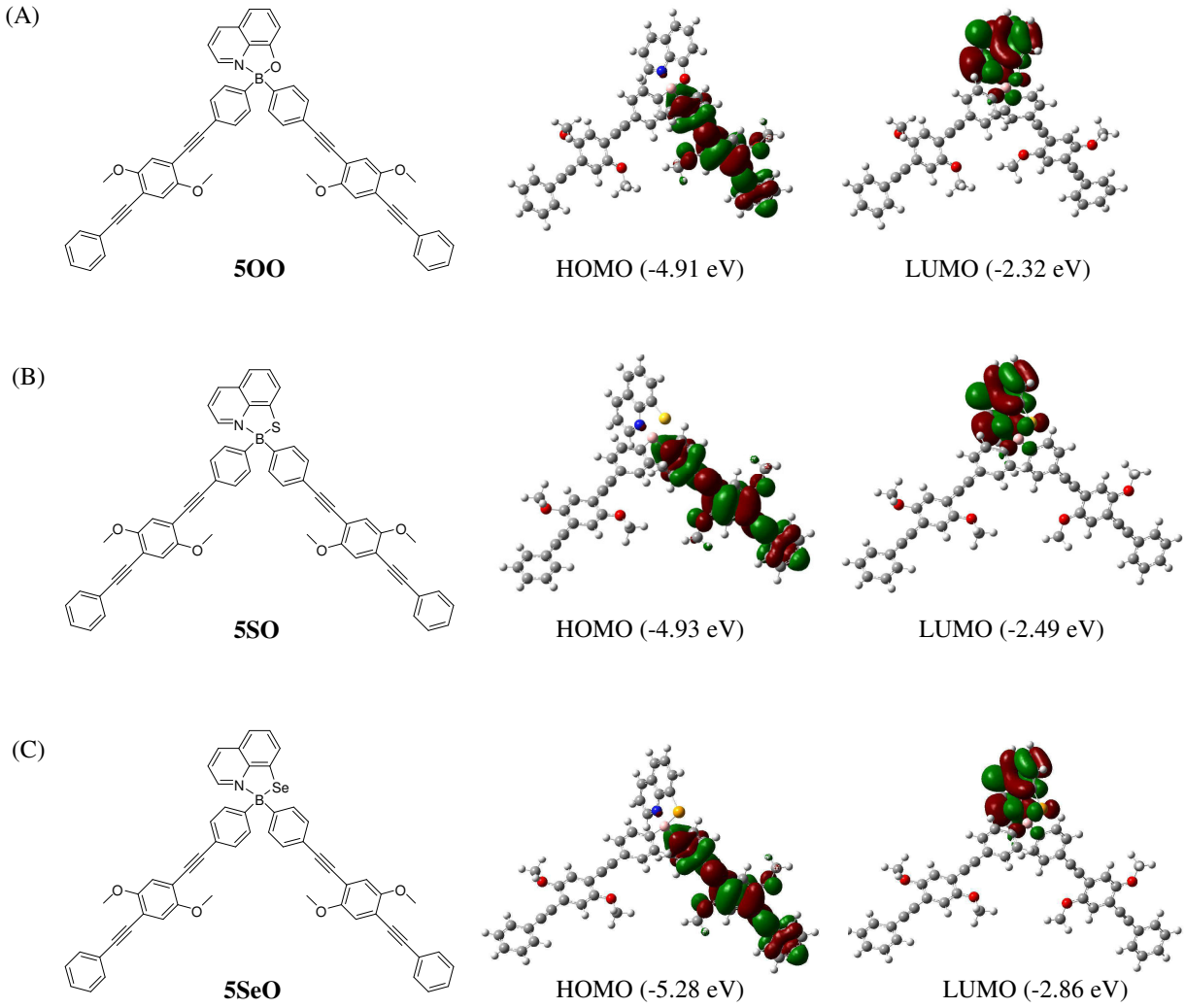

Figure 5. Structures and molecular orbital diagrams for the HOMO and LUMO of (A) **5OO** (B3LYP/6-31G(d)//B3LYP/6-31G(d)), (B) **5SO** (B3LYP/6-31G(d)//B3LYP/6-31G(d)), and (C) **5SeO** (B3LYP/6-311$_+$G(2df, 2p)//B3LYP/6-31G(d)).

Conclusion

The novel low-molecular-mass organoboron quinoline-8-thiolate and -selenolate complexes (model compounds) and the main-chain-type organoboron quinoline-8-thiolate and -selenolate polymers were prepared. These polymers were obtained by Sonogashira-Hagihara coupling in moderate yields. The emission shifted to longer wavelength as the covalent nature of the boron-ligand bonding is increased and the absolute quantum yield was reduced with increasing atomic number of the 16 Group atom adjacent to the boron atom. Emission behavior of the polymers originated efficient energy transfer from π-conjugated main chain to Q ligand and showed no difference in emission between the donating π-conjugated linker and accepting one. In addition, the polymers had high refractive indices, so that further study of these polymers may lead to a new class of materials with both luminescence and high refractive index.

Experimental Section

Measurements. ^{1}H (400 MHz), ^{13}C (100 MHz), and ^{11}B (128 MHz) NMR spectra were recorded on a JEOL JNM-EX400 spectrometer. ^{1}H and ^{13}C NMR spectra used tetramethylsilane (TMS) as an internal standard, ^{11}B NMR were referenced externally to BF_3OEt_2 (sealed capillary) in $CDCl_3$. The number-average molecular weight (M_n) and the molecular weight distribution [weight-average molecular weight/number-average molecular weight (M_w/M_n)] values of all polymers were estimated by size-exclusion chromatography (SEC) with a TOSOH G3000HXI system equipped with three consecutive polystyrene gel columns [TOSOH gels: α-4000, α-3000, and α-2500] and ultraviolet detector at 40 °C. The system was operated at a flow rate of 1.0 mL/min, with tetrahydrofuran as an eluent. Polystyrene standards were employed for calibration. UV–vis spectra were recorded on a Shimadzu UV-3600 spectrophotometer. Fluorescence emission spectra were recorded on a HORIBA JOBIN YVON Fluoromax-4 spectrofluorometer, and the absolute quantum yield was calculated by integrating sphere method on the HORIBA JOBIN YVON Fluoromax-4 spectrofluorometer in chloroform. FT-IR spectra were obtained using a Perkin-Elmer 1600 infrared spectrometer. Thermogravimetric analyses (TGA) were performed on a Seiko TG/DTA 6200 at a scan rate of 10 °C/min. X-ray crystallographic analysis was carried out by a Rigaku R-AXIS RAPID-F graphite-monochromated Mo Kα radiation diffractometer with an imaging plate. A symmetry related absorption correction was carried out by using the program ABSCOR[14]. The analysis was carried out with direct methods (SHELX-97[15] or SIR97[16]) using Yadokari-XG[17]. The program ORTEP3[18] was used to generate the X-ray structural diagram. Elemental analysis was performed at the Microanalytical Center of Kyoto University. Refractive indices were measured by an ATAGO Abbe refractometer DR-M4. All reaction was performed under nitrogen or argon atmosphere.

Materials. Tetrahydrofuran (THF) and triethylamine (Et_3N) were purified using a two-column solid-state purification system (Glasscontour System, Joerg Meyer, Irvine, CA). B(4-iodophenyl)$_2$Q (**2O**),[10] quinoline-8-selenol,[19] 1,4-diethynyl-2,5-dihexadecyloxybenzene,[20] and 1,4-diethynyl-2,5-bis(trifluoromethyl)benzene[21] were prepared according to the literature.

Synthesis of BPh2Q (1O). Triphenylborane (0.484 g, 2.00 mmol) dissolved in toluene (8 mL) was added to a solution of 8-hydroxyquinoline (0.292 g, 2.01 mmol) stirring in toluene (16 mL). After the reaction mixture was refluxed for 11.5 h, the solvent was removed under vacuum. The crude product was put in a small vial and then dissolved in CH_2Cl_2, on which hexane was slowly laid. The phase separated solution was allowed to stand for 25 h for slow evaporation and diffusion, which gave a yellow solid of **1O** (0.369 g, 1.19 mmol) in 59% yield. ^{1}H NMR ($CDCl_3$, δ, ppm): 8.58 (d, J = 5.16 Hz, 1H), 8.40 (d, J = 8.28 Hz, 1H), 7.68-7.60 (m, 2H), 7.45 (d, J = 6.56 Hz, 2H), 7.29-7.21 (m, 7H), 7.18 (d, J = 7.80 Hz, 1H).

Synthesis of BPh2Q-S (1S). Triphenylborane (1.070 g, 4.40 mmol) dissolved in toluene (16 mL) was added to a solution of 8-mercaptoquinoline hydrochloride (0.791 g, 4.00 mmol) and Et_3N (0.56 mL, 4.00 mmol) stirring in toluene (16 mL). After the reaction mixture was refluxed for 12 h, the solvent was removed under vacuum. The remaining solid was dissolved in $CHCl_3$, followed by washing with water, drying over $MgSO_4$, and removal of the solvent under vacuum. The crude product was put in a small vial and then dissolved in CH_2Cl_2, on which hexane was slowly laid. The phase separated solution was allowed to stand for 25 h for slow evaporation and diffusion, which gave a yellow solid of **1S** (0.380 g, 1.17 mmol) in 29% yield. ^{1}H NMR ($CDCl_3$, δ, ppm): 8.50 (d, J = 5.36 Hz, 1H), 8.46 (d, J = 7.32 Hz, 1H), 7.73 (d, J = 7.32 Hz, 1H), 7.62-7.56 (m, 2H), 7.49 (d, J = 8.08 Hz, 1H), 7.33 (d, J = 6.84 Hz, 4H), 7.28-7.18 (m, 6H). ^{13}C NMR ($CDCl_3$, δ, ppm): 144.58, 144.16, 143.34, 141.04, 133.20, 130.95, 129.35, 127.55, 127.00,

126.47, 121.59, 118.70. ^{11}B NMR ($CDCl_3$, δ, ppm): 3.57. HRMS (EI) Calcd for $C_{21}H_{16}NSB$: m/z 325.1097. Found: m/z 325.1100.

Synthesis of BPh2Q-Se (1Se). Triphenylborane (0.434 g, 1.79 mmol) dissolved in toluene (7.2 mL) was added to a solution of quinoline-8-selenol (0.373 g, 1.79 mmol) stirring in toluene (16 mL). After the reaction mixture was refluxed for 12 h, the solvent was slowly evaporated for recrystallization, giving a yellow solid of **1Se** (0.327 g, 0.878 mmol) in 49% yield. ^{1}H NMR ($CDCl_3$, δ, ppm): 8.49 (m, 2H), 7.97 (d, J = 7.32 Hz, 1H), 7.64-7.52 (m, 3H), 7.33 (d, J = 6.80 Hz, 4H), 7.26-7.17 (m, 6H). ^{13}CNMR ($CDCl_3$, δ, ppm): 145.88, 144.63, 141.70, 138.74, 133.54, 131.56, 130.85, 129.94, 127.54, 126.38, 121.40, 120.61. ^{11}B NMR ($CDCl_3$, δ, ppm): 3.66. HRMS (EI) Calcd for $C_{21}H_{16}NBSe$: m/z 373.0541. Found: m/z 373.0537.

Synthesis of B(4-iodophenyl)$_2$Q-S (2S). 12.5 mL (1.6 M, 20 mmol) of *n*-BuLi was slowly added to a solution of 1,4-diiodobenzene (6.60 g, 20 mmol) in 100 mL of THF at -78 °C, and the mixture was stirred at -78 °C for 1 h. BBr_3 (0.67 mL, 6.7 mmol) was added to the reaction mixture at -78 °C and then allowed to room temperature and refluxed for 3.5 h. The mixture of 8-mercaptoquinoline hydrochloride (1.38 g, 7.0 mmol) and Et_3N (0.98 mL, 7.0 mmol) dissolved in 60 mL of THF in another flask was added to the reaction mixture and then refluxed for 9 h. The solvents were removed under vacuum. The residue was dissolved in a small amount of $CHCl_3$ and reprecipitating with 100 mL of methanol, giving a yellow solid. This solid was purified by dissolving in a small amount of CH_2Cl_2 and reprecipitating with 80 mL of hexane to obtain **2S** (1.92 g, 3.3 mmol) in 50% yield as a yellow solid. ^{1}H NMR ($CDCl_3$, δ, ppm): 8.51 (d, J = 8.32 Hz, 1H), 8.43 (d, J = 4.12 Hz, 1H), 7.74 (d, J = 7.32 Hz, 1H), 7.66-7.53 (m, 7H), 7.03 (d, J = 8.04 Hz, 4H). ^{13}CNMR ($CDCl_3$, δ, ppm): 143.91, 141.53, 136.67, 135.16, 131.20, 129.40, 127.30, 121.73, 119.10, 93.12. ^{11}B NMR ($CDCl_3$, δ, ppm): 7.43. HRMS (EI) Calcd for

$C_{21}H_{14}NSBI_2$: m/z 576.9029. Found: m/z 576.9029. Anal. Calcd for $C_{21}H_{14}NSBI_2$: C, 43.71; H, 2.45; I, 43.99. Found: C, 43.69; H, 2.63; I, 43.79.

Synthesis of B(4-iodophenyl)$_2$Q-Se (2Se). 7.1 mL (1.6 M, 11 mmol) of *n*-BuLi was slowly added to the solution of 1,4-diiodobenzene (3.73 g, 11 mmol) in 57 mL of THF at -78 °C, and the mixture was stirred at –78 °C for 1 h. BBr_3 (0.36 mL, 3.8 mmol) was added to the reaction mixture at –78 °C and then allowed to room temperature and refluxed for 1 h. Quinoline-8-selenol (0.78 g, 3.8 mmol) dissolved in 50 mL of THF in another flask was added to the reaction mixture and then refluxed for 12 h. The solvents were removed under vacuum. The residue was dissolved in a small amount of $CHCl_3$ and reprecipitating with 50 mL of methanol, giving an orange solid. This solid was purified by dissolving in a small amount of CH_2Cl_2 and reprecipitating with 30 mL of hexane to obtain **2Se** (0.45 g, 0.72 mmol) in 19% yield as an orange solid. ^{1}H NMR ($CDCl_3$, δ, ppm): 8.54 (d, J = 8.28 Hz, 1H), 8.41 (d, J = 5.40 Hz, 1H), 7.98 (d, J = 7.32 Hz, 1H), 7.68-7.55 (m, 7H), 7.03 (d, J = 8.28 Hz, 4H). ^{13}C NMR ($CDCl_3$, δ, ppm): 145.59, 144.51, 142.16, 137.99, 136.65, 135.46, 131.79, 131.09, 129.99, 121.54, 120.96, 100.55, 92.95. ^{11}B NMR ($CDCl_3$, δ, ppm): 7.53. HRMS (EI) Calcd for $C_{21}H_{14}NBSeI_2$: m/z 624.8474. Found: m/z 624.8472. Anal. Calcd for $C_{21}H_{14}NBSeI_2$: C, 40.43; H, 2.26; I, 40.68. Found: C, 40.68; H, 2.46; I, 40.53.

Synthesis of Polymer 4SO. Monomer **2S** (0.127 g, 0.220 mmol), 1,4-diethynyl-2,5-dihexadecyloxybenzene (0.134 g, 0.220 mmol), CuI (0.006 g, 0.030 mmol), and $Pd(PPh_3)_4$ (0.013 g, 0.011 mmol) were dissolved in 4.4 mL of THF and 2.2 mL of Et_3N. The reaction mixture was stirred at room temperature for 96 h. The solvent was removed under vacuum. The residue was purified by repeated precipitation from a small amount of $CHCl_3$ into 25 mL of methanol to obtain **4SO** (0.169 g, 0.183 mmol) in 83% yield as a yellow solid. ^{1}H NMR ($CDCl_3$, δ, ppm): 8,50 (2H), 7.77-7.52 (5H), 7.42 (4H), 7.29 (4H), 6.96 (2H), 3.99 (4H), 1.80 (4H), 1.49

(4H), 1.23 (48H), 0.85 (6H). ^{13}C NMR ($CDCl_3$, δ, ppm): 153.58, 144.23, 144.08, 143.33, 133.04, 131.08, 130.76, 129.43, 127.21, 121.71, 121.51, 118.95, 117.06, 114.08, 95.46, 85.53, 69.63, 31.93, 29.67, 29.37, 28.89, 25.98, 22.70, 14.11. ^{11}B NMR ($CDCl_3$, δ, ppm): 6.45. IR (KBr, ν, cm^{-1}): 3063, 3016, 2923, 2852, 2205, 1598, 1573, 1499, 1463, 1414, 1373, 1307, 1279, 1217, 1020, 865, 809, 776, 719.

Synthesis of Polymer 4SeO. Similarly to the preparation of **4SO**, polymer **4SeO** was prepared from monomer **2Se** (0.137 g, 0.220 mmol) and 1,4-diethynyl-2,5-dihexadecyloxybenzene (0.134 g, 0.220 mmol) in 87% yield as an orange solid. ^{1}H NMR ($CDCl_3$, δ, ppm): 8,54 (1H), 8.46 (1H), 7.99 (1H), 7.66-7.55 (4H), 7.41 (4H), 7.28 (4H), 3.98 (4H), 1.80 (4H), 1.23 (48H), 0.87 (6H). ^{11}B NMR ($CDCl_3$, δ, ppm): 5.18. IR (KBr, ν, cm^{-1}): 3063, 3014, 2921, 2851, 2204, 1597, 1571, 1495, 1466, 1412, 1377, 1304, 1279, 1216, 1008, 862, 818, 754.

Synthesis of Polymer 4SF. Similarly to the preparation of **4SO**, polymer **4SF** was prepared from monomer **2S** (0.144 g, 0.250 mmol) and 1,4-diethynyl-2,5-bis(trifluoromethyl)benzene (0.066 g, 0.25 mmol), in 58% yield as a yellow solid. ^{1}H NMR ($CDCl_3$, δ, ppm): 8,55-8.47 (2H), 7.90 (2H), 7.77 (1H), 7.65-7.55 (4H), 7.45 (4H), 7.33 (4H). ^{11}B NMR ($CDCl_3$, δ, ppm): 3.91. IR (KBr, ν, cm^{-1}): 3069, 2214, 1605, 1574, 1500, 1462, 1422, 1372, 1304, 1245, 1222, 1156, 1071, 1019, 913, 871, 820, 762.

Synthesis of Polymer 4SeF. Similarly to the preparation of **4SO**, polymer **4SeF** was prepared from monomer **2Se** (0.156 g, 0.250 mmol) and 1,4-diethynyl-2,5-bis(trifluoromethyl)benzene (0.066 g, 0.25 mmol) in 69% yield as an orange solid. ^{1}H NMR ($CDCl_3$, δ, ppm): 8,57 (1H), 8.47 (1H), 8.00 (1H), 7.90 (2H), 7.70 (2H), 7.46 (9H), 7.29 (2H), 7.23 (1H). ^{11}B NMR ($CDCl_3$, δ, ppm): 4.89. IR (KBr, ν, cm^{-1}): 3065, 3015, 2212, 1601, 1573, 1497, 1459, 1422, 1372, 1303, 1245, 1221, 1157, 1071, 1011, 913, 870, 819, 754.

Synthesis of Polymer 4OO. Similarly to the preparation of **4SO**, polymer **4OO** was prepared from monomer **2O** (0.134 g, 0.220 mmol) and 1,4-diethynyl-2,5-dihexadecyloxybenzene (0.134 g, 0.220 mmol) at 40 °C for 48 h in 29% yield as a yellow solid. ^{1}H NMR ($CDCl_3$, δ, ppm): 8,56 (1H), 8.44 (1H), 8.00 (1H), 7.67-7.54 (2H), 7.42 (7H), 7.26-7.19 (2H), 6.96 (2H), 3.98 (4H), 1.80 (4H), 1.49 (4H), 1.22 (48H), 0.86 (6H). ^{11}B NMR ($CDCl_3$, δ, ppm): 8.89. IR (KBr, ν, cm^{-1}): 3064, 3023, 2924, 2852, 2206, 1615, 1505, 1468, 1414, 1383, 1332, 1274, 1215, 1124, 1019, 957, 906, 865, 815, 783, 720.

Synthesis of Polymer 4OF. Similarly to the preparation of **4SO**, polymer **4OF** was prepared from monomer **2O** (0.140 g, 0.250 mmol) and 1,4-diethynyl-2,5-bis(trifluoromethyl)benzene (0.066 g, 0.25 mmol) in 58% yield as a yellow solid. ^{1}H NMR ($CDCl_3$, δ, ppm): 8,56 (1H), 8.46 (1H), 8.00 (1H), 7.90 (2H), 7.70-7.56 (4H), 7.44 (4H), 7.33 (4H). ^{11}B NMR ($CDCl_3$, δ, ppm): 4.89. IR (KBr, ν, cm^{-1}): 3065, 3015, 2212, 1601, 1573, 1497, 1459, 1422, 1372, 1303, 1245, 1221, 1157, 1071, 1011, 913, 870, 819, 754.

References

(1) (a) Hadziioannou, G., van Hutten, P. F., Eds., *Semiconducting polymers: Chemistry, Physics and Engineering,* 2nd ed.; Wiley-VCH:Weinheim, Germany, 2006. (b) Skotheim, T. J., Elsenbaumer, R. L. Reynolds, J. R., Eds. *Handbook of Conducting Polymers,* 2nd ed.; Dekker: New York, 1998. (c) Martin, R. E.; Diederich, F. *Angew. Chem.* **1999,** *111*, 1440.

(2) Kraft, A.; Grimsdale, A. C.; Holmes, A. B. *Angew. Chem.* **1998,** *110*, 402.

(3) Hide, F.; Diaz-Garcia, M. A.; Schwartz, B. J.; Heeger A. J. *Acc. Chem. Res.* **1997**, *30*, 430.

(4) Screen, T. E. O.; Lawton, K. B.; Wilson, G. S.; Dolney, N.; Ispasoiu, R.; Goodson III, T.; Martin, S. J.; Bradley, D. D. C.; Anderson, H. L. *J. Mater. Chem.* **2001**, *11*, 312.

(5) Yu, G.; Gao, J.; Hummelen, J. C.; Wudl, F.; Heeger, A. J. *Science* **1995,** *270*, 1789.

(6) (a) Bao, Z; Rogers, J. A.; Katz, H. E. *J. Mater. Chem.* **1999,** *9*, 1895. (b) Calvert, P. *Chem. Mater.* **2001,** *13*, 3299.

(7) Haugland, R. P. *The Handbook-A Guide to Fluorescent Probes and Labeling Technologies*, 10th ed.; Spence, M. T. Z., Ed.; Molecular Probes: Eugene. OR, 2005; Chapter 1 Section 1.4.

(8) Gorman, A.; Killoran, J.; O'Shea, C.; Kenna, T.; Gallagher, W. M.; O'Shea, D. F. *J. Am. Chem. Soc.* **2004,** *126*, 10619.

(9) (a) García-Moreno, I.; Costela, A.; Campo, L.; Sastre, R.; Amat-Guerri, F.; Liras, M.; López Arbeloa, I. *J. Phys. Chem. A* **2004,** *108*, 3315. (b) Pavlopoulos, T. G.; Boyer, J. H.; Sathyamoorthi, G. *Appl. Opt.* **1998,** *37*, 7797.

(10) (a) Nagata, Y.; Chujo, Y. *Macromolecules* **2007,** *40*, 6. (b) Nagata, Y.; Chujo, Y. *Macromolecules* **2008,** *41*, 2809.

(11) (a) Cheng, Y. M.; Yeh, Y. S.; Ho, M. L.; Chou, P. T.; Chen, P. S.; Chi, Y. *Inorg. Chem.* **2005,** *44*, 4594. (b) Shi, Y.-W.; Shi, M.-M.; Huang, J.-C.; Chen, H.-Z.; Wang, M.; Liu, X.-D.; Ma, Y.-G.; Xu, H.; Yang, B. *Chem. Commun.* **2006,** 1941.

(12) (a) Chen, C. H.; Shi, J. C. *Coord. Chem. Rev.* **1998,** *171*, 161. (b) Ballardini, R.; Varani, G.; Indelli, M. T.; Scandola, F. *Inorg. Chem.* **1986,** *25*, 3858.

(13) Shavaleev, N. M.; Adams, H.; Best, J.; Edge, R.; Navaratnam, S.; Weinstein, J. A. *Inorg. Chem.* **2006,** *45*, 9410.

(14) Higashi, T. *ABSCOR. Program for Absorption Correction.*; Rigaku Corporation: Japan, 1995.

(15) Sheldrick, G. M. SHELX-97. Programs for Crystal Structure Analysis.; University of Göttingen: Germany, 1997.

(16) Altomare, A.; Burla, M.C.; Camalli, M.; Cascarano, G. L.; Giacovazzo, C.; Guagliardi, A.; Moliterni, A. G. G.; Polidori, G.; Spagna, R. *J. Appl. Cryst.* **1999,** *32*, 115.

(17) Wakita, K. *Yadokari-XG. Program for Crystal Structure Analysis.*; 2000.

(18) Farrugia, L. J. *J. Appl. Cryst.* **1997,** *30*, 565.

(19) Ashaks, J.; Bankovsky, Y.; Zaruma, D.; Shestakova, I.; Domracheva, I.; Nesterova, A.; Lukevics, E. *Chem. Heterocycl. Compd.* **2004,** *40*, 776.

(20) Swager, T. M.; Gil, C. J.; Wrighton, M. S. *J. Phys. Chem.* **1995,** *99*, 4886.

(21) Nagai, A.; Miyake, J.; Kokado, K.; Nagata, Y.; Chujo, Y. *J. Am. Chem. Soc.* **2008,** *130*, 15276.

(22) Wu, Q.; Esteghamatian, M.; Hu, N.-X.; Popovic, Z.; Enright, G.; Tao. Y.; D'Iorio, M.; Wang, S. *Chem. Mater.* **2000,** *12*, 79.

(23) Egbe, D. A. M.; Roll, C. P.; Brickner, E.; Grummt, U.-W.; Stockmann, R.; Klemm, E. *Macromolecules* **2002,** *35*, 3825.

(24) Okubo, T.; Kohmoto, S.; Yamamoto, M. *J. Polym. Sci., Part A: Polym. Chem.* **1998**, *68*, 1791

(25) Frisch, M. J.; Trucks, G. W.; Schlegel, H. B.; Scuseria, G. E.; Robb, M. A.; Cheeseman, J. R.; Montgomery, J. A., Jr.; Vreven, T.; Kudin, K. N.; Burant, J. C.; Millam, J. M.; Iyengar, S. S.; Tomasi, J.; Barone, V.; Mennucci, B.; Cossi, M.; Scalmani, G.; Rega, N.; Petersson, G. A.; Nakatsuji, H.; Hada, M.; Ehara, M.; Toyota, K.; Fukuda, R.; Hasegawa, J.; Ishida, M.; Nakajima, T.; Honda, Y.; Kitao, O.; Nakai, H.; Klene, M.; Li, X.; Knox, J. E.; Hratchian, H. P.; Cross, J. B.; Adamo, C.; Jaramillo, J.; Gomperts, R.; Stratmann, R. E.; Yazyev, O.; Austin, A. J.; Cammi, R.; Pomelli, C.; Ochterski, J. W.; Ayala, P. Y.; Morokuma, K.; Voth, G. A.; Salvador, P.; Dannenberg, J. J.; Zakrzewski, V. G.; Dapprich, S.; Daniels, A. D.; Strain, M. C.; Farkas, O.; Malick, D. K.; Rabuck, A. D.; Raghavachari, K.; Foresman, J. B.; Ortiz, J. V.; Cui, Q.; Baboul, A. G.; Clifford, S.;

Cioslowski, J.; Stefanov, B. B.; Liu, G.; Liashenko, A.; Piskorz, P.; Komaromi, I.; Martin, R. L.; Fox, D. J.; Keith, T.; Al-Laham, M. A.; Peng, C. Y.; Nanayakkara, A.; Challacombe, M.; Gill, P. M. W.; Johnson, B.; Chen, W.; Wong, M. W.; Gonzalez, C.; Pople, J. A. Gaussian 03, revision D.01; Gaussian, Inc., Wallingford, CT, **2004.**

Chapter 2

Synthesis of π-Conjugated Polymers Containing Organoboron Benzo[*h*]quinolate in the Main-Chain

Abstract

Novel π-conjugated polymers containing organoboron benzo[*h*]quinolate were prepared by Sonogashira-Hagihara coupling of organoboron benzo[*h*]quinolate-based bis-iodo monomer with 1,4-diethynylbenzene derivatives. Tetracoordination states of boron atoms in the obtained polymers were confirmed by ^{11}B NMR spectroscopy, and they were also characterized by ^{1}H NMR and IR spectroscopies, and size-exclusion chromatography (SEC). 10-Hydroxybenzo[*h*]quinolinato-diphenylboron was also prepared as a model compound of the polymers, and the detailed structure was determined by single-crystal X-ray diffraction analysis. The optical properties of the polymers and the model compound were studied by UV-vis absorption and photoluminescence spectroscopies. The absorption and emission bands attributed to the benzo[*h*]quinolate moiety were bathochromically shifted as compared with 8-hydroxyquinolinatodiphenylboron. The Stokes shift of the model compound sensitively depended on the orientational polarizability of the solvent. The polymers showed efficient energy transfer from π-conjugated main chain to benzo[*h*]quinolate ligand and exhibited no difference in emission between the donating π-conjugated linker and accepting one. Higher quantum yields were observed (Φ_F = 0.16 or 0.18), while the model compound displayed moderate fluorescence quantum yield (Φ_F = 0.10).

Introduction

Organoboron dyes have recently found widespread interest as species with promising optical properties in various fields. They have been used as chemical probes[1], photosensitizers[2] and optical sensing[3] due to high luminescent quantum yields, large extinction coefficients or two-photon absorption cross section. Among them, organoboron quinolates such as 8-hydroxyquinolinatodiphenylboron (BPh_2q)[4] turned out to be attractive as an alternative to tris (8-hydroxyquinolinato)aluminium (Alq_3)[5] for organic light-emitting diodes (OLEDs) because of their good thermal stabilities as well as the high emission quantum yields. BPh_2q and their derivatives emit intense light from a quinoline-based intraligand charge transfer (ILCT) excited state.[6] This ILCT state is formed when the highest occupied molecular orbital (HOMO) and the lowest unoccupied molecular orbital (LUMO) are localized on the phenolate ring and on the pyridyl ring of the quinoline ligand, respectively. Introduction of them into polymers by covalent bond is expected to be advantageous because of the improved processability such as film-formability, thermal- and photo-stability, etc. Jäkle *et al.* first reported the synthesis of well-defined polymers incorporated into the polystyrene side chain via multistage polymeric reaction of poly(4-dibromoborylstyrene),[7] and Weck, *et al.* also proposed the potentiality of organoboron quinolate-functionalized polystyrene as the excellent precursors for OLEDs.[8]

Recently, Chujo *et al.* have also prepared organoboron quinolate-containing conjugated polymers, in which *p*-phenylene-ethynylene units were embedded to boron atoms in the polymer backbones.[9] These polymers gave strong green fluorescence, and an efficient energy migration from conjugated linkers with high molar absorption coefficient to boron quinolate moieties was observed. Substituting groups can change the emission color of the polymers, i.e., polymers with methyl substituted organoboron quinolate exhibited green-blue or blue photoluminescence.[10] Elements also affect the emission wavelength of the organoboron quinolate polymer.[11] Increasing

atomic number of the 16 Group atom adjacent to the boron atom caused emission shift to longer wavelength and decreasing of absolute quantum yields for both the low-molecular-mass model compounds and the polymers.

Extension of π-conjugation is another important approach to changing the emission color. 10-Hydroxybenzo[*h*]quinoline can be regarded as π-extended 8-hydroxy quinoline and shows proton transfer emission like the emission from ILCT state,[12] so that 10-hydroxybenzo[*h*]quinolinatodiphenylboron and the benzo[*h*]quinoline-conatining polymers seem to be a reasonable candidate for that aim. Herein, the author wishes to report novel synthesis of 10-hydroxybenzo[*h*]quinolinatodiphenylboron **1** and the incorporation of **1** into π-conjugated polymer main-chain, and discuss the optical properties comparing them with BPh_2q.

Results and Discussion

Synthesis of a Model Compound. The reaction between 10-hydroxybenzo[*h*]quinoline[13] and triphenylborane in toluene under reflux condition afforded organoboron benzo[*h*]quinolate **1** as a yellow precipitate in the reaction mixture at –20°C (Scheme 1). This compound was stable under air and showed high solubility in dichloromethane and chloroform. The tetracoordination state of the boron atoms in **1** was confirmed by the ^{11}B NMR spectroscopy in $CDCl_3$ (δ_B = 6.55 ppm) and the basic structure was also characterized by ^{1}H NMR, ^{13}C NMR and EI mass spectroscopies, and besides elemental analysis.

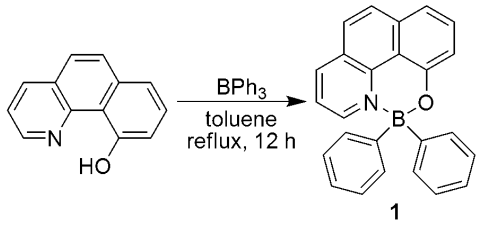

1

Scheme 1. Synthesis of model compound

Further, the molecular structure of **1** as determined by single crystal X-ray analyses is shown in Figure 1. Unlike the 8-hydroxyquinolate ligand, which forms a planar, five-membered ring with boron, the chelate ring in **1** is six membered and puckered. The sp^3 orbital-hybridized boron centers of **1** appear as a slightly distorted tetrahedron with the dihedral angle O(1)-B(1)-N(1) of 105.1° (Table 1), which is closer to an ideal orientation of four sp^3 orbitals than that of $B(C_2H_5)_2q$ (97.0°, q = 8-hydroxyquinolato)[4] and B(4-iodophenyl)$_2$q (99.9°).[10] On the other hand, the angle C(23)-O(1)-B(1) of 117.8° suggested large distortion around O atom of **1** as compared with that of $B(C_2H_5)_2q$ (111.8°).[4] The average of B(1)-N(1) bond length of **1** (1.635 Å) was same as that of $B(C_2H_5)_2q$ (1.636 Å)[4] and B(4-iodophenyl)$_2$q (1.629 Å)[10] probably indicating that 10-hydroxybenzo[*h*]quinolate possesses as high chelating ability as 8-hydroxyquinolate.

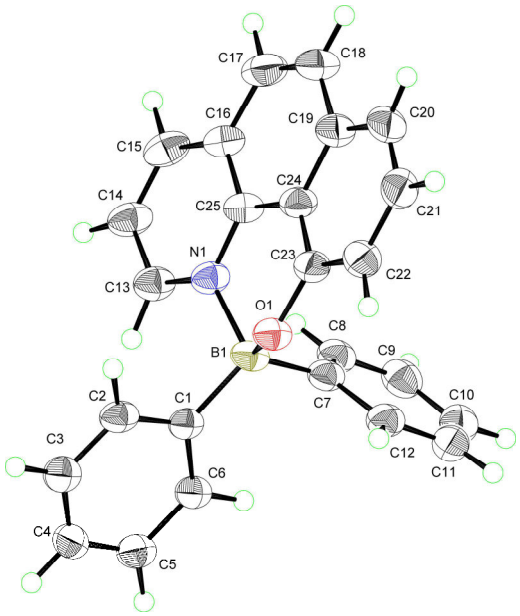

Figure 1. The X-ray crystal structure of **1** with thermal ellipsoids drawn to the 50% probability level.

Table 1. Selected bond lengths (Å) and angles (deg) for **1**

B(1)-N(1)	1.635(4)	O(1)-B(1) -N(1)	105.1(2)
B(1)-O(1)	1.500(3)	C(23)-O(1)-B(1)	117.8(2)
O(1)-C(23)	1.358(3)	O(1)-C(23)-C(24)	120.6(3)
C(23)-C(24)	1.415(5)	C(23)-C(24)-C(25)	120.7(3)
C(24)-C(25)	1.441(4)	N(1)-C(25)-C(24)	118.7(2)
N(1)-C(25)	1.369(3)	C(25)-N(1)-B(1)	118.4(2)
B(1)-C(1)	1.602(4)		
B(1)-C(7)	1.613(5)		

Synthesis of Polymers. Organoboron benzo[*h*]quinolate-based monomer **2** was prepared from 10-hydroxybenzo[*h*]quinoline according to Scheme 2. When the compound was purified by reprecipitation from methanol and hexane, respectively, the compound **2** was obtained as a yellow color solid analogous to the model compound. The monomer was stable under air and soluble in dichloromethane and chloroform. The tetracoordination state of the boron atoms in **2** was confirmed by the ^{11}B NMR spectroscopy in $CDCl_3$ (δ_B = 6.06 ppm), which is similar to the signal of the model compound. Moreover, the structure of **2** was also characterized by ^{1}H NMR, ^{13}C NMR and EI mass spectroscopies, and by elemental analysis.

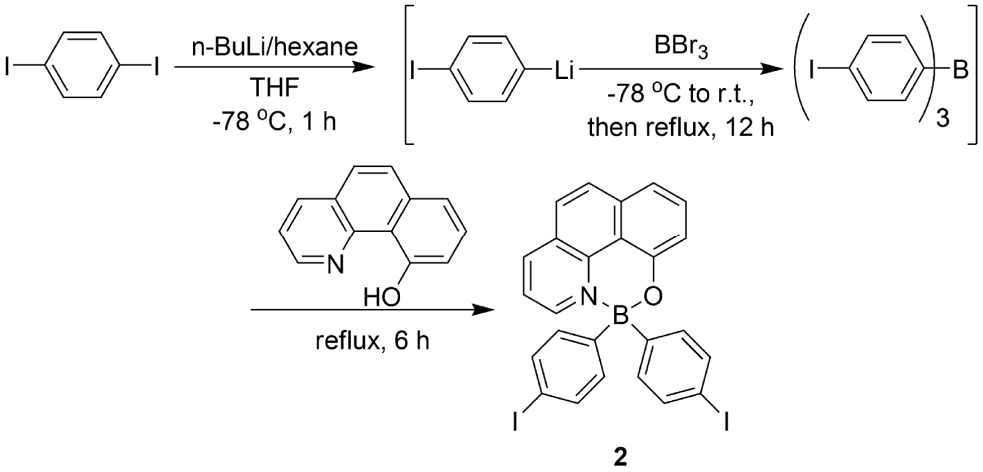

Scheme 2. Synthesis of monomer

Scheme 3 and Table 2 summarize the condition and results of the polymerization of the monomer **2** with 1,4-diethynylbenzene derivatives **3O** or **3F** in the presence of a catalytic amount of $Pd(PPh_3)_4$ and CuI in the mixed solvent of tetrahydrofuran (THF) and triethylamine. The obtained polymers **4O** and **4F** were collected as yellow solids, and their yields were 72% and 57%, respectively. The ^{11}B NMR spectra of the obtained polymers were observed at δ_B = 4.10 (for **4O**) and 4.30 (for **4F**) ppm assignable to the tetracoordination state of the boron atoms in each polymer, indicating that the polymerization proceeded without any damage of the structure in the organoboron quinolate moiety. The IR spectra of the polymers showed the absorption peaks at 2205 (for **4O**) and 2216 (for **4F**) cm^{-1}, which are attributable to stretching of the –C≡C– bond in the polymer backbone. Moreover, strong and broad peaks due to the C-F stretching band were observed at around 1200 cm^{-1} in the spectra of **4F**. The number-average molecular weights (M_n) and the molecular weight distributions (M_w/M_n) of **4O** and **4F**, measured by size-exclusion chromatography (SEC) in THF, were 10800 and 2.4, and 6400 and 2.5, respectively (Table 2). The degrees of polymerization (DPs), estimated by M_n from SEC, were 11.2 and 6.6 (**poly1** and

poly2, respectively). Thermal stabilities of the polymers were examined by thermogravimetric analysis (TGA). The starts of the thermal degradation under air for the polymers **4O** and **4F** lie at 298 and 368 °C, where 5% weight loss was recorded. These data suggest that the obtained polymers present similar thermal stability to general poly(*p*-phenylene-ethynylene)s[14] and π-conjugated polymers containing organoboron quinolates in the main-chain.[11]

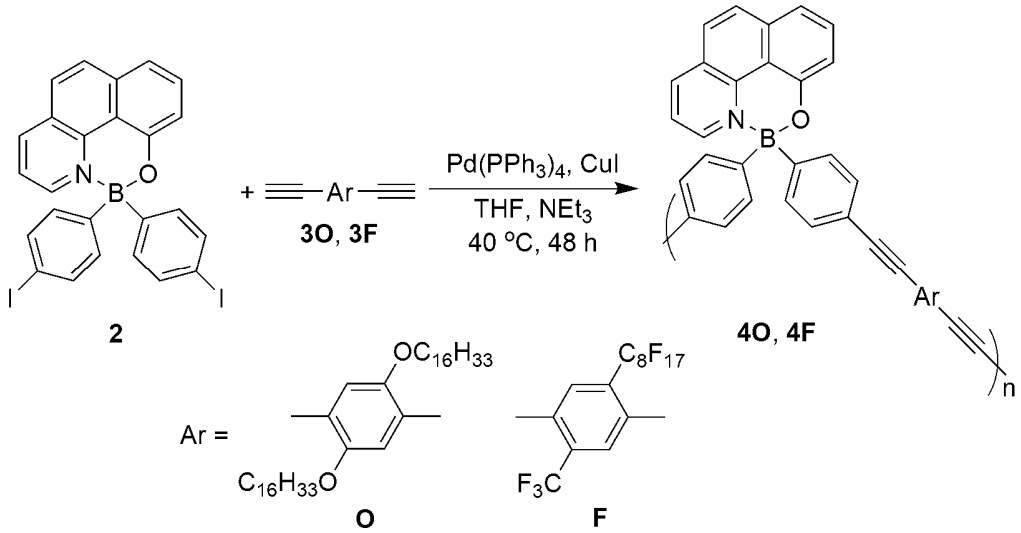

Scheme 3. Synthesis of polymers

Optical Properties. The optical properties of the obtained polymers were investigated by UV-vis absorption and photoluminescence in $CHCl_3$ solution as compared to those of model compounds. The results from the absorption and emission spectra are summarized in Table 3. The model compound **1** showed the weak absorption peak at 302 and 420 nm arising from the benzo[*h*]quinolate ligand (Figure 2). These peaks stand on the bathochromic side in comparison with those of BPh_2q (264 and 395 nm).[11] This means that the extension of π-conjugation from quinolate to benzo[*h*]quinolate reduces the width between molecular orbitals and causes the bathochromic shift of the absorption peaks. The polymers **4O** and **4F** exhibited the strong absorption bands in the region from 300 to 400 nm like other π-conjugated polymers containing organoboron quinolates in the main-chain.[11] Therefore, these bands can be assignable to the π-

conjugated linkers connecting the benzo[*h*]quinolate units each other, and the electronic structure of the π-conjugated linker is also independent from that of the benzo[*h*]quinolate.

Table 2. Polymerization of organoboron quinolate-based monomers and 1,4-diethynylbenzene derivatives[a]

polymer	Yield[b] (%)	M_n[c]	M_w[c]	M_w/M_n[c]	DPn[d]	T_5/°C[e]
4O	72	10,800	25,500	2.4	11.2	298
4F	57	6,400	16,200	2.5	6.6	368

[a] Conditions: Sonogashira-Hagihara couplings of organoboron quinolate-based monomer (1 equiv.) and 1,4-diethynylbenzene derivatives (1 equiv.) were carried out in the presence of $Pd(PPh_3)_4$ and CuI in the mixed solvent (THF/NEt_3 = 2/1) at room temperature or 40 °C for 48 h. [b] Isolated yields after precipitation. [c] Estimated by size-exclusion chromatography (SEC) based on polystyrene standard in tetrahydrofuran (THF). [d] Average number of repeating units calculated from M_n and molecular weights of repeating units. [e] Thermogravimetric analysis: heating rate 10 K/min under air; values given for weight loss of 5%.

Table 3. UV-visible absorption and photoluminescence data

compound	$\lambda_{abs,max}$ / nm[a]	ε / $M^{-1}cm^{-1}$[b]	Ex / nm[c]	$\lambda_{em,max}$ / nm[d]	Φ_F[e]
1	302, 420	3,600	420	513	0.10
4O	314, 373	39,000	373	513	0.16
4F	359, 375	47,700	375	509	0.18

[a] Absorption maxima: $CHCl_3$ (1.0×10^{-5} M). [b] Molar extinction coefficients at the longest absorption maxima. [c] Excited wavelength. [d] Fluorescence maxima: $CHCl_3$ (1.0×10^{-5} M). [e] Absolute quantum yield.

Photoluminescence spectra in $CHCl_3$ are shown in Figure 3. All emission data given here were obtained after exciting at the longest wavelength of the absorption peaks, i.e., absorption

maxima of the polymers and the model compound are corresponding to phenylene-ethynylene and benzo[*h*]quinoline, respectively. The spectra of the polymers **4O** and **4F** coincided with its model compound **1**, implying that the polymers emit the light from benzo[*h*]quinolate moiety and the polymer side chains are irresponsible to the wavelength of the emission. Although the emission bands of the organoboron benzo[*h*]quinolates were bathochromically shifted as compared with BPh_2q,[11] the Stokes shifts of the formers are smaller than that of the latter. In addition, full widths at half maximum (FWHMs) of the organoboron benzo[*h*]quinolates were narrower than that of BPh_2q. From these results, it can be said that the benzo[*h*]quinolate ligand disturbs the nuclear reorientation and oscillation in transition state. Photoluminescence property of the model compound **1** in different solvents (THF, DMSO, DMF, and acetonitrile) was also examined. Shifts of the absorption spectra and fluorescence spectra depend on the nature of the solvent, and the solvent polarity greatly affect the Stokes shift. The change in the Stokes shift ($\Delta\nu$) was roughly proportional to the orientational polarizability (Δf) of the solvent, obeying the dipole interaction theory of Lippert and Mataga (Figure 4).[15] Based on this analysis, it can be concluded that the excitation of the organoboron benzo[*h*]quinolate **1** causes ILCT like organoboron quinolate, leading to the charge separated state. Figure 5 represents fluorescence excitation spectra of the polymers in $CHCl_3$ ($c = 1.0 \times 10^{-5}$ M). These spectra displayed the similar shapes as the UV-vis absorption spectra, i.e., the strong absorption at π-conjugated linkers in the main-chain is crucial in photoluminescence. This suggests that the energy transfer from the π-conjugated linkers to the benzo[*h*]quinolate ligands on the boron centers occurs, followed by photoluminescence from the ligands. Absolute fluorescence quantum yields (Φ_F) of the polymers and the model compound in $CHCl_3$ were measured by integrating sphere method. The quantum yield of **1** ($\Phi_F = 0.10$) is lower than that of BPh_2q ($\Phi_F = 0.47$). The introduction of organoboron benzo[*h*]quinolate into the π-conjugated polymer main-chain, however, enhances

the quantum yield (Φ_F = 0.16 or 0.18). This would mean that the bulky π-conjugated linkers prevent benzo[*h*]quinolate from some quenchers.

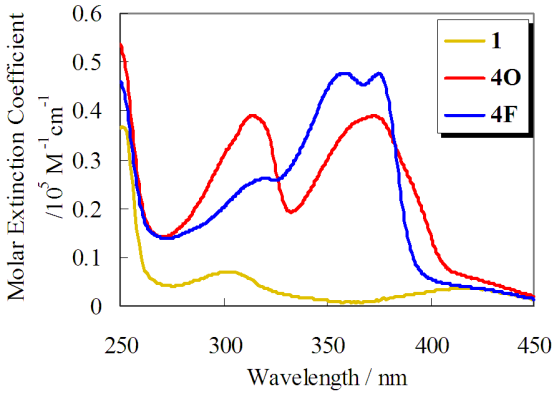

Figure 2. UV-vis spectra of polymers and model compound in $CHCl_3$ (1.0×10^{-5} M).

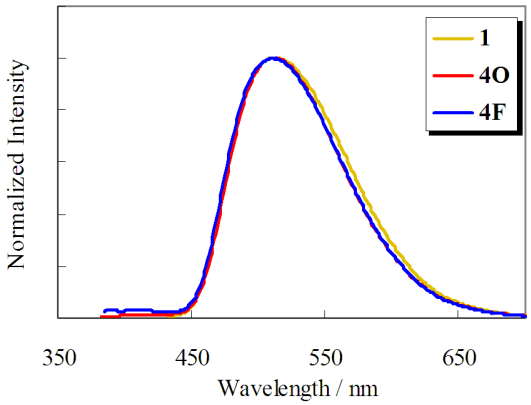

Figure 3. Normalized emission spectra of polymers and model compound in $CHCl_3$ (1.0×10^{-5} M).

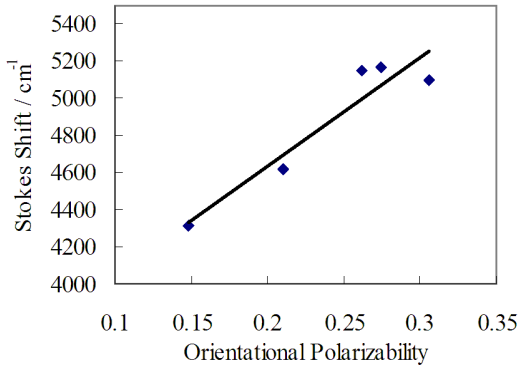

Figure 4. Lippert plot of model compound **1**.

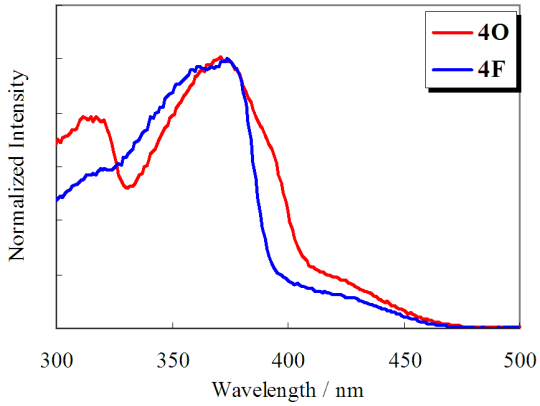

Figure 5. Normalized excitation spectra of polymers and model compound in $CHCl_3$ (1.0×10^{-5} M).

Molecular Orbital Calculations. To provide more effective understanding for the photophysical behavior of the polymers and the model compounds, we employed the theoretical calculation for compounds **1** and **5** using density-functional theory (DFT) and time-dependent DFT (TD-DFT) method at the B3LYP/6-31G(d)//B3LYP/6-31G(d).[16] Figure 6A exhibits HOMO and LUMO of the compound **1**. The geometry optimization of **1** provided the puckered chelate ring with boron similar to the X-ray crystal structure. The HOMO of **1** is located predominantly on the phenolate ring and the LUMO is mainly on the pyridinyl ring. This orbital localization probably causes ILCT as shown in organoboron quinolates. TD-DFT calculation reveals that HOMO-LUMO transition occurs at 431 nm with small oscillator strength (f = 0.0618), and this peak position gives good agreement with that of UV-vis spectra (420 nm). In the compound **5**, which has π-conjugated linkers, the HOMO is not on the benzo[*h*]quinolate ligand, but localized on the one side of the π-conjugated linker and the LUMO is localized on the ligand (Figure 6B). This result supports that π-conjugation is unable to extend through tetracoordinated boron, and that the π-conjugated linkers are irresponsible to the electronic structure of the ligand. From the TD-DFT calculation, major oscillator strength of **5** is above 1 at 390 nm (f = 1.9901), and this absorption process predominantly consists of the electronic transitions from orbitals on the linker to other orbitals on the linker. This means that the absorption peak of the polymer **4O** at 373 nm is assignable to the π-conjugated linker, and that transition in the linker is easy to take place in comparison with that concerned with the benzo[*h*]quinolate ligand.

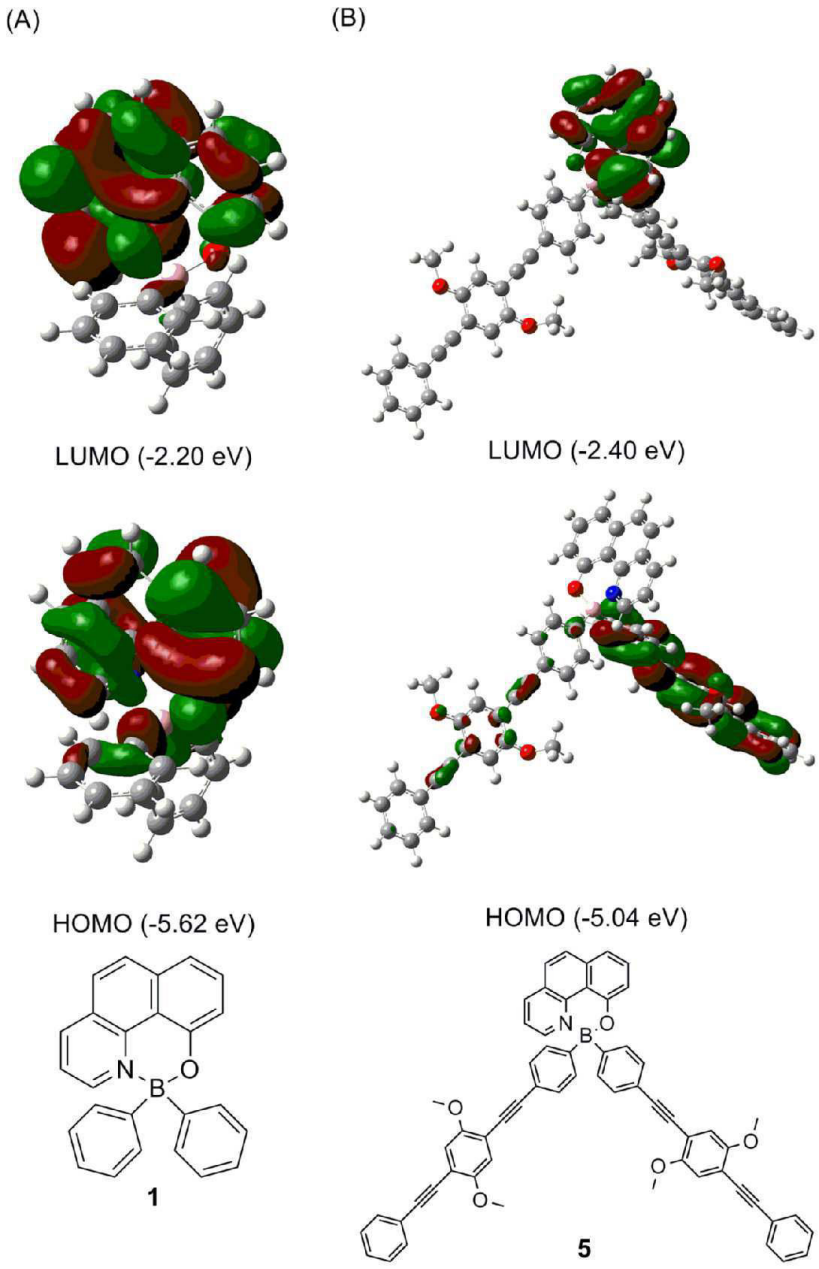

Figure 6. Molecular orbital diagrams for the HOMO and LUMO of (A) **1**and (B) **5** (B3LYP/6-31G(d)// B3LYP/6-31G(d)).

Conclusion

The author has successfully prepared the novel low-molecular-mass organoboron benzo[*h*]quinolate complexes (model compound) and the main-chain-type organoboron benzo[*h*]quinolate polymers. These polymers were obtained by Sonogashira-Hagihara coupling in moderate yields. The emission of the organoboron benzo[*h*]quinolate was responsible to ILCT, and shifted to longer wavelength as compared with BPh_2q. The polymers showed efficient energy transfer from π-conjugated main chain to benzo[*h*]quinolate ligand and they exhibited no difference in emission between the donating π-conjugated linker and accepting one. Low-molecular-mass organoboron benzo[*h*]quinolate displayed moderate fluorescence quantum yield ($\Phi_F = 0.10$). In contrast, the polymers showed higher quantum yield ($\Phi_F = 0.16$ or 0.18).

Experimental Section

Measurements. ^{1}H (400 MHz), ^{13}C (100 MHz), and ^{11}B (128 MHz) NMR spectra were recorded on a JEOL JNM-EX400 spectrometer. ^{1}H and ^{13}C NMR spectra used tetramethylsilane (TMS) as an internal standard, ^{11}B NMR were referenced externally to BF_3OEt_2 (sealed capillary) in $CDCl_3$. The number-average molecular weight (M_n) and the molecular weight distribution [weight-average molecular weight/number-average molecular weight (M_w/M_n)] values of all polymers were estimated by size-exclusion chromatography (SEC) with a TOSOH G3000HXI system equipped with three consecutive polystyrene gel columns [TOSOH gels: α-4000, α-3000, and α-2500] and ultraviolet detector at 40 °C The system was operated at a flow rate of 1.0 mL/min, with tetrahydrofuran as an eluent. Polystyrene standards were employed for calibration. UV–vis spectra were recorded on a Shimadzu UV-3600 spectrophotometer. Fluorescence emission spectra were recorded on a HORIBA JOBIN YVON Fluoromax-4 spectrofluorometer, and the absolute quantum yield was calculated by integrating sphere method on the HORIBA JOBIN YVON Fluoromax-4 spectrofluorometer in chloroform. FT-IR spectra were obtained using a SHIMADZU IRPrestige-21 infrared spectrometer. Thermogravimetric analyses (TGA) were performed on a Seiko TG/DTA 6200 at a scan rate of 10 °C/min. X-ray crystallographic analysis was carried out by a Rigaku R-AXIS RAPID-F graphite-monochromated Mo Kα radiation diffractometer with an imaging plate. A symmetry related absorption correction was carried out by using the program ABSCOR[17]. The analysis was carried out with direct methods (SHELX-97[18] or SIR97[19]) using Yadokari-XG[20]. The program ORTEP3[21] was used to generate the X-ray structural diagram. Elemental analysis was performed at the Microanalytical Center of Kyoto University.

Materials. Tetrahydrofuran (THF) and triethylamine (Et_3N) were purified using a two-column solid-state purification system (Glasscontour System, Joerg Meyer, Irvine, CA). 10-Hydroxybenzo[*h*]quinoline,[13] 1,4-diethynyl-2,5-dihexadecyloxybenzene,[22] and 1.4-diethynyl-2-perfluorooctyl-5-trifluoromethylbenzene [23] were prepared according to the literature.

Synthesis of 1. Triphenylborane (0.726 g, 3.00 mmol) and 10-hydroxybenzo[*h*]quinoline (0.59 g, 3.00 mmol) were dissolved in toluene (18 mL). After the reaction mixture was refluxed for 12 h, the mixture was allowed to stand for 1 day at –20 °C to precipitate a product. The precipitate was collected by filtration to give a yellow solid in 76% yield (0.82 g, 2.28 mmol). ^{1}H NMR ($CDCl_3$, δ, ppm): 8.47 (m, 1H, Ar), 8.42 (m, 1H, Ar), 7.84 (dd, J = 8.9, 4.8 Hz, 1H, Ar), 7.72-7.61 (m, 3H, Ar), 7.41 (d, J = 8.1 Hz, 1H, Ar), 7.33 (m, 5H, Ar), 7.24-7.15 (m, 6H, Ar). ^{11}B NMR ($CDCl_3$, δ, ppm): 6.55. ^{13}CNMR ($CDCl_3$, δ, ppm): 157.81 (Ar), 143.21 (Ar), 140.58 (Ar), 139.78 (Ar) 134.78 (Ar), 133.11 (Ar), 132.82 (Ar), 130.74 (Ar), 127.32 (Ar), 126.58 (Ar), 126.34 (Ar), 123.25 (Ar), 120.74 (Ar), 117.67 (Ar), 116.98 (Ar), 115.26 (Ar). HRMS (EI) Calcd for $C_{25}H_{18}BNO$: m/z 359.1481. Found: m/z 359.1478. Anal. Calcd for $C_{25}H_{18}BNO$: C, 83.59; H, 5.05; N, 3.90. Found: C, 83.48; H, 5.19; N, 3.77.

Synthesis of 2. 9.4 mL (1.6 M, 15 mmol) of *n*-BuLi was slowly added to the solution of 1,4-diiodobenzene (4.95 g, 15.0 mmol) in 75 mL of THF at -78 °C, and the mixture was stirred at –78 °C for 1 h. BBr_3 (0.48 mL, 5.0 mmol) was added to the reaction mixture at -78 °C and then allowed to room temperature and refluxed for 12 h. 10-Hydroxybenzo[*h*]quinoline (0.98 g, 5.00 mmol) dissolved in 15 mL of THF in another flask was added to the reaction mixture and then refluxed for 6 h. The reaction mixture was concentrated under vacuum. The remaining oil was diluted by a small amount of $CHCl_3$ and the solution was reprecipitated with 100 mL of methanol to give a yellow solid. This solid was purified by dissolving in a small amount of CH_2Cl_2 and reprecipitating with 100 mL of hexane to obtain **2** in 53% yield (1.63 g, 2.67 mmol) as a yellow

solid. ^{1}H NMR ($CDCl_3$, δ, ppm): 8.47 (d, J = 7.8 Hz, 1H, Ar), 8.38 (d, J = 4.4 Hz, 1H, Ar), 7.88 (d, J = 9.0 Hz, 1H, Ar), 7.74-7.65 (m, 3H, Ar), 7.52 (d, J = 8.1 Hz, 4H, Ar), 7.37 (dd, J = 7.8, 4.4 Hz, 2H, Ar), 7.00 (d, J = 8.0 Hz, 4H, Ar) . ^{11}B NMR ($CDCl_3$, δ, ppm): 6.06. ^{13}CNMR ($CDCl_3$, δ, ppm): 157.25 (Ar), 142.80 (Ar), 140.40 (Ar), 140.18 (Ar) 136.44 (Ar), 135.06 (Ar), 134.75 (Ar), 133.00 (Ar), 130.93 (Ar), 126.49 (Ar), 123.30 (Ar), 120.93 (Ar), 118.10 (Ar), 116.94 (Ar), 115.05 (Ar), 93.26 (Ar-I). HRMS (EI) Calcd for $C_{25}H_{16}BI_2NO$: m/z 610.9414. Found: m/z 610.9415. Anal. Calcd for $C_{25}H_{16}BI_2NO$: C, 49.14; H, 2.64; N, 2.29. Found: C, 48.99; H, 2.81; N, 2.29.

Synthesis of 4O. Monomer **2** (0.12 g, 0.20 mmol), 1,4-diethynyl-2,5-dioctyloxybenzene (0.12 g, 0.20 mmol), CuI (1.9 mg, 0.01 mmol), and $Pd(PPh_3)_4$ (12.0 mg, 0.01 mmol) were dissolved in 2.0 mL of THF and 1.0 mL of Et_3N. After the mixture was stirred at 40 °C for 48 h, a small amount of $CHCl_3$ was added and poured into a large excess of methanol to precipitate the polymer. The polymer was purified by repeated precipitations from a small amount of $CHCl_3$ into a large excess of methanol and hexane respectively to give a yellow solid in 72% yield (0.14 g, 0.14 mmol). M_n = 10,800. ^{1}H NMR ($CDCl_3$, δ, ppm): 8.46 (1H, Ar), 8.41 (1H, Ar), 7.87 (1H, Ar), 7.72-7.67 (4H, Ar), 7.42-7.36 (6H, Ar), 7.28-7.25 (4H, Ar), 6.93 (2H, Ar), 3.96 (4H, -OCH_2-), 1.78 (4H, -CH_2-), 1.58 (4H, -CH_2-), 1.47 (4H, -CH_2-), 1.21 (44H, -CH_2-), 0.86 (6H, -CH_3). ^{13}C NMR ($CDCl_3$, δ, ppm): 157.52 (Ar), 153.53 (Ar), 143.02 (Ar), 140.53 (Ar), 134.77 (Ar), 132.96 (Ar), 130.90 (Ar), 130.59 (Ar), 126.46 (Ar), 123.27 (Ar), 121.59 (Ar), 120.88 (Ar), 117.97 (Ar), 117.08 (Ar), 115.19 (Ar), 114.09 (Ar), 95.57 (–C≡C–), 85.35 (–C≡C–), 69.62 (–OCH_2–), 31.93, 29.67, 29.60, 29.38, 29.34, 25.98, 22.70, 14.15. ^{11}B NMR ($CDCl_3$, δ, ppm): 4.10. IR (KBr): ν = 3061 (Ar), 3017 (Ar), 2924, 2853, 2205 (C≡C), 1923 (Ar), 1630 (Ar), 1597 (Ar), 1510, 1468, 1437, 1379, 1342, 1294, 1215, 1148, 1076, 1049, 970, 908, 889, 835, 721 cm^{-1}. Anal. Calcd for $C_{67}H_{84}BNO_3$: C, 83.63; H, 8.80; N, 1.46. Found: C, 81.01; H, 8.44; N, 1.46.

Synthesis of 4F. Similarly to the preparation of **4O**, **4F** was prepared from Monomer **2** (97.8 mg, 0.16 mmol), and 1.4-diethynyl-2-perfluorooctyl-5-trifluoromethylbenzene (98.0 mg, 0.16 mmol) in 57% yield as a yellow solid. M_n = 6,400. ^{1}H NMR ($CDCl_3$, δ, ppm): 8.51 (1H, Ar), 8.43 (1H, Ar), 7.89 (2H, Ar), 7.79 (1H, Ar), 7.71 (4H, Ar), 7.40 (5H, Ar), 7.32 (3H, Ar), 7.28 (1H, Ar). ^{11}B NMR ($CDCl_3$, δ, ppm): 4.30. IR (KBr): ν = 3065 (Ar), 3021 (Ar), 2216 (C≡C), 1923 (Ar), 1802 (Ar), 1630 (Ar), 1597 (Ar), 1512, 1441, 1344, 1298, 1244, 1213, 1144, 1078, 1047, 1020, 970, 910, 889, 835, 721 cm^{-1}. Anal. Calcd for $C_{44}H_{18}BF_{20}NO$: C, 54.63; H, 1.88; N, 1.45. Found: C, 53.98; H, 2.25; N, 1.39.

References

(1) Haugland, R. P. *The Handbook-A Guide to Fluorescent Probes and Labeling Technologies*, 10th ed.; Spence, M. T. Z., Ed.; Molecular Probes: Eugene. OR, 2005; Chapter 1 Section 1.4.

(2) Gorman, A.; Killoran, J.; O'Shea, C.; Kenna, T.; Gallagher, W. M.; O'Shea, D. F. *J. Am. Chem. Soc.* **2004,** *126,* 10619.

(3) (a) García-Moreno, I.; Costela, A.; Campo, L.; Sastre, R.; Amat-Guerri, F.; Liras, M.; López Arbeloa, I. *J. Phys. Chem. A* **2004,** *108*, 3315. (b) Pavlopoulos, T. G.; Boyer, J. H.; Sathyamoorthi, G. *Appl. Opt.* **1998,** *37*, 7797.

(4) Wu, Q.; Esteghamatian, M.; Hu, N.-X.; Popovic, Z.; Enright, G.; Tao. Y.; D'Iorio, M.; Wang, S. *Chem. Mater.* **2000,** *12*, 79.

(5) Tang, C.W.; Vanslyke, S. A. *Appl. Phys. Lett.* **1987,** *51,* 913.

(6) (a) Cheng, Y. M.; Yeh, Y. S.; Ho, M. L.; Chou, P. T.; Chen, P. S.; Chi, Y. *Inorg. Chem.* **2005,** *44*, 4594. (b) Shi, Y.-W.; Shi, M.-M.; Huang, J.-C.; Chen, H.-Z.; Wang, M.; Liu, X.-D.; Ma, Y.-G.; Xu, H.; Yang, B. *Chem. Commun.* **2006,** 1941.

(7) (a) Qin, Y; Pagba, C.; Piotrowiak, P.; Jäkle, F. *J. Am. Chem. Soc.* **2004,** *126,* 7015. (b) Qin, Y.; Kiburu, I.; Shah, S.; Jäkle, F. *Macromolecules* **2006,** *39,* 9041.

(8) Wang, X.-Y; Weck, M. *Macromolecules* **2005,** *38,* 7219.

(9) Nagata, Y.; Chujo, Y. *Macromolecules* **2007,** *40,* 6.

(10) Nagata, Y.; Otaka, H.; Chujo, Y. *Macromolecules* **2008,** *41,* 737.

(11) Tokoro, Y; Nagai, A.; Kokado, K.; Chujo, Y. *Macromolecules* **2009,** *42,* 2988.

(12) Chen, K.-Y.; Hsieh, C.-C.; Cheng, Y.-M.; Lai, C.-H.; Chou, P.-T. *Chem. Commun.* **2006,** 4395.

(13) Dick, A. R.; Hull, K. L.; Sanford, M. S. *J. Am. Chem. Soc.* **2004,** *126,* 2300.

(14) Egbe, D. A. M.; Roll, C. P.; Brickner, E.; Grummt, U.-W.; Stockmann, R.; Klemm, E. *Macromolecules* **2002,** *35*, 3825.

(15) (a) Lippert, E. Z. *Electrochem.* **1957,** *61,* 962. (b) Mataga, N.; Kaifu, Y.; Koizumi, M. *Bull. Chem. Soc. Jpn.* **1956,** *29,* 465.

(16) Frisch, M. J.; Trucks, G. W.; Schlegel, H. B.; Scuseria, G. E.; Robb, M. A.; Cheeseman, J. R.; Montgomery, J. A., Jr.; Vreven, T.; Kudin, K. N.; Burant, J. C.; Millam, J. M.; Iyengar, S. S.; Tomasi, J.; Barone, V.; Mennucci, B.; Cossi, M.; Scalmani, G.; Rega, N.; Petersson, G. A.; Nakatsuji, H.; Hada, M.; Ehara, M.; Toyota, K.; Fukuda, R.; Hasegawa, J.; Ishida, M.; Nakajima, T.; Honda, Y.; Kitao, O.; Nakai, H.; Klene, M.; Li, X.; Knox, J. E.; Hratchian, H. P.; Cross, J. B.; Adamo, C.; Jaramillo, J.; Gomperts, R.; Stratmann, R. E.; Yazyev, O.; Austin, A. J.; Cammi, R.; Pomelli, C.; Ochterski, J. W.; Ayala, P. Y.; Morokuma, K.; Voth, G. A.; Salvador, P.; Dannenberg, J. J.; Zakrzewski, V. G.; Dapprich, S.; Daniels, A. D.; Strain, M. C.; Farkas, O.; Malick, D. K.; Rabuck, A. D.; Raghavachari, K.; Foresman, J. B.; Ortiz, J. V.; Cui, Q.; Baboul, A. G.; Clifford, S.; Cioslowski, J.; Stefanov, B. B.; Liu, G.; Liashenko, A.; Piskorz, P.; Komaromi, I.; Martin, R. L.; Fox, D. J.; Keith, T.; Al-Laham, M. A.; Peng, C. Y.; Nanayakkara, A.; Challacombe, M.; Gill, P. M. W.; Johnson, B.; Chen, W.; Wong, M. W.; Gonzalez, C.; Pople, J. A. Gaussian 03, revision D.01; Gaussian, Inc., Wallingford, CT, **2004.**

(17) Higashi, T. *ABSCOR. Program for Absorption Correction.*; Rigaku Corporation: Japan, 1995.

(18) Sheldrick, G. M. SHELX-97. Programs for Crystal Structure Analysis.; University of Göttingen: Germany, 1997.

(19) Altomare, A.; Burla, M.C.; Camalli, M.; Cascarano, G. L.; Giacovazzo, C.; Guagliardi, A.; Moliterni, A. G. G.; Polidori, G.; Spagna, R. *J. Appl. Cryst.* **1999,** *32*, 115.

(20) Wakita, K. *Yadokari-XG. Program for Crystal Structure Analysis.*; 2000.

(21) Farrugia, L. J. *J. Appl. Cryst.* **1997,** *30*, 565.

(22) Swager, T. M.; Gil, C. J.; Wrighton, M. S. *J. Phys. Chem.* **1995,** *99*, 4886.

(23) Kokado, K.; Chujo, Y. *Macromolecules* **2009,** *42,* 1418.

Chapter 3

Synthesis and Properties of Highly Luminescent Organoboron 8-Aminoquinolate-Coordination Polymers

Abstract

New organoboron aminoquinolate-based coordination polymers linked by π-conjugated bridge were prepared by Sonogashira-Hagihara coupling of organoboron aminoquinolate-based bis-iodo monomers bearing biphenyl or bithiophene moiety with 1,4-diethynylbenzene derivatives. Tetracoordination states of boron atoms in the obtained polymers were confirmed by ^{11}B NMR spectroscopy, and they were also characterized by ^{1}H NMR and IR spectroscopies, and size-exclusion chromatography (SEC). Their optical properties were studied by UV-vis absorption and photoluminescence spectroscopies. In the region above 400 nm, the polymers prepared from 1,4-diethynyl-2,5-dioctyloxybenzene showed bathochromic shifts as compared with those prepared from 1,4-diethynyl-2-perfluorooctyl-5-trifluoromethylbenzene. The polymers with biphenyl moiety showed higher absolute fluorescence quantum yields (Φ_F = 0.28 and 0.65), whereas those with bithiophene moiety led to decreasing of the low quantum yields (Φ_F = 0.19 and 0.00). The DFT and TD-DFT calculations of model compounds corresponding to the polymers were in good agreement with the results from UV-vis properties. The calculations revealed that the electronic structure of the polymer with bithiophene moiety is different from that with biphenyl moiety, and predicted the electron transfer from the bithiophene moiety to the π-extended quinoline moiety in transition state.

Chapter 3

Introduction

For a few decades, conjugated polymers have received much attention because of their extensive applications to electronic and photonic devices such as polymeric light emitting diodes,[1] plastic lasers,[2] nonlinear optical materials,[3] and polymer-based photovoltaic cells.[4] The polymers have an advantage of low cost device fabrication via solution processing methods, including dip coating, spin casting, and, ink-jet printing, as compared with inorganic or low molecular weight counterparts.[5] To control the physical properties of conjugated polymers from the view point of the molecular scale, various aromatic moieties and side chains have been incorporated into them.[6-8] One of the interesting approaches is introduction of functional dyes into the conjugated polymer backbone.[9-12] This method allows for increasing not only of the diversity of emission maxima available in the dyes, which were incorporated into the conjugated linkers, but also of stability of the dyes.

Many fluorescent organoboron dyes have been used as chemical probes, photosensitizers and optical sensing due to high emission quantum yields.[13-15] Among them, organoboron quinolates such as 8-hydroxyquinoline biphenylboron (BPh_2q)[16] turned out to be attractive as an alternative to tris(8-hydroxyquinoline)aluminium (Alq_3)[17] for organic light-emitting diodes because of their good thermal stabilities as well as the high emission quantum yields. They showed, however, lower molar absorption coefficient corresponding to the HOMO-LUMO transition relative to typical π-conjugated molecules. This weak point has been improved by the synthesis of organoboron quinolate-containing conjugated polymers, in which *p*-phenylene-ethynylene units were embedded to boron atoms in the polymer backbones.[18, 19] These polymers gave strong green fluorescence, and an efficient energy migration from conjugated linkers with high molar absorption coefficient to boron quinolate moieties was observed. However, the linkage between boron atom and two *p*-phenylene-ethynylene moieties in the polymers prevented

the phenylene-ethynylene linkers from π-conjugating to boron quinolate cores. Therefore, these polymers did not obviously change the absorption and emission maxima of boron quinolate moiety. Generally, the control of absorption and emission wavelength is as important as improvement of the molar absorption coefficient toward the application of actual device fabrication. Embedding the quinolato ligands in the various main chains of conjugated polymers accomplished the efficient control by through-bond interaction between quinolato moiety and π-conjugated bridge. There are two types of polymer architecture fit for that qualification; (i) both the boron centers and the quinolato ligands are embedded in the main chain,[20] and (ii) quinolate group is part of the polymer backbone with diphenylboron moieties as pendant group.[21] The majority of polymers prepared by this procedure represented less emission quantum yield than BPh_2q. However, Chujo *et al.* have previously reported organoboron 8-aminoquinolate-coordination polymers with red-shifts of the emission maxima and higher absolute quantum yields as compared with BPh_2q.[22] Herein, the author reports the synthesis and characterization of novel organoboron 8-aminoquinolate-coordination polymers, and discuss the relationship between the optical property and the structure of the polymer backbone in detail.

Results and Discussion

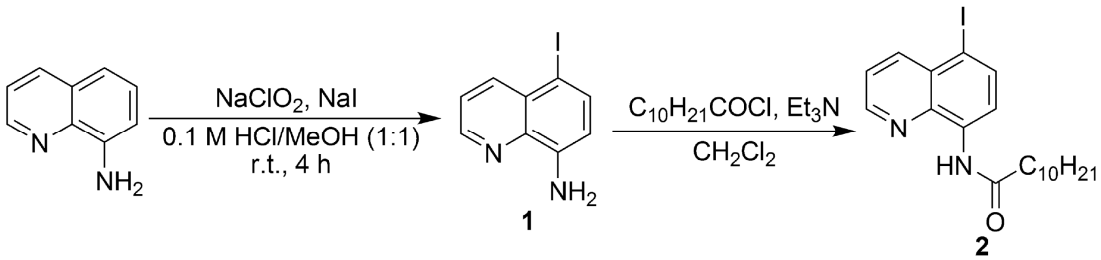

Scheme 1. Synthesis of ligand **2**

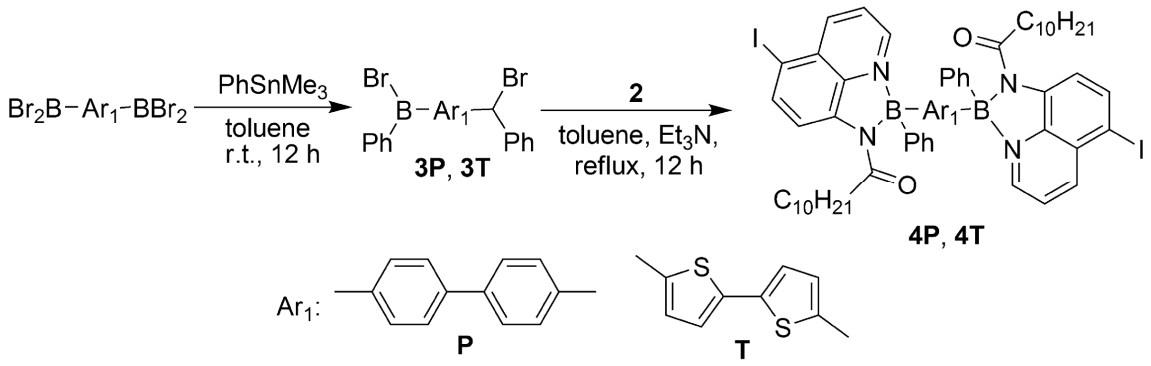

Scheme 2. Synthesis of monomers

Initially, the ligand *N*-(5-iodo-8-quinolyl)undecanamide (**2**) was synthesized from 8-aminoquinoline as a starting compound according to Scheme 1. The other precursors for organoboron monomers, 4,4'-bis(phenylbromoboryl)biphenyl **3P** and bithiophene **3T** were obtained via tin-boron exchange from 4,4'-bis(dibromoboryl)biphenyl[23] and 2,2'-bis(dibromoboryl)thiophene[23] upon reaction with trimethyl(phenyl)tin. **3P** and **3T** were not absolutely purified due to their high reactivities. The reaction of these bis(phehylbromoboryl)-functionalized compounds with the ligand **2** produced organoboron aminoquinolate-based monomers **4P** and **4T** bearing bis-iodo groups as yellow powders (Scheme 2). These monomers possess good solubility in various organic solvent due to the long alkyl chains attached by amide linkages. The tetracoordination state of the boron atoms in **4P** and **4T** were confirmed by the ^{11}B NMR spectroscopy in $CDCl_3$ [**4P**: δ_B = 6.74 ppm, **4T**: δ_B = 4.40 ppm]. Strong electron-donating nature of the bithiophene unit moved chemical shift δ_B of **4T** to the upfield relative to that of **4P**. The basic structures of **4P** and **4T** were also characterized by ^{1}H NMR, ^{13}C NMR, elemental analysis and mass spectroscopies. Coordination of the aminoquinolato generates a stereogenic center at boron. However, the stereo-conformation might be not significantly responsible for

emission behavior, so that the stereoisomers were not separated here.[20,24] Sonogashira-Hagihara coupling polymerization of **4P** or **4T** were conducted with 1,4-diethynyl-2,5-dioctyloxybenzene[25] or 1,4-diethynyl-2-(perfluorooctyl)-5-(trifluoromethyl)benzene[26] in the presence of $Pd(PPh_3)_4$ and CuI in the mixed solvent of tetrahydrofuran (THF) and triethylamine (Et_3N) at 40 ºC for 48 h (Scheme 3). The obtained polymers **6PO** and **6TO** were collected as red solids, while **6PF** and **6TF** were collected as yellow solids. The polymers were soluble in THF, CH_2Cl_2, and $CHCl_3$. The ^{11}B NMR spectra of the obtained polymers were observed at δ_B = 5.18–2.15 ppm assignable to the tetracoordination state of the boron atoms in each polymer, indicating that the polymerization proceeded without any damage of the structure in the organoboron quinolate moiety. The IR spectra of the polymers showed the weak absorption peaks at 2203-2197 cm^{-1} and the strong absorption peaks at 1663–1653 cm^{-1}, which are attributable to stretching of the C≡C bond and the C=O bond, respectively. Table 1 summarizes the polymerization results. The number-average molecular weights (M_n) and the molecular weight distribution (M_w/M_n) of the polymers, measured by size-exclusion chromatography (SEC) in THF toward polystyrene standards, were 12,600–34,000 and 1.4–3.0, respectively. The low reactivity of the monomer **5F** with electronegative substituent for Sonogashira-Hagihara coupling resulted in the low molecular weight polymers **6PF** and **6TF** as compared with the polymers **6PO** and **6TO**. To evaluate the optical properties of the polymers, a model compound **8**) for the polymer **6PO** was also prepared from boron aminoquinolate bearing mono-iodo group **7** and 1,4-diethynyl-2,5-dioctyloxybenzene under the similar condition to the polymerization (Scheme 4). After the purification by the reprecipitation, the model compound **8** was collected as a solid, which is similar color to the polymer **6PO**.

Table 1. Polymerization Results

polymer	yield[a] (%)	M_n[b]	M_w[b]	M_w/M_n[b]	DP[c]
6PO	91	34,000	100,300	3.0	25.6
6PF	85	15,400	29,800	1.9	9.9
6TO	88	28,000	102,000	3.7	20.9
6TF	89	12,600	23,200	1.8	8.0

[a] Isolated yields after reprecipitation. [b] Estimated by SEC based on polystyrene standards in THF. [c] Degree of polymerization estimated by number-average molecular weight.

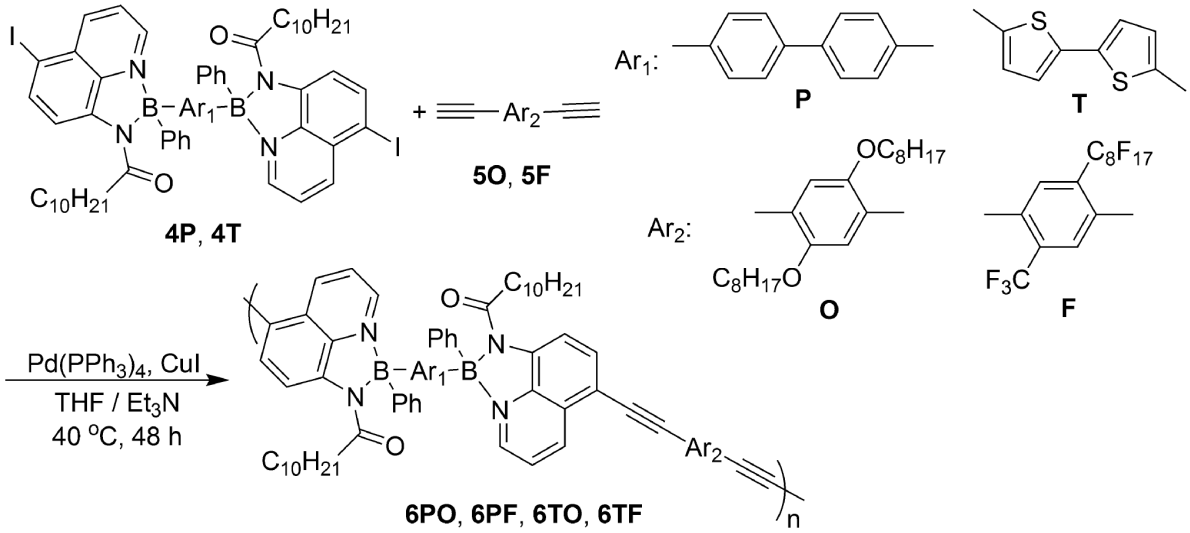

Scheme 3 Synthesis of polymers

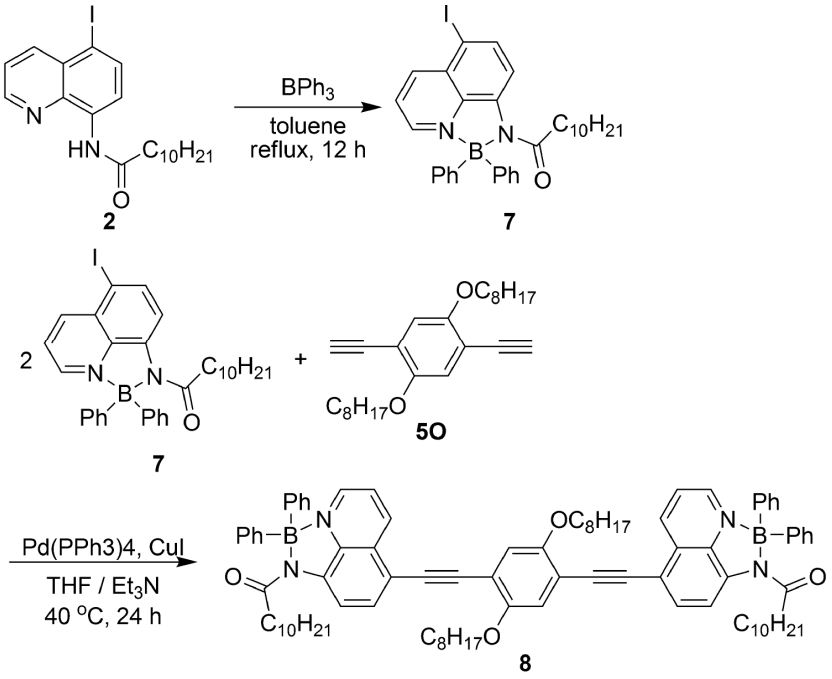

Scheme 4. Synthesis of model **8**

The optical properties of the obtained polymers and the model compound were investigated by UV-vis absorption and photoluminescence experiments. Figure 1 illustrates UV-vis absorption spectra of the polymers and the model compound in $CHCl_3$ solution ($c = 1.0 \times 10^{-5}$ M). The spectra of the polymer **6PO** and its model compound **8** overlapped in the region of the wavelength between 300 and 550 nm, obviously indicating that the polymer **6PO** consists of the scaffold of the model compound **8**, and their absorption bands in this region were probably assigned to the absorption of the unit composed of two quinoline rings and diethynylbenzene (qAr_2q-unit). In the region of the wavelength above 400 nm, the polymers having the same side chain at Ar_2 give the same absorption peaks. The absorption bands of the polymers with octyloxy group (**6PO** and **6TO**) were bathochromically shifted in comparison with those of the polymers with perfluoroalkyl group (**6PF** and **6TF**). This would mean that the absorption maximum of the

polymer with any Ar_1 unit depends on Ar_2 unit, i.e., the diethynyl-functionalized monomer in Scheme 3, and the bathochromic shift is related to the electron-donating nature of Ar_2 unit in that region. All the polymers and the model compounds strongly absorb the visible light at longer wavelength in comparison with typical organoboron quinolates and aminoquinolates, meaning coplanarity and extended π-conjugation of quinoline rings through Ar_2 unit.

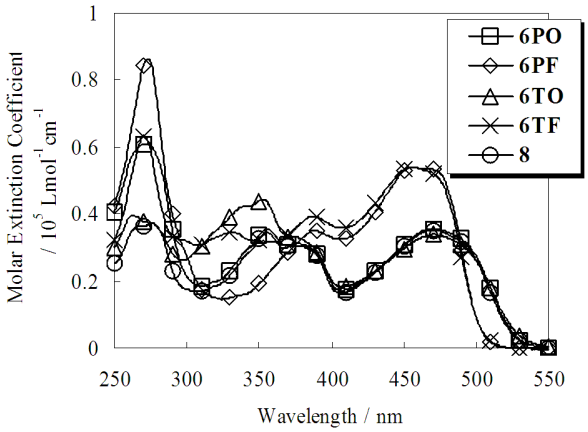

Figure 1. UV-vis spectra of polymers and model compounds in $CHCl_3$ (1.0×10^{-5} M).

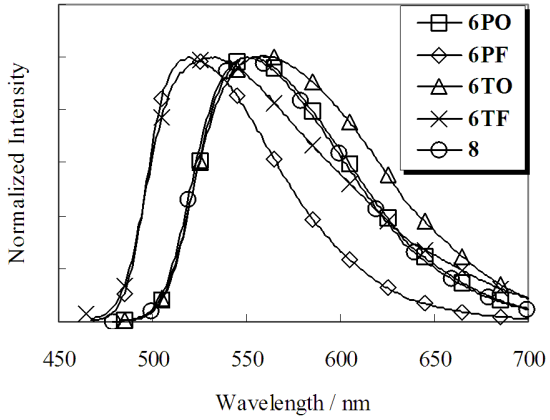

Figure 2. Normalized emission spectra of polymers and model compounds in $CHCl_3$ (1.0×10^{-5} M).

Emission spectra of the polymers and the model compound in $CHCl_3$ solution (c = 1.0 × 10^{-5} M) are represented in Figure 2. All the emission data given here were obtained after exciting at the longest wavelength of the absorption peaks, i.e., absorption maxima corresponding to qAr_2q-unit. The emission bands of the polymers with octyloxy group (**6PO** and **6TO**) were red-shifted in comparison with those with perfluoroalkyl group (**6PF** and **6TF**). Moreover, the spectrum of the polymer **6PO** coincided with that of the model compound (**8**). Based on these results, it can be concluded that the polymers emit the light from qAr_2q-unit and its wavelength is mainly controlled by electron-donating Ar_2 unit like the visible light absorption of the polymers. In the case that the polymers have the same Ar_2 group, the emission band of the polymer with bithiophene moiety (**6TO** or **6TF**) appeared in the region of longer wavelength than that with biphenyl moiety (**6PO** or **6PF**). On the contrary, Ar_1 unit shifted the emission band while that had no relation with the absorption band in the region above 400 nm. This would mean that Ar_1 affects the electronic structure of qAr_2q-unit not in the ground state but in the excited state. Absolute fluorescence quantum yields (Φ_F) of the polymers and the model compound in $CHCl_3$ were measured by integrating sphere method. The quantum yields of the polymers with bithiophene moiety (**6TO**, **6TF**) were lower than those with biphenyl moiety (**6PO** or **6PF**), and especially, the polymer with strong electron-withdrawing substituent (**6TF**) gave $\Phi_F < 0.01$. It seems to be that electron-donating ability of the bithiophene moiety is very strong, so that electron transfer from bithiophene moiety to quinoline ring leads to decreasing of the quantum yield.

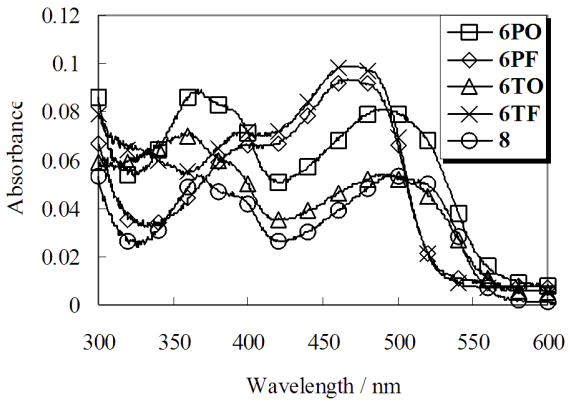

Figure 3. UV-vis spectra of polymers and model compounds in film state.

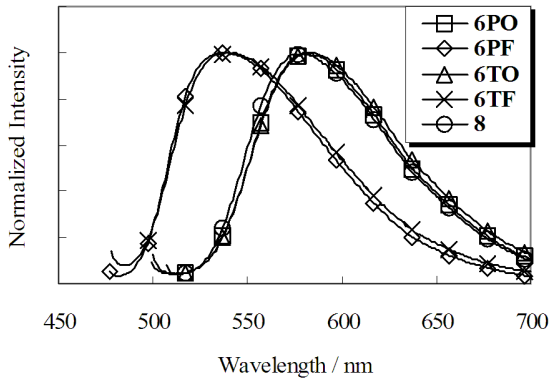

Figure 4. Normalized emission spectra of polymers and model compounds in film state.

UV-vis absorption and photoluminescence experiments in spin-coated film state were also carried out (Figures 3 and 4). All the polymers and the model compound in film state showed bathocromic shift of the absorption and photoluminescence spectra (7–29 nm) as compared with those in solution state due to intermolecular stacking interaction of π-conjugated main chain. Moreover, the polymers with perfluoroalkyl chains (**6PF**, **6TF**) represented smaller bathocromic shift than those with alkoxy chains (**6PO**, **6TO**), indicating that repulsion between

highly electronegative surfaces of perfluoroalkyl chains inhibits the stabilization by the stacking of π-conjugated main chain. In the normalized fluorescence spectra, the film state disappears the difference between the polymers with biphenyl moiety and those with bithiophene moiety as shown in the solution state (Figure 2). This is probably due to no solvation of the transition state from charge transfer in the film of **6TO** and **6TF**.

Table 2. UV-vis Absorption and Photoluminescence Properties in Solution State

compound	$\lambda_{abs,max}$ / nm[a]	ε / m^2mol^{-1}[b]	Ex / nm[c]	$\lambda_{em,max}$ / nm[d]	Φ_F[e]
6PO	272, 356, 376, 471	35800	471	555	0.28
6PF	273, 389, 457	53800	457	519	0.65
6TO	263, 353, 471	33900	471	558	0.19
6TF	271, 331, 388, 455	54000	455	531	0.00
8	268, 356, 376, 470	35200	470	550	0.29

[a] Absorption maxima: $CHCl_3$ (1.0×10^{-5} M). [b] Molar extinction coefficients at the longest absorption maxima. [c] Excited wavelength. [d] Fluorescence maxima: $CHCl_3$ (1.0×10^{-5} M). [e] Absolute quantum yield.

Table 3. UV-vis Absorption and Photoluminescence Properties in Film State

compound	$\lambda_{abs,max}$ / nm[a]	Ex / nm[b]	$\lambda_{em,max}$ / nm[c]
6PO	369, 489	489	580
6PF	467	467	537
6TO	362, 490	490	586
6TF	468	468	538
8	367, 497	497	579

[a] Absorption maxima. [b] Excited wavelength. [c] Fluorescence maxima.

Molecular Orbital Calculations

To further understand the nature of optical properties, the author has carried out theoretical calculation for model compounds **9PO** and **9TF** using density-functional theory (DFT) method at the B3LYP/6-31G(d), and also using time-dependent DFT (TD-DFT) at the B3LYP/6-31G(d,p).[27] Figures 5A and B exhibit HOMO and LUMO of **9PO** and **9TF**, respectively, and the molecular orbitals around frontier orbitals separate well into qAr_2q-unit and Ar_1 unit. The HOMO and LUMO of **9PO** are located predominantly on qAr_2q-unit and the oscillator strength (*f*) mainly responsible for HOMO–LUMO transition of **9PO** was large (*f* = 1.1089). These results indicate that the π-conjugation is extended through Ar_2 moiety, and that the HOMO–LUMO transition at qAr_2q-unit results in the absorption band of the polymer **6PO** around 470 nm as mentioned above. In contrast, the HOMO of **9TF** is localized on bithiophene moiety and the LUMO is on qAr_2q-unit. TD-DFT calculation revealed that HOMO-LUMO transition hardly occurs (*f* ~ 0.01), while transition from HOMO–2 on qAr_2q-unit to LUMO easily occurs (*f* = 1.5044) corresponding to the absorption band of the polymer **6TF** around 455 nm (Figure 1). The order of the oscillator strength was consistent with that of the molar extinction coeffifient. From the result of **9TF**, it can be said that the electron transition from HOMO–2 to LUMO provides a hole at HOMO–2 on qAr_2q-unit and that an electron localized on the bithiophene moiety transfers from HOMO to HOMO–2 in order to stabilize the transition state leading to the non-radiative relaxation.

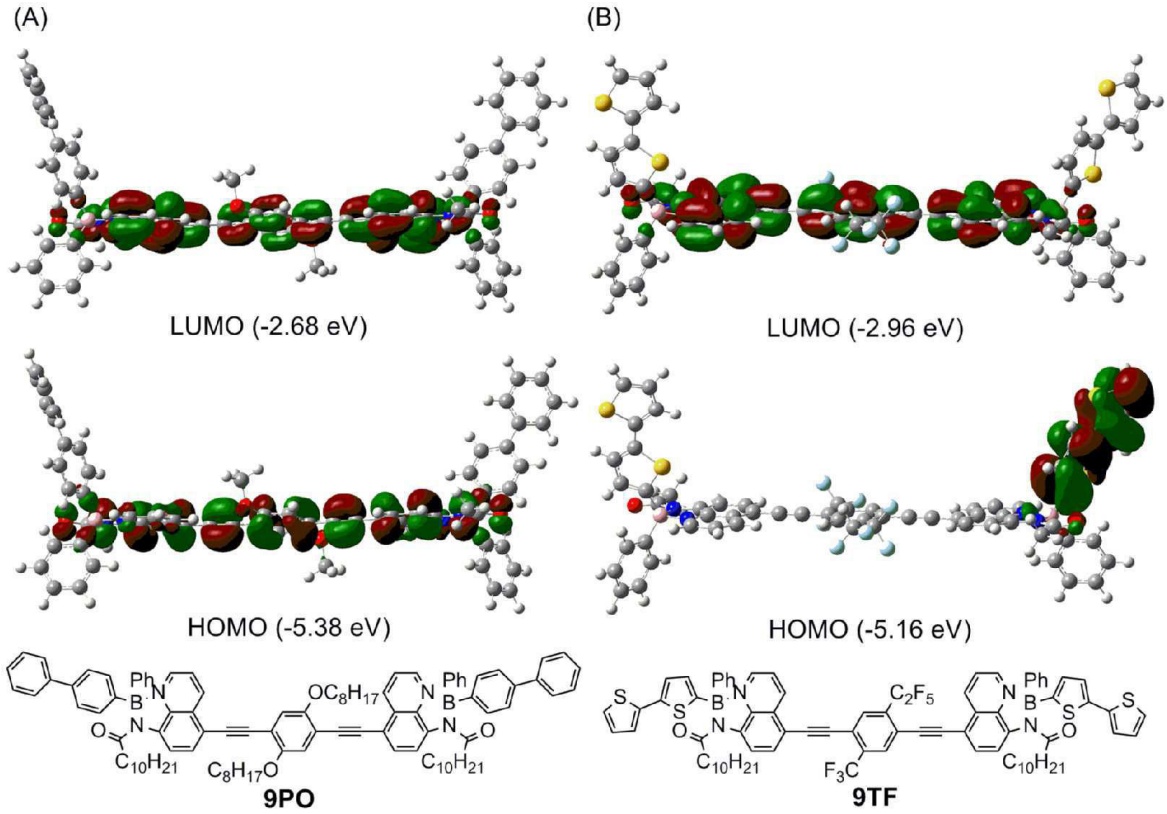

Figure 5. Molecular orbital diagrams for the HOMO and LUMO of (A) **9PO** and (B) **9TF** (B3LYP/6-31G(d)// B3LYP/6-31G(d)).

Conclusion

The author has successfully synthesized the novel organoboron aminoquinolate-based coordination polymers with high molecular weight by Sonogashira-Hagihara coupling in good yields. The color and the emission intensity of the polymers can be tuned by diethynyl-monomer and diiodo-monomer, respectively. The absorption and emission bands in the region above 400 nm predominantly depended on the backbone structure composed of two quinoline rings and diethynylbenzene. The polymers with biphenyl group exhibited the high fluorescence absolute quamtum yields, while no emission of the polymers with the bithiophene moiety and the perfluoroalkyl chain was observed. This result and the DFT calculations on the molecular model systems of the polymers suggest that the electron transfer easily occurs from bithiophene moiety to the π-extended quinoline moiety in transition state.

Experimental Section

Measurements. ^{1}H (400 MHz), ^{13}C (100 MHz), and ^{11}B (128 MHz) NMR spectra were recorded on a JEOL JNM-EX400 spectrometer. ^{1}H and ^{13}C NMR spectra used tetramethylsilane (TMS) as an internal standard, ^{11}B NMR spectra were referenced externally to BF_3OEt_2 (sealed capillary) in $CDCl_3$. The number-average molecular weights (M_n) and molecular weight distribution [weight-average molecular weight/number-average molecular weight (M_w/M_n)] values of all polymers were estimated by size-exclusion chromatography (SEC) with a TOSOH G3000HXI system equipped with three consecutive polystyrene gel columns [TOSOH gels: α-4000, α-3000, and α-2500] and ultraviolet detector at 40 °C. The system was operated at a flow rate of 1.0 mL/min, with tetrahydrofuran as an eluent. Polystyrene standards were employed for calibration. UV–vis spectra were recorded on a Shimadzu UV-3600 spectrophotometer. Fluorescence emission spectra were recorded on a HORIBA JOBIN YVON Fluoromax-4 spectrofluorometer. FT-IR spectra were obtained using a SHIMADZU IRPrestige-21 infrared spectrometer. Elemental analysis was performed at the Microanalytical Center of Kyoto University. All reaction was performed under nitrogen or argon atmosphere.

Materials. 5-Iodo-8-aminoquinoline,[22] 4,4'-bis(dibromoboryl)biphenyl,[23] 2,2'-bis(dibromoboryl)bithiophene,[23] 1,4-diethynyl-2,5-dioctyloxybenzene,[24] and 1.4-diethynyl-2-perfluorooctyl-5-trifluoromethylbenzene[25] were prepared according to the literature. Tetrahydrofuran (THF) and triethylamine (Et_3N) were purified using a two-column solid-state purification system (Glasscontour System, Joerg Meyer, Irvine, CA). Other reagents were commercially available and used as received.

Synthesis of N-(5-Iodo-8-quinolyl)undecanamide (2). 5-Iodo-8-aminoquinoline (5.40 g, 20.0 mmol) and undecanoyl chloride (4.62 mL, 21.0 mmol) were dissolved in dichloromethane (90 mL), followed by addition of triethylamine (2.93 mL, 21.0 mmol). The resulting mixture was

stirred at room temperature for 20 h. The mixture was transferred to a separating funnel and washed with aqueous $NaHCO_3$. The organic layer was dried over $MgSO_4$, and removal of the solvent under vacuum. Recrystallization from hexane gave a brown solid in 86% yield (7.52 g, 17.16 mmol). ^{1}H NMR ($CDCl_3$): δ = 9.81 (s, 1H, –N*H*–CO–), 8.77 (d, *J* = 4.1 Hz, 1H, Ar*H*), 8.57 (d, *J* = 8.3 Hz, 1H, Ar*H*), 8.37 (d, *J* = 8.6 Hz, 1H, Ar*H*), 8.07 (d, *J* = 8.3 Hz, 1H, Ar*H*), 7.53 (dd, *J* = 8.3, 4.2 Hz, 1H, Ar-*H*), 2.55 (t, *J* = 7.6 Hz, 2H, –CO–CH_2–), 1.81 (m, 2H, CO–CH_2–CH_2–), 1.43-1.26 (m, 14H, –CH_2–), 0.87 (t, *J* = 6.6 Hz, 1H, –CH_3) ppm. ^{11}B NMR ($CDCl_3$): δ = 7.13 ppm. ^{13}C NMR ($CDCl_3$): δ = 171.98 (*C*=O), 148.64 (Ar), 140.72 (Ar), 138.94 (Ar), 138.30 (Ar), 135.47 (Ar), 129.55 (Ar), 123.09 (Ar), 117.76 (Ar), 88.98 (Ar–I), 38.28, 31.87, 29.56, 29.48, 29.38, 29.27, 25.57, 22.66.

Synthesis of 4,4'-Bis(phenylbromoboryl)-biphenyl (3P). Trimethyl(phenyl)tin (4.78 mL, 26.3 mmol) was added to a solution of 4,4'-bis(dibromoboryl)biphenyl (6.49 g, 13.2 mmol) in toluene (263 mL) and the mixture was stirring for 14 h. All volatile components were removed under a high vacuum, and the solid was washed with hexane to give a crude product (3.96 g), which was used without further purification.

Synthesis of Monomer (4P). The crude product **3P** (0.746 g), *N*-(5-iodo-8-quinolyl)undecanamide (1.75 g, 4.00 mmol), and triethylamine (0.43 mL, 3.1 mmol) were dissolved in toluene (30 mL). After the reaction mixture was refluxed for 12 h, the solvent was removed by rotary evaporation. The residue was treated with water, followed by extraction with diethyl ether, drying over $MgSO_4$ and removal of the solvent under vacuum. The crude products were purified by silica gel (neutral) column chromatography eluted with hexane/dichloromethane. Recrystallization from hexane/dichloromethane gave a yellow solid in 50% yield (0.918 g, 0.763 mmol). ^{1}H NMR ($CDCl_3$): δ = 8.77 (d, *J* = 8.3 Hz, 2H, Ar*H*), 8.47 (m, 4H, Ar*H*), 8.23 (d, *J* = 8.3 Hz, 1H, Ar*H*), 7.63 (dd, *J* = 8.4, 5.3 Hz, 2H, Ar*H*), 7.52–7.44 (m, 12H, Ar*H*), 7.28–7.25 (m, 6H,

Ar*H*), 2.18 (t, *J* = 7.6 Hz, 4H, –CO–C*H*$_2$–), 1.23 (br, 8H, –C*H*$_2$–), 1.15 (br, 8H, –C*H*$_2$–), 1.09 (br, 8H, –C*H*$_2$–, 0.96 (br, 8H, –C*H*$_2$–), 0.83 (m, 6H, –CH$_3$) ppm. ^{11}B NMR ($CDCl_3$): δ = 6.74 ppm. ^{13}C NMR ($CDCl_3$): δ = 177.48 (*C*=O), 143.16 (Ar), 142.91 (Ar), 142.61 (Ar), 140.18 (Ar), 139.91 (Ar), 138.30 (Ar), 133.84 (Ar), 133.40 (Ar), 129.61 (Ar), 127.87 (Ar), 127.25 (Ar), 126.39 (Ar), 123.58 (Ar), 120.21 (Ar), 81.71 (Ar–I), 38.45 (–CO–*C*H$_2$–), 31.84, 29.49, 29.38, 29.32, 29.24, 29.08, 25.20, 22.65, 14.11 (–*C*H$_3$). IR (KBr): ν = 3069, 3048, 3013, 2926, 2855, 1647 (C=O), 1574 (Ar–H), 1503, 1462, 1433, 1387, 1308, 1207, 1190, 1148, 1107, 1057, 1043, 1003, 961, 878, 841, 818, 781, 739, 708, 665, 644 cm^{-1}. HRMS (FAB+): m/z: Calcd for $C_{60}H_{70}B_2I_2N_4O_2$: 1202.3774; found: 1202.3813 $[M]^+$. Anal. Calcd for $C_{60}H_{70}B_2I_2N_4O_2$: C, 63.91; H, 5.87; N, 4.66. Found: C, 63.47; H, 5.81; N, 4.60.

Synthesis of 2,2'-Bis(phenylbromoboryl)-5,5'-bithiophene (3T). A solution of 2,2'-bis(dibromoboryl)-5,5'-bithiophene (1.50 g, 3.00 mmol) in toluene (90 mL) was cooled to –78 ºC and then trimethyl(phenyl)tin was added. The reaction mixture was slowly allowed to warm up to room temperature, and left stirring for 16 h. All volatile components were removed under a high vacuum, and the solid was washed with CH_2Cl_2 and hexane to give a crude product (1.08 g), which was used without further purification.

Synthesis of Monomer (4T). The crude product **3T** (0.750 g), *N*-(5-iodo-8-quinolyl)undecanamide (1.45 g, 3.30 mmol), and triethylamine (0.42 mL, 3.0 mmol) were dissolved in toluene (30 mL). After the reaction mixture was refluxed for 12 h, water was added, followed by extraction with diethyl ether, drying over $MgSO_4$ and removal of the solvent under vacuum. The crude products were purified by silica gel (neutral) column chromatography eluted with dichloromethane. Recrystallization from hexane/dichloromethane gave a yellow solid in 47% yield (0.856 g, 0.705 mmol). ^{1}H NMR ($CDCl_3$): δ = 8.73 (dd, *J* = 8.3, 4.2 Hz, 2H, Ar*H*), 8.49 (d, *J* = 8.3 Hz, 2H, Ar*H*), 8.42 (d, *J* = 4.9 Hz, 2H, Ar*H*), 8.23 (dd, *J* = 8.4, 3.1 Hz, 2H, Ar*H*),

7.64 (m, 2H, Ar*H*), 7.54 (d, *J* = 3.9 Hz, 4H, Ar*H*), 7.26 (m, 6H, Ar*H)*, 7.08 (m, 4H, Ar*H*), 2.26 (m, 4H, -–CO–CH_2–), 1.35–0.98 (br, 32H, –CH_2–), 0.85 (m, 6H, –CH_3) ppm. ^{11}B NMR ($CDCl_3$): δ = 4.40 ppm. ^{13}C NMR ($CDCl_3$): δ = 177.31 (*C*=O), 143.37 (Ar), 142.57 (Ar), 142.41 (Ar), 140.63 (Ar), 130.18 (Ar), 137.73 (Ar), 133.02 (Ar), 132.81 (Ar), 132.49 (Ar), 132.24 (Ar), 129.61 (Ar), 127.95 (Ar), 127.61 (Ar), 124.18 (Ar), 123.94 (Ar), 123.66 (Ar), 123.45 (Ar), 120.22 (Ar), 81.93 (Ar–I), 38.27 (–CO–*C*H_2–), 31.85, 29.48, 29.36, 29.25, 29.07, 25.18, 22.65, 14.12 (–*C*H_3). IR (KBr): ν = 3071, 3049, 3005, 2924, 2852, 1653 (C=O), 1591, 1574 (Ar–H), 1501, 1460, 1433, 1412, 1387, 1371, 1308, 1283, 1211, 1148, 1103, 1057, 1043, 961, 885, 841, 804, 781, 725, 706, 669, 648 cm^{-1}. HRMS (FAB+): m/z: Calcd for $C_{60}H_{60}B_2I_2N_6O_4$: 1214.2903; found: 1214.2869 [*M*]$^+$. Anal. Calcd for $C_{60}H_{66}B_2I_2N_4O_2S_2$: C, 59.32; H, 5.48; N, 4.61. Found: C, 59.12; H, 5.35; N, 4.53.

Synthesis of Polymer (6PO). A typical procedure is shown as follows: Triethylamine (0.70 mL) was added to a solution of **4** (0.168 g, 0.14 mmol), 1,4-diethynyl-2,5-dioctyloxybenzene (0.054 g, 0.140 mmol), $Pd(PPh_3)_4$ (8.10 mg, 7.00 μmol), CuI (1.30 mg, 7.00 μmol) in THF (1.40 mL) at room temperature. After the mixture was stirred at 40 °C for 48 h, a small amount of $CHCl_3$ was added and poured into a large excess of methanol to precipitate the polymer. The polymer was purified by repeated precipitations from a small amount of $CHCl_3$ into a large excess of methanol and hexane respectively to give a red solid in 91% yield (0.169 g, 0.127 mmol). M_n = 34,000. ^{1}H NMR ($CDCl_3$): δ = 8.96 (4H, Ar*H*), 8.49 (2H, Ar*H*), 8.00 (2H, Ar*H*), 7.59 (2H, Ar*H*), 7.51 (12H, Ar*H*), 7.28 (4H, Ar*H*), 7.24 (2H, Ar*H*), 7.09 (2H, Ar*H*), 4.10 (4H, –OCH_2–), 2.21 (4H, –CO–CH_2–), 1.90 (4H, –CH_2–), 1.53 (4H, –CH_2–), 1.34 (4H, –CH_2–), 1.22-1.08 (36H, –CH_2–), 0.96 (8H, –CH_2–), 0.81 (12H, –CH_3) ppm. ^{11}B NMR ($CDCl_3$): δ = 2.93 ppm. ^{13}C NMR ($CDCl_3$): δ = 177.57 (*C*=O), 153.62 (Ar), 142.28 (Ar), 139.92 (Ar), 137.60 (Ar), 133.94 (Ar), 133.44 (Ar), 128.21 (Ar), 127.87 (Ar), 127.25 (Ar), 126,39 (Ar), 122.73 (Ar),

118.44 (Ar), 115.69 (Ar), 113.48 (Ar), 111.33 (Ar), 91.51 (–C≡C–), 91.13 (–C≡C–), 69.32 (–O*C*H_2–), 38.53 (–CO–*C*H_2–), 31.87, 31.74, 29.51, 29.40, 29.25, 26.02, 25.28, 22.66, 22.60, 14.12 (-*C*H_3), 14.06 (–*C*H_3) ppm. IR (KBr): ν = 3069, 3049, 3010, 2930, 2909, 2845, 2197 (C≡C), 1653 (C=O), 1570 (Ar–H), 1499, 1476, 1431, 1395, 1373, 1310, 1273, 1215, 1190, 1144, 1067, 1001, 876, 847, 818, 783, 737, 706, 683, 654 cm^{-1}. Anal. Calcd for $C_{90}H_{106}B_2N_4O_4$: C, 81.31; H, 8.04; N, 4.21. Found: C, 79.38; H, 7.98; N, 4.03.

Synthesis of Polymer (6PF). Similarly to the preparation of **6PO**, polymer **6PF** was prepared from monomer **4P** (0.144 g, 0.120 mmol) and 1.4-diethynyl-2-perfluorooctyl-5-trifluoromethylbenzene (0.0735 g, 0.120 mmol) in 85% yield as a yellow solid. M_n = 15,400. ^{1}H NMR ($CDCl_3$): δ = 8.98 (2H, Ar*H*), 8.80 (2H, Ar*H*), 8.52 (2H, Ar*H*), 8.09 (3H, Ar-*H*), 7.98 (1H, Ar*H*), 7.71 (1H, Ar*H*), 7.64 (1H, Ar*H*), 7.52 (12H, Ar*H*), 7.28 (4H, Ar*H*), 7.24 (1H, Ar*H*), 7.09 (1H, Ar-*H*), 2.22 (4H, –CO–CH_2–), 1.24–1.08 (24H, –CH_2–), 0.96 (8H, –CH_2–), 0.83 (6H, –CH_3) ppm. ^{11}B NMR ($CDCl_3$): δ = 5.18 ppm. IR (KBr): ν = 3071, 3049, 3011, 2928, 2855, 2203 (C≡C), 1663 (C=O), 1614, 1572 (Ar–H), 1499, 1476, 1433, 1395, 1379, 1310, 1240, 1213, 1202, 1148, 1117, 1088, 1053, 1016, 1003, 978, 878, 851, 820, 783, 737, 706, 677, 656 cm^{-1}. Anal. Calcd for $C_{83}H_{72}B_2F_{20}N_4O_2$: C, 63.94; H, 4.65; N, 3.59. Found: C, 63.13; H, 4.62; N, 3.56.

Synthesis of Polymer (6TO). Similarly to the preparation of **6PO**, polymer **6TO** was prepared from monomer **4T** (0.122 g, 0.100 mmol) and 1,4-diethynyl-2,5-dioctyloxybenzene (0.0383 g, 0.100 mmol) in 88% yield as a red solid. M_n = 27,900. ^{1}H NMR ($CDCl_3$): δ = 8.98 (2H, Ar*H*), 8.80 (2H, Ar*H*), 8.52 (2H, ArH), 8.09 (3H, Ar*H*), 7.98 (1H, Ar*H*), 7.71 (1H, Ar*H*), 7.64 (1H, Ar*H*), 7.52 (12H, Ar*H*), 7.28 (4H, Ar*H*), 7.24 (1H, Ar*H*), 7.09 (1H, Ar*H*), 2.22 (4H, –CO–CH_2–), 1.24–1.08 (24H, –CH_2–), 0.96 (8H, –CH_2–), 0.83 (6H, –CH_3) ppm. ^{11}B NMR ($CDCl_3$): δ = 2.15 ppm. ^{13}C NMR ($CDCl_3$): δ = 177.40 (*C*=O), 153.63 (Ar), 148.21 (Ar), 145.55 (Ar), 141.81 (Ar), 140.50 (Ar), 140.24 (Ar), 139.09 (Ar), 137.08 (Ar), 135.93 (Ar), 134.55 (Ar),

132.97 (Ar), 132.39 (Ar), 128.22 (Ar), 127.96 (Ar), 127.61 (Ar), 124.14 (Ar), 122.71 (Ar), 118.45 (Ar), 115.75 (Ar), 113.50 (Ar), 111.52 (Ar), 91.61 (–C≡C–), 91.04 (–C≡C–), 69.33 (–O*C*H_2–), 38.36 (–CO–*C*H_2–), 31.88, 31.74, 29.58, 29.51, 29.40, 29.32, 29.26, 29.11, 26.02, 25.26, 22.68, 22.60, 14.14 (–*C*H_3), 14.07 (–*C*H_3). IR (KBr): ν = 3070, 3051, 3005, 2924, 2853, 2199 (C≡C), 1653 (C=O), 1570 (Ar–H), 1499, 1468, 1431, 1395, 1375, 1312, 1271, 1217, 1190, 1146, 1113, 1067, 1051, 1024, 912, 885, 849, 804, 783, 758, 739, 704, 655 cm^{-1}. Anal. Calcd for $C_{86}H_{102}B_2N_4O_4S_2$: C, 77.00; H, 7.66; N, 4.18. Found: C, 75.67; H, 7.41; N, 4.00.

Synthesis of Polymer (6TF). Similarly to the preparation of **6PO**, polymer **6TF** was prepared from monomer **4T** (0.146 g, 0.120 mmol) and 1.4-diethynyl-2-perfluorooctyl-5-trifluoromethylbenzene (0.0735 g, 0.120 mmol) in 89% yield as a yellow solid. M_n = 12,600. ^{1}H NMR ($CDCl_3$): δ = 8.94 (2H, Ar*H*), 8.83–8.74 (2H, Ar*H*), 8.49 (2H, Ar*H*), 8.11–7.98 (4H, Ar*H*), 7.72–7.55 (6H, Ar*H*), 7.28 (6H, Ar*H*), 7.10 (4H, Ar*H*), 2.30 (4H, –CO–CH_2–), 1.16–1.10 (24H, –CH_2-), 1.00 (8H, –CH_2–), 0.84 (6H, –CH_3) ppm. ^{11}B NMR ($CDCl_3$): δ = 3.52 ppm. IR (KBr): ν = 3073, 3051, 2926, 2855, 2203 (C≡C), 1663 (C=O), 1570 (Ar–H), 1501, 1474, 1433, 1395, 1379, 1312, 1240, 1213, 1200, 1170, 1146, 1117, 1070, 1053, 910, 851, 810, 783, 743, 704, 656 cm^{-1}. Anal. Calcd for $C_{83}H_{72}B_2F_{20}N_4O_2$: C, 63.94; H, 4.65; N, 3.59. Found: C, 63.13; H, 4.62; N, 3.56.

Synthesis of N-(5-Iodo-8-quinolyl)-N-(diphenylboryl)undecanamide (7). Triphenylborane (0.969 g, 4.00 mmol) and *N*-(8-quinolyl)undecanamide (1.75 g, 4.00 mmol) were dissolved in toluene (24 mL). After the reaction mixture was refluxed for 12 h, the solvent was removed under vacuum. The crude product was purified by precipitation from a small amount of CH_2Cl_2 into a large excess of hexane, followed by precipitation from a small amount of $CHCl_3$ into a large excess of methanol to give a yellow solid in 57% yield (1.37 g, 2.27 mmol). ^{1}H NMR ($CDCl_3$) δ = 8.76 (d, *J* = 8.4 Hz, 1H, Ar*H*), 8.48 (d, *J* = 8.4 Hz, 1H, Ar*H*), 8.44 (d, *J* = 4.8 Hz, 1H, Ar*H*), 8.23 (d, *J* = 8.4 Hz, 1H, Ar*H*), 7.63 (dd, *J* = 8.4, 5.2 Hz, 1H, Ar*H*), 7.45 (m,

4H, Ar*H*), 7.29–7.25 (m, 6H, Ar*H*), 2.16 (t, *J* = 7.6 Hz, 2H, –CO–CH_2–), 1.26-1.09 (m, 12H, –CH_2–), 0.96 (m, 4H, –CH_2–), 0.87 (t, *J* = 8.0 Hz, –CH_3) ppm. ^{11}B NMR ($CDCl_3$): δ = 6.45 ppm. ^{13}C NMR ($CDCl_3$): δ = 177.47 (*C*=O), 143.12 (Ar), 142.94 (Ar), 142.59 (Ar), 140.15 (Ar), 138.30 (Ar), 133.41 (Ar), 129.58 (Ar), 127.84 (Ar), 127.21 (Ar), 123.55 (Ar), 120.19 (Ar), 81.65 (Ar-I), 38.41 (–CO–*C*H_2–), 31.88, 29.50, 29.37, 29.27, 29.03, 25.16, 22.66, 14.11 (-*C*H_3) ppm. IR (KBr): ν = 3071, 3048, 3005, 2924, 2853, 1645 (C=O), 1576 (Ar–H), 1504, 1460, 1433, 1412, 1387, 1368, 1337, 1308, 1227, 1209, 1190, 1146, 1113, 1055, 1043, 961, 895, 878, 835, 781, 741, 704, 642 cm^{-1}. HRMS (EI): m/z: Calcd for $C_{32}H_{36}BIN_2O$: 602.1965; found: 602.1955 [*M*]$^+$. Anal. Calcd for $C_{32}H_{36}BIN_2O$: C, 63.81; H, 6.02; N, 4.65. Found: C, 63.63; H, 5.98; N, 4.69.

Synthesis of Model compound (8). Triethylamine (2.0 mL) was added to a solution of *N*-(5-iodo-8-quinolyl)-*N*-(diphenylboryl)undecanamide (0.482 g, 0.800 mmol), 1,4-diethynyl-2,5-dioctyloxybenzene (0.153 g, 0.400 mmol), $Pd(PPh_3)_4$ (23.1 mg, 20.0 μmol), CuI (3.80 mg, 20.0 μmol) in THF (4.0 mL) at room temperature. After the mixture was stirred at 40 °C for 24 h, the solvent was removed under vacuum. The crude was precipitated from a small amount of $CHCl_3$ into a large excess of methanol twice. The precipitate was purified by recrystallization from hexane/dichloromethane to give a red solid in 68% (0.359 g, 0.273 mmol). ^{1}H NMR ($CDCl_3$): δ = 9.01 (d, *J* = 8.4 Hz, 2H, Ar*H*), 8.95 (d, *J* = 8.0 Hz, 2H, Ar*H*), 8.48 (d, *J* = 4.4 Hz, 2H, Ar*H*), 8.00 (d, *J* = 8.4 Hz, 2H, Ar*H*), 7.61 (dd, *J* = 8.0, 5.6 Hz, 2H, Ar*H*), 7.49 (m, 8H, Ar*H*), 7.29 (m, 10H, Ar*H*), 7.10 (s, 2H, Ar*H*), 4.11 (t, *J* = 6.8 Hz, 4H, –OCH_2–), 2.19 (t, *J* = 7.6 Hz, 4H, –CO–CH_2–), 1.93 (m, 4H, –CH_2–), 1.53 (m, 4H, –CH_2–), 1.36 (m, 4H, –CH_2–), 1.23–1.12 (m, 36H, –CH_2–), 0.97 (m, 8H, –CH_2–), 0.87 (t, *J* = 7.2 Hz, 12H, –CH_3), 0.82 (t, *J* = 6.8 Hz, 6H, –CH_3) ppm. ^{11}B NMR ($CDCl_3$): δ = 6.26 ppm. ^{13}C NMR ($CDCl_3$): δ = 177.56 (*C*=O), 153.64 (Ar), 142.33 (Ar), 140.05 (Ar), 138.78 (Ar), 137.60 (Ar), 135.93 (Ar), 133.46 (Ar), 128.19 (Ar), 127.84 (Ar), 127.19 (Ar), 122.72 (Ar), 118.38 (Ar), 115.80 (Ar), 113.54 (Ar), 111.28 (Ar), 91.47

(–C≡C–), 91.11 (–C≡C–), 69.37 (–O*C*H_2–), 38.48 (–CO–*C*H_2–), 31.89, 31.73, 29.57, 29.51, 29.40, 29.28, 29.24, 29.06, 26.03, 25.23, 22.67, 22.58, 14.11 (–*C*H_3), 14.03 (–*C*H_3) ppm. IR (KBr): ν = 3071, 3049, 3005, 2924, 2853, 2201 (–C≡C–), 1653 (C=O), 1570 (Ar–H), 1499, 1476, 1429, 1395, 1377, 1312, 1275, 1217, 1190, 1144, 1051, 877, 847, 820, 785, 760, 739, 704, 644 cm^{-1}. HRMS (FAB+): m/z: Calcd for $C_{90}H_{108}B_2N_4O_4$: 1330.8557; found: 1330.8547 $[M]^+$. Anal. Calcd for $C_{90}H_{108}B_2N_4O_4$: C, 81.19; H, 8.18; N, 4.21. Found: C, 81.12; H, 8.18; N, 4.23.

References

(1) Kraft, A.; Grimsdale, A. C.; Holmes, A. B. *Angew. Chem. Int. Ed.* **1998,** *110,* 402.

(2) Hide, F.; Diaz-Garcia, M. A.; Schwartz, B. J.; Heeger A. *J. Acc. Chem. Res.* **1997,** *30,* 430.

(3) Screen, T. E. O.; Lawton, K. B.; Wilson, G. S.; Dolney, N.; Ispasoiu, R.; Goodson III, T.; Martin, S. J.; Bradley, D. D. C.; Anderson, H. L. *J. Mater. Chem.* **2001,** *11,* 312.

(4) Yu, G.; Gao, J.; Hummelen, J. C.; Wudl, F.; Heeger, A. J. *Science* **1995,** *270,* 1789.

(5) Chang, S. C.; Liu, J.; Bharathan, J.; Yang, Y.; Onohara, J.; Kido, J. *Adv. Mater.* **1999,** *11,* 734.

(6) Jiang, H.; Taranekar, P.; Reynolds, J. R.; Schanze, K. S. *Angew. Chem. Int. Ed.* **2009,** *48,* 4300.

(7) Grimsdale A. C.; Chan K L; Martin Rainer E.; Jokisz P. G.; Holmes A. B. *Chem. Rev.* **2009,** *109,* 897.

(8) Beaujuge, P. M.; Reynolds, J. R. *Chem. Rev.* **2010,** *110,* 268.

(9) Donuru, V. R.; Vegesna, G. K.; Velayudham, S.; Meng, G.; Liu, H. *J Polym Sci Part A: Polym Chem* **2009,** *47,* 5354.

(10) Baier, M. C.; Huber, J.; Mecking, S. *J. Am. Chem. Soc.* **2009,** *131,* 14267.

(11) Alemdaroglu, F. E.; Alexander, S. C.; Ji, D.; Prusty, D. K.; Börsch M.; Herrmann A. *Macromolecules* **2009,** *42,* 6529.

(12) Nagai, A.; Chujo, Y. *Macromolecules* **2010,** *43,* 193.

(13) Loudet, A.; Burgess, K. *Chem. Rev.* **2007,** *107,* 4891.

(14) Cogné-Laage, E.; Allemand, J.-F.; Ruel, O.; Baudin, J.-B.; Croquette, V.; Blanchard-Desce, M.; Jullien, L. *Chem.-Eur. J.* **2004,** *10,* 1445.

(15) Nagai, A.; Kokado, K.; Nagata, Y.; Chujo, Y. *Macromolecules* **2008,** *41,* 8295.

(16) Wu, Q.; Esteghamatian, M.; Hu, N.-X.; Popovic, Z.; Enright, G.; Tao. Y.; D'Iorio, M.; Wang, S. *Chem. Mater.* **2000,** *12,* 79.

(17) Tang, C.W.; Vanslyke, S. A. *Appl. Phys. Lett.* **1987,** *51,* 913.

(18) Nagata, Y.; Chujo, Y. *Macromolecules* **2007,** *40,* 6.

(19) Nagata, Y.; Chujo, Y. *Macromolecules* **2008,** *41,* 3488.

(20) Li, H.; Jäkle, F. *Macromolecules* **2009,** *42,* 3448.

(21) Nagata, Y.; Otaka, H.; Chujo, Y. *Macromolecules* **2008,** *41,* 737.

(22) Tokoro, Y.; Nagai, A.; Chujo, Y. *Appl. Org. Chem.* **2010,** *51,* 3451.

(23) Sudaraman, A.; Venkatasubbaiah, K.; Victor, M.; Zakharov, L. N.; Rheingold, A. L.; Jäkle, F. *J. Am. Chem. Soc.* **2006,** *128,* 16554.

(24) Nagai, A.; Miyake, J.; Kokado, K.; Nagata, Y.; Chujo, Y. *Macromolecules* **2009**, *42,* 1560.

(25) Weder, C.; Wrighton, M. S. *Macromolecules* **1996,** *29,* 5157.

(26) Kokado, K.; Chujo, Y. *Macromolecules* **2009,** *42,* 1418-1420.

(27) Frisch, M. J.; Trucks, G. W.; Schlegel, H. B.; Scuseria, G. E.; Robb, M. A.; Cheeseman, J. R.; Montgomery, J. A., Jr.; Vreven, T.; Kudin, K. N.; Burant, J. C.; Millam, J. M.; Iyengar, S. S.; Tomasi, J.; Barone, V.; Mennucci, B.; Cossi, M.; Scalmani, G.; Rega, N.; Petersson, G. A.; Nakatsuji, H.; Hada, M.; Ehara, M.; Toyota, K.; Fukuda, R.; Hasegawa, J.; Ishida, M.; Nakajima, T.; Honda, Y.; Kitao, O.; Nakai, H.; Klene, M.; Li, X.; Knox, J. E.; Hratchian, H. P.; Cross, J. B.; Adamo, C.; Jaramillo, J.; Gomperts, R.; Stratmann, R. E.; Yazyev, O.; Austin, A. J.; Cammi, R.; Pomelli, C.; Ochterski, J. W.; Ayala, P. Y.; Morokuma, K.; Voth, G. A.; Salvador, P.; Dannenberg, J. J.; Zakrzewski, V. G.; Dapprich, S.; Daniels, A. D.; Strain, M. C.; Farkas, O.; Malick, D. K.; Rabuck, A. D.; Raghavachari, K.; Foresman, J. B.; Ortiz, J. V.; Cui, Q.; Baboul, A. G.; Clifford, S.; Cioslowski, J.; Stefanov, B. B.; Liu, G.; Liashenko, A.; Piskorz, P.; Komaromi, I.; Martin, R. L.; Fox, D. J.; Keith, T.; Al-Laham, M. A.; Peng, C. Y.; Nanayakkara, A.; Challacombe, M.; Gill, P. M. W.; Johnson, B.; Chen, W.; Wong, M. W.; Gonzalez, C.; Pople, J. A. Gaussian 03, revision D.01; Gaussian, Inc., Wallingford, CT, 2004.

Chapter 4

Luminescent Chiral Organoboron 8-Aminoquinolate-Coordination Polymers

Abstract

The author has successfully synthesized optically active organoboron aminoquinolate-based coordination polymers bearing the chiral side chain derived from $_{L}$-alanine, and studied their optical behavior by UV-vis and photoluminescence spectroscopies. Higher absolute quantum yields (Φ_F) of the obtained polymers, measured by integrating sphere method, were observed with electron-withdrawing substituent (Φ_F = 0.80) than that with electron-donating substituent (Φ_F = 0.52). The CD study in the mixed solvent of $CHCl_3$ and DMF showed that the secondary structures of the obtained polymers were stabilized by hydrogen-bonding interaction in the side chain. From concentration dependence on the CD spectra, the chirality of the obtained polymers originated from the nature of one molecule.

Chapter 4

Introduction

Active current interests in light-emitting organoboron dyes encompass both biological and material sciences, as well as chemistry. Many fluorescent organoboron dyes have been used as chemical probes,[1] photosensitizers,[2] and optical sensing[3] due to large molar extinction coefficients and two-photon absorption cross sections, high emission quantum yields, and sensitivity to the surrounding medium.[4] Incorporation of them including boron 8-aminoquinolate as electroluminescent chromophores into π-conjugated polymer main chain,[5] i.e., π-conjugated organoboron polymer, is more attractive for applications as electroluminescent devices, organic field-effect transistors, photovoltaics, and so on.[6] Recently, designs of π-conjugated organoboron polymers can be prepared by three conceivable approaches; (i) cross-coupling reaction between organoboron dye having bis-iodo groups and diyne compound,[5a,c,d,e] (ii) additional coordination to π-conjugated polymer linker by boron compound,[5b,f] and (iii) direct coordination of two ligand-functionalized compound with diborylated compound.[5g] The approach (iii) had been left unattainable until Jäkle and coworkers recently succeeded in synthesis of π-conjugated organoboron quinolate polymers through boron-induced ether cleavage. Photoluminescence properties of these polymers can be tuned by varying the degree of conjugation of the linker between the quinolate groups.

In regard to functionalization of the organoboron dyes, boron 8-aminoquinolates are more attractive than boron 8-quinolinolate because the former can introduce an additional functional group by amide linkage. The organoboron dyes need stability toward several environments such as acid, base, heat, and light. To give these stabilities to the boron complexes, we selected introduction of chiral substituent by amide linkage as stabilization of polymer main chain coordinated boron complex; i.e., if it is possible to prepare π-conjugated organoboron complex-connected polymers carrying chiral side chain, the stability of polymer backbone would be

enhanced by secondary interactions of not only π-stacking between polymer backbone but also chirally stack between polymer side chain.[7] This strategy, in which the relationship between chirality and conjugation is stricter, is the construction of chiral polymers with stable and rigid structure such as helical structure.[8]

A particularly interesting moiety with amide group for chiral induction is derived from amino acid.[9] The combination of π-stacking and hydrogen-bonding interactions favors a more rigid chiral conformation. Therefore, it seems that the chiral amide side chain leads to safe preparation and stability of π-conjugated organoboron coordination polymer. Herein, the author reports novel synthesis of chiral organoboron coordination polymers exhibiting high fluorescence quantum yield.

Results and Discussion

Initially, the ligand *N*-hexanoyl-$_L$-alanine-*N'*-5-iodo-8-quinolylamide (**4**) was prepared from 8-aminoquinoline as starting compound according to Scheme 1. The reaction of this ligand (**4**) with 4,4'-bis(bromo(phenyl)boryl)biphenyl, which was treated with bis(dibromoboryl)biphenyl[10] and trimethyl(phenyl)tin by a modification of a literature procedure,[11] produced an organoboron aminoquinolate-based monomer **6** bearing bis-iodo and amide groups (Scheme 2). Monomer **6** was obtained as a yellow powder in 24% yield. Tetracoordination state of the boron atom of **6** was confirmed by the ^{11}B NMR spectrum in $CDCl_3$ (δ_B = 7.13 ppm). The basic structure of **6** was also identified by ^{1}H NMR, ^{13}C NMR, IR, and high resolution mass spectroscopies. However, ^{1}H NMR and ^{13}C NMR spectra of **6** showed the presence of many multiple peaks attributable to diastereomers, which originates from the stereogenic borons.[5g]

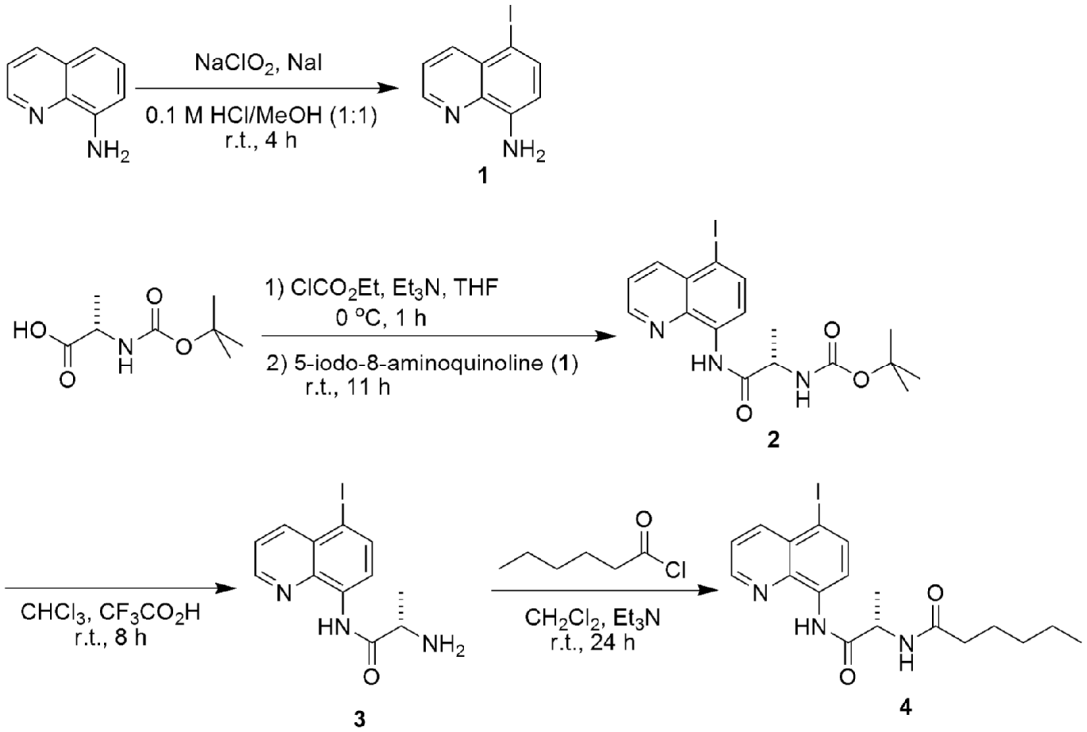

Scheme 1. Synthesis of *N*-hexanoyl-$_L$-alanine-*N'*-5-iodo-8-quinolylamide

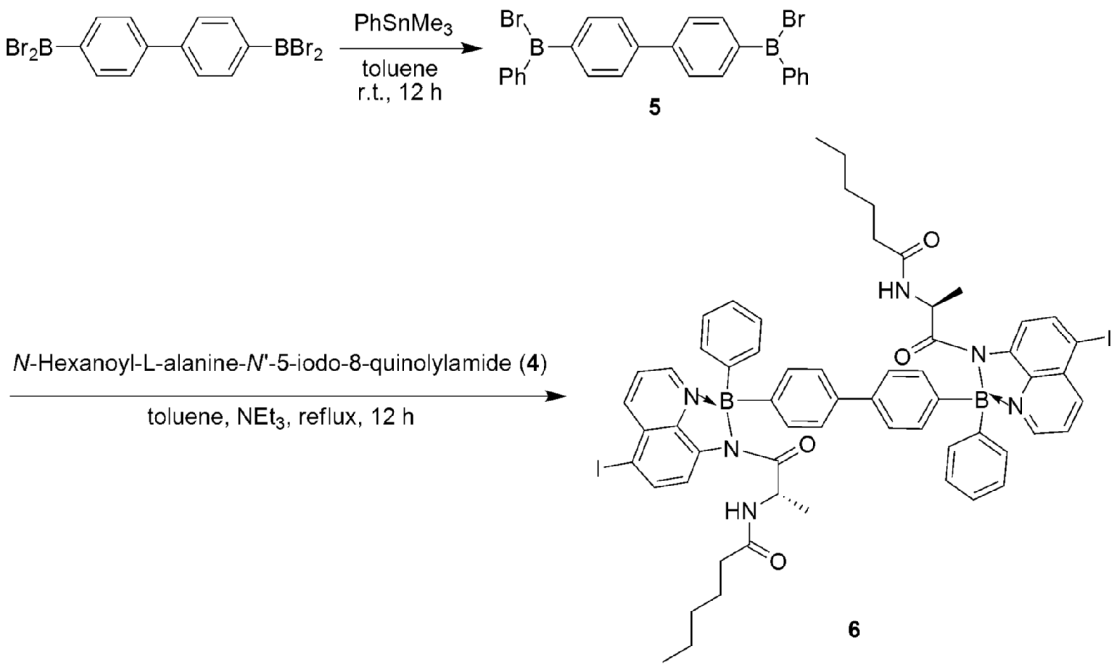

Scheme 2. Synthesis of monomer **6**

The Sonogashira-Hagihara coupling polymerization of **6** was conducted with 1,4-diethynyl-2,5-dioctyloxybenzene or 1,4-diethynyl-2-(perfluorooctyl)-5-(trifluoromethyl)benzene in the presence of $Pd(PPh_3)_4$ and CuI in the mixed solvent of tetrahydrofuran (THF) and triethylamine (NEt_3) at 40 ºC for 48 h (Scheme 3). The obtained polymers **poly1** and **poly2** were collected as orange and yellow solids, respectively, and were insoluble in methanol and their yields were 80% and 59%, respectively. The number-average molecular weights (M_n) and the molecular weight distributions (M_w/M_n) of **poly1** and **poly2**, measured by size-exclusion chromatography (SEC) in THF, were 5300 and 2.8, and 7900 and 3.1, respectively. The degrees of polymerization (DPs) estimated by M_n from SEC were 4.0 and 5.0 (**poly1** and **poly2**, respectively). The structures of the polymers were characterized spectroscopically. The ^1H, ^{11}B NMR, ^{13}C NMR, and IR spectra of the polymers exhibited signals reasonably assignable to the structures illustrated in Scheme 3. For example, the IR spectra of the polymers showed the absorption peaks at around 2208 cm^{-1}, which are attributable to stretching of the –C≡C– bond in the polymer backbone, and the characteristic peaks at 4.40–6.35 ppm, which are assigned to tetracoordination state of the boron atom of the polymers, clearly seen by ^{11}B NMR spectroscopy. These data indicate that the coupling reaction proceeded effectively without decomposition of the boron complex in the polymer main chain. The polymers were soluble in DMF, THF, $CHCl_3$, and CH_2Cl_2, and partly soluble in toluene, while insoluble in hexane, methanol, and acetone.

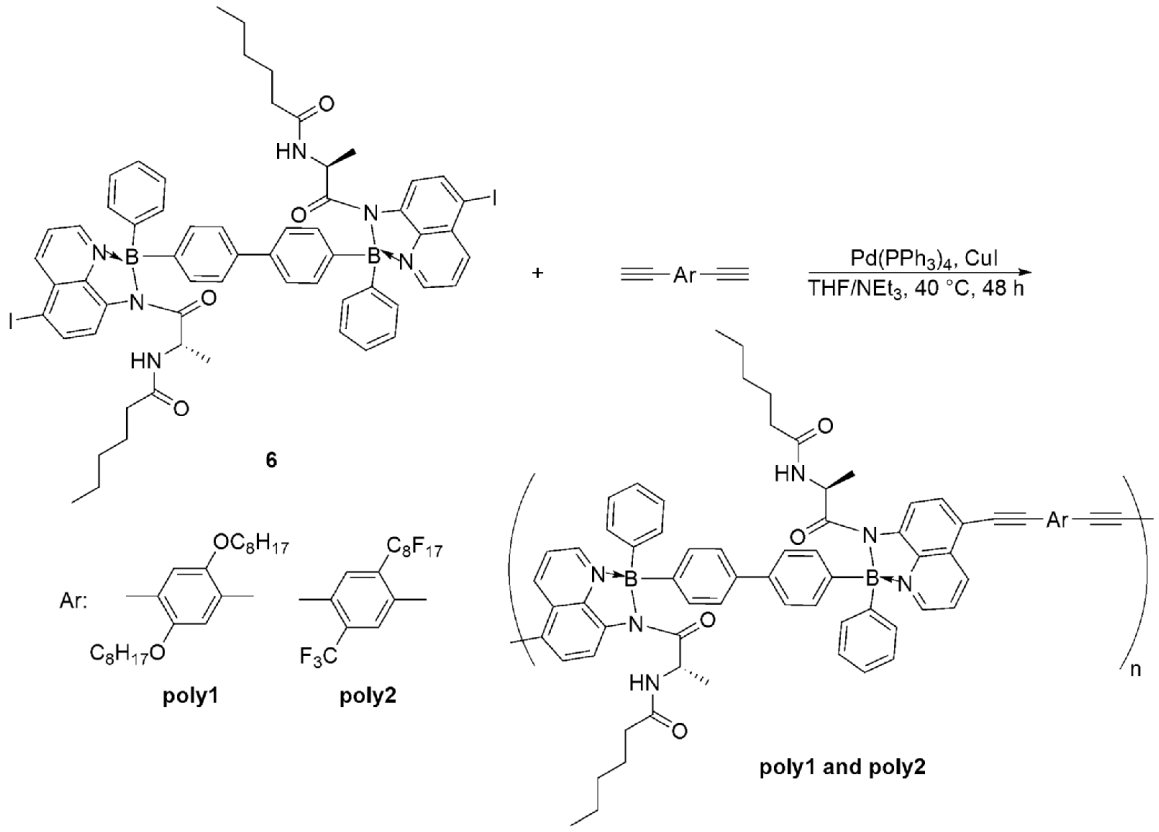

Scheme 3. Cross-coupling reaction of monomer **6** with diyne compounds

UV-vis absorption spectra of monomer and the obtained polymers were recorded in $CHCl_3$ (1.0×10^{-5} mol/L) as shown in Figure 1a. The absorption bands of all compounds at 268–270 nm could be commonly assigned to the absorption of biphenyl unit in the polymer chain, corresponding to π-π* transition. The monomer **6** showed the weak absorption band at 415 nm originating from the aminoquinoline ligand unit. In contrast to **6**, the absorption bands of both polymers (**poly1**: 461 nm, **poly2**: 446 nm) were red-shifted and significantly broadened to bathochromic side, and new bands of **poly1** and **poly2** appeared at 352 nm and 382 nm, respectively, attributable to *p*-phenylene-ethynylene units. The molar absorption coefficients (ε) of aminoquinoline moieties in the polymers (**poly1**: $\varepsilon = 0.38 \times 10^5$ $M^{-1}cm^{-1}$, **poly2**: $\varepsilon = 0.55 \times$

10^5 $M^{-1}cm^{-1}$) were higher than that in monomer (**6**: ε= 0.12 $\times$ 10^5 $M^{-1}cm^{-1}$). These results indicate that π-conjugation lengths of the polymers were extended along the polymer backbone. Further, the absorption band of **poly1** was bathochromically shifted in comparison with that of **poly2**, while the ε of **poly2** was higher than that of **poly1**. These bathochromic shifts should be caused by the electronic structures of comonomers, i.e., relation of donor-acceptor.[5d, 12] Figure 1b illustrates the emission bands of **6**, **poly1**, and **poly2** in $CHCl_3$ (1.0×10^{-5} mol/L). The emission of **poly2** was green color at 509 nm (excited at 446 nm), while it is almost identical to that at 516 nm of **6** (excited at 415 nm). In contrast, the emission band of **poly1** was red-shifted to bathochromic side as compared to those of **6** and **poly2** due to high electron-donating nature of the comonomer. Higher absolute quantum yields (Φ_F), measured by integrating sphere method, were observed with electron-withdrawing substituent (**poly2**: Φ_F = 0.80) than that with electron-donating substituent (**poly1**: Φ_F = 0.52),[12a] and **6** having bis-iodo groups on the aminoquinoline ligand displayed a lower Φ_F of 0.24 due to internal heavy-atom effect.[13] These observations suggest that the substituents in the comonomers should be responsible for the intensity of fluorescence of the obtained polymers.

To confirm the secondary structures of the obtained polymers stabilized by hydrogen-bonding interaction, which is stimulated in polar solvents such as DMF, the CD and UV-vis spectroscopic studies of **poly1** and **poly2** were carried out in the mixed solvent of $CHCl_3$/DMF as depicted in Figures 2a and b. In $CHCl_3$, the CD and UV-vis maxima of **poly1** were observed at 268, 352, and 461 nm, respectively, attributable to bisphenyl, *p*-phenylene-ethynylene and aminoquinoline units, respectively. Similarly, **poly2** also showed their signals at 272 nm and at around 446 nm, at which both *p*-phenylene-ethynylene and aminoquinoline units were overlapped. These data indicate that the ordered secondary structures in the main chain are

derived from chirality of amino acid moiety in the side chain, although it is difficult to completely control regulated higher-order structure such as helix due to the contamination of the diastereomeric conformations in the polymers. The CD signals of the polymers gradually decreased by increasing the DMF content, suggesting stabilization by hydrogen-bonding interaction. In contrast, the specific rotations ($[\alpha]^{25}_{D}$) of the polymers in $CDCl_3$ and DMF were not almost changed (**poly1**: –267 ° in $CHCl_3$ and –213 ° in DMF, and **poly2**: –264 ° in $CHCl_3$ and –279 ° in DMF). However, $[\alpha]^{25}_{D}$ of monomer **6** in $CHCl_3$ ($[\alpha]^{25}_{D}$ = –294 °) was higher than that in DMF ($[\alpha]^{25}_{D}$ = –192 °). These findings mean that the secondary structures of the obtained polymers were stabilized by stronger hydrogen-bonding interaction than that of the monomer. Next, the concentration dependence on the secondary structure of **poly1** was carried out in $CHCl_3$ (Figure 3). Increasing the concentration leads to both bathochromic shifts and decrease of the CD effect, and the CD signal of **poly1** almost completely disappeared at 1.0×10^{-3} mol/L. The observed concentration dependence clearly shows that the observed Cotton effects are not due to supramoleuclar aggregation but due to the nature of one macromolecule. Figures 4a and 4b illustrate the emission spectra of the polymers in the mixed solvent of $CHCl_3$/DMF. Similarly to CD effects of the polymers in the mixed solvents, the emission spectra of the polymers also gradually decreased together with shifting to bathochromic side by increase of the DMF content, ruling out the possibility of effect on hydrogen-bonding interaction in the polymers. In other hands, the red-shift and decrease of intensity in emission spectra mean the excited state after intramolecular charge transfer (CT) is stabilized in the polar solvent. Further, the intensity of **poly1** with electron-donating group exceedingly decreased in comparison with that of **poly2** having electron-withdrawing group due to higher stabilization of the charge separated state,[14] and the Φ_F of **poly1** (Φ_F = 0.15) was also smaller than that of **poly2** (Φ_F = 0.52) in DMF.

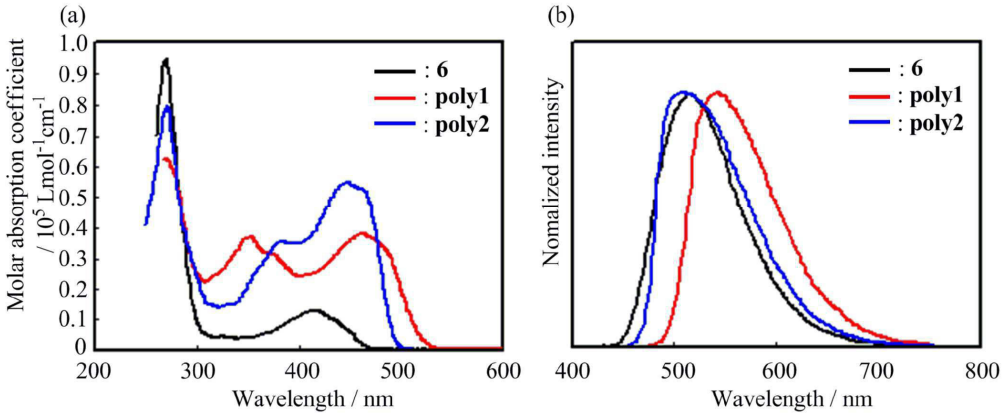

Figure 1. (a) UV-vis spectra of **6**, **poly1**, and **poly2** in $CHCl_3$(1.0×10^{-5} mol/L), and (b) normalized emission spectra of **6**, **poly1**, and **poly2** in $CHCl_3$ (1.0×10^{-5} mol/L).

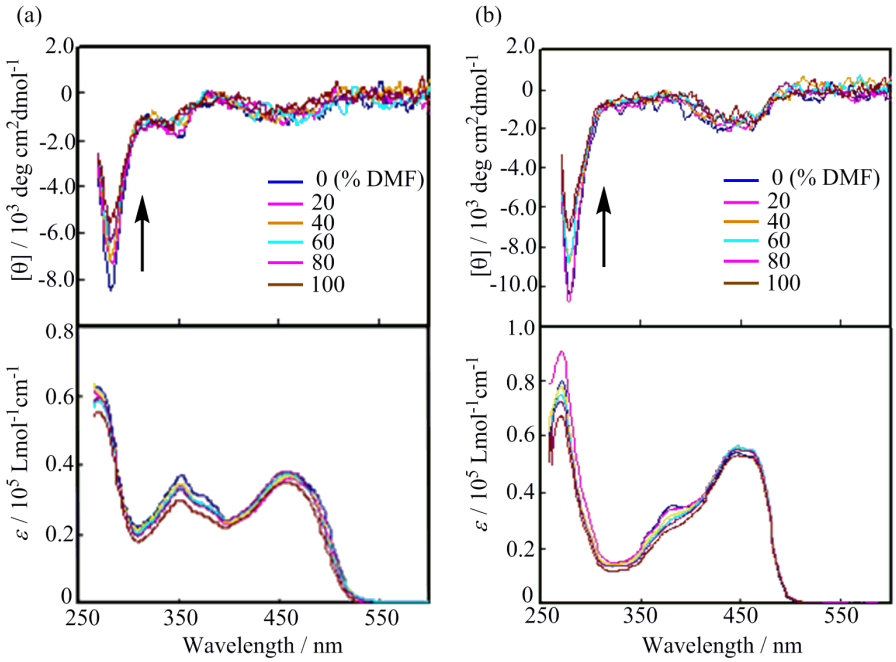

Figure 2. CD and UV-vis spectra of (a) **poly1** and (b) **poly2** in $CHCl_3$ and $CHCl_3$/DMF mixtures (1.0×10^{-5} mol/L).

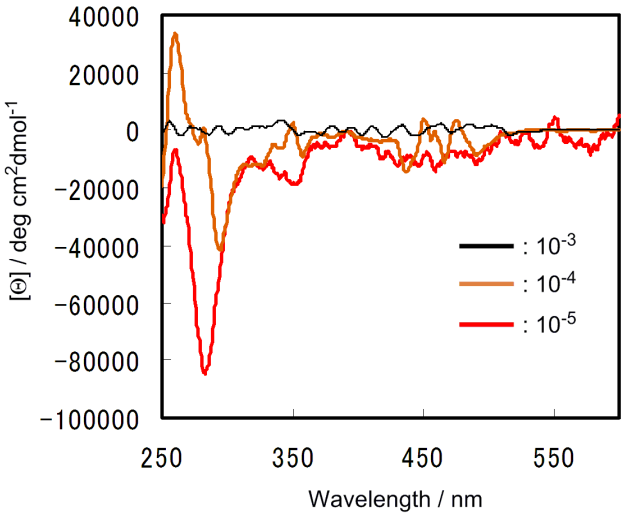

Figure 3. Concentration dependence in $CHCl_3$ of CD spectrum of **poly1.**

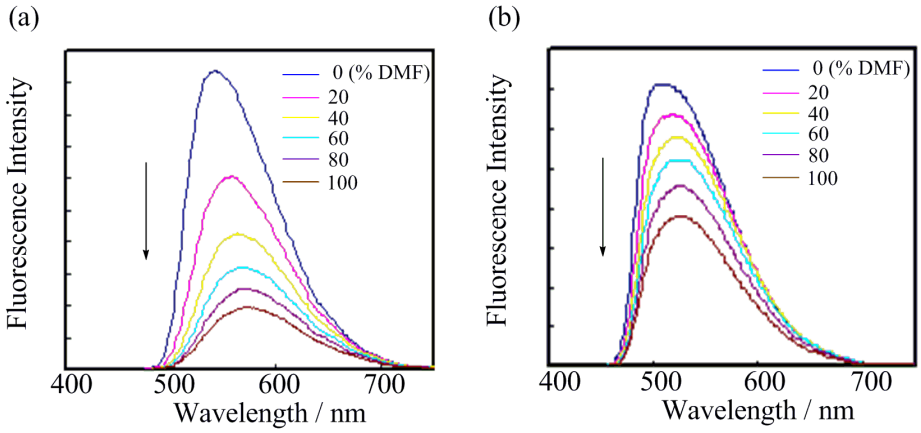

Figure 4. Emission spectra of (c) **poly1** and (d) **poly2** in $CHCl_3$ and $CHCl_3$/DMF mixtures (1.0 $\times$ 10^{-5} mol/L).

Conclusion

The author has successfully synthesized optically active organoboron aminoquinolate-based coordination polymers bearing the chiral side chain derived from $_{L}$-alanine, and studied their optical behavior by UV-vis and photoluminescence spectroscopies. The dependence of photoluminescence property on the solvent's polarity suggested the existence of intramolecular charge transfer. The CD study in the mixed solvents of $CHCl_3$ and DMF showed that the secondary structures of the obtained polymers were stabilized by hydrogen-bonding interaction in the side chain. The concentration dependence on the CD spectra demonstrated that the regulated high-order structures of the obtained polymers consist of macromolecules in nature.

Experimental Section

Measurements. ^{1}H (400 MHz), ^{13}C (100 MHz), and ^{11}B (128 MHz) NMR spectra were recorded on a JEOL JNM-EX400 spectrometer. ^{1}H and ^{13}C NMR spectra used tetramethylsilane (TMS) as an internal standard, ^{11}B NMR spectra were referenced externally to BF_3OEt_2 (sealed capillary) in $CDCl_3$. The number-average molecular weights (M_n) and molecular weight distribution [weight-average molecular weight/number-average molecular weight (M_w/M_n)] values of all polymers were estimated by size-exclusion chromatography (SEC) with a TOSOH G3000HXI system equipped with three consecutive polystyrene gel columns [TOSOH gels: α-4000, α-3000, and α-2500] and ultraviolet detector at 40 °C. The system was operated at a flow rate of 1.0 ml/min, with tetrahydrofuran as an eluent. Polystyrene standards were employed for calibration. UV-vis spectra were recorded on a Shimadzu UV-3600 spectrophotometer. Fluorescence emission spectra were recorded on a HORIBA JOBIN YVON Fluoromax-4 spectrofluorometer. FT-IR spectra were obtained using a Perkin-Elmer 1600 infrared spectrometer. Elemental analysis was performed at the Microanalytical Center of Kyoto University. All reaction was performed under nitrogen or argon atmosphere.

Materials. 1,4-Diethynyl-2,5-dioctyloxybenzene [15] , 4,4'-bis(dibromoboryl)biphenyl [16], and 1.4-diethynyl-2-perfluorooctyl-5-trifluoromethylbenzene [17] were prepared according to the literature. Tetrahydrofuran (THF) and triethylamine (Et_3N) were purified using a two-column solid-state purification system (Glasscontour System, Joerg Meyer, Irvine, CA). Other reagents were commercially available and used as received.

Synthesis of 5-Iodo-8-aminoquinoline (1). 0.1 M HCl (900 mL) was added to a solution of 8-aminoquinoline (13.0 g, 90.0 mmol), $NaClO_2$ (4.08 g, 45.0 mmol), and NaI (13.5 g, 90.0 mmol) in methanol, and the mixture was stirred at room temperature for 4 h. The precipitate was collected, and rinsed with aqueous $Na_2S_2O_3$ and water to afford 5-iodo-8-aminoquinoline in 68%

yield (16.6 g, 61.4 mmol). ^{1}H NMR ($CDCl_3$): δ = 5.07 (s, 2H, –N*H*$_2$), 6.72 (d, *J* = 8.0 Hz, 1H, quinoline ring, H_7), 7.45 (dd, *J* = 8.6, 4.1 Hz, 1H, H_3), 7.82 (d, *J* = 8.0 Hz, 1H, H_6), 8.27 (d, *J* = 8.6 Hz, 1H, H_4), 8.71 (d, *J* = 4.1 Hz, 1H, H_2) ppm. ^{13}C NMR (DMSO-d_6): δ = 147.60, 146.43, 139.19, 138.23, 138.11, 129.45, 123.43, 110.41, 77.85 (Ar-I). Anal. Calcd for $C_9H_7IN_2$: C, 40.03; H, 2.61; N, 10.37. Found: C, 40.14; H, 2.62; N, 10.35.

Synthesis of N-(tert-Butoxycarbonyl)-$_{L}$-alanine-N'-5-iodo-8-quinolylamide (2). *N*-(*tert*-Butoxycarbonyl)-L-alanine (3.41 g, 18.0 mmol) was dissolved in THF (90 mL), and triethylamine (2.50 mL, 18.0 mmol) and ethyl chlorocarbonate (1.72 mL, 18.0 mmol) were added to the mixture at 0 °C. After the mixture was stirred at 0 °C for 1 h, 5-iodo-8-aminoquinoline was added. The reaction was continued at 0 °C for 1 h, and then stirred at room temperature for 11 h. The resulting mixture was filtered, and the filtrate was concentrated under vacuum. The crude product was purified by silica gel column chromatography eluted with hexane/ethyl acetate to give a brown solid in 73 % yield (5.81 g, 13.2 mmol). ^{1}H NMR ($CDCl_3$): δ = 1.49 (m, 12H, –C*H*$_3$), 4.51 (m, 1H, -C*H*<), 5.19 (m, 1H), 7.53 (dd, *J* = 8.6, 4.0 Hz, 1H, Ar*H*), 8.07 (d, *J* = 8.3 Hz, 1H, Ar*H*), 8.36 (d, *J* = 8.6 Hz, 1H, Ar*H*), 8.53 (d, *J* = 8.3 Hz, 1H, Ar*H*), 8.77 (d, *J* = 4.0 Hz, 1H, Ar*H*), 10.36 (s, 1H, –N*H*–CO–CH<) ppm. ^{13}C NMR ($CDCl_3$): δ = 171.37 (–NH–*C*O–CH<), 155.34 (–NH–*C*O–O–), 148.83 (Ar), 140.59 (Ar), 139.11 (Ar), 138.09 (Ar), 135.02 (Ar), 129.54 (Ar), 123.15 (Ar), 117.88 (Ar), 89.68 (Ar–I), 80.23 (–O–*C*(CH$_3$)$_3$), 51.33 (–C*H*<), 28.33 (–O–C(*C*H$_3$)$_3$), 18.55 (>CH–*C*H$_3$) ppm. IR(KBr): ν = 3320, 2972, 2929, 1695, 1506, 1368, 1315, 1248, 1160, 1101, 1061, 1028, 942, 912, 861, 832, 784, 750, 704, 639 cm^{-1}. HRMS: m/z: Calcd for $C_{17}H_{20}IN_3O_3$: 441.0549; found: 441.0548 [*M*]$^{+}$. Anal. Calcd for $C_{17}H_{20}IN_3O_3$: C, 46.27; H, 4.57; N, 9.52. Found: C, 46.25; H, 4.64; N, 9.44.

Synthesis of Alanine-N'-5-iodo-8-aminoquinolylamide (3). N-(tert-Butoxycarbonyl)-$_{L}$-alanine-*N'*-5-iodo-8-quinolylamide (5.00 g, 11.3 mmol) was treated with TFA (17 mL) in $CHCl_3$

(17 mL) for 32 h. 10 % aqueous ammonia was added to the resulting mixture, followed by extraction with diethyl ether, drying over $MgSO_4$, and removal of the solvent to give a brown solid in 77.3% yield (2.98 g, 8.73 mmol). ^{1}H NMR ($CDCl_3$): δ = 1.52 (d, J = 7.48 Hz, 3H, –CH_3), 1.87 (s, 2H, –NH_2), 3.78 (q, J = 6.96 Hz, –C*H*<), 7.53 (dd, J = 4.28 and 8.44 Hz), 8.07 (d, J = 8.32 Hz, 1H, Ar*H*), 8.36 (dd, J = 8.56 and 1.48 Hz, 1H, Ar*H*), 8.60 (d, J = 8.32 Hz, 1H, Ar*H*), 8.83 (dd, J = 4.16 and 1.48 Hz, 1H, Ar*H*), 11.43 (s, 1H, –N*H*–CO–CH<) ppm. ^{13}C NMR ($CDCl_3$): δ = 174.61 (>*C*=O), 149.06 (Ar), 140.59 (Ar), 139.66 (Ar), 138.18 (Ar), 135.37 (Ar), 129.66 (Ar), 123.03 (Ar), 117.75 (Ar), 89.43 (Ar-I), 52.04 (–*C*H<), 21.77 (–*C*H_3) ppm. HRMS: m/z: Calcd for $C_{12}H_{12}IN_3O$: 341.0025; found: 341.0030 [M]$^+$. Anal. Calcd for $C_{12}H_{12}IN_3O_3$: C, 42.25; H, 3.55; N, 12.32. Found: C, 42.53; H, 3.71; N, 12.11.

Synthesis of N-Hexanoyl-$_L$-alanine-N'-5-iodo-8-quinolylamide (4). Alanine-*N'*-5-iodo-8-aminoquinolylamide (2.73 g, 8.00 mmol) and triethylamine (1.17 mL, 8.40 mmol) were dissolved in dichloromethane (36 mL), followed by addition of hexanoyl chloride (1.17 ml, 8.40 mmol). The resulting mixture was stirred at room temperature for 24 h. The mixture was transferred to a separating funnel and washed with aqueous $NaHCO_3$. The organic layer was dried over $MgSO_4$. Filtration and evaporation of the solvent gave a pale brown solid in 85.5% yield (3.01 g, 6.84 mmol). ^{1}H NMR ($CDCl_3$): δ = 0.88 (t, J = 6.8 Hz, 3H, –CH_2–CH_3), 1.33 (m, 4H, –CH_2–), 1.56 (d, J = 7.1 Hz, 3H, >CH–CH_3), 1.68 (m, 2H, –CH_2–), 2.28 (t, J = 7.6 Hz, 2H), 4.86 (m, 1H, –C*H*<), 6.24 (d, J = 7.1 Hz, 1H, –N*H*–CO–CH_2–), 7.54 (dd, J = 8.6, 4.1 Hz, 1H, Ar*H*), 8.07 (d, J = 8.3 Hz, 1H, Ar*H*), 8.36 (d, J = 8.6 Hz, 1H, Ar*H*), 8.48 (d, J = 8.3 Hz, 1H, Ar*H*), 8.78 (d, J = 4.1 Hz, 1H, Ar*H*), 10.20 (s, 1H, –N*H*–CO–CH<) ppm. ^{13}C NMR ($CDCl_3$): δ = 173.97 (>*C*=O), 170.91 (>*C*=O), 149.06 (Ar), 140.73 (Ar), 139.02 (Ar), 138.08 (Ar), 134.91 (Ar), 129.60 (Ar), 123.29 (Ar), 118.00 (Ar), 89.92 (Ar-I), 49.77 (–*C*H<), 36.65, 31.42, 25.34, 22.39, 18.92, 18.82, 13.93 ppm. IR(KBr): ν = 3280, 3059, 2927, 2865, 1698, 1652, 1540, 1474, 1380,

1357, 1315, 1250, 1211, 1151, 1103, 1076, 1036, 961, 934, 908, 837, 785, 724, 694 cm^{-1}. HRMS: m/z: Calcd for $C_{18}H_{22}IN_3O_2$: 439.0757; found: 439.0760 $[M]^+$. Anal. Calcd for $C_{18}H_{22}IN_3O_2$: C, 49.21; H, 5.05; N, 9.57. Found: C, 49.38; H, 5.06; N, 9.52.

Synthesis of Monomer (6). Trimethyl(phenyl)tin (4.78 mL, 26.3 mmol) was added to a solution of 4,4'-bis(dibromoboryl)biphenyl (6.49 g, 13.2 mmol) in toluene (263 mL) and the mixture was stirring for 14 h. All volatile components were removed under a high vacuum, and the crude product was washed with hexane. This product (1.17 g), *N*-hexanoyl-$_L$-alanine-*N'*-5-iodo-8-quinolylamide (2.11 g, 4.80 mmol), and triethylamine (0.67 mLl, 4.8 mmol) were dissolved in toluene (38 ml). After the reaction mixture was refluxed for 12 h, the solvent was removed by rotary evaporation. The residue was treated with water, followed by extraction with ethyl acetate, drying over $MgSO_4$ and removal of the solvent under vacuum. The crude product was purified by silica gel (neutral) column chromatography eluted with hexane/ethyl acetate. Recrystallization from hexane/dichloromethane gave a yellow solid in 24% yield (0.70 g, 0.58 mmol). ^{1}H NMR ($CDCl_3$): δ = 0.53 (6H, –CH_2–CH_3), 0.70 (1H), 0.86 (5H), 1.24 (8H, –CH_2–), 1.51 (4H, –CH_2–), 2.02 (4H, –CO–CH_2–), 4.71 (2H, –C*H*<), 6.18 (2H, –N*H*–CO–CH_2–), 7.27 (6H, Ar*H*), 7.37 (4H, Ar*H*), 7.52 (8H, Ar*H*), 7.70 (2H, Ar*H*), 8.26 (2H, Ar*H*), 8.53 (4H, Ar*H*), 8.72 (2H, Ar*H*) ppm. ^{11}B NMR ($CDCl_3$): δ = 7.13 ppm. ^{13}C NMR ($CDCl_3$): δ = 177.00 (>*C*=O), 171.11 (>*C*=O), 143.50 (Ar), 143.39 (Ar), 142.34 (Ar), 142.24 (Ar), 141.95 (Ar), 140.88 (Ar), 140.73 (Ar), 140.14 (Ar), 140.07 (Ar), 139.84 (Ar), 138.18 (Ar), 134.69 (Ar), 134.59 (Ar), 134.29 (Ar), 132.74 (Ar), 132.57 (Ar), 132.29 (Ar), 129.60 (Ar), 128.07 (Ar), 127.65 (Ar), 127.50 (Ar), 126.71 (Ar), 126.58 (Ar), 126.46 (Ar), 123.99 (Ar), 123.93 (Ar), 120.76 (Ar), 120.63 (Ar), 83.48 (Ar–I), 50.31 (–*C*H<), 36.50, 31.28, 25.32, 22.40, 18.75, 13.96 ppm. IR(KBr): ν = 3418, 3331, 3070, 3045, 3006, 2954, 2926, 2855, 1645, 1578, 1575, 1504, 1462, 1393, 1307, 1276, 1192, 1145, 1114, 1070, 1022, 1003, 962, 882, 840, 818, 782, 738, 706, 666, 642 cm^{-1}.

HRMS: m/z: Calcd for $C_{60}H_{60}B_2I_2N_6O_4$: 1204.2952; found: 1204.2997 $[M]^+$. Anal. Calcd for $C_{60}H_{60}B_2I_2N_6O_4$: C, 59.82; H, 5.02; N, 6.98. Found: C, 59.50; H, 4.88; N, 6.99.

Synthesis of Poly1. A typical procedure is shown as follows: Triethylamine (0.70 mL) was added to a solution of **6** (0.170 g, 0.14 mmol), 1,4-diethynyl-2,5-dioctyloxybenzene (0.053 g, 0.140 mmol), $Pd(PPh_3)_4$ (8.10 mg, 7.00 μmol), CuI (2.60 mg, 14.0 μmol) in THF (1.40 mL) at room temperature. After the mixture was stirred at 40 °C for 48 h, a small amount of $CHCl_3$ was added and poured into a large excess of methanol to precipitate the polymer. The polymer was purified by repeated precipitations from a small amount of $CHCl_3$ into a large excess of methanol and hexane respectively to give a red solid in 81% yield (0.15 g, 0.11 mmol). M_n = 5320. ^{1}H NMR ($CDCl_3$): δ = 0.55 (6H, –CH_2–CH_3), 0.70 (1H), 0.86 (9H), 1.23(20H, –CH_2–), 1.37 (6H), 1.53 (8H, –CH_2–), 1.94 (4H, –CH_2–), 2.02 (4H, –CO–CH_2–), 4.12 (4H), 4.74 (2H, –C*H*<), 6.22 (2H, –N*H*–CO–CH_2–), 7.11 (2H, Ar–*H*), 7.29 (6H, Ar*H*), 7.42 (4H, Ar*H*), 7.55 (8H, Ar*H*), 7.68 (2H, Ar*H*), 8.02 (2H, Ar*H*), 8.58 (2H, Ar*H*), 9.05 (2H, Ar*H*), 9.07 (2H, Ar*H*) ppm. ^{11}B NMR ($CDCl_3$): δ = 4.40 ppm. ^{13}C NMR ($CDCl_3$): δ = 177.08 (>*C*=O), 171.17 (>*C*=O), 153.70 (Ar), 141.29 (Ar), 140.72 (Ar), 137.59 (Ar), 135.48 (Ar), 134.65 (Ar), 134.32 (Ar), 132.85 (Ar), 132.69 (Ar), 132.39 (Ar), 128.12 (Ar), 127.64 (Ar), 127.50 (Ar), 126,74 (Ar), 126.60 (Ar), 126.49 (Ar), 123.11 (Ar), 119.00 (Ar), 115.7 (Ar), 113.49 (Ar), 112.67 (Ar), 92.03 (Ar), 90.91 (Ar), 69.35 (–O*C*H_2–), 50.47 (–*C*H<), 36.69, 36.62, 31.74, 31.46, 31.31, 29.57, 29.40, 29.26, 26.02, 25.36, 22.60, 22.43, 22.37, 22.30, 19.01, 18.82, 14.07, 13.96, 13.83 ppm. IR(KBr): ν = 3418, 2926, 2854, 2208 (–C≡C–), 1645, 1574, 1498, 1395, 1309, 1270, 1197, 1192, 1143, 1034, 1003, 860, 848, 820, 783, 738, 705 cm^{-1}. Anal. Calcd for $C_{86}H_{96}B_2N_6O_6$: C, 77.58; H, 7.27; N, 6.31. Found: C, 76.22; H, 7.03; N, 6.21.

Synthesis of Poly2. Yield = 59% (0.11 g, 0.07 mmol). M_n = 7880. ^{1}H NMR ($CDCl_3$): δ = 0.55 (6H, –CH_2–CH_3), 0.71 (1H), 0.87 (5H), 1.22 (8H, –CH_2–), 1.52 (4H, –CH_2–), 2.03 (4H, –

CO–C*H*$_2$–), 4.75 (2H, –C*H*<), 6.19 (2H, –N*H*–CO–CH$_2$–), 7.29 (4H, Ar*H*), 7.41 (6H, Ar*H*), 7.54 (8H, Ar*H*), 7.71 (1H, Ar*H*), 7.79 (1H, Ar*H*), 8.01 (1H, Ar*H*), 8.12 (3H, Ar*H*), 8.61 (2H, Ar*H*), 8.79 (1H, Ar*H*), 8.85 (1H, Ar*H*), 8.94 (2H, Ar*H*) ppm. ^{11}B NMR ($CDCl_3$): δ = 6.35 ppm. IR (KBr): ν = 3419, 3071, 3007, 2955, 2926, 2862, 2205 (–C≡C–), 1652, 1574, 1499, 1475, 1447, 1396, 1310, 1252, 1240 (C–F), 1201 (C–F), 1144 (C–F), 1035, 1003, 882, 849, 820, 783, 711, 706 cm^{-1}. Anal. Calcd for $C_{79}H_{62}B_2N_6O_4F_{20}$: C, 60.79; H, 4.00; N, 5.38. Found: C, 59.40; H, 4.07; N, 5.16.

References

(1) Haugland, R. P. *The Handbook-A Guide to Fluorescent Probes and Labeling Technologies*, 10th ed.; Spence, M. T. Z., Ed.; Molecular Probes: Eugene. OR, 2005; Chapter 1 Section 1.4.

(2) Gorman, A.; Killoran, J.; O'Shea, C.; Kenna, T.; Gallagher, W. M.; O'Shea, D. F. *J. Am. Chem. Soc.* **2004,** *126,* 10619.

(3) (a) García-Moreno, I.; Costela, A.; Campo, L.; Sastre, R.; Amat-Guerri, F.; Liras, M.; López Arbeloa, I. *J. Phys. Chem. A* **2004,** *108*, 3315. (b) Pavlopoulos, T. G.; Boyer, J. H.; Sathyamoorthi, G. *Appl. Opt.* **1998,** *37*, 7797.

(4) (a) Chow, Y. L.; Johansson, C. I; Zhang, Y.-H.; Gautron, R.; Yang, L.; Rassat, A.; Yang, S.-Z. *J. Phys. Org. Chem.* **1996,** *9,* 7. (b) Cogné-Laage, E.; Allemand, J.-F.; Ruel, O.; Baudin, J.-B.; Croquette, V.; Blanchard-Desce, M.; Jullien, L. *Chem. Eur. J.* **2004,** *10,* 1445. (c) Karolin, J.; Johansson, L. B.-Å.; Strandberg, L.; Ny, T. *J. Am, Chem. Soc.* **1994**, *116,* 7801. (d) Wan, C.–W.; Burghart, A.; Chen, J.; Bergström, F.; Johanson, L. B.-Å.; Wolford, M. F.; Kim, T. G.; Topp, M. R.; Hochstrasser, R. M.; Burgess, K. *Chem. Eur. J.* **2003**, *9*, 4430. (e) Wu, Q.; Esteghamatian, M.; Hu, N.–X.; Popovic, Z.; Enright, G.; Tao, Y.; D'Iorio, M.; Wang, S. *Chem. Mater.* **2000**, *12*, 79. (f) Kappaun, S.; Rentenberger, S.; Pogantsch, A.; Zojer, E.; Mereiter, K.; Trimmel, G.; Saf, R.; Möller, K. C.; Stelzer, F.; Slugovc, C. *Chem. Mater.* **2006**, *18*, 3539. (g) Cui, Y.; Wang, S. *J. Org. Chem.* **2006**, *71*, 6485. (h) Nagai, A.; Kokado, K.; Nagata, Y.; Chujo, Y. *J. Org. Chem.* **2008**, *73*, 8605.

(5) (a) Nagata, Y.; Chujo, Y. *Macromolecules* **2008**, *41*, 2809. (b) Nagata, Y.; Otaka, H.; Chujo, Y.; *Macromolecules* **2008**, *41*, 737. (c) Nagata, Y.; Chujo, Y. *Macromolecules*

2007, *40*, 6. (d) Nagata, Y.; Chujo, Y. *Macromolecules* **2008**, *41*, 3488. (e) Nagai, A.; Miyake, J.; Kokado, K.; Nagata, Y.; Chujo, Y. *J. Am. Chem. Soc.* **2008**, *130*, 15276. (f) Nagai, A.; Kokado, K.; Nagata, Y.; Chujo, Y. *Macromolecules* **2008**, *41*, 8295. (g) Li, H.; Jäkle, F. *Macromolecules* **2009,** *42,* 3448.

(6) (a) Hadziioannou, G., van Hutten, P. F., Eds., *Semiconducting polymers: Chemistry, Physics and Engineering,* 2nd ed.; Wiley-VCH:Weinheim, Germany, 2006. (b) Hughes, G.; Bryce, M. H. *J. Mater. Chem.* **2005**, *15*, 94. (c) Kulkarni, A. P.; Tonzola, C. J.; Babel, A.; Jenekhe, S. A. *Chem. Mater.* **2004**, *16*, 4556. (d) Skotheim, T. J., Elsenbaumer, R. L. Reynolds, J. R., Eds. *Handbook of Conducting Polymers,* 2nd ed.; Dekker: New York, 1998.

(7) (a) Bidan, G.; Guillerez, S.; Sorokin, V. *Adv. Mater.* **1996**, *8*, 157. (b) Goto, H.; Okamoto, Y.; Yashima, E. *Macromolecules* **2002**, *35*, 4590. (c) Azmi, R.; Mena-Osteritz, E.; Bose, R.; Benet-Buchholz, J.; Bauerle, P. *J. Mater. Chem.* **2006**, *16*, 728.

(8) (a) Havinga, E. E.; Bouman, M. M.; Meijer, E. W.; Pomp, A.; Simenon, M. M. J. *Synth. Met.* **1994**, *66*, 93. (b) Majidi, M. R.; Kane-Maguire, L. A. P.; Wallace, G. G. *Polymer* **1994**, *35*, 3113. (c) Su, S.–J.; Takeishi, M.; Kuramoto, N. *Macromolecules* **2002**, *35*, 5752. (d) Goto, H.; Akagi, K. *Macromol. Rapid Commun.* **2004**, *25*, 1482.

(9) (a) Liu, R.; Sanda, F.; Masuda, T. *Macromolecules* **2008**, *41*, 5089. (b) Nomura, R.; Tabei, J.; Masuda, T. *Macromolecules*, **2001**, *123*, 8430.

(10) Haberecht, M. C.; Heilmann, J. B.; Haghiri, A.; Bolte, M.; Bats, J. W.; Lerner, H. –W.; Holthausen, M. C.; Wagner, M. *Z. Anorg. Allg. Chem.* **2004**, *630*, 904.

(11) Sundararaman, A.; Venkatasubbaiah, K.; Victor, M.; Zakharov, L. N.; Rheingold, A. L.; Jäkle, F. *J. Am. Chem. Soc.* **2006**, *128*, 16554.

(12) (a) Qin, Y.; Kiburu, I.; Shah, S.; Jäkle, F. *Org. Lett.* **2006**, *8*, 5227. (b) Kappaum, S.; Rentenberger, S.; Pogantsch, A.; Zojer, E.; Mereiter, K.; Trimmel, G.; Saf, R.; Möller, K. C.; Stelzer, F.; Slugovc, C. *Chem. Mater.* **2006**, *18*, 3539. (c) Qin, Y.; Kiburu, I.; Shah, S.; Jäkle, F. *Macromolecules* **2006**, *39*, 9041.

(13) (a) Yuster, P.; Weissman, S. I. J. *J. Chem. Phys.* **1949**, *17*, 1182. (b) McClure, D. S. *J. Chem. Phys.* **1949**, *17*, 905. (c) Yogo, T.; Urano, Y.; Ishitsuka, Y.; Maniwa, F.; Nagano, T. *J. Am. Chem. Soc.* **2005**, *127*, 12162.

(14) (a) Sarkar, N.; Das, K.; Das, S.; Datta, A.; Dutta, R.; Bhattacharyya, K. *J. Chem. Soc., Faraday Trans.* **1996**, *92*, 3097. (b) Seliskar, C. J.; Brand, L. *J. Am. Chem. Soc.* **1971**, *93*, 5414. (c) Sadkowski, P. J.; Fleming, G. R. *Chem. Phys.* **1980**, *54*, 79.

(15) Weder, C.; Wrighton, M. S. *Macromolecules* **1996,** *29,* 5157.

(16) Sudaraman, A.; Venkatasubbaiah, K.; Victor, M.; Zakharov, L. N.; Rheingold, A. L.; Jäkle, F. *J. Am. Chem. Soc.* **2006,** *128,* 16554.

(17) Kokado, K.; Chujo, Y. *Macromolecules* **2009,** *42,* 1418.

Chapter 5

Synthesis of π-Conjugated Polymers Containing Aminoquinoline-Borafluorene Complexes in the Main-Chain

Abstract

The author reports here the regulation of the electron transferring between the conjugated polymers and the orthogonally-connected ligands to the main chain. Poly(arylene-ethynylene)s containing aminoquinoline-borafluorene complexes in the main-chain were synthesized in good yields by Sonogashira-Hagihara coupling. Single crystal X-ray analysis of a model compound elucidated the complex's structure in which the aminoquinolate moiety and the borafluorene ring were connected directly and orthogonally. Moreover, the optical properties of the polymers were characterized by UV-vis absorption and photoluminescence spectra. Perfluorinated alkyl chain-containing polymers showed strong emission, while hydrocarbon chain-containing ones exhibited only slight emission. DFT calculation suggested that an electron transfer from the excited-main chain to the aminoquinolate ligand was suppressed because of the lowered LUMO level by introducing the electron withdrawing groups, resulting in the significant emission.

Introduction

The π-conjugated polymers have drawn considerable attention as charge transporting or emissive materials in organic light-emitting diodes (OLEDs),[1] organic solar cells[2] and sensing materials.[3] Their extended π- and π*-orbitals or narrow band gaps make it possible for irradiation in the visible or near infrared regions to excite the long conjugation system along the main chains, resulting in fluorescence and charge separation.[4] Exciton's migration through the orbitals can be enhanced or restricted by the preprogrammed connection between electron-donating groups and electron-withdrawing ones.[5,6] For tuning the orbital levels and regulating the conjugation lengths, various elements were incorporated into their main-chains.[7] Boron is one of the candidates as a strong electron-withdrawing unit because of their electropositivity and moderate affinity to carbon.[8] Kinetically stabilized tricoordinate boron possesses a vacant 2p-orbital extending π-conjugation in the conjugated polymers and these exhibit red-shifted absorption and fluorescence.[9] On the other hand, tetracoordinate organoboron complexes such as boron quinolates,[10] boron diketonates[11] and boron-dipyrromethenes[12] are also attractive because of their strong fluorescence and high stability against air and water. Boron quinolates, which have the same ligands as aluminium quinolates used in OLEDs as typical electron transporting materials,[13] showed not only high quantum yield but also low LUMO (Lowest Unoccupied Molecular Orbital) level leading to high electron-carrier ability.

Recently, Chujo and coworkers have demonstrated the synthesis of the π-conjugated polymers incorporating boron quinolate, boron aminoquinolate or other boron complexes into the main-chain.[14,15] In these polymers, the fluorescence band of the π-conjugated linker and the absorption band of the boron quinolate well overlapped, and also the π-conjugated linker freely rotated. Consequently, strong interaction between orbitals or dipoles resulted in the strong

fluorescence via energy transferring from the linkers with high molar extinction coefficient to the boron quinolate moieties. Moreover, low LUMO level is useful for the application to photofunctional materials based on donor-acceptor conjugation systems. Moieties with low LUMO level mediate electron transfer from excited donor moieties resulting in fluorescence quenching[16] or charge separation.[17] The former is applicable for the on/off switching of emission.[18] The latter is the key steps to determine the efficiencies in artificial photosynthesis,[19] solar cells,[20] and photocatalytic reactions.[21] Thus, the controls of exciton migration in the conjugated boron polymers are of significance not only for understanding electronic structures involving heteroatoms, but also for producing advanced opt-electronic devices. According to the Marcus theory of electron transfer, the electron transfer state can be maintained in the conjugated molecule involved direct and orthogonal linkage between a plane donor and a plane acceptor.[22] For example, in 9-mesityl-10-methylacridinium ion, two aromatic rings contact orthogonally and it showed long life time of electron transfer state (~2 h).[23] Herein, the author synthesized π-conjugated polymers containing aminoquinoline-borafluorene complexes in the main-chain by a Sonogashira-Hagihara cross coupling. In the complex, the borafluorene and the quinoline ring are orthogonally connected. The energy transferring via Förster mechanism observed from the previous polymers composed of the boron quinolate units should be prohibited through such orthogonal conformations due to the mismatches of the directions of the transition dipole moments. [24] In addition, π-conjugation along the main chains through the borafluorene moieties and the accumulation of the quinoline rings on the polymer chains could induce the electron transfer. These were investigated by UV-vis and fluorescence spectrometry, and also density functional theory (DFT) calculation.

Results and Discussion

The synthetic routes for the preparation of a monomer and a model compound are shown in Scheme 1. According to the literature, [25] 2,7-bis(triazenyl)-9-stanafluorene was synthesized and it was treated with iodotrimethylsilane to give 2,7-diiodo-9-stanafluorene (**1**). Tin-boron exchange of **1** by BBr_3 followed by adding of 8-acetylaminoquinoline and triethylamine accomplished the transformation from **1** to aminoquinoline-borafluorene monomer (**2**). Additionally, the same procedure provided the model compound without iodide (**3**). The tetracoordination states of the boron atoms in **2** and **3** were confirmed by the ^{11}B NMR spectroscopy in $CDCl_3$ (**2**: δ_B = 5.08 ppm, **3**: δ_B = 5.96 ppm). The basic structures of **2** and **3** were also characterized by ^{1}H NMR, ^{13}C NMR and mass spectroscopies. Further, Figure 1 presents the molecular structure of **3** as determined by single crystal X-ray analyses. It is observed that the quinolyl ring and the borafluorene moiety contacted orthogonally. The B(1)–N(1) and B(1)–N(2) bond lengths (1.603 and 1.569 Å) were similar to those of (κ^2-(*N,N'*)-8-acetylaminoquinolate)diphenylborane (BPh_2aq, 1.619 and 1.587 Å),[14] respectively. Moreover, the N(1)–B(1)–N(2) angle of **3** (97.1°) was almost same as that of BPh_2aq (96.2°). These structural similarities mean that the borafluorene moiety keeps stability of the structure with tetracoordinate boron. Sonogashira-Hagihara coupling polymerization of **2** was conducted with 1,4-diethynyl-2-(perfluorooctyl)-5-(trifluoromethyl)benzene[26] or 1,4-diethynyl-2,5-didodecylbenzene[27] in the presence of $Pd(PPh_3)_4$ and CuI in the mixed solvent of tetrahydrofuran (THF) and triethylamine (Et_3N) at 40 °C for 48 h (Scheme 3). The polymers were soluble in THF, CH_2Cl_2, and $CHCl_3$. The ^{11}B NMR spectra of the obtained polymers were observed at δ_B = –1.18 (**4F**) and 4.01 (**4C**) ppm assigned as the tetracoordination state of the boron atoms in each polymer. These data indicate that the polymerization proceeded without any degradation in the

organoboron quinolate moiety. The number-average molecular weights (M_n) and the molecular weight distribution (M_w/M_n) of the polymers, measured by size-exclusion chromatography (SEC) in THF toward polystyrene standards, were 10,400 and 2.5 for **4F**, and 20,300 and 2.8 for **4C**, respectively (Table 1). The obtained polymers possessed adequate lengths for ignoring the influence from the chain ends and the unexpected aggregation on the measurements of optical properties.

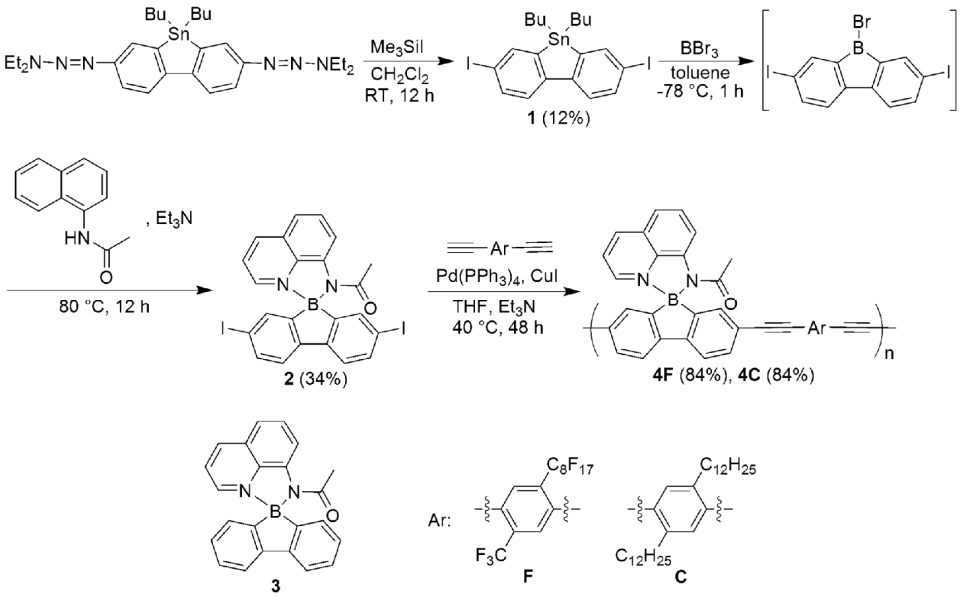

Scheme 1. Synthesis of polymers

Table 1. Properties of compounds

Polymers	M_n[a)]	PDI[a)]	λ_{max} [nm][b)]	Em [nm][c)]	Φ_F[d)]
4F	10,400	2.5	418	512	0.53
4C	20,300	2.8	437	453, 500	0.02
3	—	—	406	508	0.51

[a)]Estimated by SEC based on polystyrene standards in THF; [b)]Absorption maxima in $CHCl_3$ (1.0×10^{-5} M); [c)]Emission maxima in $CHCl_3$ (1.0×10^{-5} M); [d)]Absolute fluorescence quantum yields.

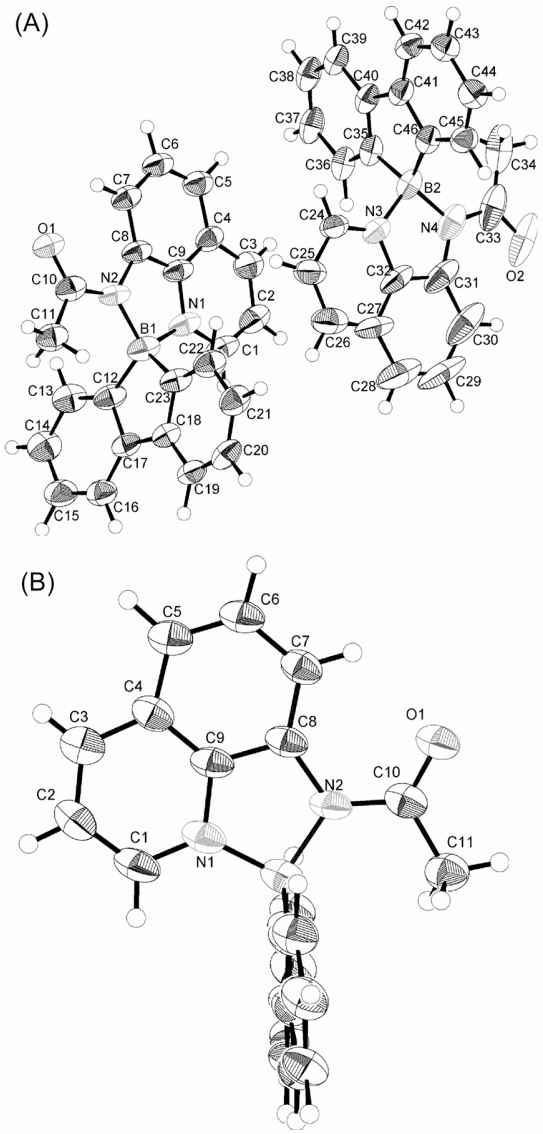

Figure 1. (A) The X-ray crystal structure of **3** with thermal ellipsoids drawn to the 50% probability level. (B) Displaying orthogonal connection of two aromatic rings.

The optical properties of the obtained polymers were investigated by UV-vis absorption and photoluminescence measurements in $CHCl_3$ solution and compared to those of the model compound. The compound **3** showed a weak and broad absorption peak at 406 nm arising from the aminoquinolate ligand (Figure 2A). In contrast, the polymers **4F** and **4C** exhibited the strong

absorption bands around 400 nm assignable to the π-conjugated main-chain. Although there are slight absorption bands from the boron complexes in this region, their contributions to the emissions with the excitation lights in this region are negligible because the magnitudes of the absorptions are approximately 5% compared to those of the main-chains. Thereby, the emissions observed from the polymers should be originated from the main-chain excitation. Emission spectra of the polymers and the model compound in $CHCl_3$ solution (c = 1.0 × 10^{-5} M) are represented in Figure 2B. All the emission data given here were obtained after exciting at the longest wavelength of the absorption peaks (**4C**: 418 nm, **4F**: 437 nm, **3**: 406 nm). The spectrum of **4C** has subtle emission (Φ_F = 0.02) with a similar shape as that of **3** (Φ_F = 0.51). The intrinsic emission of the boron complex should be observed. In contrast, the polymer **4F** displayed strong emission (Φ_F = 0.51) with the peaks at 452 nm assigned to the main-chain emission and at 500 nm to the aminoquinolate. These data indicate that the large contribution of the non-radiative process should be considered to the decay of the polymer **4C**. Figure 2C represents fluorescence excitation spectra of the polymers in $CHCl_3$ (c = 1.0 × 10^{-5} M) detected at fluorescence maxima. This result means that the fluorescence emissions from the polymers **4F** and **4C** was caused from the excitation at the main chains. However, the lower intensity of **4C** between 300 and 430 nm was observed in the excitation spectrum expected from the UV-vis spectrum. These data also represent the existence of the annihilation process after the main chain excitation in the polymer **4C**.

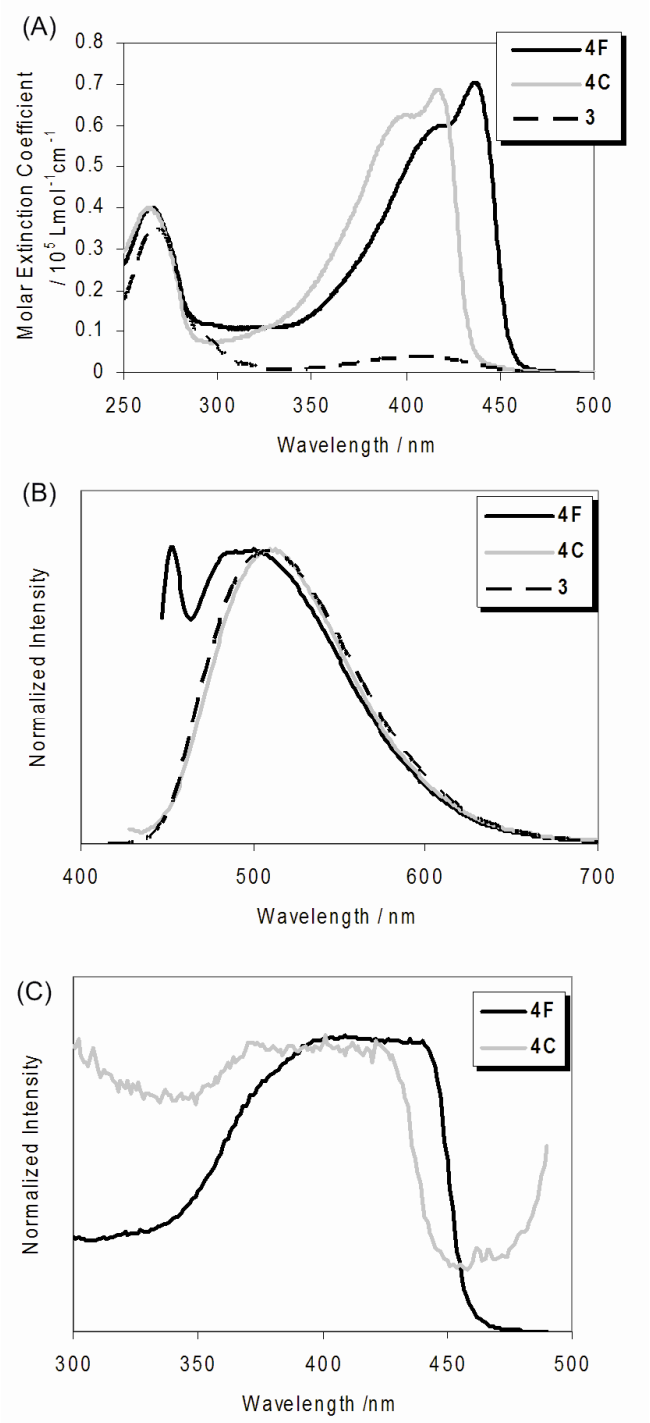

Figure 2. UV-vis (A), fluorescence (B), and excitation (C) spectra of **3** and **4** (in $CHCl_3$, c = 1.0 × 10^{-5} M).

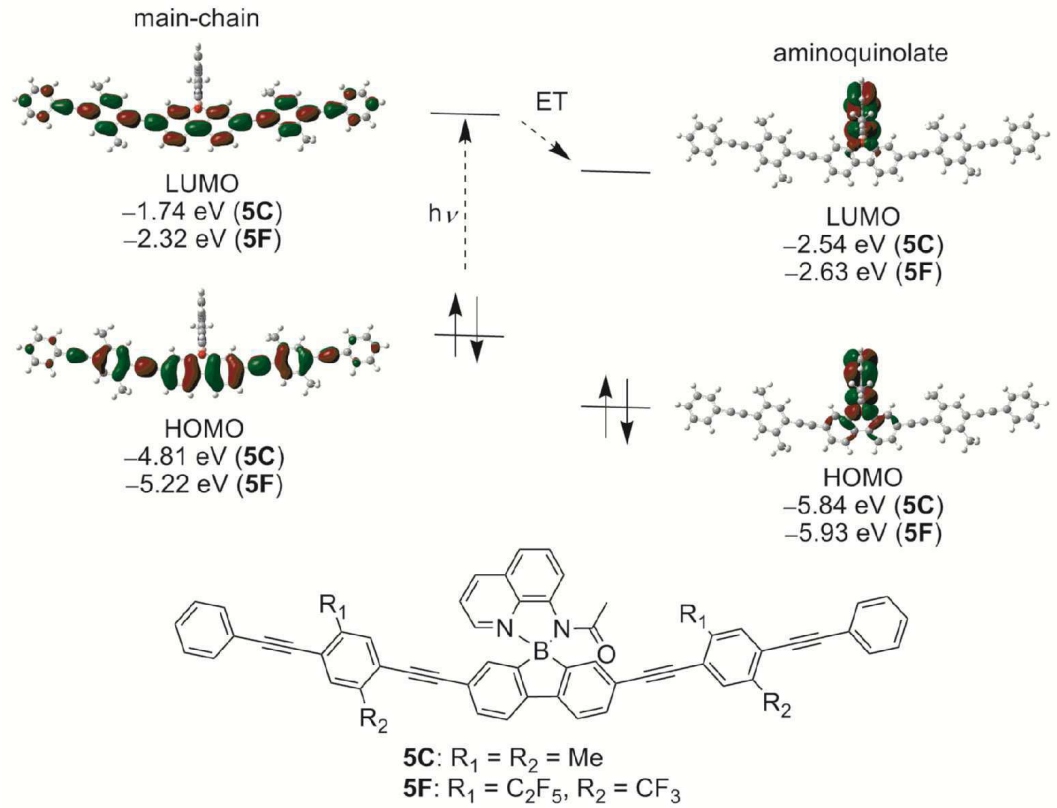

Figure 3. Kohn-Sham orbital diagrams for the HOMO and LUMO of **5C** corresponding to main-chain or aminoquinolate (B3LYP/6-31G(d)//B3LYP/6-31G(d)).

To understand the difference of the luminescent behavior induced by the side-chain of the comonomers, the author has carried out theoretical calculation for model compounds **5C** and **5F** using density-functional theory (DFT) method at the B3LYP/6-31G(d).[28] Figure 3 illustrates Kohn-Sham orbital diagrams of **5C** around frontier orbitals, HOMO (Highest Occupied Molecular Orbital) and LUMO (Lowest Unoccupied Molecular Orbital). The HOMO, HOMO-1, HOMO-2 and LUMO+1 were located on the main-chains while the HOMO-3 and LUMO were localized on the aminoquinolate ring. To put it differently, the HOMO and LUMO+1 were regarded as HOMO and LUMO of the main-chain, and the HOMO-3 and LUMO of the model compounds corresponded to HOMO and LUMO of the aminoquinolate moiety. These shapes are

almost similar as the orbitals of **5F** but HOMO-2 of **5F** was equivalent to HOMO of the aminoquinolate moiety. Considering that the dipole moments are parallel to aromatic rings in flat molecules during π-π* transition, the localization of the orbitals and orthogonal contact of the main-chain and the aminoquinolate moieties should inhibit energy transferring from the main-chain to the aminoquinolate moiety via Förster mechanism because of unfavorable distribution of the moments. In addition, the HOMO-LUMO gaps of the aminoquinolate moieties are larger than those of the main-chain due to π-conjugation through borafluorene. These facts suggest that the energy transfer mentioned above should hardly occur. Indeed, boron aminoquinolate **3** displayed an absorption peak at shorter wavelength than the polymers in UV-vis absorption spectra. Direct contact of the aminoquinolate moiety to the main-chain, however, allows electron transfer between the polymer chain and the ligand. Moreover, electron transfer induced by photoexcitation is accelerated as a gap between donor's LUMO level and acceptor's one increases. In **5C**, LUMO+1 was 0.80 eV higher than LUMO while the gap of **5F** was 0.31 eV due to electron-withdrawing side-chains which lowers the LUMO level of the main-chain. From these results, it can be concluded that electron transfer effectively occurs from the excited main-chain to the aminoquinolate moiety, leading to non-radiative process.

Conclusion

Novel π-conjugated polymers containing aminoquinoline-borafluorene complexes in the main-chain were synthesized by Sonogashira-Hagihara coupling in good yields. Energy transfer from the main-chain to the aminoquinolate moiety was regulated in these polymers by narrow band gap of the main-chain and orthogonal contact between them. Direct connection of them brought about electron transfer induced by photoexcitation, using the aminoquinolate moiety as an acceptor. Side chains of the polymers tuned degree of electron transfer and fluorescence quantum yields. It is anticipated that optimization of substituents on these polymers affords a new charge separation material available for solar cells, photocatalysts and sensing materials.

Experimental Section

Measurements. ^{1}H (400 MHz), ^{13}C (100 MHz), and ^{11}B (128 MHz) NMR spectra were recorded on a JEOL JNM-EX400 spectrometer. ^{1}H and ^{13}C NMR spectra used tetramethylsilane (TMS) as an internal standard, ^{11}B NMR were referenced externally to BF_3OEt_2 (sealed capillary) in $CDCl_3$. The number-average molecular weight (M_n) and the molecular weight distribution [weight-average molecular weight/number-average molecular weight (M_w/M_n)] values of all polymers were estimated by a size-exclusion chromatography (SEC) with a TOSOH G3000HXI system equipped with three consecutive polystyrene gel columns [TOSOH gels: α-4000, α-3000, and α-2500] and ultraviolet detector at 40 °C. The system was operated at a flow rate of 1.0 mL/min, with tetrahydrofuran (THF) as an eluent. Polystyrene standards were employed for calibration. UV–vis spectra were recorded on a Shimadzu UV-3600 spectrophotometer. Fluorescence emission spectra were recorded on a HORIBA JOBIN YVON Fluoromax-4 spectrofluorometer, and the absolute quantum yield was calculated by integrating sphere method on the HORIBA JOBIN YVON Fluoromax-4 spectrofluorometer in chloroform. FT-IR spectra were obtained using a SHIMADZU IRPrestige-21 infrared spectrometer. X-ray crystallographic analysis was carried out by a Rigaku R-AXIS RAPID-F graphite-monochromated Mo Kα radiation diffractometer with an imaging plate. A symmetry related absorption correction was carried out by using the program ABSCOR.[29] The analysis was carried out with direct methods (SHELX-97[30] or SIR97[31]) using Yadokari-XG.[32] The program ORTEP3[33] was used to generate the X-ray structural diagram. Elemental analysis was performed at the Microanalytical Center of Kyoto University. Computations were performed using the Gaussian 03 suite of programs.[28]

Materials. 3,7-Bis(*N*,*N*-diethyltriazenyl)-5,5-di(*n*-butyl)dibenzo[*b*,*d*]stannole,[25] 5,5-di(n-butyl)dibenzo[*b,d*]stannole,[34] 1.4-diethynyl-2-perfluorooctyl-5-trifluoromethylbenzene,[26] and

1.4-diethynyl-2,5-didodecylbenzene,[27] were prepared according to the literature. Tetrahydrofuran (THF) and triethylamine (Et_3N) were purified using a two-column solid-state purification system (Glasscontour System, Joerg Meyer, Irvine, CA). Other reagents were commercially available and used as received.

Synthesis of 3,7-diiodo-5,5-dibutyldibenzo[b.d]stannole (1). To a solution of 3,7-bis(*N*,*N*-diethyltriazenyl)-5,5-di(*n*-butyl)dibenzo[*b*,*d*]stannole (12.1 g, 20.7 mmol) in dichloromethane (20 mL), iodotrimethylsilane (11.8 mL, 82.8 mmol) was added. The reaction mixture was refluxed for 12 h, and then quenched by aqueous $NaHCO_3$ solution. After the aqueous layer was extracted with dichloromethane (100 mL), the organic extract was dried over $MgSO_4$, filtered, and concentrated under reduced pressure. The crude residue was purified by silica gel column chromatography eluted with hexane to give a colorless oil in 12% yield (1.58 g, 2.48 mmol). The analytical data agree with the literature's values.[25]

Synthesis of Monomer (2). Boron tribromide in dichloromethane (1.0 M, 2.48 mL) was added into a solution of **1** (1.58 g, 2.48 mmol) in toluene (20 mL) at –78 °C. The mixture was stirred at –78 °C for 1 h and then allowed to warm to room temperature. A solution of 8-acetylaminoquinoline (0.555 g, 2.98 mmol) in toluene (12 mL) and triethylamine (0.415 mL, 2.98 mmol) were added to the reaction mixture. After the reaction mixture was stirred at 80 °C for 12 h, water was added, followed by extraction with toluene (100 mL), drying over $MgSO_4$ and removal of the solvent under vacuum. The crude residue was purified by silica gel (neutral) column chromatography eluted with cyclopentyl methyl ether/hexane (7/3). Recrystallization from hexane/dichloromethane gave a yellow solid in 24% yield (0.432 g, 0.720 mmol). ^{1}H NMR (400 MHz, $CDCl_3$, δ): 8.84 (d, J = 7.6 Hz, 1H, ArH), 8.47 (d, *J* = 8.4 Hz, 1H, ArH), 7.84 (m, 2H, ArH), 7.66 (dd, *J* = 8.0, 2.0 Hz, 1H, ArH), 7.57-7.42 (m, 6H, ArH), 1.69 (s, 1H, CH_3), ^{13}CNMR (100 MHz, $CDCl_3$, δ): 173.43 (C=O), 147.24 (Ar), 142.05 (Ar), 139.64 (Ar), 139.30 (Ar), 138.81

(Ar), 138.49 (Ar), 137.64 (Ar), 132.76 (Ar), 127.96 (Ar), 122.49 (Ar), 121.96 (Ar), 118.38(Ar), 117.07 (Ar), 94.51 (Ar), 24.48 (CH_3). ^{11}B NMR (128 MHz, $CDCl_3$, δ, ppm): 5.08. HRMS (EI) Calcd for $C_{23}H_{15}BI_2N_2O$: m/z 599.9367. Found: m/z 599.9368. Anal. Calcd for $C_{23}H_{15}BI_2N_2O$: C, 46.04; H, 2.52; N, 4.67. Found: C, 45.78; H, 2.48; N, 4.63. IR (KBr): ν = 3422 (NH), 3048 (CH), 2986 (CH), 1653 (CO), 1599, 1582, 1504, 1468, 1383, 1325, 1269, 1167, 824, 741 cm^{-1}.

Synthesis of 3. Similarly to the preparation of **2**, **3** was prepared from 5,5-di(n-butyl)dibenzo[*b,d*]stannole (1.16 g, 3.00 mmol), boron tribromide in dichloromethane (1.0 M, 3.0 mL), 8-acetylaminoquinoline (1.68 g, 9.00 mmol), and triethylamine (1.25 mL, 9.00 mmol) in 45% yield as a yellow solid (0.473 g, 1.36 mmol). ^{1}H NMR (400 MHz, $CDCl_3$, δ): 8.85 (d, J = 7.6 Hz, 1H, ArH), 8.40 (dd, *J* = 8.2, 1.0 Hz, 1H, ArH), 7.87 (d, *J* = 4.4 Hz, 1H, ArH), 7.83 (t, *J* = 8.2 Hz, 1H, ArH), 7.74 (d, *J* = 7.6 Hz, 2H, ArH), 7.52 (d, *J* = 8.4 Hz, 1H, ArH), 7.44 (dd, *J* = 8.0, 5.0 Hz, 1H, ArH), 7.33 (td, *J* = 7.4, 1.0 Hz, 2H, ArH), 7.13-7.06 (m, 4H, ArH), 1.68 (s, 1H, CH_3), ^{13}CNMR (100 MHz, $CDCl_3$, δ): 173.93 (C=O), 149.01 (Ar), 142.50 (Ar), 139.26 (Ar), 138.97 (Ar), 138.74 (Ar), 132.56 (Ar), 129.75 (Ar), 128.63 (Ar), 127.89 (Ar), 127.28 (Ar), 122.31 (Ar), 119.82 (Ar), 118.00 (Ar), 24.41 (CH_3). ^{11}B NMR (128 MHz, $CDCl_3$, δ, ppm): 5.96. HRMS (EI) Calcd for $C_{23}H_{17}BN_2O$: m/z 348.1434. Found: m/z 348.1436. IR (KBr): ν =3422 (NH), 3059 (CH), 3003 (CH), 1633 (CO), 1599, 1582, 1508, 1472, 1445, 1423, 1395, 1383, 1325, 1240, 1177, 1159, 1146, 1125, 1099, 1049, 1003, 922, 826, 787 cm^{-1}.

Synthesis of 4F. Monomer **2** (0.108 g, 0.180 mmol), 1.4-diethynyl-2-perfluorooctyl-5-trifluoromethylbenzene (0.110 g, 0.180 mmol), CuI (1.7 mg, 9.0 μmol), and $Pd(PPh_3)_4$ (10.4 mg, 9.0 μmol) were dissolved in 1.8 mL of THF and 0.9 mL of triethylamine. After the mixture was stirred at 40 °C for 48 h, a small amount of $CHCl_3$ was added and poured into a large excess of methanol to precipitate the polymer. The polymer was purified by repeated precipitations from a small amount of $CHCl_3$ into a large excess of methanol and hexane respectively to give a yellow

solid in 84% yield (0.145 g, 0.151 mmol). M_n = 10,400.^{1}H NMR (400 MHz, $CDCl_3$, δ): 8.86 (1H, ArH), 8.44 (1H, ArH), 7.83-7.72 (6H, ArH), 7.55-7.48 (4H, ArH), 7.33-7.30 (2H, ArH), 1.68 (3H, CH_3). ^{11}B NMR (128 MHz, $CDCl_3$, δ, ppm): –1.18.

Synthesis of 4C. Similarly to the preparation of **Poly1F**, **Poly1C** was prepared from Monomer **2** (0.120 g, 0.200 mmol), and 1.4-diethynyl-2,5-didodecylbenzene (0.0926 g, 0.200 mmol) in 84% yield as a yellow solid. M_n = 20,300. ^{1}H NMR (400 MHz, $CDCl_3$, δ): 8.86 (1H, ArH), 8.43 (1H, ArH), 7.83 (2H, ArH), 7.71 (2H, ArH), 7.54-7.47 (4H, ArH), 7.28 (2H, ArH), 7.20 (2H, ArH), 2.67 (4H, $ArCH_2$), 1.71 (3H, $COCH_3$), 1.56 (4H, CH_2), 1.23-1.18 (36H, CH_2), 0.87 (6H, CH_3). ^{11}B NMR (128 MHz, $CDCl_3$, δ, ppm): 4.01. IR(KBr): ν = 3439 (NH), 3048 (CH), 3013 (CH), 2922 (CH), 2851 (CH), 2195 (C≡C), 1661 (CO), 1506, 1491, 1456, 1387, 1321, 1236, 1177, 1117, 1003, 895, 824, 783 cm^{-1}.

References

(1) Kraft, A.; Grimsdale, A. C.; Holmes, A. B. *Angew. Chem. Int. Ed.* **1998,** *110,* 402.

(2) Yu, G.; Gao, J.; Hummelen, J. C.; Wudl, F.; Heeger, A. J. *Science* **1995,** *270,* 1789.

(3) Zheng, J.; Swager, T. M.; *Adv. Polym. Sci.* **2005,** *177,* 151.

(4) Bunz, U. H. F. *Macromol. Rapid Commun.* **2009,** *30,* 772.

(5) Lee, S. K.; Cho, S.; Tong, M.; Seo, J. H.; Heeger, A. J. *J. Polym. Sci. A: Polym. Chem.* **2011,** *49,* 1821.

(6) Blouin, N.; Michaud, A.; Gendron, D.; Wakim, S.; Blair, E.; Neagu-Plesu, R.; Belletête, M.; Durocher, G.; Tao, Y.; Leclerc, M. *J. Am. Chem. Soc.* **2008,** *130,* 732.

(7) Hissler, M.; Dyer, P. W.; Rèau, R. *Coord. Chem. Rev.* **2003,** *244,* 1.

(8) Entwistle, C. D.; Marder, T. B. *Angew. Chem. Int. Ed.* **2002,** *41,* 2927.

(9) Matsumi, N.; Naka, K.; Chujo, Y. *J. Am. Chem. Soc.* **1998,** *120,* 5112.

(10) Wu, Q.; Esteghamatian, M.; Hu, N.-X.; Popovic, Z.; Enright, G.; Tao, Y.; D'Iorio, M.; Wang, S.; *Chem. Mater.* **2000,** *12*, 79.

(11) Cogné-Laage, E.; Allemand, J.-F.; Ruel, O.; Baudin, J.-B.; Croquette, V.; Blanchard-Desce, M.; Jullien, L. *Chem. Eur. J.* **2004,** *10,* 1445.

(12) Loudet, A.; Burgess, K. *Chem. Rev.* **2007,** *107,* 4891.

(13) Tang, C. W.; Vanslyke, S. A. *Appl. Phys. Lett.* **1987,** *51,* 913.

(14) Nagata, Y.; Chujo, Y. *Macromolecules* **2008,** *41,* 3488.

(15) Tokoro, Y.; Nagai, A.; Kokado, K.; Chujo Y. *Macromolecules* **2009,** *42,* 2988.

(16) Wang, M.; Sun, Y.; Tong, M.; Chesnut, E. S.; Seo, J. H.; Kumar, R.; Wudl, F. *J. Polym. Sci. A: Polym. Chem.* **2011,** *49,* 441.

(17) D'Souza, F.; Ito, O. *Chem. Commun.* **2009,** 4913.

(18) Raymo, F. M.; Tomasulo, M. *J. Phys. Chem. A* **2005,** *109,* 7343.

(19) Kloz, M.; Pillai, S.; Kodis, G.; Gust, D.; Moore, T. A.; Moore, A. L.; van Grondelle, R.; Kennis, J. T. M. *J. Am. Chem. Soc.* **2011,** *133,* 7007.

(20) Seri, M.; Marrocchi, A.; Bagnis, D.; Ponce, R.; Taticchi, A.; Marks, T. J.; Facchetti, A. *Adv. Mater.* **2011,** *23,* 3827.

(21) Tschierlei, S.; Karnahl, M.; Presselt, M.; Dietzek, B.; Guthmuller, J.; González, L.; Schmitt, M.; Rau, S.; Popp, J. *Angew. Chem. Int. Ed.* **2010,** *49,* 3981.

(22) Marcus, R. A. *Annu. Rev. Phys. Chem.* **1964,** *15,* 155.

(23) Fukuzumi, S.; Kotani, H.; Ohkubo, K.; Ogo, S.; Tkachenko, N. V.; Lemmetyinen, H. *J. Am. Chem. Soc.* **2004,** *126,* 1600.

(24) Mårtensson, J. *Chem. Phys. Lett.* **1994,** *229,* 449.

(25) Wakamiya, A.; Mishima, K.; Ekawa, K.; Yamaguchi, S. *Chem. Commun.* **2008,** 579.

(26) Kokado, K.; Chujo, Y. *Macromolecules* **2009,** *42,*1418.

(27) Englert, B. C.; Smith, M. D.; Hardcastle, K. I.; Bunz, U. H. F. *Macromolecules,* **2004,** *37,* 8212.

(28) Gaussian 09, Revision **A.1**, Frisch, M. J.; Trucks, G. W.; Schlegel, H. B.; Scuseria, G. E.; Robb, M. A.; Cheeseman, J. R.; Scalmani, G.; Barone, V.; Mennucci, B.; Petersson, G. A.; Nakatsuji, H.; Caricato, M.; Li, X.; Hratchian, H. P.; Izmaylov, A. F.; Bloino, J.; Zheng, G.; Sonnenberg, J. L.; Hada, M.; Ehara, M.; Toyota, K.; Fukuda, R.; Hasegawa, J.; Ishida, M.; Nakajima, T.; Honda, Y.; Kitao, O.; Nakai, H.; Vreven, T.; Montgomery, Jr., J. A.; Peralta, J. E.; Ogliaro, F.; Bearpark, M.; Heyd, J. J.; Brothers, E.; Kudin, K. N.; Staroverov, V. N.; Kobayashi, R.; Normand, J.; Raghavachari, K.; Rendell, A.; Burant, J. C.; Iyengar, S. S.; Tomasi, J.; Cossi, M.; Rega, N.; Millam, J. M.; Klene, M.; Knox, J. E.; Cross, J. B.; Bakken, V.; Adamo, C.; Jaramillo, J.; Gomperts, R.; Stratmann, R. E.; Yazyev, O.; Austin, A. J.; Cammi, R.; Pomelli, C.; Ochterski, J. W.; Martin, R. L.; Morokuma, K.; Zakrzewski, V. G.; Voth, G. A.; Salvador, P.; Dannenberg, J. J.; Dapprich, S.; Daniels, A. D.; Farkas, Ö.; Foresman, J. B.; Ortiz, J. V.; Cioslowski, J.; Fox, D. J. Gaussian, Inc., Wallingford CT, 2009.

(29) Higashi, T. *ABSCOR. Program for Absorption Correction.*; Rigaku Corporation: Japan, 1995.

(30) Sheldrick, G. M. SHELX-97. Programs for Crystal Structure Analysis.; University of Göttingen: Germany, 1997.

(31) Altomare, A.; Burla, M.C.; Camalli, M.; Cascarano, G. L.; Giacovazzo, C.; Guagliardi, A.; Moliterni, A. G. G.; Polidori, G.; Spagna, R. *J. Appl. Cryst.* **1999,** *32*, 115.

(32) Wakita, K. *Yadokari-XG. Program for Crystal Structure Analysis.*; 2000.

(33) Farrugia, L. J. *J. Appl. Cryst.* **1997,** *30*, 565.

(34) Nagao, I.; Shimizu, M. Hiyama, T. *Angew. Chem. Int. Ed.* **2009,** *48,* 7573.

Part II

Pentacoordinate Silicon Induced by a Benzo[*h*]quinolyl Ligand

Chapter 6

Synthesis of Benzo[*h*]quinoline-Based Neutral Pentacoordinate Organosilicon Complexes

Abstract

Reactions of 10-benzo[h]quinolyllithium with a series of organosilanes led to the formation of neutral pentacoordinate complexes. The diethynyl-substituted complex was able to be converted to di(arylethynyl)-substituted ones by the Sonogashira-Hagihara coupling reaction. Electronegative substituents shortened N–Si distances and enhanced fluorescence intensity from the complexes.

Chapter 6

Introduction

Conjugated organosilicon compounds have received much attention because of their unique electronic and optical properties. Interaction between π* (Si–C) and π* (C–C) orbital lowers their lowest unoccupied molecular orbital (LUMO), leading to n-type conductivity and red-shifted fluorescence.[1] These functional organosilicon materals were mainly developed in the context of tertracoordinate silicon owing to the stability and accessibility. In the case of electronegative substituents,[2] π-conjugated moieties,[3] or polydentate ligands[4] on the silicon atoms, neutral pentacoordinate silicon complexes were obtained, and they usually have weak dative bonds sensitive to substituents. The bond strength between the silicon atom and the ligand with the lone pair significantly influences their fluorescence intensity, because strong bond suppresses vibrational deactivation. In addition, the absorption and luminescence properties of the π-conjugated organic chromophores can be tuned by introducing electron donating or withdrawing substituents and by modulating the length of π-conjugation. Facile introduction of substituents to pentacoordinate silicon complexes is feasible for resulting their optical properties.

For preparing conjugated molecules with pentacoordinate silicon, the limited numbers of the ligands can be applied. One of the common bidentate ligands is 8-aminonaphthyl ligand.[5] Using this, the Si–N dative bond lengths are extremely longer than covalent bond length of Si–N. Accordingly, an establishment of synthetic procedures for the variety of complexes should be strongly required to gather the information on the optical properties of the pentacoordinate silicon-containing compounds. Herein, the author reports the synthesis and characterization of novel pentacoordinate organosilicon complexes with benzo[*h*]quinoline. The author also demonstrates an arylation of the diethynyl-substituted complex by the Sonogashira-Hagihara

coupling reaction and their unique fluorescence property derived from the pentacoordinate silicon.

Results and Discussion

According to Scheme 1, 10-trimethylsilyl-, 10-trifluorosilyl-, and 10-(diethynylmethylsilyl)benzo[*h*]quinoline (**1C**, **1F**, and **1E**) were prepared from 10-bromobenzo[*h*]quinoline. These silyl-substituted compounds showed good solubility in chloroform, dichloromethane, and tetrahydrofuran (THF). They were characterized by a multinuclear NMR spectroscopy in $CDCl_3$ as well as by a single crystal X-ray diffraction. The ^{29}Si NMR signals of **1F** (δ = –105.1 ppm) and **1C** (δ = –11.14 ppm) appeared in upper field than those of the corresponding phenyl-substituted compounds (δ($PhSiF_3$) = –73.7 ppm, δ($PhSiMe_3$) = –4.1 ppm),[6] respectively. The large difference of the chemical shifts between the fluorinated compounds means that the electronegative fluoride strongly attracts the lone pair on the nitrogen to the silicon.[7] The diethynyl derivative **1E** displayed the ^{29}Si NMR signal in upfield (δ = –70.85 ppm) as compared with 8-(diethynyl(methyl)silyl)-*N*,*N*-dimethylnaphthalen-1-amine (δ = –56.65 ppm).[6] It was found that 10-benzo[*h*]quinolyl ligands were more favorable to form pentacoordinate silicon complexes than 8-aminonaphthyl ligands.

In the crystals, the silicon centers adopted a trigonal-bipyramidal or a pseudo-trigonal-bipyramidal geometry (Figure 1). As the Si—N distance shortens in the order of **1C** (2.701 Å) > **1E** (2.427 Å) > **1F** (2.055 Å), the sum of the three angles formed by the equatorial atoms increased the order of **1C** (343.6º) < **1E** (349.5º) < **1F** (357.5º). Moreover, the Si—N bond length of **1E** was shorter than that of the corresponding 8-aminonaphthyl compound (2.725 Å).[5] These results present that the benzo[*h*]quinolyl moiety efficiently induced the pentacoordinate state of

the silicon atom, and that the ethynyl moiety, as well as fluoride should stabilize the pentacoordination state. The pentacoordinate characters, $\%TBP_a$ and $\%TBP_e$ were determined as 29% and 62% for **1C**, 44% and 67% for **1E**, and 73% and 92% for **1F**, respectively.[8] These values suggest that the configurations around the silicon atoms of **1C** and **1E** are intermediate structures between tetrahedral and trigonal-bipyramidal structures. In contrast, the silicon atom of **1F** is almost trigonal-bipyramidal structure.

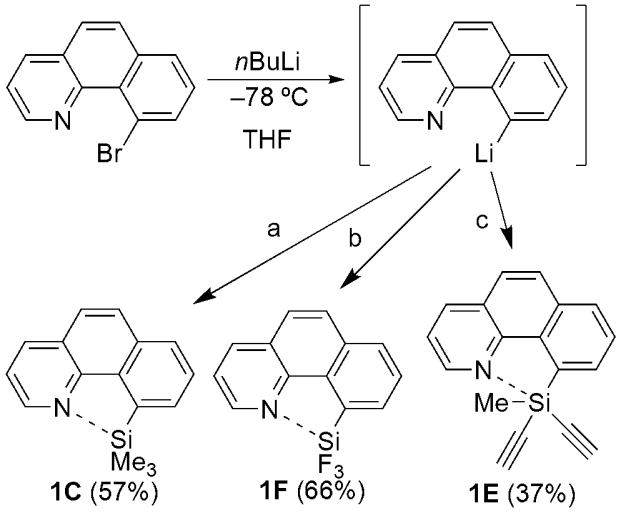

Scheme 1. Synthesis of pentacoordinate silicon complexes. Conditions and reagents: a) Me_3SiCl, RT, 12 h; b) i. chlorotriethoxysilane, RT, 12 h, ii. boron trifluoride diethyl etherate, Et_2O, RT, 12 h; c) i. chlorodiethoxymethylsilane, RT 12 h, ii. ethynylmagnesium bromide, THF, reflux, 12 h

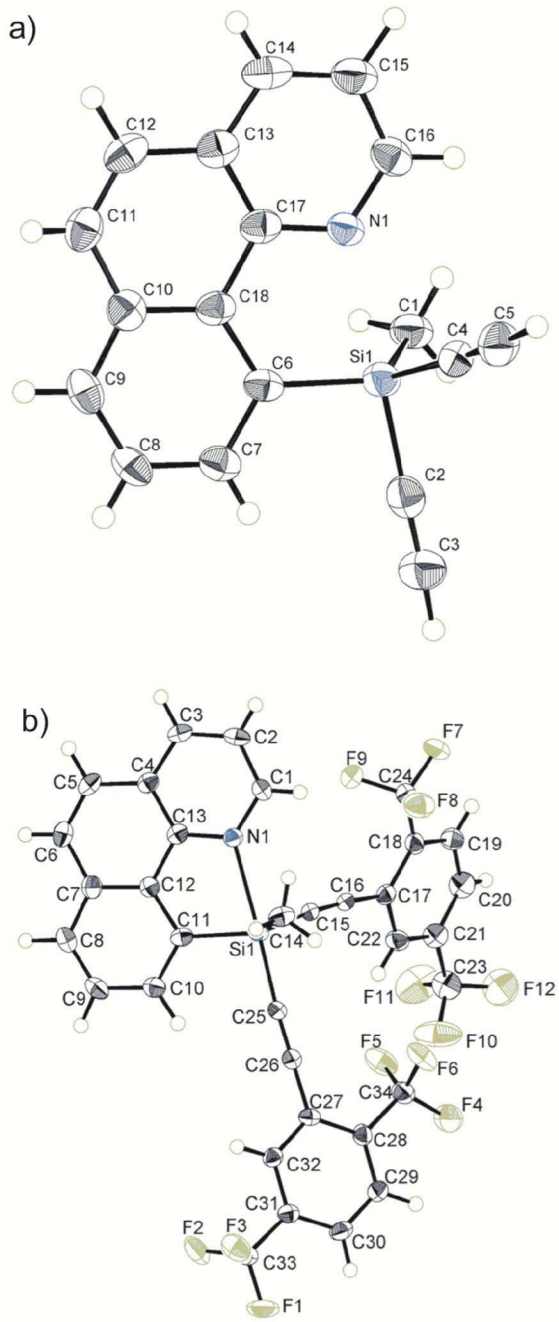

Figure 1. The X-ray crystal structures of a) **1E** and b) **2F** with thermal ellipsoids drawn to the 50% probability level. Selected bond lengths [Å] and angles[°]: **1E**: Si1–N1 2.434, C1–Si1–C4 116.5(2), C4–Si1–C6 114.12(19), C1–Si1–C6 119.48(18), C2–Si1–C4 101.03(18), C1–Si1–C2 99.25(19), C2–Si1–C6 101.52(18); **2F**: Si1–N1 2.3454(17), C15–Si1–C14 113.8(11), C15–Si1–C11 117.9(9), C14–Si1–C11 122.4(11), C15–Si1–C25 95.8(10).

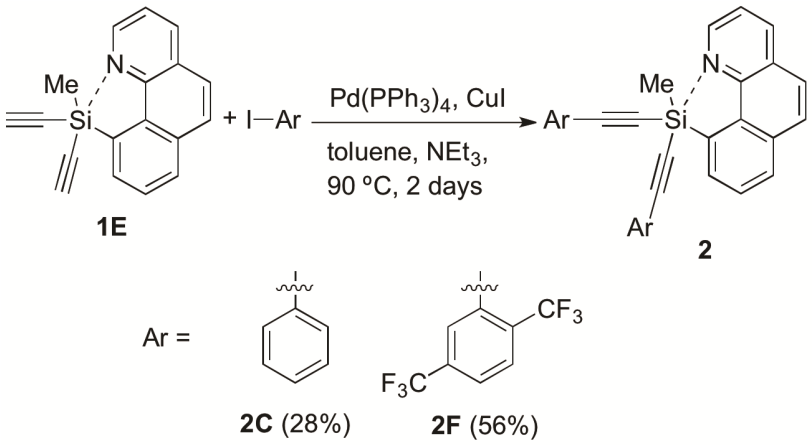

Scheme 2. Arylation of **1E**

The Sonogashira-Hagihara coupling of **1E** with iodobenzene or 1,4-bis(trifluoromethyl)-2-iodobenzene in the presence of $Pd(PPh_3)_4$ and CuI gave the aryl-substituted complexes, **2C** and **2F** (Scheme 2) in good yields. It was found that **2C** ((δ= –66.2 ppm) and **2F** (δ = –72.3 ppm) gave the ^{29}Si NMR signals at the similar positions to that of **1E**. Noteworthily, trifluoromethyl group on the phenyl group caused upfield shift of the ^{29}Si NMR resonance, implying that the electronegativity enhanced the pentacoordinate nature of the silicon. The crystal structures of **2C** and **2F** clearly show that the silicon centers adopted the pseudo-trigonal-bipyramidal geometries and that one of the arylethynyl substituents occupies an apical coordination site directly opposite to the nitrogen on the benzo[*h*]quinoline ring (Figure 1). Selective formation of this structure can be explained by the fact that the apical site of the pentacoordinate silicon should be occupied by a substituent which tends to stabilize negative charge.[9] The Si–N bond length of **2C** (2.428 Å) was similar to that of **1E**, whereas that of **2F** (2.345 Å) was shorter than those of **1E** and **2C**. The pentacoordinate characters, $\%TBP_a$ and $\%TBP_e$ were determined as 51% and 74% for **2C**, and 59% and 82% for **2F**, respectively. These mean that the electronegative substituents at the phenyl groups should strengthen the Si—N bond through ethynyl bridges.

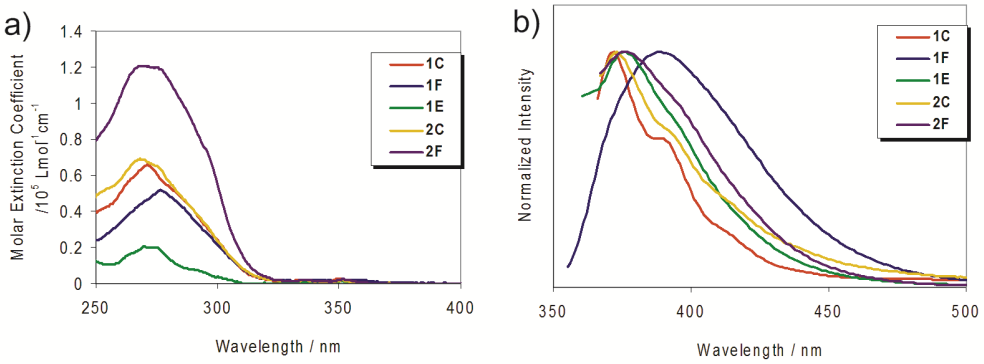

Figure 2. a) UV–vis spectra and b) normalized photoluminescence spectra in $CHCl_3$ (1.0×10^{-5} M).

The optical properties of the obtained silicon complexes were investigated by UV–vis absorption (Figure 2a) and photoluminescence (Figure 2b) experiments in $CHCl_3$ solution (c = 1.0×10^{-5} M). The absorption band around 270 nm was probably assigned to the absorption of both benzo[*h*]quinolyl and arylethynyl moieties. Very weak absorption peak was also observed around 350 nm, which corresponded to the absorption of benzo[*h*]quinoline. The former absorption peak of **1F** was bathochromically shifted in comparison with that of **1C**. Moreover, the π-conjugated substituent hardly affected the position of the absorption band. It can be summarized that the difference of absorption spectra tends to reflect not interaction between π* (Si–C) and the π * (C–C) orbital but pentacoordinate nature. This speculation was supported by photoluminescence spectra in which the excitation wavelength was the longest absorption maxima (~350 nm). An increase of electronegativity of the substituents on the silicon seems to be related to red-shift and broadening of the luminescent peak. Absolute fluorescence quantum yields (Φ_F) in $CHCl_3$ were measured by an integrated sphere method. The quantum yields of the silicon complexes with the electronegative substituents (**1F** and **2F**) were higher than the others

(Φ_F = 0.02 (**1C**), 0.11 (**1F**), 0.06 (**1E**), 0.02 (**2C**), 0.11(**2F**)). It is suggested that pentacoordinate state could inhibit vibrations of benzo[*h*]quinoline rings bringing about non-radiative relaxation.

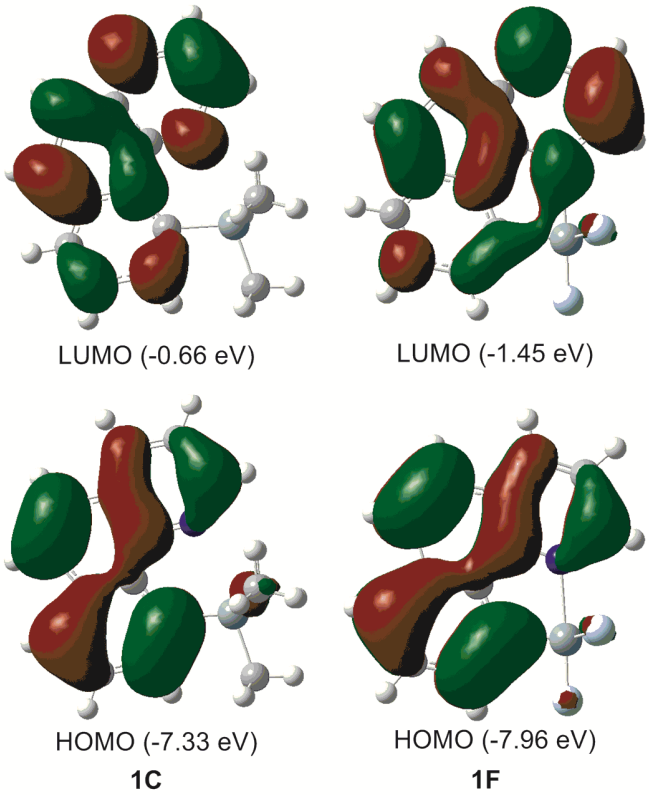

Figure 3. Kohn-Sham orbital diagrams for the HOMO and LUMO of **1C** and **1F** (M06-2X/cc-pVDZ).

To further understand the nature of pentacoordinate state and the optical property, the author carried out theoretical calculations for **1C** and **1F** using DFT (M06-2X/cc-pVDZ) method.[10] The Si—N bond lengths of **1C** and **1F** were 2.847 Å and 2.161 Å. These values agreed with those experimentally determined, qualitatively. Figure 3 illustrates Kohn-Sham orbital diagrams of **1C** and **1F** around frontier orbitals, HOMO (highest occupied molecular orbital) and LUMO (lowest unoccupied molecular orbital). While HOMO and LUMO of **1C** were localized

on the benzo[*h*]quinoline moiety, LUMO of **1F** was extended from the benzo[*h*]quinoline moiety to the silicon atoms. Moreover, the HOMO-LUMO gap of **1F** (6.51 eV) was smaller than that of **1C** (6.67 eV). The calculation result would mean that the additional lobe contributes to red-shift of **1F** in UV–vis and photoluminescence spectra.

Concluision

The author has found that benzo[*h*]quinoline was used for preparation of neutral pentacoordinate silicon complexes. The Si–N bond length was tuned by substituents on the silicon atoms. The short Si–N bond length of these complexes enhanced the fluorescence quantum yield.

Experimental Section

Measurements. ^{1}H (400 MHz), ^{13}C (100 MHz), and ^{11}B (128 MHz) NMR spectra were recorded on a JEOL JNM-EX400 spectrometer. ^{1}H and ^{13}C NMR spectra used tetramethylsilane (TMS) as an internal standard. ^{29}Si NMR spectra were referenced externally to TMS in $CDCl_3$. UV-vis spectra were recorded on a Shimadzu UV-3600 spectrophotometer. Fluorescence emission spectra were recorded on a HORIBA JOBIN YVON Fluoromax-4 spectrofluorometer. X-ray crystallographic analysis was carried out by a Rigaku R-AXIS RAPID-F graphite-monochromated Mo Kα radiation diffractometer with an imaging plate. A symmetry related absorption correction was carried out by using the program ABSCOR.[11] The analysis was carried out with direct methods (SHELX-97[12] or SIR97[13]) using Yadokari-XG.[14] The program ORTEP3[15] was used to generate the X-ray structural diagram. Molecular orbital calculations were performed using Gaussian 09. Elemental analysis was performed at the Microanalytical Center of Kyoto University. All reactions were performed under nitrogen or argon atmosphere.

Materials. Tetrahydrofuran (THF), diethyl ether, and triethylamine (Et_3N) were purified using a two-column solid-state purification system (Glasscontour System, Joerg Meyer, Irvine, CA). 10-Bromobenzo[*h*]quinoline,[16] chlorodiethoxymethylsilane,[17] and 2-iodo-1,4-bis(trifluoromethyl)benzene[18] were prepared according to the literature. Other reagents were commercially available and used as received.

Synthesis of 10-trimethylsilylbenzo[*h*]quinoline (1C). 6.25 mL (1.6 M in hexane, 10.0 mmol) of *n*-BuLi was slowly added to a solution of 10-bromobenzo[*h*]quinoline (2.58 g, 10.0 mmol) in 40 mL of THF at –78 °C, and the mixture was stirred at –78 °C for 20 min. Trichloromethylsilane (1.26 mL, 10.0 mmol) was added to the reaction mixture at -78 °C and then allowed to room temperature. After stirring for 12 h, NH_4Cl (aq) was added, followed by extraction with diethyl ether, drying over $MgSO_4$, and removal of the solvent under vacuum. The

crude product was purified by silica gel column chromatography eluted with hexane. Recrystallization from hexane gave a white solid in 57% yield (1.42 g, 5.66 mmol). ^{1}H NMR (400 M Hz, $CDCl_3$): δ = 8.89 (d, J = 4.2 Hz, 1H), 8.17 (d, J = 8.0 Hz, 1H), 8.11 (d, J = 6.9 Hz, 1H), 7.94 (d, J = 7.8 Hz, 1H), 7.84 (d, J = 8.8 Hz, 1H), 7.71 (m, 1H), 7.68 (m, 1H), 7.51 (q, J =4.4 Hz, 1H), 0.46 (s, 3H) ppm. ^{13}C NMR (100 M Hz, $CDCl_3$): δ = 146.53, 145.52, 138.73, 136.04, 135.81, 135.28, 133.60, 129.28, 128.81, 127.42, 126.62, 124.68, 121.42, 3.16 ppm. ^{29}Si NMR (80 M Hz, $CDCl_3$): δ = −11.14 ppm. HRMS (EI): m/z: calcd for $C_{16}H_{17}NSi$ (M^+): 251.1130; found : 251.1128.

Synthesis of 10-trifluorosilylbenzo[*h*]quinoline (1F). 7.76 mL (1.6 M in hexane, 12.5 mmol) of *n*-BuLi was slowly added to a solution of 10-bromobenzo[*h*]quinoline (3.20 g, 12.5 mmol) in 60 mL of THF at –78 °C, and the mixture was stirred at –78 °C for 20 min. Chlorotriethoxysilane (1.26 mL, 10.0 mmol) was added to the reaction mixture at –78 °C and then allowed to room temperature. After stirring for 12 h, all volatile components were removed under vacuum. Boron trifluoride diethyl etherate (1.8 mL, 14.6 mmol) was added to a suspension of the remaining solid in diethyl ether (30 mL), and stirring for 12 h. The reaction mixture was concentrated under vacuum. The remaining solid was dissolved in a small amount of dichloromethane, and the solution was reprecipitated with hexane. Recrystallization from hexane gave a white solid in 66% yield (2.18 g, 8.29 mmol). ^{1}H NMR (400 M Hz, $CDCl_3$): δ = 8.83 (d, J = 4.8 Hz, 1H), 8.44 (d, J = 8.0 Hz, 1H), 8.36 (d, J = 7.0 Hz, 1H), 8.07 (d, J = 8.0 Hz, 1H), 7.95 (d, J = 9.0 Hz, 1H), 7.87 (t, J = 7.4 Hz, 1H), 7.79 (d, J = 9.0 Hz, 1H), 7.76 (q, J = 4.9 Hz, 1H) ppm. ^{13}C NMR (100 M Hz, $CDCl_3$): δ = 150.8, 143.8, 142.0, 138.9, 138.1, 137.1, 134.3, 131.1, 128.6, 125.2, 123.4, 123.3 ppm. ^{29}Si NMR (80 M Hz, $CDCl_3$): δ = −105.3 ppm. HRMS (EI): m/z: calcd for $C_{13}H_8F_3NSi$ (M^+): 263.0378; found: 263.0388. elemental analysis: calcd for $C_{13}H_8F_3NSi$: C 59.30, H 3.06, N 5.32; found: C 59.41, H 3.06, N 5.38.

Synthesis of 10-(diethynylmethylsilyl)benzo[*h*]quinoline (1E). 18.0 mL (1.6 M in hexane, 30.0 mmol) of *n*-BuLi was slowly added to a solution of 10-bromobenzo[*h*]quinoline (7.66 g, 30.0 mmol) in 300 mL of THF at –78 °C, and the mixture was stirred at –78 °C for 20 min. Chlorodiethoxymethylsilane (6.12 mL, 36.0 mmol) was added to the reaction mixture at –78 °C and then allowed to room temperature. After stirring for 12 h, all volatile components were removed under vacuum. Ethynylmagnesium bromide (0.5 M in THF, 120 mL, 60 mmol) was slowly added to a solution of the remaining solid in THF (300 mL), and then the solution was refluxed for 12 h. After the solvent was removed under vacuum, the crude product was purified by silica gel column chromatography eluted with toluene/hexane (2/1). Recrystallization from hexane/dichloromethane gave a white solid in 37% yield (3.02 g, 11.1 mmol). ^{1}H NMR (400 M Hz, $CDCl_3$) : δ = 8.95 (dd, J = 4.4, 1.5 Hz, 1H), 8.82 (dd, J = 6.5, 1.0 Hz, 1H), 8.28 (dd, J = 6.6, 1.5 Hz, 1H), 8.03 (d, J = 6.9 Hz, 1H), 7.91 (d, J = 8.9 Hz, 1H), 7.84 (t, J = 7.5 Hz, 1H), 7.77 (d, J = 9.0 Hz, 1H), 7.63 (q, J = 4.1 Hz, 1H), 2.52 (s, 2H), 0.77 (t, J = 4.1 Hz, 3H) ppm. ^{13}C NMR (100 M Hz, $CDCl_3$): δ = 144.08, 137.94, 135.76, 134.61, 132.38, 130.16, 129.84, 128.34, 128.12, 125.71, 123.99, 122.06, 93.08, 90.95, 4.65 ppm. ^{29}Si NMR (80 M Hz, $CDCl_3$): δ = –70.85 ppm..HRMS (EI): m/z: calcd for $C_{18}H_{13}NSi$ (M^+): 271.0817; found: 271.0807. elemental analysis: calcd for $C_{18}H_{13}NSi$: C 79.66, H 4.83, N 5.16; found: C 79.39, H 4.75, N 5.15.

Synthesis of 10-(methylbis(phenylethynyl)silyl)benzo[h]quinoline (2C). Triethylamine (5.0 mL) was added to a solution of **1E** (0.271 g, 1.00 mmol), iodobenzene (0.223 g, 2.00 mmol), $Pd(PPh_3)_4$ (0.115 g, 0.100 mmol), CuI (0.020 g, 0.100 mmol) in toluene (10 mL) at room temperature. After the mixture was stirred at 90 °C for 36 h, the solvent was removed under vacuum. The crude product was purified by silica gel column chromatography eluted with hexane/chloroform (3/2). Recrystallization from hexane/dichloromethane gave a yellow solid in 28% yield (0.120 g, 0.284 mmol). ^{1}H NMR (400 M Hz, $CDCl_3$) : δ = 9.04 (dd, J = 4.4, 1.1 Hz,

1H), 8.93 (dd, *J* = 7.0, 1.0 Hz, 1H), 8.23 (dd, *J* = 7.9, 1.3 Hz, 1H), 8.02 (d, *J* = 7.7 Hz, 1H), 7.88 (d, *J* = 8.7 Hz, 1H), 7.83 (d, *J* = 7.5 Hz, 1H), 7.73 (d, *J* = 8.9 Hz, 1H), 7.60 (q, *J* = 4.3 Hz, 1H), 7.50 (q, *J* = 2.7 Hz, 4H), 7.27 (t, *J* = 3.1 Hz, 6H), 0.89 (s, 3H) ppm. ^{13}C NMR (100 M Hz, $CDCl_3$): δ = 144.8, 144.5, 138.3, 135.7, 135.2, 132.8, 131.9, 129.9, 128.5, 128.0, 126.1, 124.3, 124.1, 122.1, 103.1, 97.2, 4.9 ppm. ^{29}Si NMR (80 M Hz, $CDCl_3$): δ = −66.2 ppm. HRMS (EI): m/z: calcd for $C_{30}H_{21}NSi$ (M^+): 423.1443; found: 423.1432.

Synthesis of 10-(bis((2,5-bis(trifluoromethyl)phenyl)ethynyl)-(methyl)silyl)benzo[*h*]quinoline (2F). Triethylamine (10 mL) was added to a solution of **1E** (0.540 g, 2.00 mmol), 2-iodo-1,4-bis(trifluoromethyl)benzene (1.36 g, 4.00 mmol), $Pd(PPh_3)_4$ (0.240 g, 0.200 mmol), CuI (0.040 g, 0.200 mmol) in toluene (20 mL) at room temperature. After the mixture was stirred at 90 °C for 18 h, the solvent was removed under vacuum. The crude product was purified by silica gel column chromatography eluted with hexane/ethyl acetate (7/1). Recrystallization from hexane/dichloromethane gave a yellow solid in 56% yield (0.779 g, 1.12 mmol). ^{1}H NMR (400 M Hz, $CDCl_3$) : δ = 8.99 (s, 1H), 8.88 (d, *J* = 6.9 Hz, 1H), 8.21 (d, *J* = 7.8 Hz, 1H), 7.99 (d, *J* = 7.8 Hz, 1H), 7.93 (s, 2H), 7.85 (d, *J* = 7.8 Hz, 1H), 7.82 (d, *J* = 8.5 Hz, 1H), 7.70 (d, *J* = 8.2 Hz, 2H), 7.66 (d, *J* = 9.0 Hz, 1H), 7.61 (q, *J* = 4.9 Hz, 1H), 7.55 (d, *J* = 8.1 Hz, 2H), 0.96 (s) ppm. ^{13}C NMR (100 M Hz, $CDCl_3$): δ = 144.6, 144.2, 138.1, 136.3, 135.1, 134.8, 134.4, 134.2, 133.8, 133.5, 133.2, 132.6, 131.5, 130.4, 130.2, 128.8, 128.4, 127.9, 127.1, 126.4, 126.0, 124.3, 123.6, 122.3, 121.7, 118.9, 106.9, 96.8, 4.4 ppm. ^{29}Si NMR (80 M Hz, $CDCl_3$): δ = −72.3 ppm. HRMS (ESI): m/z: calcd for $C_{34}H_{18}F_{12}NSi$ ($M-H^+$): 696.1017; found: 696.1011.

References

(1) (a) Chen, J.; Cao, Y. *Macromol. Rapid Commun.* **2007,** *28,* 1714. (b) Yamaguchi, S.; Tamao, K. *J. Chem. Soc., Dalton Trans.* **1998,** 3693. (c) Uchida, M.; Izumizawa, T.; Nakano, T.; Yamaguchi, S.; Tamao, K.; Furukawa, K. *Chem. Mater.* **2001,** *13,* 2680. (d) Chan, K. L.; McKiernan, M. J.; Towns, C. R.; Holmes, A. B. *J. Am. Chem. Soc.* **2005,** *127,* 7662. (e) Sanchez, J. C.; Urbas, S. A.; Toal, S. J.; DiPasquale, A. G.; Rheingold, A. L.; Trogler, W. C. *Macromolecules* **2008,** *41,* 1237.

(2) (a) Chuit, C.; Corriu, R. J. P.; Reye, C.; Young, J. C. *Chem. Rev.* **1993,** *93,* 1371. (b) Nakash, M.; Goldvaser, M. *J. Am. Chem. Soc.* **2004,** *126,* 3436. (c) Setaka, W.; Nirenji, T.; Kabuto, C.; Kira, M. *J. Am. Chem. Soc.* **2008,** *130,* 15762. (d) Ghadwai, R. S.; Pröper, K.; Dittrich, B.; Jones, P. G.; Roesky, H. W. *Inorg. Chem.* **2011,** *50,* 358. (e) Ghadwal, R. S.; Sen, S. S.; Roesky, H. W.; Tavcar, G.; Merkel, S.; Stalke, D. *Organometalics* **2009,** *28,* 6374. (f) Kawachi, A.; Tani, A.; Shimada, J.; Yamamoto, Y. *J. Am. Chem. Soc.* **2008,** *130,* 4222.

(3) (a) Deerenberg, S.; Schakel, M.; de Keijzer, A. H. J. F.; Kranenburg, M.; Lutz, M.; Spek, A. L.; Lammertsma, K. *Chem. Commun.* **2002.** 348. (b) Couzijn, E. P. A.; Schakel, M.; de Kanter, F. J. J.; Ehlers, A. W.; Lutz, M.; Spek, A. L.; Lammertsma, K. *Angew. Chem. Int. Ed.* **2004,** *43,* 3440.

(4) (a) Metz, S.; Burschka, C.; Platte, D.; Tacke, R. *Angew. Chem. Int. Ed.* **2007,** *46,* 7006. (b) Ghadwal, R. S.; Sen, S. S.; Roesky, H. W.; Grantizka, M.; Kratzert, D.; Merkel, S.; Stalke, D. *Angew. Chem. Int. Ed.* **2010,** *49,* 3952. (c) Wagler, J.; Böhme, U.; Roewer, G. *Angew. Chem. Int. Ed.* **2002,** *41,* 1732. (d) Driess, M.; Muresan, N.; Merz, K. *Angew. Chem. Int.*

Ed. **2005,** *44,* 6738. (e) Sergani, S.; Kalikhman, I.; Yakubovich, S.; Kost, D. *Organometalics* **2007,** *26,* 5799.

(5) Bushuk, S. B.; Carré, F. H.; Guy, D. M. H.; Douglas, W. E.; Kalvinkovskya, Y. A.; Klapshina, L. G.; Rubinov, A. N.; Stupak, A. P.; Bushuk, B. A. *Polyhedron* **2004,** *23,* 2615.

(6) (a) Brelière, C.; Carré, F.; Corriu, R. J. P.; Poirier, M.; Royo, G. *Organometalics* **1986,** *5,* 388. (b) Williams, E. A.; Cargioli, J. D. in *Annual Reports on NMR Spectroscopy*, *Vol. 9* (Eds.: Webb, G. A.), Academic Press: New York, **1979**.

(7) Kano, N.; Komatsu, F.; Yamamura, M.; Kawashima, T. *J. Am. Chem. Soc.* **2006,** *128,* 7097.

(8) Tamao, K.; Hayashi, T.; Ito, Y. *Organometallics* **1992,** *11,* 2099.

(9) Couzijn, E. P. A.; Ehlers, A. W.; Schakel, M.; Lammertsma, K. *J. Am. Chem. Soc.* **2006,** *128,* 13634.

(10) Gaussian 09, Revision **A.1**, Frisch, M. J.; Trucks, G. W.; Schlegel, H. B.; Scuseria, G. E.; Robb, M. A.; Cheeseman, J. R.; Scalmani, G.; Barone, V.; Mennucci, B.; Petersson, G. A.; Nakatsuji, H.; Caricato, M.; Li, X.; Hratchian, H. P.; Izmaylov, A. F.; Bloino, J.; Zheng, G.; Sonnenberg, J. L.; Hada, M.; Ehara, M.; Toyota, K.; Fukuda, R.; Hasegawa, J.; Ishida, M.; Nakajima, T.; Honda, Y.; Kitao, O.; Nakai, H.; Vreven, T.; Montgomery, Jr., J. A.; Peralta, J. E.; Ogliaro, F.; Bearpark, M.; Heyd, J. J.; Brothers, E.; Kudin, K. N.; Staroverov, V. N.; Kobayashi, R.; Normand, J.; Raghavachari, K.; Rendell, A.; Burant, J. C.; Iyengar, S. S.; Tomasi, J.; Cossi, M.; Rega, N.; Millam, J. M.; Klene, M.; Knox, J. E.; Cross, J. B.;

Bakken, V.; Adamo, C.; Jaramillo, J.; Gomperts, R.; Stratmann, R. E.; Yazyev, O.; Austin, A. J.; Cammi, R.; Pomelli, C.; Ochterski, J. W.; Martin, R. L.; Morokuma, K.; Zakrzewski, V. G.; Voth, G. A.; Salvador, P.; Dannenberg, J. J.; Dapprich, S.; Daniels, A. D.; Farkas, Ö.; Foresman, J. B.; Ortiz, J. V.; Cioslowski, J.; Fox, D. J. Gaussian, Inc., Wallingford CT, 2009.

(11) Higashi, T. *ABSCOR. Program for Absorption Correction.*; Rigaku Corporation: Japan, 1995.

(12) Sheldrick, G. M. SHELX-97. Programs for Crystal Structure Analysis.; University of Göttingen: Germany, 1997.

(13) Altomare, A.; Burla, M.C.; Camalli, M.; Cascarano, G. L.; Giacovazzo, C.; Guagliardi, A.; Moliterni, A. G. G.; Polidori, G.; Spagna, R. *J. Appl. Cryst.* **1999,** *32*, 115.

(14) Wakita, K. *Yadokari-XG. Program for Crystal Structure Analysis*; 2000.

(15) Farrugia, L. J. *J. Appl. Cryst.* **1997,** *30*, 565.

(16) Dick, A. R.; Hull, K. L.; Sanford, M. S. *J. Am. Chem. Soc.* **2004,** *126,* 2300.

(17) Zhang, J.; Chen, Z.; Fu, W.; Xie, P.; Li, Z.; Yan, S.; Zhang, R. *J. Polym. Sci., Part A: Polym. Chem.* **2010,** *48,* 2491.

(18) Satyanarayana. K.; Srinivas, K.; Himabindu, V.; Reddy, G. M. *Org. Process Res. Dev.* **2007,** *11,* 842.

Chapter 7

Structure-Dependent Electronic Communication around Pentacoordinate Silicon in Benzo[*h*]quinolyldibenzo[*b*,*f*]silepins

Abstract

A benzo[*h*]quinolyl ligand provided pentacoordinate character for silicon in dibenzo[*b*,*f*]silepins. The molecular structures were dominated by substituents on the silicon centre. The cross-shaped structure strongly fixed by fluoride induced charge transfer from the dibenzosilepin moiety to the benzoquinolyl ligand in photoexcitation

Introduction

Silicon in organic molecules has shown various coordination and oxidation numbers and also provided attractive structures and unique properties. Tetracoordinate silicon compounds with C–Si single bonds are so stable under the air that many π-conjugated organosilicons have been already applied to organic electronics devices.[1,2] In recent years, stabilizing strategies for multiple bonds containing silicon has been evolved dramatically. Kinetically stabilized disilenes[3] and silabenzenes[4] exhibited bathochromic shift in UV–vis absorption spectra as compared with corresponding hydrocarbons.

Pentacoordinate silicon compounds possess distinct structure from well known tetracoordinate ones.[5] The pentacoordinate center shows a trigonal-bipyramidal geometry giving two inequivalent sites of substitution, apical and equatorial. The apical positions were generally occupied by dative moieties or electronegative substituents. Switching between tetracoordinate and pentacoordinate state of the silicon compounds induces the changes not only in the structure but also in the electronic states, resulting in intriguing optical characteristics such as stimuli-responsive changes.[6] In spite of their promising useful optical properties, there are only a few versatile methods for preparing and isolating neutral pentacoordinate organosilicon compounds.[7] In Chapter 6, the author demonstrated that 10-benzo[*h*]quinolyl ligand can stabilize N–Si dative bond in trimethylsilyl, trifluorosilyl and diethynyl(methyl)silyl derivatives.[8] Pentacoordination of the silicon centre induced a bathochromic shift and enhancement to fluorescence from the benzo[*h*]quinolyl ligand. The characteristic optical property was related to orbitals localized on the benzoquinolyl ligand, only depending on the degree of ligand's fixation.

To make full use of the trigonal-bipyramidal geometry and construct cooperative system between substituents on the pentacoordinate silicon centre, the author now reports the synthesis

and properties of benzo[*h*]quinolyldibenzo[*b,f*]silepins with bending structure by vinyliden group. The apical and equatorial positions of silicon produce two distinct patterns to place the 1,2-diarylethene moiety. Tuning of the comformation was achieved by the substituent on the silicon centre (Me or F). Moreover, the conformation and the substituent influenced charge transfer efficiencies between the dibenzosilepin moiety and the benzoquinolyl ligand by photoirradiation.

Results and Discussion

Entry to the desired dibenzo[*b,f*]silepins begins with a dibrominared 1,2-diphenylethene **1** and its dilithiation (Scheme 1).[9] The dilithiated species reacted with trichlroro(methyl)silane followed by addition of 10-benzo[*h*]quinolyllithium to give the methylated benzo[*h*]quinolyldibenzo[*b,f*]silepin **2**. For preparing the fluorinated dibenzo[*b,f*]silepins, synthesis of an alkoxylated dibenzo[*b,f*]silepins was executed as the same procedure for **2** by an alkoxytrichlorosilane. After column chromatography and recrystallization, the prododucts were separated. Although the structures were not definitely determined in ^{1}H NMR spectra because of the diverse peaks, elemental analysis and mass spectra supported that the product was hydrolyzed during purification, resulting in hydroxylated dibenzo[*h*]quinolyldibenzo[*b,f*]silepin **3**. Boron trifluoride diethyl etherate successfully exchanged hydroxy group of **3** for fluoride to give compound **4**.

The solid-state structures of the obtained dibenzosilepins were determined by X-ray diffraction analysis (Figure 1). In compound **2**, the methyl group, which is electrodonating, occupied the equatorial position. Therefore, the diphenylethene moiety was arranged in the apical-equatorial manner. The structure of **3** also looked like apical-equatorial conformation. The

benzoquinoline's nitrogen, however, pointed to the hydroxy group. This means that the structure of **3** was governed not only by pentacoordination of the silicon centre but also by hydrogen bond. In compound **4**, fluoride occupied apical position and directed the diphenylethene moiety to equatorial-equatorial conformation. As the N–Si distance shortens in the order of **3** (2.818 Å) > **2** (2.761 Å) > **4** (2.341 Å), the sum of the three angles formed by the equatorial atoms increases in the order of **3** (341.55°) < **2** (343.84°) < **4** (353.26°). The order suggested that hydrogen bond disturbed pentacoordination of the silicon centre, and that fluoride enhanced the pentacoordinte character. The pentacoordinate characters, $\%TBP_a$ and $\%TBP_e$,[10] were determined as 25% and 42% for **3**, 30% and 49% for **2**, and 55% and 79% for **4**, respectively. From these values, the configurations around the silicon centre are intermediate structures between tetrahedron and trigonal-bipyramid. The dihedral angles between phenyl and vinylene moieties of **2** and **4** were 46° and 29° (averaged four dihedral angles, and neglecting front or back side of the surface), respectively. The conformation of the diphenylethene moiety, apical-equatorial and equatorial-equatorial, plays a crucial role in the silepin structure.

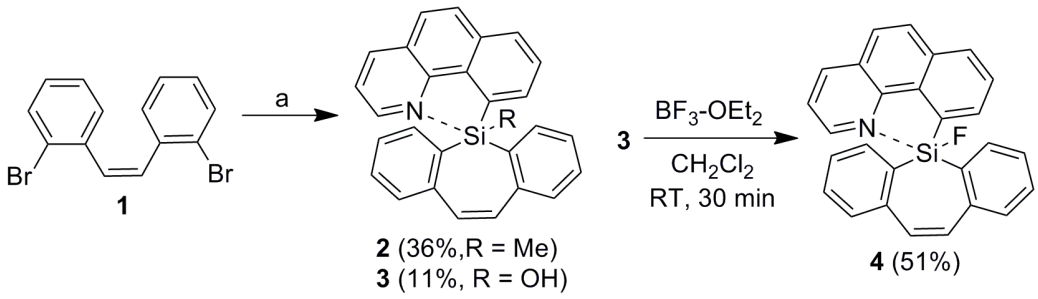

Scheme 1. Synthesis of benzo[*h*]quinolyldibenzo[*b,f*]silepins. Conditions and reagents: (a) i. *n*BuLi, THF, –78 °C, ii. *N,N,N',N'*-tetramethylethylenediamine (TMEDA), –78 °C, iii. R^1SiCl_3 (R^1 = Me for **2**, $R^1 = O(CH_2)_2O(CH_2)_2OEt$ for **3**), RT, iv. 10-benzo[*h*]quinolyllithium, TMEDA, THF, RT, v. NH_4Cl (aq)

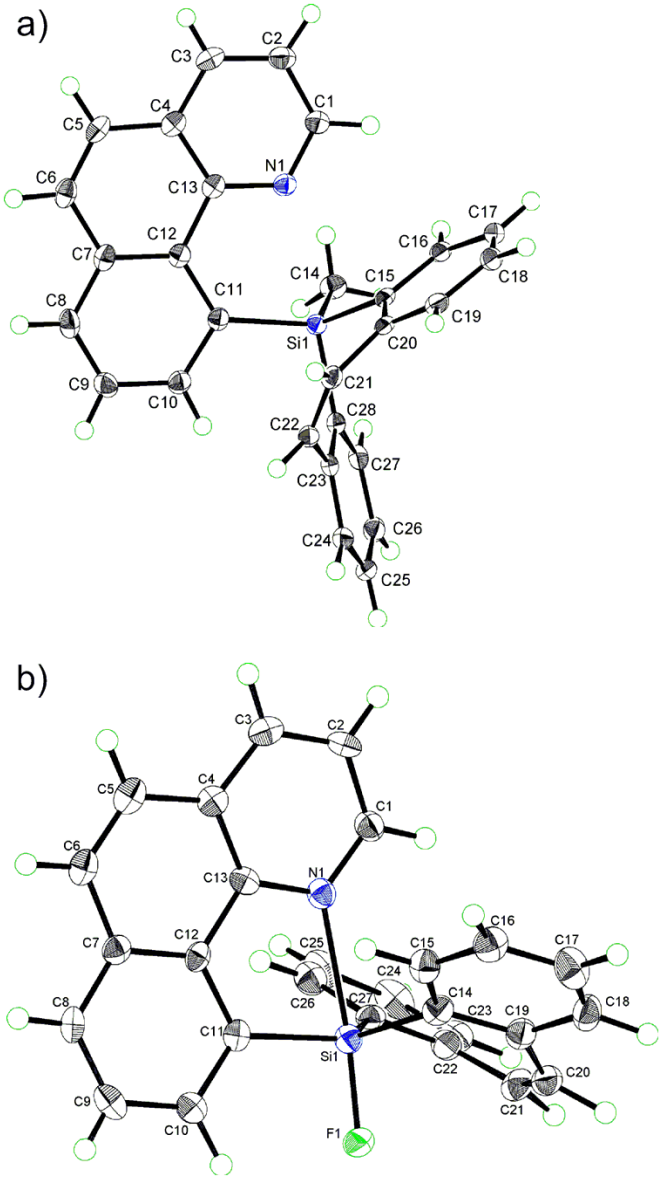

Figure 1. The X-ray crystal structures of (a) **2** and (b) **4** with thermal ellipsoids drawn to 50% probability level. Selected bond lengths [Å] and angles [°]: **2**: Si1–N1 = 2.761, C28–Si1–C11 = 104.47(8), C14–Si1–C28 = 107.73(9), C15–Si1–C28 = 99.00(8), C14–Si1–C15 = 113.09(9), C19–C20–C21–C22 = 134.4(2), C21–C22–C23–C24 = 134.8(2); **4**: Si1-N1 = 2.341(2), F1–Si1–C11 = 97.04(12), F1–Si1–C27 = 99.34(11), F1–Si1–C14 = 99.78(12), C27–Si1–C11 =120.34(15), C14–Si1–C11 = 119.98(15), C27–Si1–C14 = 112.94(15), C18–C19–C20–C21 = 149.7(4), C18–C19–C20–C21 = 153.4(4).

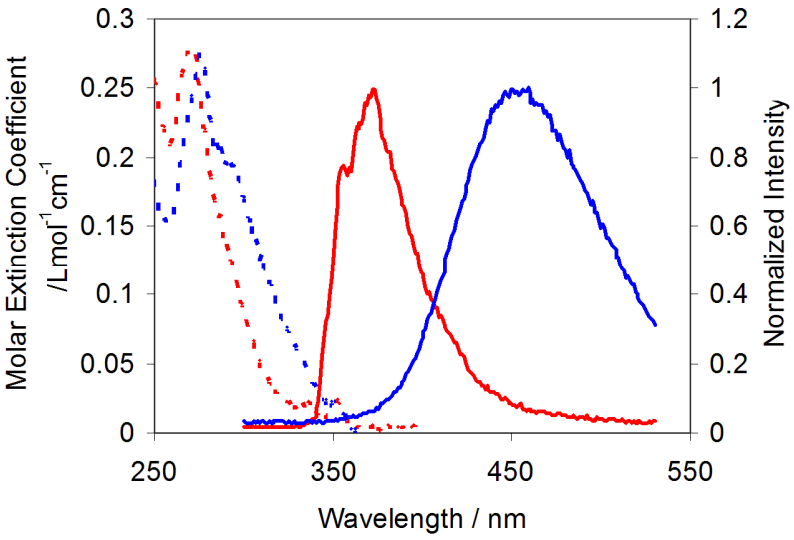

Figure 2. UV–vis (left, dotted line) and normalized photoluminescence spectra (right, solid line, excited at absorption maxima) of **2** (red) and **4** (blue) in CH_2Cl_2 (1.0×10^{-5} M).

The structures of **2** and **4** in solution-state were investigated by NMR spectroscopy at room temperature. The ^{29}Si NMR signal of **4** (δ = –40.3 ppm) appeared in upper field than that of **2** (δ = –20.2 ppm), representing strong N–Si interaction in **4**. Although the extent of the pentacoordination character was different, both of them showed upfield shift by the nitrogen's electron pair as compared with tetracoordinate analogues (δ ~ –10 ppm).[2] In ^{1}H NMR spectra of **2**, no separation of peak derived from apical-equatorial conformation was observed, implying rotation of the diarylethene moiety in solution-state. While there was only one ^{1}H NMR signal (2 protons) of **2** between 6.0 and 7.0 ppm assignable to the vinylene group, two signals (2 and 4 protons) appeared in ^{1}H NMR spectra of **4**. One is assignable to the vinylene group, and the other is 3,4,6,7-protons of dibenzo[*b*,*f*]silepin shielded by the benzoquinolyl ring. This shielding

indicates that the equatorial-equatorial conformation of the diphenylethene moiety remained in solution-state by strong electrowithdrawing character of fluoride.

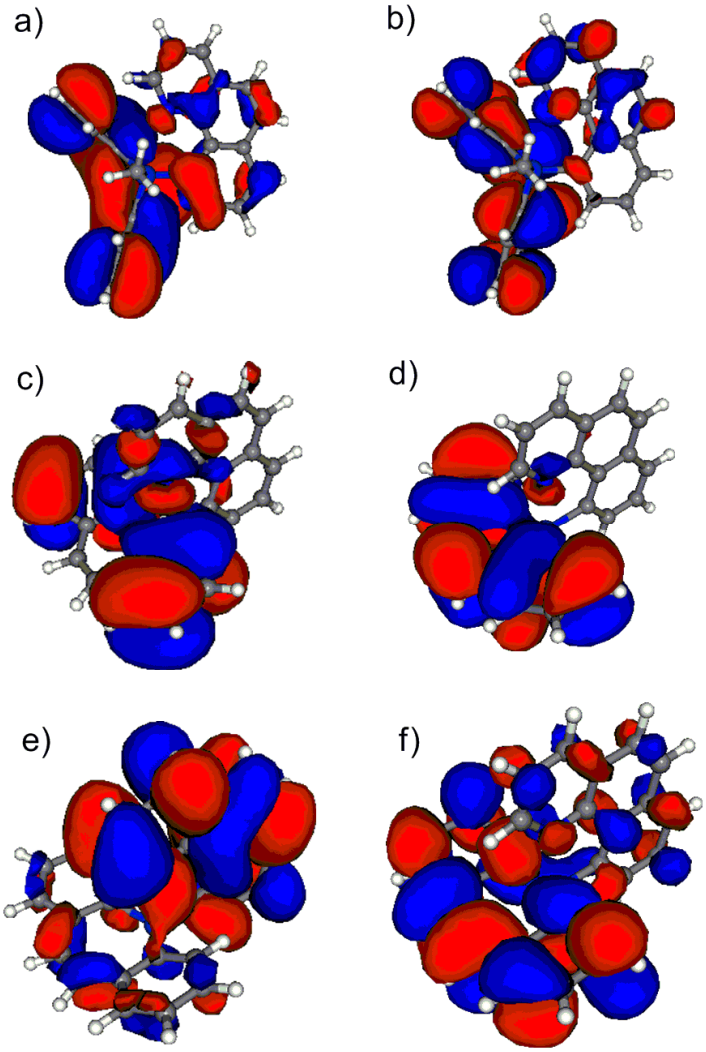

Figure 3. Kohn-Sham orbital diagrams: (a) HOMO of **2**, (b) LUMO+2 of **2**, (c) HOMO-3 of **4**, (d) HOMO of **4**, (e) LUMO of **4**, (f) LUMO+2 of **4**.

Figure 2 displays the UV–vis absorption and photoluminescence spectra of **2** and **4** excited at those absorption maxima in dichloromethane (c = 1.0 × 10^{-5} M). The absorption peak

of **4** with a shoulder around 300 nm slightly shifted to longer wavelength region as compared with that of **2**. In photoluminescence spectra, compound **4** showed larger Stokes-shift than compound **2**, and those peak shapes were different. Photoluminescence spectrometry in other solvents (cyclohexane, tetrahydrofuran and *N,N*-dimethylformamide) revealed that the peak position of **2** also remained. The peak of **4** shifted to longer wavelength region as the solvent polarity increased. It can be deduced that fluorescence was derived from local excited state of the benzoquinolyl ligand in compound **2** and from charge transfer state from the dibenzosilepin moiety to the benzoquinolyl ligand in compound **4**.

To have a better understanding of the structures and properties of the obtained benzoquinolyldibenzosilepins, density functional theory (DFT) calculations of **2** and **4** were performed.[11] The structures were optimized by RI-TPSS-D3(BJ)/def2-SVP and the N–Si distances (2.738 Å for **2** and 2.410 Å for **4**) were almost identical to those of the crystal structures.[12] Moreover, the optimization was applied to the opposite conformers, equatorial-equatorial for **2** and apical-equatorial for **4**. Single point calculation of them (RIJCOSX-PW6B95-D3(BJ)/def2-TZVP)[13] revealed that apical-equatorial conformation of **2** was more stable by 0.69 kcal/mol at 298 K than that equatorial-equatorial conformation. This small stabilization was inefficient to hold the conformation. In the compound **4**, equatorial-equatorial conformation was more stable by 3.10 kcal/mol at 298 K than apical-equatorial conformation. This value supported the fixed structure in the solution state. From Mayer population analysis, total valences for the silicon centres were determined as 4.36 for **2** and 4.39 for **4**, implying the pentacoordinate character. Time-dependent DFT calculation (RIJCOSX-PBE0/def2-TZVPP)[14] with Tamm-Dancoff approximation (TDDFT/TDA)[15] suggested that excitation between the orbitals mainly localized on the dibenzosilepin moiety (HOMO → LUMO+2) were easy to occur

for **2** (λ = 286 nm, f = 0.1962) and **4** (λ = 310 nm, f = 0.2854). In the compound **4**, additional transition was permitted from the orbital localized on the dibenzosilepin moiety to that on the benzoquinolyl ligand (HOMO-3 → LUMO, λ = 299 nm, f = 0.2709) and the two calculated transitions of **4** can explain the shoulder in the UV–vis absorption spectrum. The results from TDDFT/TDA calculation mean that the fixed equatorial-equatorial conformation and fluoride could be responsible for the electronic interaction to induce charge transfer from the dibenzosilepin moiety to the benzoquinolyl ligand.

Conclusion

Benzo[*h*]quinolyldibenzo[*b*,*f*]silepins have been synthesized successfully, and their pentacoordinate characters of the silicon centre were confirmed by X-ray diffraction analysis, NMR spectroscopy, and DFT calculation. The methyl and fluoride derivatives favored apical-equatorial and equatorial-equatorial conformation, respectively. The fixed equatorial-equatorial conformation and the electrowithdrawing substituent on the silicon centre provided large Stokes-shift in absorption and luminescence spectra.

Experimental Section

Measurements. ^{1}H (400 MHz), ^{13}C (100 MHz), and ^{29}Si (80 MHz) NMR spectra were recorded on a JEOL JNM-EX400 spectrometer. ^{1}H and ^{13}C NMR spectra used tetramethylsilane (TMS) as an internal standard. ^{29}Si NMR spectra were referenced externally to TMS in $CDCl_3$. UV–vis spectra were recorded on a Shimadzu UV-3600 spectrophotometer. Fluorescence emission spectra were recorded on a HORIBA JOBIN YVON Fluoromax-4 spectrofluorometer. X-ray crystallographic analysis was carried out by a Rigaku R-AXIS RAPID-F graphite-monochromated Mo Kα radiation diffractometer with an imaging plate. A symmetry related absorption correction was carried out by using the program ABSCOR.[16] The analysis was carried out with direct methods (SHELX-97[17] or SIR97[18]) using Yadokari-XG.[19] The program ORTEP3[20] was used to generate the X-ray structural diagram. Molecular orbital calculations were performed using ORCA. Elemental analysis was performed at the Microanalytical Center of Kyoto University. All reactions were performed under nitrogen or argon atmosphere.

Materials. Tetrahydrofuran (THF) and diethyl ether were purified using a two-column solid-state purification system (Glasscontour System, Joerg Meyer, Irvine, CA). 10-Bromobenzo[*h*]quinoline[21] and (*Z*)-1,2-bis(2-bromophenyl)ethene[22] were prepared according to the literature. Other reagents were commercially available and used as received.

Synthesis of 5-(10-benzo[*h*]quinolyl)-5-methyldibenzo[*b*,*f*]silepin (2). To a solution of (*Z*)-1,2-bis(2-bromophenyl)ethene (1.49 g, 4.00 mmol) in THF (40 mL), A solution of *n*-butyllithium in hexane (1.6 M, 5.0 mL, 8.0 mmol) was added dropwise at –78 °C and the resulting mixture was held at –78 °C for 10 min followed by the addition of TMEDA (1.19 mL, 8.00 mmol). After the mixture was stirred for 45 min at –78 °C, trichloro(methyl)silane (0.47 mL,

4.00 mmol) was added. The resulting mixture was allowed to warm to room temperature and left to stir for 6 h. The solvent was removed at room temperature under reduced pressure. The obtained solid was dissolved in THF (20 mL) and the solution and TMEDA (0.60 mL, 4.0 mmol) were added to a solution of 10-benzo[*h*]quinolyllithium in THF (generated by treating 10-bromobenzo[*h*]quinoline (1.03 g, 4.00 mmol) with *n*-butyllithium (1.6 M in hexane, 2.5 mL, 4.0 mmol) in THF (24 mL) for 30 min at –78 °C). After stirring at room temperature for 11 h, NH_4Cl (aq) was added, followed by extraction with cyclopentyl methyl ether, drying over $MgSO_4$, and removal of the solvent under vacuum. The crude product was purified by silica gel column chromatography eluted with hexane/chloroform (4/1). Recrystallization from dicloromethane/hexane gave a white solid in 36% yield (0.570 g, 1.43 mmol). ^{1}H NMR (400 MHz, $CDCl_3$): δ = 8.62 (br, 1H, Ar*H*), 8.00 (dd, *J* = 8.0, 1.6 Hz, 1H, Ar*H*), 7.87 (m, 3H, Ar*H*), 7.76 (d, *J* = 8.8 Hz, 1H, Ar*H*), 7.59 (d, *J* = 8.8 Hz, 1H, Ar*H*), 7.48 (m, 2H, Ar*H*), 7.32-7.21 (m, 7H, Ar*H*), 6.67 (s, 2H, -C*H*=C*H*-), 1.14 (s, 3H, -CH_3) ppm. ^{13}C NMR (100 MHz, $CDCl_3$): δ = 145.7, 141.7, 140.5, 137.7, 136.4, 135.1, 133.7, 133.0, 132.7, 132.5, 129.7, 128.6, 127.5, 127.1, 126.7, 126.3, 124.7, 121.4, –3.1 ppm. ^{29}Si NMR (80 MHz, $CDCl_3$): δ = –20.2 ppm. HRMS (ESI+): m/z: calcd for $C_{28}H_{22}NSi$ ($M+H^+$): 400.1516; found: 400.1515. elemental analysis: calcd for $C_{28}H_{21}NSi$: C 83.60, H 5.13, N 3.75; found: C 82.95, H 5.14, N 3.75.

Synthesis of Trichloro((2-ethoxyethoxy)ethoxy)silane. (2-Ethoxyethoxy)ethanol (27.1 mL, 200 mmol) was added to a solution of tetrachlorosilane (23.0 mL, 200 mmol) in hexane (30 mL) at room temperature. After the mixture was stirred at 60 °C for 12 h, vacuum distillation (110 °C, 1 torr) gave a colorless liquid in 48% yield (25.8 g, 96.3 mmol). ^{1}H NMR (400 MHz, $CDCl_3$): δ = 4.15 (t, *J* = 4.8 Hz, 2H, -CH_2OSiCl_3), 3.71-3.65 (m, 4H, -CH_2-), 3.61-3.51 (m, 4H, -

CH_2-), 1.22 (t, J = 7.2 Hz, 3H, -CH_3) ppm. ^{13}C NMR (100 MHz, $CDCl_3$): δ = 70.9, 70.8, 69.8, 66.7, 65.8, 15.1 ppm.

Synthesis of 5-(10-Benzo[*h*]quinolyl)-5-hydroxydibenzo[*b*,*f*]silepin (3). To a solution of (*Z*)-1,2-bis(2-bromophenyl)ethene (1.49 g, 4.00 mmol) in THF (40 mL), A solution of *n*-butyllithium in hexane (1.6M, 5.0 mL, 8.0 mmol) was added dropwise at –78 °C and the resulting mixture was held at –78 °C for 10 min followed by the addition of TMEDA (1.19 mL, 8.00 mmol). After the mixture was stirred for 30 min at –78 °C, trichloro((2-ethoxyethoxy)ethoxy)silane (1.07 g, 4.00 mmol) in THF (4.0 mL) was added. The resulting mixture was allowed to warm to room temperature and left to stir for 7 h. The solvent was removed at room temperature under reduced pressure. The obtained solid was dissolved in THF (20 mL) and the solution and TMEDA (0.60 mL, 4.0 mmol) were added to a solution of 10-benzo[*h*]quinolyllithium in THF (generated by treating 10-bromobenzo[*h*]quinoline (1.03 g, 4.00 mmol) with *n*-butyllithium (1.6 M in hexane, 2.5 mL, 4.0 mmol) in THF (24 mL) for 30 min at –78 °C). After stirring at room temperature for 12 h, NH_4Cl (aq) was added, followed by extraction with cyclopentyl methyl ether, drying over $MgSO_4$, and removal of the solvent under vacuum. The crude product was purified by silica gel column chromatography eluted with hexane/ethyl acetate (3/1). Recrystallization from chloroform/hexane gave a yellow solid in 11% yield. (0.180 g, 0.447 mmol) that was used without further purification. HRMS (ESI+): m/z: calcd for $C_{27}H_{20}NOSi$ ($M+H^+$): 402.1309; found: 402.1313. elemental analysis: calcd for $C_{27}H_{19}NOSi$: C 80.76, H 4.77, N 3.49; found: C 80.28, H 4.91, N 3.46.

Synthesis of 5-(10-Benzo[*h*]quinolyl)-5-fluorodibenzo[*b*,*f*]silepin (4). Boron trifluoride diethyl etherate (0.040 mL, 0.33 mmol) was added to a solution of 5-(10-benzo[*h*]quinolyl)-5-hydroxydibenzo[*b*,*f*]silepin (120 mg, 0.300 mmol) in dichloromethane (12 mL) at room

temperature. After the solution was stirred at room temperature for 30 min, sodium bicarbonate (saturated aqueous) was added. The organic layer was separated, dried over Na_2SO_4, filtered, and concentrated under vacuum. The resulting oil was added dropwise to methanol (10 mL) to give a colorless solid in 51% yield (62.0 mg, 0.154 mmol). ^{1}H NMR (400 MHz, $CDCl_3$): δ = 8.61 (d, *J* = 7.2 Hz,1H, Ar*H*), 8.16 (d, *J* = 8.4 Hz, 1H, Ar*H*), 8.13 (d, *J* = 8.0 Hz, 1H, Ar*H*), 8.01 (d, *J* = 8.8 Hz, 1H, Ar*H*), 7.96 (d, *J* = 7.2 Hz, 1H, Ar*H*), 7.90 (d, *J* = 4.4 Hz, 2H, Ar*H*), 7.77 (d, *J* = 9.2 Hz, 1H, Ar*H*), 7.41 (d, *J* = 7.6 Hz, 2H, Ar*H*) 7.21 (m, 3H, Ar*H*), 6.91 (s, 2H, –C*H*=C*H*–), 6.78 (m, 4H, Ar*H*) ppm. ^{13}C NMR (100 MHz, $CDCl_3$): δ = 145.2, 143.5, 140.2, 138.7, 138.7, 138.6, 138.5, 138.4, 136.0, 132.93, 132.86, 132.4, 131.8, 130.9, 130.7, 129.8, 129.5, 128.6, 126.5, 125.4, 124.1, 122.7 ppm. ^{29}Si NMR (80 MHz, $CDCl_3$): δ = –40.3 (d, *J* = 270 Hz) ppm. HRMS (ESI+): m/z: calcd for $C_{27}H_{19}NFSi$ ($M+H^+$): 404.1265; found: 404.1264. elemental analysis: calcd for $C_{27}H_{18}NFSi$: C 80.36, H 4.50, N 3.47; found: C 80.10, H 4.48, N 3.54.

References

(1) (a) Sanchez, J. C.; Trogler, W. C. *Macromol. Chem. phys.* **2008,** *209,* 1527. (b) Yamaguchi, S.; Tamao, K. *Chem. Lett.* **2005,** *34,* 2. (c) Choi, J.-K.; Jang, S.; Kim, K.-J.; Sohn, H. Jeong, H.-D. *J. Am. Chem. Soc.* **2011,** *133,* 7764. (d) Zhao, Z.; Wang, Z. Lu, P. Chan, C. Y. K.; Liu, D.; Lam, J. W. Y.; Sung, H. H. Y.; Tang, B. Z. *Angew. Chem. Int. Ed.* **2009,** *48,* 7608. (e) Zhan, X.; Barlow, S.; Marder, S. R. *Chem. Commun.* **2009,** 1948. (f) Booker, C.; Wang, X.; Haroun, S.; Zhou, J.; Jennings, M.; Pagenkopf, B. L.; Ding, Z. *Angew. Chem. Int. Ed.* **2008,** *47,* 7731. (g) Hou, J.; Chen, H.-Y.; Zhang, S.; Li, G. Yang, Y. *J. Am. Chem. Soc.* **2008,** *130,* 16144.

(2) (a) Mercier, L. G.; Furukawa, S.; Piers, W. E.; Wakamiya, A.; Yamaguchi, S.; Parvez, M.; Harrington, R. W.; Clegg, W. *Organometallics* **2011,** *30,* 1719. (b) Kira, M.; Ishida, S.; Iwamoto, T.; Kabuto, C. *J. Am. Chem. Soc.* **2002,** *124,* 3830. (c) Nishigata, T.; Izukawa, Y.; Komatsu, K. *Tetrahedron* **2001,** *57,* 3645.

(3) (a) Takeuchi, K.; Ichinohe, M.; Sekiguchi, A. *J. Am. Chem. Soc.* **2012,** *134,* 2954. (b) Tamao, K.; Kobayashi, M.; Matsuo, T.; Furukawa, S.; Tsuji, H. *Chem. Commun.* **2012,** *48,* 1030. (c) Kira, M. *Organometallics* **2011,** *30,* 4459. (d) Jeck, J.; Bejan, I,; White, A. J. P.; Nied, D.; Brecher, F.; Scheschkewitz, D. *J. Am. Chem. Soc.* **2010,** *132,* 17306.

(4) (a) Tanabe, Y.; Mizuhata, Y.; Tokitoh, N. *Organometallics* **2010,** *29,* 721. (b) Tokitoh, N. *Acc. Chem. Res.* **2004,** *37,* 86.

(5) (a) Chuit, C.; Corriu, R. J. P.; Reye, C.; Young, J. C. *Chem. Rev.* **1993,** *93,* 1371. (b) Nakash, M.; Goldvaser, M. *J. Am. Chem. Soc.* **2004,** *126,* 3436. (c) Setaka, W.; Nirenji, T.; Kabuto, C.; Kira, M. *J. Am. Chem. Soc.* **2008,** *130,* 15762. (d) Ghadwai, R. S.; Pröper, K.; Dittrich,

B.; Jones, P. G.; Roesky, H. W. *Inorg. Chem.* **2011,** *50,* 358. (e) Ghadwal, R. S.; Sen, S. S.; Roesky, H. W.; Tavcar, S. Merkel, G.; Stalke, D. *Organometalics* **2009,** *28,* 6374. (f) Kawachi, A.; Tani, A.; Shimada, J.; Yamamoto, Y. *J. Am. Chem. Soc.* **2008,** *130,* 4222.

(6) (a) Kano, N.; Komatsu, F.; Yamamura, M.; Kawashima, T. *J. Am. Chem. Soc.* **2006,** *128,* 7097. (b) Yamaguchi, S.; Akiyama, S.; Tamao. K. *J. Am. Chem. Soc.* **2000,** *122,* 6793.

(7) (a) Bushuk, S. B.; Carré, F. H.; Guy, D. M. H.; Douglas, W. E.; Kalvinkovskya, Y. A.; Klapshina, L. G.; Rubinov, A. N.; Stupak, A. P.; Bushuk, B. A. *Polyhedron* **2004,** *23,* 2615. (b) Sen, S. S.; Hey, J.; Herbst-Irmer, R. H. Roesky, W.; Stalke, D. *J. Am. Chem. Soc.* **2011,** *133,* 12311.

(8) Tokoro, Y. Yeo. H.; Tanaka, K.; Chujo, Y. *Chem. Commun.* **2012,** *48,* 8541.

(9) Harrowven, D. C.; Guy, I. L.; Nanson, L. *Synlett.* **2006,** *18,* 2977.

(10) Tamao, K. Hayashi, T. Ito, Y. *Organometallics* **1992,** *11,* 2099.

(11) ORCA (version 2.9): Neese, F.; Wennmohs, F.; Becker, U.; Bykov, D.; Ganyushin, D.; Hansen, A.; Izsak, R.; Liakos, D. G.; Kollmar, C.; Kossmann, S.; Pantazis, D. A.; Petrenko, T.; Reimann, C.; Riplinger, C.; Roemelt, M.; Sandhöfer, B.; Schapiro, I.; Sivalingam, K.; Wezisla, B.; Kállay, M.; Grimme, S.; Valeev. E.

(12) (a) Tao, J.; Perdew, J. P.; Staroverov, V. N.; Scuseria, G. E. *Phys. Rev. Lett.* **2003,** *91,* 146401. (b) Grimme, S.; Ehrlich, S.; Goerigk, L. *J. Comput. Chem.* **2011,** *32,* 1456.(c) Grimme, S.; Anthony, J.; Ehrlich, S.; Krieg, H. *J. Chem. Phys.* **2010,** *132,* 154104. (d) Schaefer, A.; Horn, H.; Ahlrichs, R. *J. Phys. Chem.* **1992,** *97,* 2571. (e) Eichkorn, K.; Treutler, O.; Öhm, H.; Häser, M.; Ahlrichs, R. *Chem. Phys. Lett*. **1998**, *286,* 243. (f) Hättig,

C.; Weigend, F. *J. Chem. Phys*. **2000,** *113,* 5154. (g) Weigend, F. *Phys. Chem. Chem. Phys.* **2006**, *8,* 1057.

(13) (a) Zhao, Y.; Truhlar, D. G. *J. Phys. Chem. A* **2005,** *109,* 5656. (b) Weigend, F.; Ahlrichs, R. *Phys. Chem. Chem. Phys.* **2005,** *7,* 3297. (c) Iszák, R.; Neese, F. *J. Chem. Phys.* **2011,** *135,* 144105.

(14) (a) Adamo, C.; Barone, V. *J. Chem. Phys.* **1999,** *110,* 6158. (b) Petrenko, T.; Kossmann, S.; Neese, F. *J. Chem. Phys.* **2011,** *134,* 054116.

(15) Hirata, S.; Head-Gordon, M. *Chem. Phys. Lett.* **2004,** *314,* 291.

(16) Higashi, T. *ABSCOR. Program for Absorption Correction.*; Rigaku Corporation: Japan, 1995.

(17) Sheldrick, G. M. SHELX-97. Programs for Crystal Structure Analysis.; University of Göttingen: Germany, 1997.

(18) Altomare, A.; Burla, M.C.; Camalli, M.; Cascarano, G. L.; Giacovazzo, C.; Guagliardi, A.; Moliterni, A. G. G.; Polidori, G.; Spagna, R. *J. Appl. Cryst.* **1999,** *32*, 115.

(19) Wakita, K. *Yadokari-XG. Program for Crystal Structure Analysis*; 2000.

(20) Farrugia, L. J. *J. Appl. Cryst.* **1997,** *30*, 565.

(21) Dick, A. R.; Hull, K. L.; Sanford, M. S. *J. Am. Chem. Soc.* **2004,** *126,* 2300.

(22) Harrowven, D. C.; Guy, I. L.; Nanson, L. *Synlett.* **2006,** *18,* 2977.

Chapter 8

Integration of Benzo[*h*]quinoline and π-Extended Dibenzo[*b*,*f*]silepins on Pentacoordinate Silicon

Abstract

Substitutent effects on structures and electronic properties of dibenzo[*b*,*f*]silepins containing pentacoordinate silicon were investigated by NMR, UV–vis absorption and photoluminescence spectroscopies. It was found that the structures of the complex were strongly influenced by the type of substituents on the silicon centre regardless of those on the dibenzosilepin moiety. In 2,8-diaryl-substituted compounds, an electron-donating substituent induced the luminescence peak shifts to longer wavelength regions than those by electron-withdrawing substituent. In 3,7-diaryl-substituted dibenzo[*b*,*f*]silepins, combination of fluorine on the silicon centre and methoxy group on the dibenzosilepin moiety led bathochromic shifts.

Chapter 8

Introduction

Silicon is classified into a metalloid, and a wide variety of silicon-containing compounds were synthesized in organic and inorganic chemistry. Although the sp^3-hybridization of carbon can hardly form the conjugation, the tetracoordinate silicon can significantly influence on the conjugation systems and offer unique optical properties. Polysilanes show absorption and luminescence in near-ultraviolet regions originated from the σ-conjugation through polymer main-chains.[1] In siloles, σ * orbitals on the silicon interact with π* orbitals on carbons, leading to bathochromic shifts of absorption and emission bands.[2] Therefore, the construction of the conjugated systems involving silicon is expected for realizing highly-efficient optical materials.[3]

The orbital interaction as representatively shown in siloles should be considered regarding an aromaticity of heterocycles. Neutral 6-membered rings with 6π electrons and tropylium cation are well-known as a typical aromatic ring according to Hückel's rule. On the other hand, neutral 7-membered rings such as 1,3,5-cycloheptatriene and tropone exhibit homoaromaticity confirmed by computational and NMR studies.[4] The methylene group in ground state of cycloheptatriene is located out of plane, leading to a boat structure to avoid antiaromatic unstabilization. Both through-space and through-bond interactions of 1,6-π-electrons contributed to the formation of homoaromaticity of cyclohexatriene. Borepins are analogues to cycloheptatrienes in which the methylene group is replaced to a borylene group.[5] The vacant p-orbital on tricoordinate boron interacts with p-orbitals on the adjacent carbon atoms, resulting in a flat 7-membered ring with 6π-electrons. Silepins have the similar structures as cycloheptatrienes where the methylene group was replaced to a silylene group.[6] Tetracoordinate silicon has no p-orbitals, resulting in a boat structure of silepins.

The tetracoordinate species can accept a lone pair in the presence of fluoride or alkoxide ions, resulting in anionic pentacoordinate silicates.[7] Moreover, intramolecular donation by a structurally-restricted donor enhances to the coordination of the fifth bond.[8] The structural feature of pentacoordinate silicon is the trigonal-bipyramidal molecular geometry with two inequivalent sites of substituents, apical and equatorial.

In the previous chapter, the author demonstrated the synthesis of pentacoordinate silicon complexes using benzo[*h*]quinolyl ligand.[9,10] Pentacoordinate silicon involved the weak dative bond, and the author showed the strength of the dative bond can be tuned by substituents on the silicon centre. Electron-donating substituents occupied an equatorial position in crystal structure weakened the dative bond. In contrast, electron-withdrawing substituents at an apical position which can stabilize a three-centre four-electron bond enhanced the pentacoordinate nature. Herein, the author explains orbital interaction between the benzo[*h*]quinolyl ligand and dibenzo[*b,f*]silepins by UV–vis absorption and photoluminescence properties. The author synthesized the series of pentacoordinate silicon complexes with substituents at the silicon centre and the benzene ring of the dibenzosilepin moiety. The former compounds were designed to control optical properties not only by inductive effect but also by molecular conformation. The latter series are expected to possess the tenability of orbital energy levels and extent of orbital interaction.

Results and Discussion

Benzo[*h*]quinolyldibenzo[*b,f*]silepins dichlorinated at 2,8- or 3,7-positions were synthesized according to our previous report of the unsubstituted ones (Scheme 1).[10]

Trichlorosilanes were added to dilithiated di(chlorophenyl)ethenes (**1p** and **1m**) in tetrahydrofuran (THF) prepared from di(bromochlorophenyl)ethenes and *n*-butyllithium. The generated trichlorodibenzo[*b,f*]silepins were reacted with benzo[*h*]quinolyllithium to give the desired dichlorinated dibenzo[*b,f*]silepins with the benzoquinolyl ligand. The alkoxirated dibenzosilepins (**2pO** and **2mO**) were semi-purified and converted to fluorodibenzosilepins by boron trifluoride etherate immediately. Suzuki-Miyaura coupling of them with arylboronic acids provided diaryl-substituted benzoquinolyldibenzosilepins in good yields.[11]

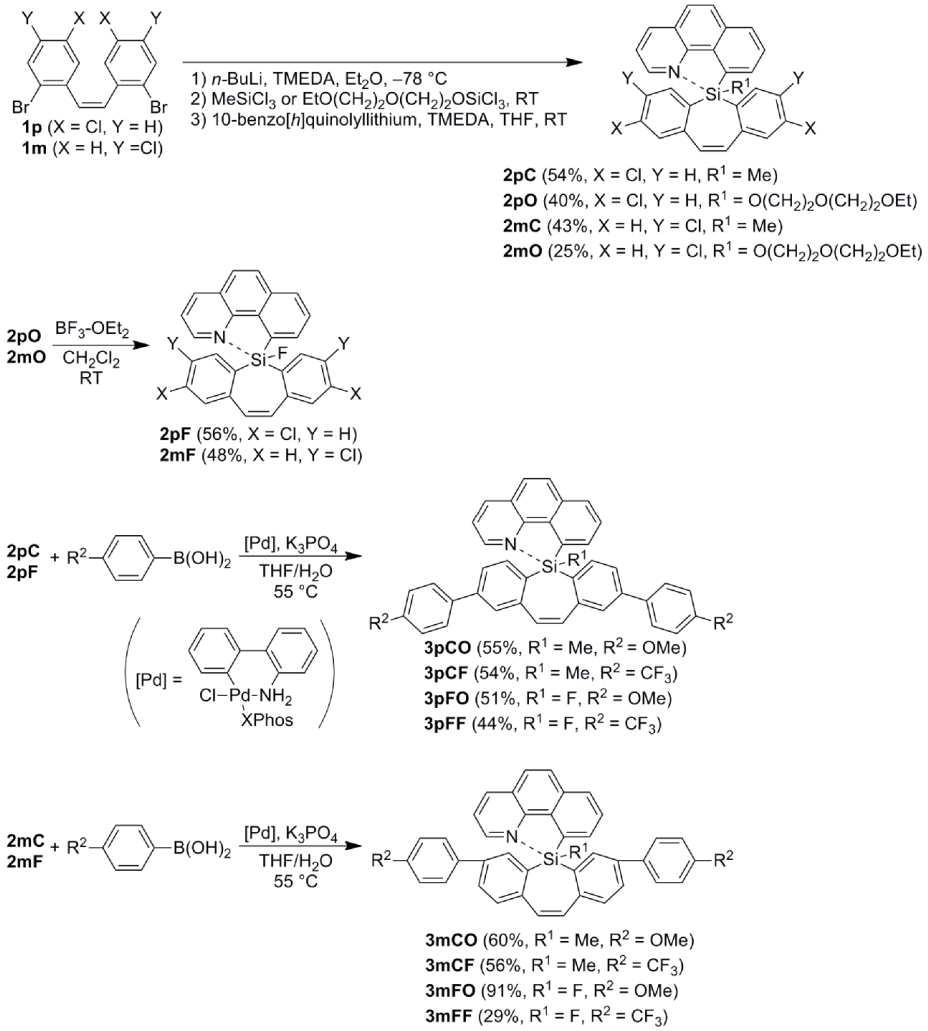

Scheme 1. Synthesis of 5-benzo[*h*]quinolyldibenzo[*b,f*]silepins

The obtained compounds were characterized by ^{29}Si and ^{1}H NMR spectroscopies. In ^{29}Si NMR spectra, the dibenzosilepins substituted by the methyl group on the silicon centre showed a singlet peak around –20 ppm, and the fluorinated ones displayed a doublet peak around –40 ppm. Meanwhile, the substituents on the phenyl group hardly influenced the resonance. It can be deduced that the substituents on the silicon centre governed the structure and pentacoordinate nature of silicon. The molecular structures of the unsubstituted compounds have been already determined by X-ray diffraction analysis, and their characters probably apply to the aryl-substituted ones.[10] In the fluorinated compound, fluorine occupied an apical position because of strong electronegativity, and the dibenzosilepin moiety occupied two equatorial positions. Moreover, fluorine contributed to shortening the distance between nitrogen and silicon by 0.4 Å as compared with that in the methyl group-substituted complex. In contrast, the methyl group, which is electron-donating, favored to locate at the equatorial position, so that the dibenzosilepin moiety occupied an equatorial and an apical position in the crystal structure of the methyl-derivatives. As well as ^{29}Si NMR spectra, ^{1}H NMR spectra offered valuable information for the pentacoordinate nature in the solution state. The methyl-substituted complexes showed only a singlet between 7.20 and 6.50 ppm corresponding to two protons of the vinylene moiety and the peaks assignable to the remained aromatic protons between 9.00 and 7.20 ppm. If the conformation was fixed as obtained in the crystal structure, the two protons of vinylene from the apical- and the equatorial-side would be distinguished and give two doublets. This presumption suggests that the dibenzosilepin moiety could rotate without restraint derived from the pentacoordinate nature. The fluorinated dibenzosilepin displayed not only the singlet from two protons of the vinylene moiety but also the peaks of aromatic protons between 7.20 and 6.50 ppm. The number of the aromatic protons corresponded to the substitution pattern. Unsubstituted and 2,8-substituted dibenzo[*b,f*]silepins provided four protons, and 3,7-substituted ones offered two

protons. The data strongly suggest that the strong dative N–Si bond should fix the dibenzosilepin moiety even in the solution as observed in the crystal structure and that the upfield shift of the aromatic protons could be induced by the ring current effect of the benzo[*h*]quinoline.

Optical properties in the solution state were examined by UV–vis absorption and photoluminescence spectroscopies. In UV–vis absorption spectra (Figure 1 and Table 1), 2,8-substituted dibenzosilepins exhibited the peaks around 275 nm, and their shapes were similar to those of the unsubstituted ones. The peaks were mainly assignable to two transitions localized on the dibenzosilepin moiety and the benzoquinolyl ligand. The slight changes in absorption spectra of the complex with the aryl groups at *para*-positions mean that the transition hardly influences to the energy levels of molecular orbitals. In addition, the pentacoordinate silicon could interrupt the extension of π-conjugation. In contrast, 3,7-substituted silepins displayed weak and broad absorption peaks around 330 nm in company with the peaks around 275 nm (Figure 2). The peaks at longer wavelength region were corresponding to the π-extended dibenzosilepin moiety through vinylene groups, and the wavelength depended on the combination of the substituents on the silicon centre and on the phenyl group. Only **3mFO** showed a bathochromic shift, and the others presented similar spectra. These difference could be explained by two factors; conformation of the dibenzosilepin moiety and perturbation of the orbital energy level by the benzoquinolyl ligand. Considering the results and discussion about the structure described above, the fluorination at the silicon centre fixed the dibenzosilepin moiety in the flat conformation, leading to the efficient π-conjugation through the vinylene group with the large bathochromic shift of **3mFO**. On the other hand, taking into account of low frontier orbital energy levels of benzo[*h*]quinoline, the trifluoromethyl group, which lowers the orbital energy levels, provided an opportunity for frontier orbitals of the diaryldibenzosilepin moiety to interact strongly with that

of the benzoquinoline ligand. These interactions should mix with those orbitals and inhibit the π-π* transition entirely localized on the diaryldibenzosilepin moiety. Thus, **3mCF** and **3mFF** could show little differences in the absorption spectra.

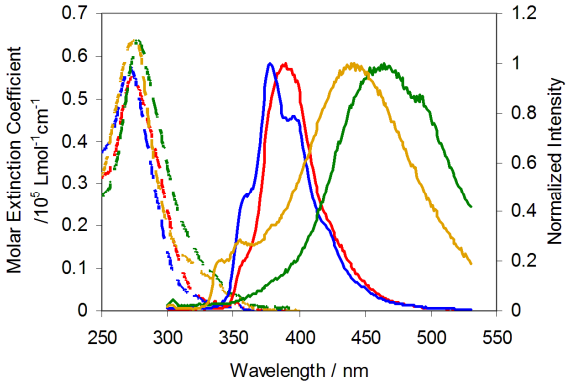

Figure 1. UV–vis absorption (dotted line) and normalized photoluminescence (solid line) spectra of **3pCO** (red), **3pCF** (blue), **3pFO** (green) and **3pFF** (yellow) in dichloromethane solutions (1.0×10^{-5} M).

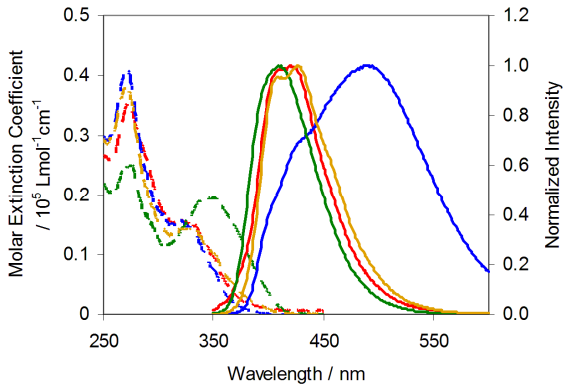

Figure 2. UV–vis absorption (dotted line) and normalized photoluminescence (solid line) spectra of **3mCO** (red), **3mCF** (blue), **3mFO** (green) and **3mFF** (yellow) in dichloromethane solutions (1.0×10^{-5} M).

Table 1. Optical data for dibenzosilepins

Compound	$\lambda_{abs,DCM}$ [nm][a]	$\lambda_{abs,DMF}$ [nm][b]	$\lambda_{em,\ DCM}$ [nm][c]	$\lambda_{em,\ DMF}$ [nm][d]	τ [ns][e]	Φ_f[f]
3pCO	273	273	390	396	1. (14%), 14 (86%)	n.d.[g]
3pCF	271	272	378	381	1.5 (28%), 2.9 (38%) 5.8 (34%)	n.d.[g]
3pFO	277	279	464	485	0.66 (53%), 2.7 (47%)	n.d.[g]
3pFF	276	278	440	463	0.55 (26%), 2.2 (74%)	n.d.[g]
3mCO	272, 320	271, 333	420	421	1.5	0.04
3mCF	271, 320	270, 321	409	413	0.12 (75%), 0.49 (25%)	0.10
3mFO	274, 351	274, 351	491	499	2.5 (9%), 9.9 (91%)	0.11
3mFF	271, 334	271, 332	426	429	0.34 (38%), 1.3 (62%)	0.22

[a] Absorption maxima of dichloromethane solution. [b] Absorption maxima of *N,N*-dimethylformamide solution. [c] Emission maxima of dichloromethane solution excited at the longest absorption maxima. [d] Emission maxima of *N,N*-dimethylformamide solution excited at the longest absorption maxima. [e] Fluorescence life time of dichloromethane solution. [f] Absolute fluorescence quantum yield of dichloromethane solution. [g] Not determined due to weak fluorescence.

In photoluminescence spectra of the 2,8-substituted compounds in dichloromethane (DCM), emission behaviors mainly depended on the substituent on the silicon centre (Figure 1). The methylated derivatives displayed the peaks below 400 nm, and the fluorinated ones showed

broad peaks over 400 nm. The former was derived from the localized excited state (LE state), and the latter was resulted from the charge transfer state (CT state). To confirm these assignments, fluorescence properties of *N,N*-dimethylformamide (DMF) solution of them were also analyzed. The peaks of the methylated compounds remained, while those of fluorinated ones shifted to longer wavelength in DMF. The peak shift in DMF indicates that the stabilization of the CT states of **3pFO** and **3pFF** should occur. Fluorescence lifetimes of the complexes also support the assignments. The methylated compounds exhibited longer lifetime (1.5–14 ns) than those of the fluorinated ones (0.55–2.7 ns). Comparing to **3pFF**, **3pFO** displayed the fluorescence peak in longer wavelength region than that of **3pFF**. This peak shift means that the methoxy group promotes transfer of negative charge from the dibenzosilepin moiety to the benzoquinolyl ligand due to the electron-donating nature. In contrast to **3pFO** and **3pFF**, **3pCO** and **3pCF** showed peaks at the almost same position. These results indicate that their fluorophore should be localized around the benzoquinolyl ligand.

Similar photoluminescence spectra of the 3,7-substituted dibenzosilepins in DCM were obtained with the peaks around 420 nm except for **3mFO** (Figure 2). As shown in UV–vis spectra, only the peak of **3mFO** appeared at longer wavelength than those of the other 3,7-substituted complexes. The fluorescence lifetime of **3mFO** was also differed from those of the other complexes. The lifetimes of **3mFO** were determined as 9.9 ns (91%) and 2.5 ns (9%), and these values were larger than those of the others (0.12–1.5 ns). These results can be explained by the discussion on UV–vis absorption spectra of 3.7-substituted dibenzosilepins. The red-shift of **3mFO** could be derived from effective π-conjugation through nearly flat conformation of the dibenzosilepin moiety. In addition, from weak perturbation in π-π* transition of the diphenyldibenzosilepin moiety by the benzoquinolyl ligand could be responsible for the shifts.

Absolute fluorescence quantum yields of 2,8-substituted dibenzosilepins were below detectable level. These data imply that substituents can hardly enhance fluorescence due to highly localized excited state around the benzoquinolyl ligand. In contrast, the substituents on the 3,7-positions increased fluorescence quantum yield derived from π-π^* transition of diphenyldibenzosilepins. It is worth noting that the compounds with trifluoromethyl groups gave higher quantum yield than those with methoxy groups. It can be deduced that methoxy groups could enhance electron transfer in excited state from the dibenzosilepin moiety to the benzoquinolyl ligand, leading to radiationless deactivation.

Table 2. Results from TD-DFT calculations

Compound	Energy gap [eV (nm)]	Oscillator strength	MO contributions
3mCO	3.66 (339)	0.744	HOMO → LUMO+2
3mCF	3.72 (333)	0.229	HOMO → LUMO+1
	3.52 (353)	0.504	HOMO → LUMO
3mFO	3.44 (361)	1.295	HOMO → LUMO+2
3mFF	3.53 (351)	0.982	HOMO → LUMO+1
	3.25 (382)	0.121	HOMO → LUMO

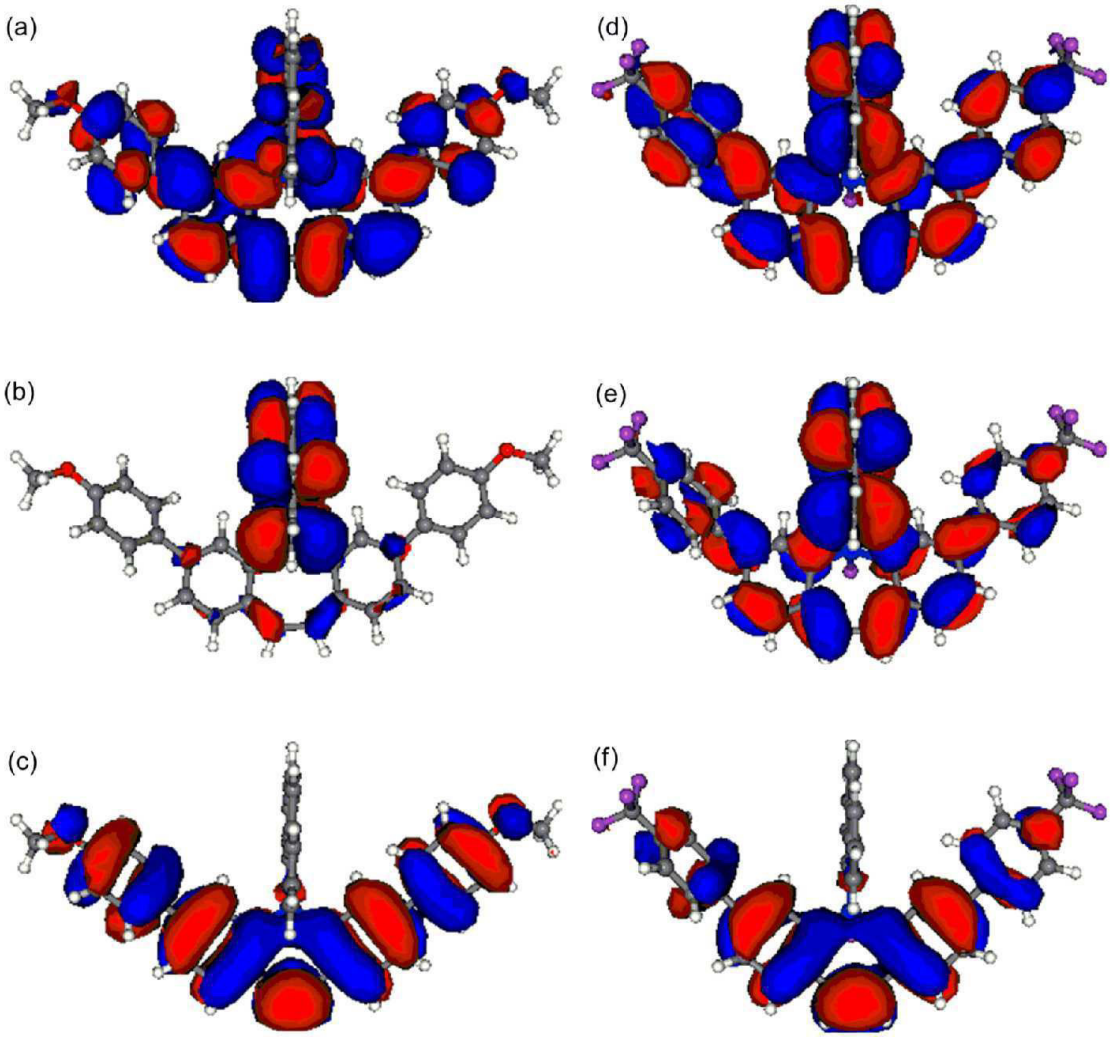

Figure3. Kohn-Sham orbital diagrams: (a) LUMO+2 of **3mFO**, (b) LUMO of **3mFO**, (c) HOMO of **3mFO**, (d) LUMO+1 of **3mFF**, (e) LUMO of **3mFF**, (f) HOMO of **3mFF**.

For further understanding optical properties of the 3,7-substituted derivatives, density functional theory (DFT) calculations were carried out (Table 2 and Figure 3). The molecular structures were optimized at TPSS-D3(bj)/def2-TZVP level, and transitions were estimated by time-dependent DFT (TD-DFT) at the PBE0-D3(bj)/def2-TZVP level. Their conformation determined in single-crystal of the unsubstituted complex was used for the initial structure.

Methyl group in **3mCO** and **3mCF** occupied an equatorial position, and fluorine in **3mFO** and **3mFF** was directed to an apical position. Transitions from HOMO to LUMO+2 in **3mCO** and **3mFO** were allowed. Both of the orbitals were distributed mainly on the diphenyldibenzosilepin moiety and slightly on the benzoquinolyl ligand. The transition energy of **3mFO** (3.44 eV) was smaller than that of **3mCO** (3.66 eV). Moreover, the similar conformation such as **3mCO** in **3mFO** increased the transition energy (3.64 eV), and the value was almost same as that of **3mCO**. These results indicate that the flat conformation can be fixed by fluorine effectively. Therefore, the π-conjugation should be extended in the diphenyldibenzosilepin. As a result, small perturbation from the benzoquinolyl ligand occurs. Finally, red-shifts in UV–vis spectra were observed. In contrast to HOMO and LUMO+2, LUMOs of **3mCO** and **3mFO** were localized on the benzoquinolyl ligand. The clear separation of the orbitals could induce charge transfer and subsequently separation of charges in excited state, leading to weak fluorescence.

In **3mCF**, the transition from HOMO to LUMO (3.52 eV) showed the largest oscillator strength, whereas the largest value in **3mFF** was corresponding to the transition from HOMO to LUMO+1 (3.53 eV). These similar transition energies were consistent with subtle peak shifts by the substituent on the silicon centre in UV–vis absorption spectra. The selective transition from the diphenyldibenzosilepin moiety to LUMO or LUMO+1 can be presumed according to the orbital contribution. The transitions from HOMO to LUMO in **3mCF** and LUMO+1 in **3mFF** were allowed. The differences in the orbital configuration indicate that fluorine on the silicon centre could lower the orbital level of the benzoquinoline ligand and maintained orbital level of the dibenzosilepin moiety. Although LUMOs of **3mCO** and **3mFO** were primarily localized on the benzoquinolyl ligand, LUMOs of **3mCF** and **3mFF** were delocalaized on the ligand and the

diphenyldibenzosilepin moiety. The delocalization could suppress charge transfer and separation in excited state, resulting in a high fluorescence quantum yield.

Conclusion

Diaryl-substituted benzoquinolyl dibenzosilepins were synthesized from dichlorinated species by Suzuki–Miyaura reaction in good yields. From NMR spectra in $CDCl_3$, the methyl group on the silicon centre can rotate and allow many conformations. In contrast, fluorine introduction fixed the planar conformation of the dibenzosilepin. In UV–vis absorption spectra, the substitution at 2,8-positions of dibenzo[*b,f*]silepin maintained the character of the unsubstituted complexes, and their spectra depended on substituents on the silicon centre. By photoexcitation, LE and CT states were observed in methylated and fluorinated derivatives, respectively. Diaryl-substitutions at 3,7-positions of dibenzo[*b,f*]silepin extended π-conjugation through vinylene groups, resulting in the observation of distinct π-π* absorption band and high fluorescence quantum yield. Combination of the methoxy group on the dibenzosilepin moiety and fluorine on the silicon centre provided the flat conformation. Finally, a little perturbation from a π*-orbital of the benzoquinolyl ligand could occur, leading to bathochromic shift in the absorption and emission spectra.

Experimental Section

Measurements. ^{1}H (400 MHz), ^{13}C (100 MHz), and ^{29}Si (80 MHz) NMR spectra were recorded on a JEOL JNM-EX400 spectrometer. ^{1}H and ^{13}C NMR spectra used tetramethylsilane (TMS) as an internal standard. ^{29}Si NMR spectra were referenced externally to TMS in $CDCl_3$. UV–vis spectra were recorded on a Shimadzu UV-3600 spectrophotometer. Fluorescence emission spectra were recorded on a HORIBA JOBIN YVON Fluoromax-4 spectrofluorometer. Elemental analysis was performed at the Microanalytical Center of Kyoto University. All reactions were performed under nitrogen or argon atmosphere.

Materials. Tetrahydrofuran (THF) and diethyl ether were purified using a two-column solid-state purification system (Glasscontour System, Joerg Meyer, Irvine, CA). 10-Bromobenzo[*h*]quinoline,[12] (*Z*)-1,2-bis(2-bromo-4-chlorophenyl)ethene[13] and (*Z*)-1,2-bis(2-bromo-5-chlorophenyl)ethene[13] were prepared according to the literatures. Other reagents were commercially available and used as received.

5-(10-Benzo[*h*]quinolyl)-2,8-dichloro-5-methyldibenzo[*b*,*f*]silepin (2pC). To a solution of (*Z*)-1,2-bis(2-bromo-5-chlorophenyl)ethene (3.26 g, 8.00 mmol) in diethyl ether (320 mL), a solution of *n*-butyllithium in hexane (1.6 M, 10.0 mL, 16 mmol) was added dropwise at –78 °C, and the resulting mixture was held at –78 °C for 10 min, followed by the addition of TMEDA (2.38 mL, 16.0 mmol). After the mixture was stirred for 2 h at –78 °C, trichloro(methyl)silane (0.94 mL, 8.00 mmol) was added. The resulting mixture was allowed to warm to room temperature and left to stir for 18 h. The solvent was removed at 65 °C under argon, and then at room temperature under reduced pressure at ambient temperature. The obtained solid was dissolved in THF (40 mL), and the solution and TMEDA (1.19 mL, 8.00 mmol) were added to a solution of 10-benzo[*h*]quinolyllithium in THF (generated by treating 10-

bromobenzo[*h*]quinoline (2.06 g, 8.00 mmol) with *n*-butyllithium (1.6 M in hexane, 5.0 mL, 8.0 mmol) in THF (48 mL) for 30 min at –78 °C). After stirring at room temperature for 22 h, NH_4Cl (aq) was added, followed by extraction with cyclopentyl methyl ether, drying over $MgSO_4$, and removal of the solvent under vacuum. The solid was dissolved in chloroform again and filtered through a short plug of silica gel. Recrystallization from chloroform/ethanol gave a pale yellow solid in 54% yield (2.02 g, 4.32 mmol). ^{1}H NMR (400 M Hz, $CDCl_3$): δ = 8.58 (br, 1H, Ar*H*), 8.06 (dd, *J* = 8.0, 1.6 Hz, 1H, Ar*H*), 7.91 (d, *J* = 7.6 Hz, 1H, Ar*H*), .7.79 (m, 3H, Ar*H*), 7.64 (d, *J* = 8.8 Hz, 1H, Ar*H*), 7.50 (br, 2H, Ar*H*), 7.37 (m, 1H, Ar*H*), 7.32 (br, 2H, Ar*H*) 7.21 (s, 2H, Ar*H*), 6.59 (s, 2H, -C*H*=C*H*-), 1.12 (s, 3H, -CH_3) ppm. ^{13}C NMR (100 M Hz, $CDCl_3$): δ = 145.6, 141.7, 140.1, 137.6, 136.2, 135.4, 134.4, 133.8, 132.5, 131.4, 130.1, 128.7, 128.4, 127.2, 127.0, 126.4, 124.9, 121.6, –3.1 ppm. ^{29}Si NMR (80 M Hz, $CDCl_3$): δ = –21.1 ppm. HRMS (ESI+): m/z: calcd for $C_{28}H_{20}NSiCl_2$ ($M+H^+$): 468.0737; found: 468.0738.

5-(10-Benzo[*h*]quinolyl)-2,8-dichloro-5-(2-(2-ethoxyethoxy)ethoxy)-dibenzo[*b*,*f*]silepin (2pO). To a solution of (*Z*)-1,2-bis(2-bromo-5-chlorophenyl)ethene (3.26 g, 8.00 mmol) in diethyl ether (320 mL), a solution of *n*-butyllithium in hexane (1.6 M, 10.0 mL, 16 mmol) was added dropwise at –78 °C and the resulting mixture was held at –78 °C for 10 min followed by the addition of TMEDA (2.38 mL, 16.0 mmol). After the mixture was stirred for 2 h at –78 °C, trichloro((2-ethoxyethoxy)ethoxy)silane (2.14 g, 8.00 mmol) in diethyl ether (8.0 mL) was added. The resulting mixture was allowed to warm to room temperature and left to stir for 5 h at ambient temperature. The solvent was removed at room temperature under reduced pressure. The obtained solid was dissolved in THF (40 mL), and the solution and TMEDA (1.19 mL, 8.00 mmol) were added to a solution of 10-benzo[*h*]quinolyllithium in THF (generated by treating 10-bromobenzo[*h*]quinoline (2.06 g, 8.00 mmol) with *n*-butyllithium (1.6 M in hexane, 5.0 mL, 8.0

mmol) in THF (48 mL) for 30 min at –78 °C). After stirring at room temperature for 11 h, NH_4Cl (aq) was added, followed by extraction with cyclopentyl methyl ether, drying over $MgSO_4$, and removal of the solvent under vacuum. The crude product was purified by silica gel column chromatography eluted with hexane/ethyl acetate (4/1), followed by precipitation in hexane to give a yellow solid in 40% yield (1.87 g, 3.19 mmol). The product was used without further purification. HRMS (ESI+): m/z: calcd for $C_{33}H_{30}NO_3SiCl_2$ ($M+H^+$): 586.1371; found: 586.1367.

5-(10-Benzo[*h*]quinolyl)-3,7-dichloro-5-methyldibenzo[*b*,*f*]silepin (2mC). Similarly to the preparation of **2pC**, **2mC** was synthesized from (*Z*)-1,2-bis(2-bromo-4-chlorophenyl)ethene (3.26 g, 8.00 mmol) in 63% yield as a white solid (2.37 g, 5.05 mmol). ^{1}H NMR (400 M Hz, $CDCl_3$): δ = 8.64 (br,1H, Ar*H*), 8.07 (d, *J* = 6.8 Hz, 1H, Ar*H*), 7.91 (m, 3H, Ar*H*), .7.79 (d, *J* = 8.8 Hz, 1H, Ar*H*), 7.64 (d, *J* = 8.8 Hz, 1H, Ar*H*), 7.48–7.41 (m,3H, Ar*H*), 7.26–7.23 (m, 2H, Ar*H*), 7.15 (s, 2H, Ar*H*), 6.59 (s, 2H, -C*H*=C*H*-), 0.88 (s, 3H, -CH_3) ppm. ^{13}C NMR (100 M Hz, $CDCl_3$): δ = 145.6, 143.8, 138.6, 137.5, 136.1, 135.5, 135.4, 133.8, 133.5, 132.7, 132.2, 131.9, 130.8, 130.1, 128.7, 127.7, 127.2, 126.5, 124.8, 121.8, –3.3 ppm. ^{29}Si NMR (80 M Hz, $CDCl_3$): δ = –21.9 ppm. HRMS (ESI+): m/z: calcd for $C_{28}H_{20}NSiCl_2$ ($M+H^+$): 468.0737; found: 468.0739.

5-(10-Benzo[*h*]quinolyl)-3,7-dichloro-5-(2-(2-ethoxyethoxy)ethoxy)-dibenzo[*b*,*f*]silepin (2mO). Similarly to the preparation of **2pO**, **2mO** was synthesized from (*Z*)-1,2-bis(2-bromo-4-chlorophenyl)ethene (3.26 g, 8.00 mmol) in 25% yield as a yellow solid (1.19 g, 2.03 mmol). The product was used without further purification. HRMS (ESI+): m/z: calcd for $C_{33}H_{30}NO_3SiCl_2$ ($M+H^+$): 586.1372; found: 586.1367.

5-(10-Benzo[*h*]quinolyl)-2,8-dichloro-5-fluorodibenzo[*b*,*f*]silepin (2pF). Boron trifluoride diethyl etherate (0.754 mL, 6.00 mmol) was added to a solution of **2pO** (1.76 g, 3.00 mmol) in dichloromethane (15 mL) at room temperature. After the solution was stirred at room

temperature for 2 h, sodium bicarbonate (saturated aqueous) was added. The organic layer was separated, dried over $MgSO_4$, filtered, and concentrated under vacuum. The crude product was purified by silica gel column chromatography eluted with hexane/chloroform (3/2) to give a colorless solid in 56% yield (0.800 g, 1.69 mmol). ^{1}H NMR (400 M Hz, $CDCl_3$): δ = 8.57 (d, *J* = 6.8 Hz, 1H, Ar*H*), 8.19 (m, 2H, Ar*H*), 8.03 (d, *J* = 8.8 Hz, 1H, Ar*H*), 7.97 (m, 1H, Ar*H*), 7.81 (m, 2H, Ar*H*), 7.40 (s, 2H, Ar*H*), 7.28 (m, 1H, Ar*H*), 6.84 (s, 2H, -C*H*=C*H*-) 6.77 (d, *J* = 7.6 Hz, 2H, Ar*H*), 6.64 (d, *J* = 8.0 Hz, 2H, Ar*H*) ppm. ^{29}Si NMR (80 M Hz, $CDCl_3$): δ = –42.2 (d, *J* = 270 Hz) ppm. HRMS (ESI+): m/z: calcd for $C_{27}H_{17}NFSiCl_2$ ($M+H^+$): 472.0491; found: 472.0486. elemental analysis: calcd for $C_{27}H_{16}NFSiCl_2$: C 68.65, H 3.41, N 2.96; found: C 68.61, H 3.31, N 3.17.

5-(10-Benzo[*h*]quinolyl)-3,7-dichloro-5-fluoro-dibenzo[*b*,*f*]silepin (2mF). Similarly to the preparation of **2pF**, **2mF** was synthesized from **2mO** (1.05 g, 1.80 mmol) in 48% yield as a colorless solid (0.405 g, 0.858 mmol). ^{1}H NMR (400 M Hz, $CDCl_3$): δ = 8.58 (d, *J* = 6.8 Hz, 1H, Ar*H*), 8.21 (d, 2H, Ar*H*), 8.05 (d, *J* = 8.8 Hz, 1H, Ar*H*), 7.97 (m, 2H, Ar*H*), 7.82 (d, *J* = 9.2 Hz, 1H, Ar*H*), 7.35–7.29 (m, 3H, Ar*H*), 7.19 (d, *J* = 6.8 Hz, 2H, Ar*H*), 6.83 (s, 2H, -C*H*=C*H*-) 6.67 (s, 2H, Ar*H*) ppm. ^{29}Si NMR (80 M Hz, $CDCl_3$): δ = –45.3 (d, *J* = 270 Hz) ppm. elemental analysis: calcd for $C_{27}H_{16}NFSiCl_2$: C 68.65, H 3.41, N 2.96; found: C 67.98, H 3.39, N 2.95.

5-(10-Benzo[*h*]quinolyl)-2,8-bis(4-methoxyphenyl)-5-methyldibenzo[*b*,*f*]silepin (3pCO). A mixture of **2pC** (0.187 g, 0.400 mmol), 4-methoxyphenylboronic acid (0.182 g, 1.20 mmol), tripotassium phosphate (0.340 g, 0.016 mmol), and chloro(2-dicyclohexylphosphino-2′,4′,6′-triisopropyl-1,1′-biphenyl)[2-(2′-amino-1,1′-biphenyl)]palladium(II) (12.6 mg, 0.016 mmol) was heated at 55 °C in THF (2.0 mL) and water (0.4 mL) with stirring for 12 h. Then, water was poured into the solution. After extraction with cyclopentyl methyl ether, drying over

$MgSO_4$, and condensation under vacuum, the crude product was purified by silica gel column chromatography eluted with hexane/ethyl acetate (9/1 to 4/1) to give a colorless solid in 55% yield (0.135 g, 0.220 mmol). ^{1}H NMR (400 M Hz, $CDCl_3$): δ = 8.72 (br, 1H, Ar*H*), 8.01 (m, 3H, Ar*H*), 7.89 (d, *J* = 7.6 Hz, 1H, Ar*H*), .7.77 (d, *J* = 8.8 Hz, 1H, Ar*H*), 7.60 (d, *J* = 8.8 Hz, 2H, Ar*H*), 7.51 (m, 7H, Ar*H*), 7.43 (s, 2H, Ar*H*), 7.33 (dd, *J* = 8.0, 4.4 Hz, 1H, Ar*H*) 6.94 (d, *J* = 8.8 Hz, 4H, Ar*H*), 6.77 (s, 2H, -C*H*=C*H*-), 3.82 (s, 6H, -OCH_3), 1.20 (s, 3H, -CH_3) ppm. ^{13}C NMR (100 M Hz, $CDCl_3$): δ = 159.1, 145.8, 140.9, 139.9, 137.9, 136.4, 135.2, 135.1, 133.8, 133.7, 133.1, 132.5, 129.8, 128.6, 128.1, 128.0, 127.1, 126.9, 126.4, 125.1, 124.7, 121.5, 121.4, 114.1, 55.3, −3.04 ppm. ^{29}Si NMR (80 M Hz, $CDCl_3$): δ = −20.6 ppm. HRMS (ESI+): m/z: calcd for $C_{42}H_{34}NO_2Si$ ($M+H^+$): 612.2353; found: 612.2340.

5-(10-Benzo[*h*]quinolyl)-5-fluoro-2,8-bis(4-methoxyphenyl)dibenzo[*b*,*f*]silepin (3pFO). A mixture of **2pF** (0.189 g, 0.400 mmol), 4-methoxyphenylboronic acid (0.182 g, 1.20 mmol), tripotassium phosphate (0.340 g, 0.016 mmol), and chloro(2-dicyclohexylphosphino-2′,4′,6′-triisopropyl-1,1′-biphenyl)[2-(2′-amino-1,1′-biphenyl)]palladium(II) (12.6 mg, 0.016 mmol) was heated at 55 °C in THF (2.0 mL) and water (0.4 mL) with stirring for 12 h. Then, water was poured into the solution. After extraction with cyclopentyl methyl ether, drying over $MgSO_4$, and condensation under vacuum, the crude product was purified by silica gel column chromatography eluted with hexane/ethyl acetate (3/1) to give a colorless solid in 51% yield (0.126 g, 0.204 mmol). ^{1}H NMR (400 M Hz, $CDCl_3$): δ = 8.64 (d, *J* = 6.8 Hz, 1H, Ar*H*), 8.17 (m, 2H, Ar*H*), 8.05–7.96 (m, 3H, Ar*H*), 7.79 (d, *J* = 8.8 Hz, 1H, Ar*H*), 7.62 (d, *J* = 1.2 Hz, 2H, Ar*H*), 7.46 (d, *J* = 8.0 Hz, 4H, Ar*H*), 7.26 (d, *J* = 8.0 Hz, 1H, Ar*H*), 7.01 (m, 4H, Ar*H*, -C*H*=C*H*-), 6.92 (d, *J* = 9.2 Hz, 4H, Ar*H*), 6.82 (d, *J* = 8.0 Hz, 2H, Ar*H*), 3.81 (s, 6H, -OCH_3) ppm. ^{29}Si NMR (80 M Hz, $CDCl_3$): δ = −40.4 (d, *J* = 270 Hz) ppm. HRMS (ESI+): m/z: calcd for $C_{41}H_{31}FNO_2Si$

(M+H$^+$): 616.2103; found: 616.2088. elemental analysis: calcd for $C_{41}H_{30}FNO_2Si$: C 79.97, H 4.91, N 2.27; found: C 79.33, H 5.12, N 2.29.

5-(10-Benzo[*h*]quinolyl)-3,7-bis(4-methoxyphenyl)-5-methyldibenzo[*b*,*f*]silepin (3mCO). A mixture of **2mC** (0.187 g, 0.400 mmol), 4-methoxyphenylboronic acid (0.182 g, 1.20 mmol), tripotassium phosphate (0.340 g, 0.016 mmol), and chloro(2-dicyclohexylphosphino-2′,4′,6′-triisopropyl-1,1′-biphenyl)[2-(2′-amino-1,1′-biphenyl)]palladium(II) (12.6 mg, 0.016 mmol) was heated at 55 °C in THF (2.0 mL) and water (0.4 mL) with stirring for 6 h. Then, water was poured into the solution. After extraction with cyclopentyl methyl ether, drying over $MgSO_4$, and condensation under vacuum, the crude product was purified by silica gel column chromatography eluted with hexane/ethyl acetate (4/1). Recrystallization from dichloromethane/hexane gave a pale yellow solid in 60% yield (0.146 g, 0.239 mmol). ^{1}H NMR (400 M Hz, $CDCl_3$): δ = 8.51 (br, 1H, Ar*H*), 8.12 (br, 2H, Ar*H*), 7.99 (d, *J* = 8.0 Hz, 1H, Ar*H*), .7.88 (d, *J* = 7.6 Hz, 1H, Ar*H*), 7.77 (d, *J* = 8.8 Hz, 1H, Ar*H*), 7.60 (m, 5H, Ar*H*), 7.47 (m, 3H, Ar*H*), 7.35–7.29 (m, 4H, Ar*H*) 6.99 (d, *J* = 8.4 Hz, 4H, Ar*H*), 6.70 (s, 2H, -C*H*=C*H*-), 3.85 (s, 6H, -OCH_3), 1.25 (s, 3H, -CH_3) ppm. ^{13}C NMR (100 M Hz, $CDCl_3$): δ = 159.0, 145.8, 145.6, 141.9, 139.3, 138.8, 137.8, 136.4, 135.1, 134.0, 133.7, 132.4, 132.3, 131.3, 129.8, 129.2, 128.7, 128.0, 127.2, 126.4, 126.0, 124.7, 121.4, 55.3, −3.1 ppm. ^{29}Si NMR (80 M Hz, $CDCl_3$): δ = −20.0 ppm. HRMS (ESI+): m/z: calcd for $C_{42}H_{34}NO_2Si$ (M+H$^+$): 612.2353; found: 612.2340.

5-(10-Benzo[*h*]quinolyl)-5-fluoro-3,7-bis(4-methoxyphenyl)dibenzo[*b*,*f*]silepin (3mFO). A mixture of **2mF** (0.189 g, 0.400 mmol), 4-methoxyphenylboronic acid (0.182 g, 1.20 mmol), tripotassium phosphate (0.340 g, 0.016 mmol), and chloro(2-dicyclohexylphosphino-2′,4′,6′-triisopropyl-1,1′-biphenyl)[2-(2′-amino-1,1′-biphenyl)]palladium(II) (12.6 mg, 0.016 mmol) was heated at 55 °C in THF (2.0 mL) and water (0.4 mL) with stirring for 6 h. Then,

water was poured into the solution. After extraction with cyclopentyl methyl ether, drying over $MgSO_4$, and condensation under vacuum, the crude product was purified by silica gel column chromatography eluted with hexane/ethyl acetate (7/3) to give a pale yellow solid in 91% yield (0.225 g, 0.365 mmol). ^{1}H NMR (400 M Hz, $CDCl_3$): δ = 8.66 (d, J = 6.8 Hz, 1H, Ar*H*), 8.14 (m, 3H, Ar*H*), 7.96 (m, 2H, Ar*H*), 7.76 (d, J = 8.8 Hz, 1H, Ar*H*), 7.43 (m, 2H, Ar*H*), 7.41 (m, 2H, Ar*H*), 7.23 (m, 1H, Ar*H*), 7.01−6.93 (m, 8H, Ar*H*), 6.99 (d, J = 8.4 Hz, 4H, Ar*H*), 6.70 (s, 2H, -C*H*=C*H*-), 6.68 (s, 2H, Ar*H*), 3.69 (s, 6H, -OCH_3) ppm. HRMS (ESI+): m/z: calcd for $C_{41}H_{31}FNO_2Si$ ($M+H^+$): 616.2103; found: 616.2084. elemental analysis: calcd for $C_{41}H_{30}FNO_2Si$: C 79.97, H 4.91, N 2.27; found: C 79.33, H 5.12, N 2.29.

5-(10-Benzo[*h*]quinolyl)-5-methyl-2,8-bis[(4-tirfluoromethyl)phenyl]-dibenzo[*b*,*f*]silepin (3pCF). A mixture of **2pC** (0.187 g, 0.400 mmol), 4-(trifluoromethyl)phenylboronic acid (0.228 g, 1.20 mmol), tripotassium phosphate (0.340 g, 0.016 mmol), and chloro(2-dicyclohexylphosphino-2′,4′,6′-triisopropyl-1,1′-biphenyl)[2-(2′-amino-1,1′-biphenyl)]palladium(II) (12.6 mg, 0.016 mmol) was heated at 55 °C in THF (2.0 mL) and water (0.4 mL) with stirring for 12 h. Then, water was poured into the solution. After extraction with cyclopentyl methyl ether, drying over $MgSO_4$, and condensation under vacuum, the crude product was purified by silica gel column chromatography eluted with hexane/ethyl acetate (95/5) to give a colorless solid in 54% yield (0.148 g, 0.215 mmol). ^{1}H NMR (400 M Hz, $CDCl_3$): δ = 8.70 (br, 1H, Ar*H*), 8.06 (m, 3H, Ar*H*), 7.93 (d, J = 8.0 Hz, 1H, Ar*H*), 7.81 (d, J = 8.8 Hz, 1H, Ar*H*), 7.67 (m, 10H, Ar*H*), 7.60 (m, 2H, Ar*H*), 7.53 (d, J = 7.6 Hz, 1H, Ar*H*), 7.48 (s, 2H, Ar*H*), 7.37 (m, 1H, Ar*H*), 6.81 (s, 2H, -C*H*=C*H*-), 1.23 (s, 3H, -CH_3) ppm. ^{29}Si NMR (80 M Hz, $CDCl_3$): δ = −21.0 ppm. HRMS (ESI+): m/z: calcd for $C_{42}H_{28}F_6NSi$ ($M+H^+$): 688.1890;

found: 688.1877. elemental analysis: calcd for $C_{42}H_{27}F_6NSi$: C 73.35, H 3.96, N 2.04; found: C 72.81, H 4.13, N 1.96.

5-(10-Benzo[*h*]quinolyl)-5-fluoro-2,8-bis[(4-tirfluoromethyl)phenyl]-dibenzo[*b*,*f*]silepin (3pFF). A mixture of **2pF** (0.189 g, 0.400 mmol), 4-(trifluoromethyl)phenylboronic acid (0.228 g, 1.20 mmol), tripotassium phosphate (0.340 g, 0.016 mmol), and chloro(2-dicyclohexylphosphino-2′,4′,6′-triisopropyl-1,1′-biphenyl)[2-(2′-amino-1,1′-biphenyl)]palladium(II) (12.6 mg, 0.016 mmol) was heated at 55 °C in THF (2.0 mL) and water (0.4 mL) with stirring for 12 h. Then, water was poured into the solution. After extraction with cyclopentyl methyl ether, drying over $MgSO_4$, and condensation under vacuum, the crude product was purified by silica gel column chromatography eluted with hexane/ethyl acetate (4/1). Recrystallization from dichloromethane/hexane gave a colorless solid in 44% yield (0.121 g, 0.174 mmol). ^{1}H NMR (400 M Hz, $CDCl_3$): δ = 8.65 (d, *J* = 6.8 Hz, 1H, Ar*H*), 8.20 (m, 2H, Ar*H*), 8.05 (d, *J* = 8.8 Hz, 1H, Ar*H*), 7.99 (m, 2H, Ar*H*), 7.82 (d, *J* = 9.2 Hz, 1H, Ar*H*), 7.67−7.59 (m, 10H, Ar*H*), 7.27 (dd, *J* = 8.0, 4.8 Hz, 1H, Ar*H*), 7.05 (m, 4H, Ar*H*, -C*H*=C*H*-), 6.87 (d, *J* = 7,6 Hz, 4H, Ar*H*) ppm. HRMS (ESI+): m/z: calcd for $C_{41}H_{25}F_7NSi$ ($M+H^+$): 692.1639; found: 692.1622. elemental analysis: calcd for $C_{41}H_{24}F_7NSi$: C 71.19, H 3.50, N 2.02; found: C 71.25, H 3.75, N 2.02.

5-(10-Benzo[*h*]quinolyl)-5-methyl-3,7-bis[(4-tirfluoromethyl)phenyl]-dibenzo[*b*,*f*]silepin (3mCF). A mixture of **2mC** (0.187 g, 0.400 mmol), 4-(trifluoromethyl)phenylboronic acid (0.228 g, 1.20 mmol), tripotassium phosphate (0.340 g, 0.016 mmol), and chloro(2-dicyclohexylphosphino-2′,4′,6′-triisopropyl-1,1′-biphenyl)[2-(2′-amino-1,1′-biphenyl)]palladium(II) (12.6 mg, 0.016 mmol) was heated at 55 °C in THF (2.0 mL) and water (0.4 mL) with stirring for 12 h. Then, water was poured into the solution. After

extraction with cyclopentyl methyl ether, drying over $MgSO_4$, and condensation under vacuum, the crude product was purified by silica gel column chromatography eluted with hexane/ethyl acetate (95/5). Recrystallization from dichloromethane/hexane gave a colorless solid in 56% yield (0.155 g, 0.225 mmol). ^{1}H NMR (400 M Hz, $CDCl_3$): δ = 8.45 (br, 1H, Ar*H*), 8.15 (br, 2H, Ar*H*), 8.03 (d, *J* = 8.0 Hz, 1H, Ar*H*), 7.92 (d, *J* = 7.6 Hz, 1H, Ar*H*), 7.81 (d, *J* = 8.8 Hz, 1H, Ar*H*), 7.71 (br, 8H, Ar*H*), 7.64 (d, *J* = 8.8 Hz, 1H, Ar*H*), 7.52 (d, *J* = 7.6 Hz, 4H, Ar*H*), 7.35 (d, *J* = 7.6 Hz, 2H, Ar*H*), 7.28 (d, *J* = 8.0 Hz, 1H, Ar*H*), 6.75 (s, 2H, -C*H*=C*H*-), 1.26 (s, 3H, -CH_3) ppm. ^{29}Si NMR (80 M Hz, $CDCl_3$): δ = −21.0 ppm. HRMS (ESI+): m/z: calcd for $C_{42}H_{28}F_6NSi$ ($M+H^+$): 688.1890; found: 688.1872. elemental analysis: calcd for $C_{42}H_{27}F_6NSi$: C 73.35, H 3.96, N 2.04; found: C 73.37, H 4.08, N 2.06.

5-(10-Benzo[*h*]quinolyl)-5-fluoro-3,7-bis[(4-tirfluoromethyl)phenyl]-dibenzo[*b*,*f*]silepin (3mFF). A mixture of **2mF** (0.189 g, 0.400 mmol), 4-(trifluoromethyl)phenylboronic acid (0.228 g, 1.20 mmol), tripotassium phosphate (0.340 g, 0.016 mmol), and chloro(2-dicyclohexylphosphino-2′,4′,6′-triisopropyl-1,1′-biphenyl)[2-(2′-amino-1,1′-biphenyl)]palladium(II) (12.6 mg, 0.016 mmol) was heated at 55 °C in THF (2.0 mL) and water (0.4 mL) with stirring for 12 h. Then, water was poured into the solution. After extraction with cyclopentyl methyl ether, drying over $MgSO_4$, and condensation under vacuum, the crude product was purified by silica gel column chromatography eluted with hexane/ethyl acetate (4/1). Recrystallization from dichloromethane/hexane gave a colorless solid in 29% yield (79.3 mg, 0.115 mmol). ^{1}H NMR (400 M Hz, $CDCl_3$): δ = 8.66 (br, 1H, Ar*H*), 8.12 (m, 2H, Ar*H*), 7.99 (m, 2H, Ar*H*), 7.85 (m, 2H, Ar*H*), 7.68–7.61 (m, 8H, Ar*H*), 7.53 (dd, *J* = 8.0, 1.0 Hz, 1H, Ar*H*), 7.40 (m, 3H, Ar*H*), 7.13 (m, 2H, Ar*H*), 6.87 (s, 2H, -C*H*=C*H*-) ppm. ^{13}C NMR (100 M Hz, $CDCl_3$): δ = 146.3, 144.5, 140.3, 139.6, 138.7, 136.5, 136.0, 133.9, 132.8, 132.6, 130.7, 130.1,

129.6, 129.3, 129.2, 129.0, 128.4, 127.7, 127.3, 127.2, 126.8, 126.6, 126.2, 126.0, 125.6, 124.7, 123.0, 122.0 ppm. HRMS (ESI+): m/z: calcd for $C_{41}H_{24}F_6NSi$ ($M–F^+$): 672.1577; found: 672.1599. elemental analysis: calcd for $C_{41}H_{24}F_7NSi$: C 71.19, H 3.50, N 2.02; found: C 71.03, H 3.76, N 1.96.

Computational details. All calculations were carried with ORCA 2.9.[14] The geometry of the singlet ground state was optimized by the TPSS functional[15] and the def2-TZVP basis set.[16] On the basis of the optimized structure, the absorption properties were calculated by TD-DFT within the Tamm-Dancoff approximation.[17] The TD-DFT calculations performed at the PBE0 hybrid functional level[18] with the def2-TZVP basis set. The resolution of the identity (RI) approximation[19] was applied for the TPSS functional, and RI and chain of spheres approximation (RIJCOSX)[20] were also applied for the hybrid functional. The auxiliary basis function for coulomb fitting[24] was used as the fitting basis in the RI and RIJCOSX treatments. In all cases, the empirical London dispersion correction (DFT-D3(bj))[21] was applied.

References

(1) (a) Miller, R. D.; Michl, J. *Chem. Rev.* **1989,** *89,* 1359.

(2) (a) Yamaguchi, S.; Tamao, K. *Chem. Lett.* **2005,** *34,* 2. (b) Sanchez, J. C.; Trogler, W. C. *Macromol. Chem. Phys.* **2008,** *209,* 1527. (c) Uchida, M.; Izumizawa, T.; Nakano, T.; Yamaguchi, S.; Tamao, K.; Furukawa, K. *Chem. Mater.* **2001,** *13,* 2680.

(3) (a) Chen, J.; Cao, Y. *Macromol. Rapid. Commun.* **2007,** *28,* 1714. (b) Yuan, M.; Yang, P.; Durban, M. M.; Luscombe, C. K. *Macromolecules* **2012,** *45,* 5934. (c) Lu, G.; Usta, H.; Risko, C.; Wang, L.; Facchetti, A.; Ratner, M. A.; Marks, T. J. *J. Am. Chem. Soc.* **2008,** *130,* 7670. (d) Keyworth, C. W.; Chan, K. L.; Labram, J. G.; Anthopoulos, T. D.; Watkins, S. E.; McKiernan, M.; White, A. J. P.; Holmes, A. B.; Williams, C. K. *J. Mater. Chem.* **2011,** *21,* 11800.

(4) (a) Williams, R. V.; Edwards, W. D.; Zhang, P.; Berg, D. J.; Mitchell, R. H. *J. Am. Chem. Soc.* **2012,** *134,* 16742. (b) Chen, Z.; Jiao, H.; Wu, J. I.; Herges, R.; Zhang, S. B.; Schleyer, P. v. R. *J. Phys. Chem. A* **2008,** *112,* 10586.

(5) (a) Ashe III, A. J.; Kampf, J. W.; Nakadaira, Y.; Pace, J. M. *Angew, Chem. Int. Ed.* **1992,** *31,* 1255. (b) Mercier, L. G.; Piers, W. E.; Parvez, M. *Angew. Chem. Int. Ed.* **2009,** *48,* 6108. (c) Levine, D. R.; Caruso Jr., A.; Siegler, M. A.; Tovar, J. D. *Chem. Commun.* **2012,** *48,* 6256.

(6) (a) Corey, J. Y.; Corey, E. R. *Tetrahedron Lett.* **1972,** *13,* 4669. (b) Nishihara, T.; Izukawa, Y.; Komatsu, K. *Chem. Lett.* **1998,** *3,* 269.

(7) (a) Chuit, C.; Corriu, R. J. P.; Reye, C.; Young, J. C. *Chem. Rev.* **1998,** *93,* 1371. (b) Johnson, S. E.; Day, R. O.; Holmes, R. R. *Inorg. Chem.* **1989,** *28,* 3182. (c) Bréfort, J. L.; Corriu, R. J. P.; Guérin, C.; Henner, B. J. L.; Wong Chi Man, W. W. C. *Organometallics* **1990,** *9,* 2080.

(8) (a) Metz, S.; Burschka, C.; Platte, D.; Tacke, R. *Angew. Chem. Int. Ed.* **2007,** *46,* 7006. (b) Ghandwal, R. S.; Sen, S. S.; Roesky, H. W.; Grantizka, M.; Kratzert, D.; Merkel, S.; Stalke, D. *Angew. Chem. Int. Ed.* **2010,** *49,* 3952. (c) Wagler, J.; Böhme, U.; Roewer, G. *Angew. Chem. Int. Ed.* **2002,** *41,* 1732. (d) Driess, M.; Muresan, N.; Merz, K. *Angew. Chem. Int. Ed.* **2005,** *44,* 6738. (e) Kano, N.; Komatsu, F.; Yamamura, M.; Kawashima, T. *J. Am. Chem. Soc.* **2006,** *128,* 7097. (f) Sakamoto, N.; Ikeda, C.; Yamamura, M.; Nabeshima, T. *J. Am. Chem. Soc.* **2011,** *133,* 4726.

(9) Tokoro, Y.; Yeo, H.; Tanaka, K.; Chujo, Y. *Chem. Commun.* **2012,** *48,* 8541.

(10) See Chapter 7.

(11) Kinzel, T.; Zhang, Y.; Buchwald, S. L. *J. Am. Chem. Soc.* **2010,** *132,* 14073.

(12) Dick, A. R.; Hull, K. L.; Sanford, M. S. *J. Am. Chem. Soc.* **2004,** *126,* 2300.

(13) (a) Caruso, Jr. A.; Siegler, M. A.; Tovar, J. D. *Angew. Chem. Int. Ed.* **2010,** *49,* 4213. (b) Mercier, L. G.; Furukawa, S.; Piers, W. E.; Wakamiya, A.; Yamaguchi, S.; Parvez, M.; Harrington, R. W.; Clegg, W. *Organometallics* **2011,** *30,* 1719.

(14) ORCA (version 2.9): Neese, F.; Wennmohs, F.; Becker, U.; Bykov, D.; Ganyushin, D.; Hansen, A.; Izsak, R.; Liakos, D. G.; Kollmar, C.; Kossmann, S.; Pantazis, D. A.; Petrenko, T.; Reimann, C.; Riplinger, C.; Roemelt, M.; Sandhöfer, B.; Schapiro, I.; Sivalingam, K.; Wezisla, B.; Kállay, M.; Grimme, S.; Valeev. E.

(15) Tao, J.; Perdew, J. P.; Staroverov, V. N.; Scuseria, G. E. *Phys. Rev. Lett.* **2003,** *91,* 146401.

(16) (a) Schaefer, A.; Horn, H.; Ahlrichs, R. *J. Phys. Chem.* **1992,** *97,* 2571. (b) Weigend, F.; Ahlrichs, R. *Phys. Chem. Chem. Phys.* **2005,** *7,* 3297.

(17) Hirata, S.; Head-Gordon, M. *Chem. Phys. Lett.* **1999,** *314,* 291.

(18) (a) Adamo, C.; Barone, V. *J. Chem. Phys.* **1999,** *110,* 6158. (b) Goerigk, L.; Moellmann, J.; Grimme, S. *Phys. Chem. Chem. Phys.* **2009,** *11,* 4611.

(19) Weigend, F.; Häser, M. *Theor. Chem. Acc.* **1997,** *97,* 331.

(20) (a) Neese, F.; Wennmohs, F.; Hansen, A.; Becker, U. *Chem. Phys.* **2009,** *356,* 98. (b) Izsák, R.; Neese, F. *J. Chem. Phys.* **2011,** *135,* 144105. (c) Petrenko, T.; Kossmann, S.; Neese, F. J. *Chem. Phys.* **2011,** *134,* 054116.

(21) Weigend, F. *Phys. Chem. Chem. Phys.* **2006,** *8,* 1057.

(22) (a) Grimme, S.; Ehrlich, S.; Goerigk, L. *J. Comput. Chem.* **2011,** *32,* 1456. (b) Grimme, S.; Antony, J.; Ehrlich, S.; Krieg, H. *J. Chem. Phys.* **2010,** *132,* 154104.

Chapter 9

Synthesis of π-Conjugated Polymers Containing Dibenzosilepin Moieties with Pentacoordinate Silicon

Abstract

Benzo[*h*]quinolyldibenzo[*b,f*]silepin containing pentacoordinate silicon was incorporated into π-conjugated polymers. Substituent effects were investigated from UV–vis absorption and photoluminescence spectra. The author found that π-conjugation involving pentacoordinate silicon was extended by elongating the polymer chain at *meta*-positions toward silicon in the silepin rings. The author also obtained the characteristic absorption bands and emissions originated from π-conjugation. The polymer containing the fluorinated silicon showed bathochromic shift compared to that from the methylated silicon-containing polymer. Polymerization at *para*-positions toward silicon resulted in the formation of short conjugation length. Finally, the emission from the CT band was observed in photoluminescence spectra of the fluorinated polymer.

Chapter 9

Introduction

Conjugated polymers are most attractive candidates for optoelectronic materials with the applicability to low cost printing process.[1] For fabricating organic light-emitting diodes (OLEDs)[2] and solar cells based on conjugated polymers,[3] tuning of the energy levels of the orbitals is necessary to improve efficiency. Introduction of heteroatoms to π-conjugated systems through the polymer chains perturbs the energy level. Conjugated polymers containing silicon-bridged biphenyls or bithiophenes have been often employed for blue-emitting layer in OLEDs and low-band gap components in organic solar cells.[4]

Conformations of π-conjugated molecules influence on the band gaps and colors. Bond rotation of a single bond gives broad peaks in absorption and luminescence spectra.[5] In π-conjugated polymers, flat conformations contribute to extending π-conjugation system. Therefore, bulky substituents would increase dihedral angles between π-conjugated units, leading to large band gaps and hypsochromic shifts. Moreover, kinking and bending in the conjugation units should change the band gap and transition-dipole moments.[6]

Large rings such as cycloheptatriene and cyclooctatetraene have flexible structures because of their weak aromaticity.[7] In ground state, they take boat conformations and flip easily. A flat conformation appears only in excited states. Dibenzo[*b*,*f*]silepins have silicon-containing 7-membered ring and take a boat conformation in the crystal structure.[8] In previous chapters, the author demonstrated tuning of the conformation of dibezo[*b*,*f*]silepins by the substituent effects on pentacoordinate silicons in which the benzo[*h*]quinolyl ligand served an intramolecular dative bond. In summary, pentacoordinate silicon possesses two inequivalent substitution sites, apical and equatorial. Methyl groups on the silicon centre weakened the dative bond. Thereby, the

dibenzosilepin moiety can take many conformations in solution states. In contrast, fluorine substituents enhanced the strength of the dative bond and fixed the flat conformations even in solution states. Moreover, in fluorinated compounds, the benzoquinolyl ligand distributed perpendicularly to the dibenzo[*b,f*]silepin moiety, leading to similar π-orbital interaction with spiroconjugation.[9] Herein, the author reports the synthesis of π -conjugated polymers containing dibenzo[*b,f*]silepin moieties with a benzo[*h*]quinolyl ligand on the main-chain. Their optical properties were investigated by UV–vis absorption and photoluminescence spectra. Density functional theory (DFT) calculations were also performed for estimating their electronic structures.

Results and Discussion

Dichlorinated dibenzo[*b,f*]silepins on 2,8- or 3,7-positions (**1**) were prepared according to Chapter 8 (Scheme 1). Pd-catalyzed borylations of **1** were conducted using bis(pinacolato)diboron.[10] Suzuki–Miyaura coupling reactions of the diborylated dibenzosilepins **2** and dibromofluorene gave the polymers **3**. The number-averaged molecular weights were determined as 4720–37900 by size-exclusion chromatography.[11] Molecular weights of the 2,8-substituted rings (**3pC** and **3pF**) were larger than those of the 3,7-substituted rings (**3mC** and **3mF**). To compare the effect of the conjugation length, difluorenyldibenzosilepins (**4**) were also synthesized from the dichlorinated dibenzosilepins and fluoreneboronic acids by Suzuki–Miyaura coupling (Scheme 2).[12] They showed ^{29}Si NMR signals around –20 ppm for 5-methylated dibenzosilepins and around –40 ppm for 5-fluorinated rings, respectively. These values were similar to benzo[*h*]quinolyldibenzo[*b,f*]silepins without substituents at 2-, 3-, 7- and

8-positions. These data indicate that the structures around silicon should be preserved during introducing substituents and polymerization.[13]

Absorbance peaks (Figure 1) of the **3pC** (338 nm) and **3pF** (341 nm) in dichloromethane appeared at the almost same wavelength. The similar results were obtained from **4pC** (317 nm) and **4pF** (318 nm). The slight substituent effects on the silicon centre suggest that π-conjugation was interrupted by pentacoordinate silicon. The absorptions of the polymers and the low-molecular-mass compounds were derived from the diphenylfluorene unit and the phenylfluorene unit, respectively. The substituent on the silicon centre influenced photoluminescence of the 2,8-substituted compounds in solution states. The fluorinated dibenzosilepins showed fluorescence peaks at longer wavelength regions than the methylated complexes. Fluorescence of the fluorinated complexes could be assigned as the charge transfer state because the *N,N*-dimethylformamide solution of **4pF** exhibited bathochromic shift as compared to that from the dichloromethane solution (14 nm). Luminescence of the methylated complexes could be from the excited state mainly localized on the fluorene and dibenzosilepin moieties because of bathochromic shift of **3pC** as observed in the absorption spectra. It is noteworthy that the fluorescence band of **3pF** was broadening. The data indicated that the polymer chain prohibited reorientation in the excited state.

In absorption spectra of 3,7-substituted dibenzo[*b,f*]silepins in dichloromethane, the polymers showed bathochromic shifts as compared to the low-molecular-mass compounds and 2,8-substituted rings with the corresponded substituents on the silicon centre. These data indicate that π-conjugation should be extended through the vinylene moiety. Moreover, the substituents on silicon induced to shift absorption bands. The 5-fluorinated compounds displayed absorption peaks in longer wavelength regions (389 nm for **3mF** and 356 nm for **4mF**) than the

corresponded methyl-derivatives (351 nm for **3mC** and 316 nm for **4mC**). These differences could be explained in terms of the conformation depending on the substituents on silicon as described in the previous chapters. The fluorinated derivatives have nearly flat conformations in which π-conjugation should be extended through vinylene moiety. In contrast, the methylated rings bend the main-chain, resulting in the distoration of π-conjugation. In photoluminescence spectra, bathochromic shifts derived from fluorine on the silicon centre diminished. It is suggested that the conformations of the dibenzosilepins could be similar to each other in the excited states.

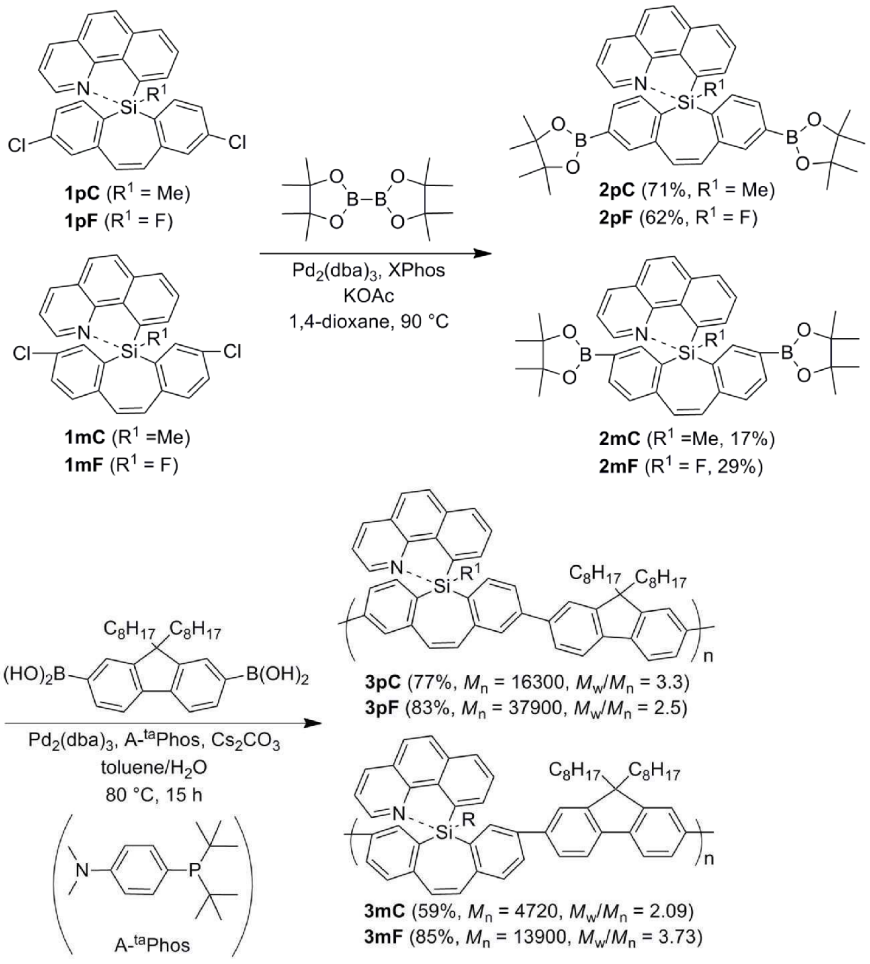

Scheme 1. Synthesis of polymers

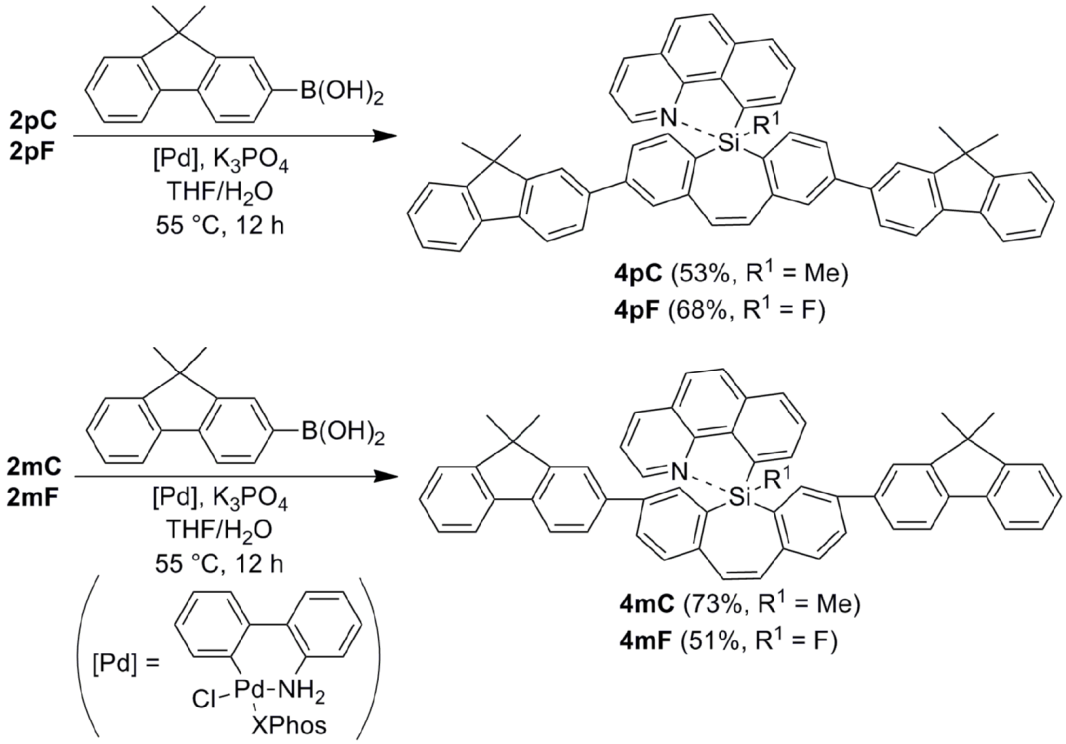

Scheme 2. Synthesis of low-molecular-mass model compounds

Absolute fluorescence quantum yields of 2,8-substituted dibenzosilepins were very low. In contrast, the extending π-conjugation through vinylene moiety contributed to the enhance of the quantum yields. The 3,7-substituted polymers exhibited higher fluorescence quantum yields (0.54 for **3mC** and 0.76 for **3mF**) than the corresponding low-molecular-mass compounds (0.53 for **4mC** and 0.27 for **4mF**). It is implied that long conjugation on the main-chain might be realized in the excited states. As a result, energy or charge transfer which decreases fluorescence intensity could be suppressed.

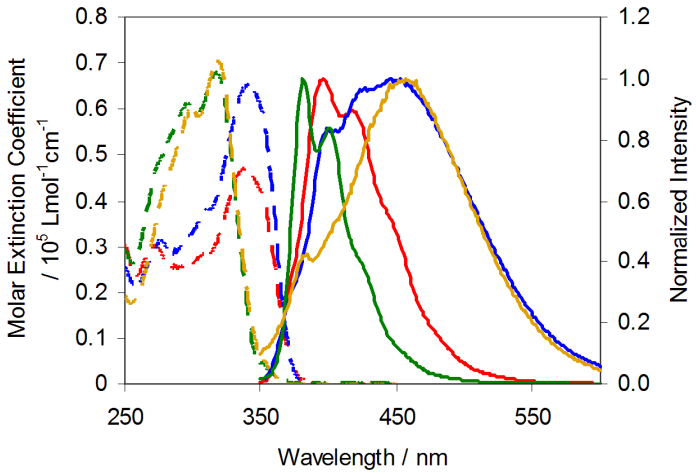

Figure 1. UV–vis absorption (dotted line) and photoluminescence (solid line) spectra of **3pC** (red), **3pF** (blue), **4pC** (green) and **4pF** (yellow) in CH_2Cl_2 (1.0×10^{-5} M).

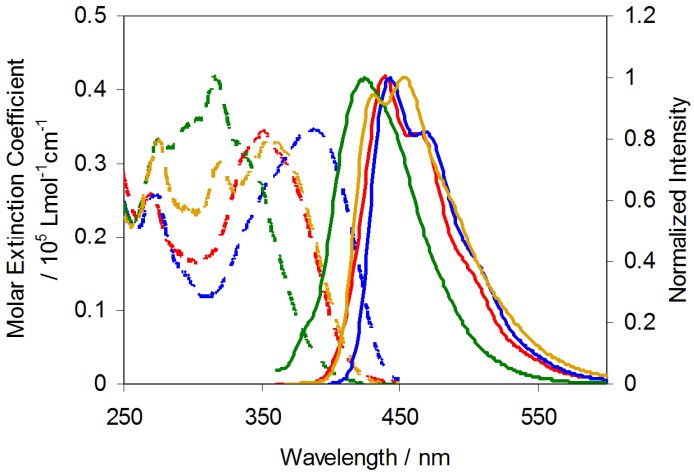

Figure 2. UV–vis absorption (dotted line) and photoluminescence (solid line) spectra of **3mC** (red), **3mF** (blue), **4mC** (green) and **4mF** (yellow) in CH_2Cl_2 (1.0×10^{-5} M).

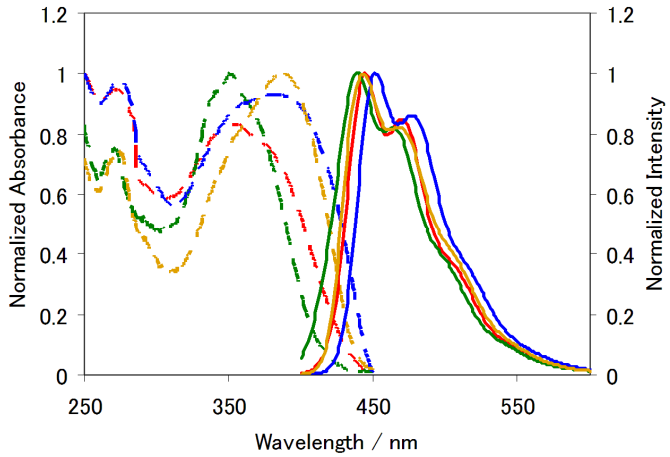

Figure 3. UV–vis absorption (dotted line) and photoluminescence (solid line) spectra of **3pC** (red) and **3pF** (blue) in film state, and **3pC** (green) and **3pF** (yellow) in CH_2Cl_2 (1.0×10^{-5} M).

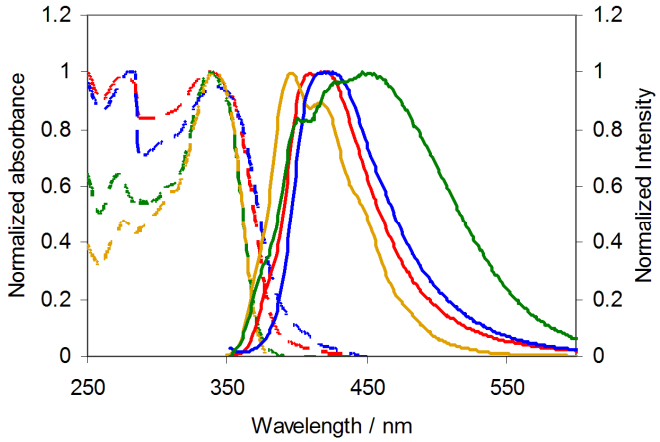

Figure 4. UV–vis absorption (dotted line) and photoluminescence (solid line) spectra of **3mC** (red) and **3mF** (blue) in film state, and **3mC** (green) and **3mF** (yellow) in CH_2Cl_2 (1.0×10^{-5} M).

Polymer films showed broad absorption peaks at similar positions of the polymer solutions. These results imply that benzoquinolyl ligands standing on the polymer chains inhibited strong stacking interaction between π-conjugated domains. Photoluminescence spectra of the polymer films except for **3pF** displayed little bathochromic shifts. The film of **3pF** decreased fluorescence intensity in long wavelength region, and the shape of the fluorescence spectrum was similar to that of **3pC**. It is expected for these data that the synthetic polymers could be versatile for highly emissive solid materials.

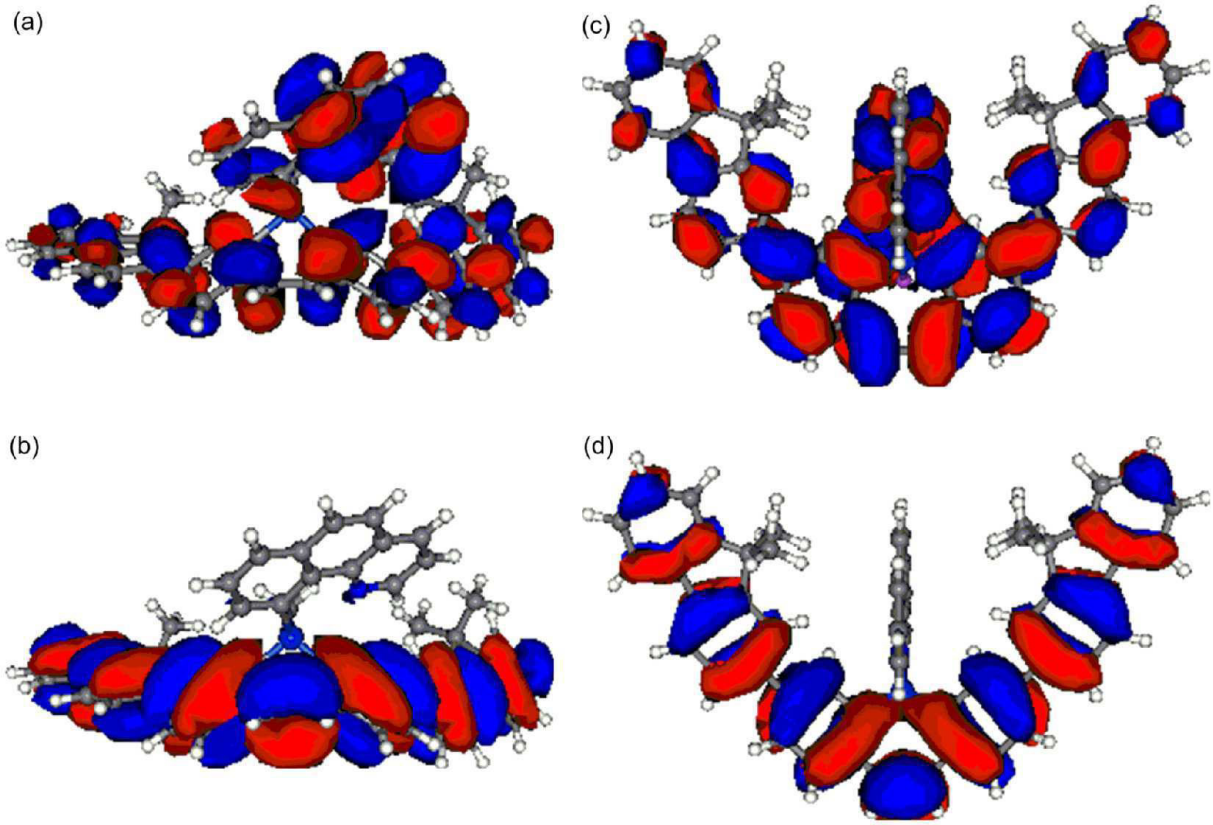

Figure 5. Kohn-Sham orbital diagrams: (a) LUMO+1 of **4mC**, (b) HOMO of **4mC**, (c) LUMO+2 of **4mF**, (d) HOMO of **4mF**.

DFT calculations were performed at TPSS-D3(bj)/def2-TZVP for optimization of structures and at TD-PBE0/def2-TZVP for estimation of absorption to elucidate the origin of the bathochromic shift of **4mF** compared to **4mC**.[14-22] Their structures were referred to the crystal structures of 5-benzo[*h*]quinolyl-5-fluorodibenzo[*b*,*f*]silepin with small bending and 5-benzo[*h*]quinolyl-5-methyldibenzo[*b*,*f*]silepin with large bending.[13] HOMOs of both **4mF** and **4mC** were localized on the difluorenyldibenzosilepin moiety. For **4mC**, transitions from HOMO to LUMO (384 nm, $f = 0.407$) and to LUMO+1 (362 nm, $f = 0.702$) were classified as allowed according to the oscillator strength. LUMO was mainly distributed to the benzoquinolyl ligand whereas LUMO+1 to the difluorenyldibenzosilepin moiety. The transition to LUMO+1 could provide the shoulder in the UV–vis absorption spectrum. With **4mF**, TD-DFT calculation suggested that transition from HOMO to LUMO+2 corresponded to π-π^* transition of the difluorenyldibenzosilepin moiety was allowed (375 nm, $f = 1.088$). In addition, it is noteworthy that an 0rbital on the benzoquinolyl ligand effectively interacted with the π^*-orbital of the dibenzosilepin moiety. The calculated wavelength of **4mF** was longer than that of **4mC**. The calculation data propose that the small bending conformation of **4mF** efficiently might extend π-conjugation. In addition, interaction between π-orbitals of the dibenzosilepin moiety and the benzoquinolyl ligand stabilized their excited state. Thus, bathochromic shifts could be obtained.

Conclusion

The author has obtained conjugated polymers containing pentacoordinate silicon in the 2,8- or 3,7-substituted dibenzo[*b*,*f*]silepin moieties by Suzuki–Miyaura coupling reaction. Emission behaviors were almost dominated by the benzoquinolyl ligand for the 2,8-substituted rings and by the fluorenyldibenzosilepin moiety for 3,7-substituted rings. Emission from CT state of the fluorinated and 2,8-substituted polymer was suppressed in the film state. Substituents on the silicon centre can tune the conjugated length in the 3,7-substituted polymers in ground states.

Experimental Section

Measurements. ^{1}H (400 MHz), ^{13}C (100 MHz), and ^{29}Si (80 MHz) NMR spectra were recorded on a JEOL JNM-EX400 spectrometer. ^{1}H and ^{13}C NMR spectra used tetramethylsilane (TMS) as an internal standard. ^{29}Si NMR spectra were referenced externally to TMS in $CDCl_3$. UV–vis spectra were recorded on a Shimadzu UV-3600 spectrophotometer. Fluorescence emission spectra were recorded on a HORIBA JOBIN YVON Fluoromax-4 spectrofluorometer. Elemental analysis was performed at the Microanalytical Center of Kyoto University. All reactions were performed under nitrogen or argon atmosphere.

Materials. Tetrahydrofuran (THF) and diethyl ether were purified using a two-column solid-state purification system (Glasscontour System, Joerg Meyer, Irvine, CA). 5-(10-benzo[*h*]quinolyl)-2,8-dichloro-5-methyldibenzo[*b*,*f*]silepin (**1pC**), 5-(10-benzo[*h*]quinolyl)-3,7-dichloro-5-methyldibenzo[*b*,*f*]silepin (**1mC**), 5-(10-benzo[*h*]quinolyl)-2,8-dichloro-5-fluorodibenzo[*b*,*f*]silepin (**1pF**) and 5-(10-benzo[*h*]quinolyl)-3,7-dichloro-5-fluoro-dibenzo[*b*,*f*]silepin (**1mF**) were synthesized according to Chapter 8. Other reagents were commercially available and used as received.

Synthesis of 5-(10-Benzo[*h*]quinolyl)-5-methyl-2,8-bis(4,4,5,5-tetramethyl-1,3,2-dioxaborolan-2-yl)dibenzo[*b*,*f*]silepin (2pC). A mixture of 5-(10-benzo[*h*]quinolyl)-5-methyl-2,8-dichlorodibenzo[*b*,*f*]silepin (1.87 g, 4.00 mmol), bis(pinacolato)diboron (6.09 g, 24.0 mmol), potassium acetate (2.36 g, 24.0 mmol), Pd_2dba_3 (54.9 mg, 0.060 mmol) and XPhos (0.114 g, 0.240 mmol) was heated to 90 °C in 1,4-dioxane (20 mL) with stirring for 39 h. The reaction mixture was then filtered through a thin pad of celite (eluting with THF) at room temperature, and the filtrate was concentrated under vacuum. The resulting solid was dissolved in chloroform (20 mL) and added to methanol (100 mL). The precipitate was collected by filtration and purified

by silica gel column chromatography eluted with hexane/ethyl acetate (9/1) to give a colorless solid in 71% yield (1.84 g, 2.82 mmol). ^{1}H NMR (400 M Hz, $CDCl_3$): δ = 8.61 (br, 1H, Ar*H*), 8.01 (d, *J* = 6.8 Hz, 1H, Ar*H*), 7.88 (m, 3H, Ar*H*), .7.78-7.68 (m, 5H, Ar*H*), 7.60 (d, *J* = 8.8 Hz, 1H, Ar*H*), 7.46 (br,2H, Ar*H*), 7.32 (m, 1H, Ar*H*), 6.71 (s, 2H, -C*H*=C*H*-), 1.32 (s, 24H, -CH_3), 1.13 (s, 3H, SiCH_3) ppm. ^{13}C NMR (100 M Hz, $CDCl_3$): δ = 145.8, 145.5, 145.1, 139.8, 137.6, 136.2, 135.1, 133.6, 132.7, 132.5, 132.3, 132.1, 129.7, 128.5, 127.6, 127.1, 126.2, 124.7, 121.5, 83.6, 24.8, −3.2 ppm. ^{29}Si NMR (80 M Hz, $CDCl_3$): δ = −20.9 ppm. HRMS (ESI+): m/z: calcd for $C_{40}H_{44}B_2NO_4Si$ ($M+H^+$): 652.3220; found: 652.3235. elemental analysis: calcd for $C_{40}H_{43}B_2NO_4Si$: C 73.74, H 6.65, N 2.15; found: C 72.24, H 6.55, N 2.04.

Synthesis of 5-(10-Benzo[*h*]quinolyl)-5-fluoro-2,8-bis(4,4,5,5-tetramethyl-1,3,2-dioxaborolan-2-yl)dibenzo[*b*,*f*]silepin (2pF). A mixture of 5-(10-benzo[*h*]quinolyl)-5-methyl-2,8-dichlorodibenzo[*b*,*f*]silepin (0.850 g, 1.80 mmol), bis(pinacolato)diboron (2.74 g, 10.8 mmol), potassium acetate (1.06 g, 10.8 mmol), Pd_2dba_3 (24.7 mg, 0.027 mmol) and XPhos (51.5 mg, 0.108 mmol) was heated at 90 °C in 1,4-dioxane (9.0 mL) with stirring for 13 h. The reaction mixture was then filtered through a thin pad of celite (eluting with THF) at room temperature, and the filtrate was concentrated under vacuum. The resulting solid was dissolved in a small amount of chloroform and added to methanol (75 mL). The precipitate was collected by filtration and purified by silica gel column chromatography eluted with hexane/ethyl acetate (7/3) to give a colorless solid in 62% yield (0.725 g, 1.11 mmol). ^{1}H NMR (400 M Hz, $CDCl_3$): δ = 8.61 (br, 1H, Ar*H*), 8.15 (d, *J* = 7.6 Hz, 2H, Ar*H*), 8.07 (d, *J* = 6.8 Hz, 1H, Ar*H*), 7.98 (m, 2H, Ar*H*), 7.87 (m, 3H, Ar*H*), 7.73 (d, *J* = 8.4 Hz, 1H, Ar*H*), 7.20 (m, 3H, Ar*H*), 6.95 (s, 2H, −C*H*=C*H*−) 6.78 (d, *J* = 6.8 Hz, 2H, Ar*H*) ppm. ^{13}C NMR (100 M Hz, $CDCl_3$): δ = 145.7, 143.3, 141.9, 141.7, 139.4, 138.5, 138.3, 136.3, 135.9, 132.8, 132.3, 132.1, 130.7, 130.5, 129.8, 129.4,

128.4, 125.3, 124.1, 122.7, 83.7, 24.8 ppm. ^{29}Si NMR (80 M Hz, $CDCl_3$): δ = –41.2 (d, J = 272 Hz) ppm. HRMS (ESI+): m/z: calcd for $C_{39}H_{41}B_2NO_4FSi$ ($M+H^+$): 656.2970; found: 656.2980.

Synthesis of 5-(10-Benzo[*h*]quinolyl)-5-methyl-3,7-bis(4,4,5,5-tetramethyl-1,3,2-dioxaborolan-2-yl)dibenzo[*b*,*f*]silepin (2mC). A mixture of 5-(10-benzo[*h*]quinolyl)-5-methyl-3,7-dichlorodibenzo[*b*,*f*]silepin (0.360 g, 0.768 mmol), bis(pinacolato)diboron (1.17 g, 4.61 mmol), potassium acetate (0.452 g, 4.61 mmol), Pd_2dba_3 (14.1 mg, 0.0154 mmol) and XPhos (29.4 mg, 0.0616 mmol) was heated at 90 °C in 1,4-dioxane (3.8 mL) with stirring for 3 h. The reaction mixture was then filtered through a thin pad of celite (eluting with THF) at room temperature, and the filtrate was concentrated under vacuum. The crude product was purified by silica gel column chromatography eluted with hexane/ethyl acetate (9/1). The resulting solid was dissolved in a small amount of chloroform and added to methanol to give a colorless solid in 17% yield (86.2 mg, 0.132 mmol). ^{1}H NMR (400 M Hz, $CDCl_3$): δ = 8.79 (d, J = 2.8 Hz, 1H, Ar*H*), 8.51 (br, 2H, Ar*H*), 8.00 (d, J = 8.0 Hz, 1H, Ar*H*), .7.83 (d, J = 7.2 Hz, 1H, Ar*H*), 7.73 (m, 3H, Ar*H*), 7.58 (d, J = 8.4 Hz, 1H, Ar*H*), 7.40 (m, 2H, Ar*H*), 7.30 (m, 1H, Ar*H*), 7.25 (m, 2H, Ar*H*), 6.68 (s, 2H, –C*H*=C*H*–), 1.39 (s, 24H, –CH_3), 1.33 (s, 3H, SiCH_3) ppm. ^{13}C NMR (100 M Hz, $CDCl_3$): δ = 146.1, 146.0, 140.3, 137.7, 136.3, 135.0, 133.8, 133.4, 132.7, 129.6, 128.6, 127.5, 126.9, 126.3, 124.6, 121.3, 83.6, 24.8, –3.4 ppm. ^{29}Si NMR (80 M Hz, $CDCl_3$): δ = –20.1 ppm. HRMS (ESI+): m/z: calcd for $C_{40}H_{44}B_2NO_4Si$ ($M+H^+$): 652.3220; found: 652.3215.

Synthesis of 5-(10-Benzo[*h*]quinolyl)-5-fluoro-3,7-bis(4,4,5,5-tetramethyl-1,3,2-dioxaborolan-2-yl)dibenzo[*b*,*f*]silepin (2mF). A mixture of 5-(10-benzo[*h*]quinolyl)-3,7-dichloro-5-fluorodibenzo[*b*,*f*]silepin (0.350 g, 0.741 mmol), bis(pinacolato)diboron (1.13 g, 4.45 mmol), potassium acetate (0.437 g, 4.45 mmol), Pd_2dba_3 (13.6 mg, 0.0148 mmol) and XPhos (28.2 mg, 0.0592 mmol) was heated at 90 °C in 1,4-dioxane (3.7 mL) with stirring for 3 h. The

reaction mixture was then filtered through a thin pad of celite (eluting with THF) at room temperature, and the filtrate was concentrated under vacuum. The crude product was purified by silica gel column chromatography eluted with hexane/ethyl acetate (9/1 to 4/1). The resulting solid was dissolved in a small amount of chloroform and added to methanol to give a colorless solid in 17% yield (86.2 mg, 0.132 mmol). ^{1}H NMR (400 M Hz, $CDCl_3$): δ = 8.58 (d, J = 7.2 Hz, 1H, Ar*H*), 8.23 (br, 1H, Ar*H*), 8.14 (d, J = 8.0 Hz, 1H, Ar*H*), .8.08 (d, J = 8.0 Hz, 1H, Ar*H*), 7.95 (m, 2H, Ar*H*), 7.69 (m, 3H, Ar*H*), 7.43 (s, 2H, Ar*H*), 7.37 (d, J = 7.6 Hz, 2H, Ar*H*), 7.20 (dd, J = 8.0, 4.8 Hz, 1H, Ar*H*), 6.91 (s, 2H, –C*H*=C*H*–), 1.13 (s, 12H, -CH_3), 1.09 (s, 12H, -CH_3) ppm. ^{29}Si NMR (80 M Hz, $CDCl_3$): δ = −39.0 (J = 274 Hz) ppm. HRMS (ESI+): m/z: calcd for $C_{39}H_{41}B_2FNO_4Si$ (M+H$^+$): 656.2970; found: 656.2960. elemental analysis: calcd for $C_{39}H_{40}B_2FNO_4Si$: C 71.47, H 6.15, N 2.14; found: C 71.19, H 6.09, N, 2.24.

Synthesis of Polymer 3pC. Monomer **2pC** (0.130 g, 0.200 mmol), 2,7-dibromo-9,9-dioctylfluorene (0.110 g, 0.200 mmol), cesium carbonate (0.391 g, 1.20 mmol), and Pd_2dba_3 (1.8 mg, 2.0 μmol), (4-(*N*,*N*-dimethylamino)phenyl)di-*tert*-butylphosphine (2.1 mg, 8.0 μmol) were dissolved in 2.0 mL of toluene and 0.2 mL of water. After the mixture was stirred at 80 °C for 15 h, the reaction mixture was cooled to room temperature and poured into a large excess of methanol to precipitate the polymer. The polymer was purified by repeated precipitations from a small amount of $CHCl_3$ into a large excess of methanol and hexane respectively to give a white solid in 77% yield (0.121 g, 0.154 mmol). ^{1}H NMR (400 M Hz, $CDCl_3$): δ = 8.78 (1H, Ar*H*), 8.02 (3H, Ar*H*), 7.90 (1H, Ar*H*), 7.73–7.54 (13H, Ar*H*), 7.36 (1H, Ar*H*), 6.86 (2H, –C*H*=C*H*–), 1.99 (4H, $Ar_2C(CH_2(CH_2)_6CH_3)_2$), 1.23 (3H, Si$CH_3$), 1.16–1.01 (20H, $Ar_2C(CH_2CH_2(CH_2)_5CH_3)_2$), 0.76 (6H, $Ar_2C(CH_2(CH_2)_6CH_3)_2$, 0.68 (4H, $Ar_2C(CH_2CH_2(CH_2)_5CH_3)_2$) ppm. ^{13}C NMR (100 M Hz, $CDCl_3$): δ = 151.6, 145.9, 141.0, 140.8,

140.1, 139.9, 137.9, 135.2, 133.82, 133.76, 133.2, 132.5, 129.9, 128.7, 127.2, 126.5, 125.9, 125.6, 124.8, 121.5, 119.9, 55.2, 40.4, 31.8, 30.0, 29.19, 29.16, 23.8, 22.6, 14.0, −3.0 ppm. ^{29}Si NMR (80 M Hz, $CDCl_3$): δ = −20.6 ppm. M_n = 16300. elemental analysis: calcd for $C_{57}H_{59}NSi$: C 87.08, H 7.56, N 1.78; found: C 86.80, H 7.84, N, 1.79.

Synthesis of Polymer 3pF. Similarly to the preparation of **3pC**, **3pF** was obtained from **2pF** (0.131 g, 0.200 mmol), and 2,7-dibromo-9,9-dioctylfluorene (0.110 g, 0.200 mmol) in 83% yield as a white solid. ^{1}H NMR (400 M Hz, $CDCl_3$): δ = 8.67 (1H, Ar*H*), 8.19 (2H, Ar*H*), 8.06–7.97 (3H, Ar*H*), 7.80 (1H, Ar*H*), 7.74–7.67 (4H, Ar*H*), 7.50 (4H, Ar*H*), 7.27 (1H, Ar*H*), 7.12 (4H, Ar*H*), 6.90 (2H, −C*H*=C*H*−), 1.94 (4H, $Ar_2C(CH_2(CH_2)_6CH_3)_2$), 1.12−1.03 (20H, $Ar_2C(CH_2CH_2(CH_2)_5CH_3)_2$), 0.74 (6H, $Ar_2C(CH_2(CH_2)_6CH_3)_2$, 0.64 (4H, $Ar_2C(CH_2CH_2(CH_2)_5CH_3)_2$) ppm. ^{13}C NMR (100 M Hz, $CDCl_3$): δ = 151.7, 145.4, 143.7, 141.8, 140.8, 140.1, 139.7, 138.7, 137.4, 137.1, 136.5, 136.1, 133.7, 133.3, 132.5, 130.9, 130.5, 129.9, 129.6, 128.6, 125.9, 125.5, 124.2, 122.8, 121.4, 119.9, 55.2, 40.3, 31.7, 30.0, 29.2, 29.1, 23.8, 22.6, 14.0, −3.1 ppm. ^{29}Si NMR (80 M Hz, $CDCl_3$): δ = −40.0 (d, J = 270 Hz) ppm. M_n = 37900. elemental analysis: calcd for $C_{56}H_{56}FNSi$: C 85.12, H 7.14, N 1.77; found: C 84.95, H 7.05, N, 1.83.

Synthesis of Polymer 3mC. Similarly to the preparation of **3pC**, **3mC** was obtained from **2mC** (71.7 mg, 0.110 mmol), and 2,7-dibromo-9,9-dioctylfluorene (60.3 mg, 0.110 mmol) in 59% yield as a pale yellow solid. ^{1}H NMR (400 M Hz, $CDCl_3$): δ = 8.53 (1H, Ar*H*), 8.20 (2H, Ar*H*), 8.02 (1H, Ar*H*), 7.92 (1H, Ar*H*), 7.75 (4H, Ar*H*), 7.58 (7H, Ar*H*), 7.37 (3H, Ar*H*), 7.24 (1H, Ar*H*), 6.79 (2H, −C*H*=C*H*−), 1.98 (4H, $Ar_2C(CH_2(CH_2)_6CH_3)_2$), 1.29 (3H, $SiCH_3$), 1.06 (20H, $Ar_2C(CH_2CH_2(CH_2)_5CH_3)_2$), 0.74 (4H, $Ar_2C(CH_2CH_2(CH_2)_5CH_3)_2$) ppm. ^{13}C NMR (100

M Hz, $CDCl_3$): δ = 151.7, 145.8, 145.6, 141.7, 140.2, 139.9, 139.7, 138.0, 136.5, 135.1, 133.8, 132.5, 132.4, 132.2, 132.0, 130.0, 129.4, 128.8, 127.6, 127.3, 126.8, 126.4, 125.8, 124.8, 121.5, 119.9, 55.1, 40.4, 31.7, 30.1, 29.2, 23.9, 22.6, 22.5, 14.0, −3.0 ppm. ^{29}Si NMR (80 M Hz, $CDCl_3$): δ = ppm. M_n = 4700. elemental analysis: calcd for $C_{57}H_{59}NSi$: C 87.08, H 7.56, N 1.78; found: C 86.82, H 7.72, N, 1.85.

Synthesis of Polymer 3mF. Similarly to the preparation of **3pC**, **3mF** was obtained from **2mF** (105 mg, 0.160 mmol), and 2,7-dibromo-9,9-dioctylfluorene (87.8 mg, 0.160 mmol) in 83% yield as a pale yellow solid. ^{1}H NMR (400 M Hz, $CDCl_3$): δ = 8.68 (1H, Ar*H*), 8.20 (1H, Ar*H*), 8.14 (2H, Ar*H*), 8.02−7.93 (2H, Ar*H*), 7.82 (1H, Ar*H*), 7.51 (4H, Ar*H*), 7.31 (2H, Ar*H*), 7.27 (1H, Ar*H*), 7.10 (2H, Ar*H*), 6.98 (2H, Ar*H*), 6.91 (2H, Ar*H*), 6.81 (2H, −C*H*=C*H*−), 1.56 (4H), 1.16 (4H), 1.07−1.00 (8H), 0.81 (14H), 0.28 (4H, $Ar_2C(CH_2CH_2(CH_2)_5CH_3)_2$) ppm. ^{13}C NMR (100 M Hz, $CDCl_3$): δ = 151.2, 145.4, 143.7, 139.8, 139.6, 139.5, 139.3, 138.9, 138.7, 138.6, 136.4, 135.9, 132.4, 131.7, 130.6, 130.3, 130.0, 129.5, 128.8, 127.3, 125.4, 125.3, 124.1, 122.7, 120.9, 119.5, 54.7, 40.1, 31.7, 29.9, 29.2, 29.0, 23.5, 22.6, 14.1 ppm. ^{29}Si NMR (80 M Hz, $CDCl_3$): δ = −39.0 (d, J = 272 Hz) ppm. M_n = 13900. elemental analysis: calcd for $C_{56}H_{56}FNSi$: C 85.12, H 7.14, N 1.77; found: C 84.64, H 7.12, N, 2.06.

Synthesis of 5-(10-Benzo[*h*]quinolyl)-2,8-bis(9,9-dimethylfluoren-2-yl)-5-methyldibenzo[*b*,*f*]silepin (4pC). A mixture of **1pC** (0.187 g, 0.400 mmol), 9,9-dimethylfluorene-2-boronic acid (0.286 g, 1.20 mmol), tripotassium phosphate (0.340 g, 0.016 mmol), and chloro(2-dicyclohexylphosphino-2′,4′,6′-triisopropyl-1,1′-biphenyl)[2-(2′-amino-1,1′-biphenyl)]palladium(II) (12.6 mg, 0.016 mmol) was heated at 55 °C in THF (2.0 mL) and water (0.4 mL) with stirring for 12 h. Then, water was added to the solution. After extraction with cyclopentyl methyl ether, drying over $MgSO_4$, and condensation under vacuum, the crude

product was purified by silica gel column chromatography eluted with hexane/ethyl acetate (100/0 to 95/5) to give a pale yellow solid in 53% yield (0.167 g, 0.213 mmol). ^{1}H NMR (400 M Hz, $CDCl_3$): δ = 8.77 (br, 1H, Ar*H*), 8.04 (m, 3H, Ar*H*), 7.92 (d, *J* = 7.6 Hz, 1H, Ar*H*), 7.81 (d, *J* = 8.8 Hz, 1H, Ar*H*), 7.74 (m, 4H, Ar*H*), 7.64 (m, 6H, Ar*H*), 7.58 (m, 5H, Ar*H*), 7.43 (m, 2H, Ar*H*) 7.32 (m, 5H, Ar*H*), 6.85 (s, 2H, -C*H*=C*H*-), 1.52 (s, 12H, ArCH_3), 1.24 (s, 3H, -SiCH_3) ppm. ^{13}C NMR (100 M Hz, $CDCl_3$): δ = 154.2, 153.9, 145.8, 141.0, 140.7, 140.3, 138.9, 138.4, 137.9, 136.4, 135.2, 133.8, 133.1, 132.4, 129.9, 128.7, 127.3, 127.2, 127.0, 126.4, 126.1, 125.6, 124.7, 122.6, 121.5, 121.3, 120.2, 120.0, 46.9, 27.2, –3.0 ppm. ^{29}Si NMR (80 M Hz, $CDCl_3$): δ = –20.6 ppm. HRMS (ESI+): m/z: calcd for $C_{58}H_{46}NSi$ ($M+H^+$): 784.3394; found: 784.3383.

Synthesis of 5-(10-Benzo[*h*]quinolyl)-2,8-bis(9,9-dimethylfluoren-2-yl)-5-fluorodibenzo[*b*,*f*]silepin (4pF). A mixture of **1pF** (0.189 g, 0.400 mmol), 9,9-dimethylfluorene-2-boronic acid (0.286 g, 1.20 mmol), tripotassium phosphate (0.340 g, 0.016 mmol), and chloro(2-dicyclohexylphosphino-2′,4′,6′-triisopropyl-1,1′-biphenyl)[2-(2′-amino-1,1′-biphenyl)]palladium(II) (12.6 mg, 0.016 mmol) was heated at 55 °C in THF (2.0 mL) and water (0.4 mL) with stirring for 12 h. Then, water was added to the solution. After extraction with cyclopentyl methyl ether, drying over $MgSO_4$, and condensation under vacuum, the crude product was purified by silica gel column chromatography eluted with hexane/ethyl acetate (10/0 to 4/1) to give a pale yellow solid in 68% yield (0.215 g, 0.273 mmol). ^{1}H NMR (400 M Hz, $CDCl_3$): δ = 8.68 (d, *J* = 6.8 Hz, 1H, Ar*H*), 8.19 (d, *J* = 7.6 Hz, 1H, Ar*H*), 8.13 (m, 1H, Ar*H*), 8.04–7.97 (m, 3H, Ar*H*), 7.78 (d, *J* = 9.2 Hz, 1H, Ar*H*), 7.74–7.69 (m, 6H, Ar*H*), 7.57 (d, *J* = 0.8 Hz, 2H, Ar*H*), 7.50 (dd, *J* = 8.0, 1.2 Hz, 2H, Ar*H*) 7.41 (m, 2H, Ar*H*), 7.32–7.22 (m, 5H, Ar*H*), 7.12 (dd, *J* = 7.6, 1.2 Hz, 2H, Ar*H*), 7.09 (s, 2H, -C*H*=C*H*-), 6.89 (d, *J* = 8.0 Hz, 1H, Ar*H*), 1.48 (s, 12H, -CH_3) ppm. ^{29}Si NMR (80 M Hz, $CDCl_3$): δ = –40.3 (d, *J* = 270 Hz) ppm. HRMS

(ESI+): m/z: calcd for $C_{57}H_{43}FNSi$ ($M+H^+$): 788.3143; found: 788.3123. elemental analysis: calcd for $C_{57}H_{42}FNSi$: C 86.88, H 5.37, N 1.78; found: C 86.61, H 5.58, N, 1.71.

Synthesis of 5-(10-Benzo[*h*]quinolyl)-3,7-bis(9,9-dimethylfluoren-2-yl)-5-methyldibenzo[*b*,*f*]silepin (**4mC**). A mixture of **1mC** (0.187 g, 0.400 mmol), 9,9-dimethylfluorene-2-boronic acid (0.286 g, 1.20 mmol), tripotassium phosphate (0.340 g, 0.016 mmol), and chloro(2-dicyclohexylphosphino-2′,4′,6′-triisopropyl-1,1′-biphenyl)[2-(2′-amino-1,1′-biphenyl)]palladium(II) (12.6 mg, 0.016 mmol) was heated to 55 °C in THF (2.0 mL) and water (0.4 mL) with stirring for 12 h. Then, water was added to the solution. After extraction with cyclopentyl methyl ether, drying over $MgSO_4$, and condensation under vacuum, the crude products was purified by silica gel column chromatography eluted with hexane/ethyl acetate (9/1). Recrystallization from dichloromethane/hexane gave a pale yellow solid in 73% yield (0.227 g, 0.290 mmol). ^{1}H NMR (400 M Hz, $CDCl_3$): δ = 8.51 (br, 1H, Ar*H*), 8.19 (br, 2H, Ar*H*), 8.00 (d, *J* = 6.4 Hz, 1H, Ar*H*), 7.91 (d, *J* = 7.6 Hz, 1H, Ar*H*), 7.81–7.72 (m, 6H, Ar*H*), 7.63–7.55 (m, 7H, Ar*H*), 7.43 (m, 3H, Ar*H*), 7.32 (m, 6H, Ar*H*), 7.21 (m, 1H, Ar*H*), 6.76 (s, 2H, -C*H*=C*H*-), 1.48 (s, 12H, -CH_3), 1.26 (s, 12H, -SiCH_3) ppm. ^{13}C NMR (100 M Hz, $CDCl_3$): δ = 154.2, 153.9, 145.6, 141.9, 140.7, 139.7, 138.9, 138.3, 137.9, 136.4, 135.1, 133.8, 132.5, 132.3, 131.8, 129.9, 129.4, 128.7, 127.3, 127.2, 127.0, 126.9, 126.5, 126.4, 126.0, 124.7, 122.6, 121.5, 121.3, 120.2, 120.0, 46.9, 27.2, –3.0 ppm. ^{29}Si NMR (80 M Hz, $CDCl_3$): δ = –19.3 ppm. HRMS (ESI+): m/z: calcd for $C_{58}H_{46}NSi$ ($M+H^+$): 784.3394; found: 784.3380. elemental analysis: calcd for $C_{58}H_{45}NSi$: C 88.85, H 5.78, N 1.79; found: C 89.08, H 6.06, N, 1.60.

Synthesis of 5-(10-Benzo[*h*]quinolyl)-3,7-bis(9,9-dimethylfluoren-2-yl)-5-fluorodibenzo[*b*,*f*]silepin (**4mF**). A mixture of **1mF** (0.189 g, 0.400 mmol), 9,9-dimethylfluorene-2-boronic acid (0.286 g, 1.20 mmol), tripotassium phosphate (0.340 g, 0.016

mmol), and chloro(2-dicyclohexylphosphino-2′,4′,6′-triisopropyl-1,1′-biphenyl)[2-(2′-amino-1,1′-biphenyl)]palladium(II) (12.6 mg, 0.016 mmol) was heated to 55 °C in THF (2.0 mL) and water (0.4 mL) with stirring for 12 h. Then, water was added to the solution. After extraction with cyclopentyl methyl ether, drying over $MgSO_4$, and condensation under vacuum, the crude product was purified by silica gel column chromatography eluted with hexane/ethyl acetate (4/1). Recrystallization from dichloromethane/hexane gave a pale yellow solid in 51% yield (0.159 g, 0.202 mmol). ^{1}H NMR (400 M Hz, $CDCl_3$): δ = 8.70 (d, *J* = 6.8 Hz, 1H, Ar*H*), 8.22 (d, *J* = 8.4 Hz, 1H, Ar*H*), 8.16 (d, *J* = 7.6 Hz, 1H, Ar*H*), 8.11 (d, *J* = 4.4 Hz, 1H, Ar*H*), 8.02 (d, *J* = 8.8 Hz, 1H, Ar*H*), 7.95 (m, 1H, Ar*H*), 7.82 (d, *J* = 9.2 Hz, 1H, Ar*H*), 7.59 (m, 2H, Ar*H*), 7.54 (s, 4H, Ar*H*), 7.49 (d, *J* = 7.6 Hz, 2H, Ar*H*), 7.35 (m, 2H, Ar*H*), 7.30 (dd, *J* = 8.0, 4.8 Hz, 1H, Ar*H*), 7.30 (m, 2H, Ar*H*), 7.25 (m, 4H, Ar*H*), 7.12 (s, 2H, Ar*H*), 7.02 (m, 4H, Ar*H*), 6.94 (s, 2H, -C*H*=C*H*-), 1.29 (d, *J* = 12.0 Hz, 12H, -CH_3) ppm. ^{13}C NMR (100 M Hz, $CDCl_3$): δ = 153.8, 153.7, 145.4, 143.8, 139.7, 139.4, 139.3, 138.9, 138.7, 138.2, 136.5, 136.0, 132.5, 132.3, 131.9, 130.6, 130.3, 130.0, 129.6, 128.8, 127.4, 127.2, 126.9, 125.6, 125.5, 124.0, 122.8, 122.5, 121.0, 120.0, 119.9, 46.6, 27.0 ppm. ^{29}Si NMR (80 M Hz, $CDCl_3$): δ = −39.1 (d, *J* = 272 Hz) ppm. HRMS (ESI+): m/z: calcd for $C_{57}H_{43}FNSi$ ($M+H^+$): 788.3143; found: 788.3119. elemental analysis: calcd for $C_{57}H_{42}FNSi$: C 86.88, H 5.37, N 1.78; found: C 86.36, H 5.38, N, 1.86.

Computational details. All calculations were carried with ORCA 2.9.[14] The geometry of the singlet ground state was optimized by the TPSS functional[15] and the def2-TZVP basis set.[16] On the basis of the optimized structure, the absorption properties were calculated by TD-DFT within the Tamm-Dancoff approximation.[17] The TD-DFT calculations performed at the PBE0 hybrid functional level[18] with the def2-TZVP basis set. The resolution of the identity (RI) approximation[19] was applied for the TPSS functional, and RI and chain of spheres approximation

(RIJCOSX)[20] were also applied for the hybrid functional. The auxiliary basis function for coulomb fitting[21] was used for the fitting basis in the RI and RIJCOSX treatments. In all cases, the empirical London dispersion correction (DFT-D3(bj))[22] was applied.

References

(1) (a) Kertesz, M.; Choi, C. H.; Yang, S. *Chem. Rev.* **2005,** *105,* 3448. (b) Grimsdale, A. C.; Müllen, K. *Macromol. Rapid Commun.* **2007,** *28,* 1676.

(2) (a) Grimsdale, A. C.; Chan, K. L.; Martin, R. E.; Jokisz, P. G.; Holmes, A. B. *Chem. Rev.* **2009,** *109,* 897. (b) Neher, D. *Macromol. Rapid Commun.* **2001,** *22,* 1365. (c) Mitschke, U.; Bäuerle, P. *J. Mater. Chem.* **2000,** *10,* 1471.

(3) (a) Günes, S.; Neugebauer, H.; Sariciftci, N. S. *Chem. Rev.* **2007,** *107,* 1324. (b) Zhan, X.; Zhu, D. *Polym. Chem.* **2010,** *1,* 409. (c) Coakley, K. M.; Mcgehee, M. D. *Chem. Mater.* **2004,** *16,* 4533. (d) Winder, C.; Sariciftci, N. S. *J. Mater. Chem.* **2004,** *14,* 1077.

(4) (a) Beaupré, S.; Boudreault, P.-L. T.; Leclerc, M. *Adv. Mater.* **2010,** *22,* E6. (b) Chen, J.; Cao, Y. *Macromol. Rapid. Commun.* **2007,** *28,* 1714. (c) Yuan, M.; Yang, P.; Durban, M. M.; Luscombe, C. K. *Macromolecules* **2012,** *45,* 5934. (d) Lu, G.; Usta, H.; Risko, C.; Wang, L.; Facchetti, A.; Ratner, M. A.; Marks, T. J. *J. Am. Chem. Soc.* **2008,** *130,* 7670. (e) Keyworth, C. W.; Chan, K. L.; Labram, J. G.; Anthopoulos, T. D.; Watkins, S. E.; McKiernan, M.; White, A. J. P.; Holmes, A. B.; Williams, C. K. *J. Mater. Chem.* **2011,** *21,* 11800.

(5) (a) Roncali, J. *Macromol. Rapid. Commun.* **2007,** *28,* 1761. (b) Gierchner, J.; Cornil, J.; Egelhaaf, H.-J. *Adv. Mater.* **2007,** *19,* 173. (c) Andersson, M. R.; Berggren, M.; Inganäs, O.; Gustafsson, G.; Gustafsson-Carlberg, J. C.; Selse, D.; Hjertberg, T.; Wennerström, O. *Macromolecules* **1995,** *28,* 7525. (d) Lupton, J. M. *ChemPhysChem* **2012,** *13,* 901.

(6) (a) Beenken, W. J. D.; Pullerits, T. *J. Phys. Chem. B* **2004,** *108,* 6164. (b) Becker, K.; Como, E. D.; Feldman, J.; Scheliga, F.; Csányi, T.; Tretiak, S.; Lupton, J. M. *J. Phys. Chem. B* **2008,** *112,* 4859.

(7) (a) Chen, Z.; Jiao, H.; Wu, J. I.; Herges, R.; Zhang, S. B.; Schleyer, P. v. R. *J. Phys. Chem. A* **2008,** *112.* 10586. (b) Williams, R. V.; Edwards, W. D.; Zhang, P.; Berg, D. J.; Mitchell, R. H. *J. Am. Chem. Soc.* **2012,** *134,* 16742. (c) Wenthold, P. G.; Hrovat, D. A.; Borden, W. T.; Lineberger, W. C. *Science* **1996,** *272,* 1456.

(8) (a) Corey, J. Y.; Corey, E. R. *Tetrahedron Lett.* **1972,** *13,* 4669. (b) Nishihara, T.; Izukawa, Y.; Komatsu, K. *Chem. Lett.* **1998,** *3,* 269.

(9) Saragi, T. P. I.; Spehr, T.; Siebert, A.; Fuhrmann-Lieker, T.; Salbeck, J. *Chem. Rev.* **2007,** *107,* 1011.

(10) Billingsley, K. L.; Barder, T. E.; Buchwald, S. L. *Angew. Chem. Int. Ed.* **2007,** *46,* 5359.

(11) Guram, A. S.; Wang, X.; Bunel, E. E.; Faul, M. M.; Larsen, R. D.; Martinelli, M. J. *J. Org. Chem.* **2007,** *72,* 5104.

(12) Kinzel, T.; Zhang, Y.; Buchwald, S. L. *J. Am. Chem. Soc.* **2010,** *132,* 14073.

(13) See Chapter 7.

(14) ORCA (version 2.9): Neese, F.; Wennmohs, F.; Becker, U.; Bykov, D.; Ganyushin, D.; Hansen, A.; Izsak, R.; Liakos, D. G.; Kollmar, C.; Kossmann, S.; Pantazis, D. A.; Petrenko, T.; Reimann, C.; Riplinger, C.; Roemelt, M.; Sandhöfer, B.; Schapiro, I.; Sivalingam, K.; Wezisla, B.; Kállay, M.; Grimme, S.; Valeev. E.

(15) Tao, J.; Perdew, J. P.; Staroverov, V. N.; Scuseria, G. E. *Phys. Rev. Lett.* **2003,** *91,* 146401.

(16) (a) Schaefer, A.; Horn, H.; Ahlrichs, R. *J. Phys. Chem.* **1992,** *97,* 2571. (b) Weigend, F.; Ahlrichs, R. *Phys. Chem. Chem. Phys.* **2005,** *7,* 3297.

(17) Hirata, S.; Head-Gordon, M. *Chem. Phys. Lett.* **1999,** *314,* 291.

(18) (a) Adamo, C.; Barone, V. *J. Chem. Phys.* **1999,** *110,* 6158. (b) Goerigk, L.; Moellmann, J.; Grimme, S. *Phys. Chem. Chem. Phys.* **2009,** *11,* 4611.

(19) Weigend, F.; Häser, M. *Theor. Chem. Acc.* **1997,** *97,* 331.

(20) (a) Neese, F.; Wennmohs, F.; Hansen, A.; Becker, U. *Chem. Phys.* **2009,** *356,* 98. (b) Izsák, R.; Neese, F. *J. Chem. Phys.* **2011,** *135,* 144105. (c) Petrenko, T.; Kossmann, S.; Neese, F. J. *Chem. Phys.* **2011,** *134,* 054116.

(21) Weigend, F. *Phys. Chem. Chem. Phys.* **2006,** *8,* 1057.

(22) (a) Grimme, S.; Ehrlich, S.; Goerigk, L. *J. Comput. Chem.* **2011,** *32,* 1456. (b) Grimme, S.; Antony, J.; Ehrlich, S.; Krieg, H. *J. Chem. Phys.* **2010,** *132,* 154104.

List of Publications

Chapter 1

Synthesis of Organoboron Quinoline-8-thiolate and -selenolate Complexes and Their Incorporation into π-Conjugated Polymer Main-Chain

Yuichiro Tokoro, Atsushi Nagai, Kenta Kokado and Yoshiki Chujo

Macromolecules **2009,** *42,* 2988–2993.

Chapter 2

Synthesis of π-Conjugated Polymer Containing Organoboron Benzo[h]quinolate in the Main-Chain

Yuichiro Tokoro, Atsushi Nagai and Yoshiki Chujo

Macromolecules **2010,** *43,* 6299–6233.

Chapter 3

Synthesis of Highly Luminescent Organoboron Polymers Connected by Bifunctional 8-Aminoquinolate Linkers

Yuichiro Tokoro, Atsushi Nagai and Yoshiki Chujo

J. Polym. Sci. Part A: Polym. Chem. **2010,** *48,* 3693–3701.

Chapter 4

Luminescent Chiral Organoboron 8-Aminoquinolate-Coordination Polymers

Yuichiro Tokoro, Atsushi Nagai and Yoshiki Chujo

Appl. Organomet. Chem. **2010,** *24,* 563–568.

Chapter 5

Synthesis of π-Conjugated Polymers Containing Aminoquinoline-Borafluorene Complexes in the Main-Chain

Yuichiro Tokoro, Atsushi Nagai, Kazuo Tanaka and Yoshiki Chujo

Macromol. Rapid Commun. **2012,** *33,* 550–555.

Chapter 6

Synthesis of Benzo[h]quinoline-Based Neutral Pentacoordinate Organosilicon Complexes

Yuichiro Tokoro, Hyeonuk Yeo, Kazuo Tanaka and Yoshiki Chujo

Chem. Commun. **2012,** *48,* 8541–8543.

Chapter 7

Structure-Dependent Electronic Communication around Pentacoordinate Silicon in Benzo[h]quinolyldibenzo[b,f]silepins

Yuichiro Tokoro, Kazuo Tanaka and Yoshiki Chujo

To be submitted.

Chapter 8

Integration of Benzo[h]quinoline and π-Extended Dibenzo[b,f]silepins on Pentacoordinate Silicon

Yuichiro Tokoro, Kazuo Tanaka and Yoshiki Chujo

To be submitted.

Chapter 9

Synthesis of π-Conjugated Polymers Containing Dibenzosilepin Moieties with Pentacoordinate Silicon

Yuichiro Tokoro, Kazuo Tanaka and Yoshiki Chujo

To be submitted.

Other publications not included in this thesis

Luminescent m-Carborane-Based π-Conjugated Polymer

Kenta Kokado, Yuichiro Tokoro and Yoshiki Chujo

Macromolecules **2009,** *42,* 2925–2930.

Luminescent and Axially Chiral π-Conjugated Polymers Linked by Carboranes in the Main Chain

Kenta Kokado, Yuichiro Tokoro and Yoshiki Chujo

Macromolecules **2009,** *42,* 9238–9242.

Nanoparticles via H-Aggregation of Amphiphilic BODIPY Dyes

Yuichiro Tokoro, Atsushi Nagai and Yoshiki Chujo

Tetrahedron Lett. **2010,** *51,* 3451–3454.